Identification of a novel putative PrP receptor

Filippo Cipriani

Thesis submitted to the University of London

for the degree of Doctor of Philosophy

September 2005

Mammalian Genetics Laboratory, Cancer Research UK, London

Department of Biochemistry, University College London

ProQuest LLC
789 East Eisenhower Parkway
P.O. Box 1346
Ann Arbor, MI 48106-1346

In memory of Giuliano

(1975-2001)

Abstract

Prion diseases, also known as Transmissible Spongiform Encephalopathies (TSEs), are fatal conditions which affect humans and animals. The hallmark of Transmissible Spongiform Encephalopathies is the accumulation in the brain of PrP^{Sc}, which is an abnormal isoform of the cellular protein PrP^{C}. It has been proposed that PrP^{Sc} is able to impose its own conformation on PrP^{C}, but the molecular mechanism by which PrP^{C} is converted into PrP^{Sc} is unclear.

PrP^{C} and PrP^{Sc} share the same primary sequence but they are different in their biochemical properties. PrP^{C} is rich in alpha helices, detergent soluble and Protease K sensitive; on the other hand, PrP^{Sc} is mainly composed of beta sheets, detergent insoluble and Protease K resistant.

To better understand PrP^{Sc} generation, a genetic screen to identify proteins that preferentially interact with a misfolded version of PrP has been employed. This novel protein-protein interaction system takes place in the yeast cytoplasm where PrP has been reported to adopt a beta sheet-rich conformation characterised by increased Protease K resistance.

Initial analysis revealed that one candidate molecule, PrP Interacting Protein 7 (PIP7), encoded a transmembrane protein present on the cell surface, suggesting a potential function as a novel PrP receptor. The interaction between PIP7 and PrP has been confirmed *in vitro* by GST pull down experiments and *in vivo* by co-immunoprecipitation studies. A panel of monoclonal antibodies directed against the C-terminus of PIP7, which contains the PrP binding region, has been generated.

FACS analysis using these antibodies confirmed the presence of PIP7 on the cell surface of N2a cells, commonly used to study PrP^{Sc} propagation, and PIP7 immunohistochemistry has revealed an intense staining in all brain regions including the cortex, hippocampus and cerebellum. Overexpression of PrP in N2a cells resulted in an accumulation of PIP7 surface levels. Furthermore, PIP7 levels appear to be reduced in the brains of PrP knockout mice. The direct correlation between the levels of PIP7 and PrP suggests a potential role for PIP7 as a regulator in prion biology.

Acknowledgements

First of all, I wish to thank my supervisor Dr Axel Behrens for giving me the great opportunity to do my PhD in his laboratory and for its constant support during the past years.

I would also like to thank all the members of the Mammalian Genetics Laboratory for their encouragement. I am especially indebted to Nnennaya Kanu for her incredible encouragement and sincere friendship. Special thanks to Clive Da Costa, Lluis Riera Sans and Ken Nakagawa for being always available for discussion. I am also grateful to Karel Dorey for the critical suggestions during the writing of the thesis.

I deeply want to thank my parents, Angela and Fernando, for always supporting me with their unconditional love and for being a constant presence in my life. A big thanks to my little sister Federica, whom I am really proud of, and to Giovanna for her support in the past years.

This work would not be possible without the facilities and services provided by CRUK.

Table of contents

List of figures

Abbreviations

BSA	bovine serum albumin
BSE	bovine spongiform encephalopathy
cDNA	complementary deoxyribonuvleic acid
CJD	Creutzfeldt-Jakob disease
CNS	central nervous system
Cu	copper
CWD	Chronic Wasting Disease
DC	dendritic cells
DNA	deoxyribonuvleic acid
Dpl	Doppel
ER	endoplasmatic reticulum
fCJD	familial Creutzfeldt-Jakob disease
FCS	foetal calf serum
FDC	follicular dendritic cell
FFI	fatal familial insomnia
GC	germinal centre
GFAP	glial fibrillary acidic protein
GPI	glycosylphosphatidylinositol
GSS	Gerstmann-Sträussler-Scheinker disease
H&E	Hematoxylin and Eosin
iCJD	iatrogenic Creutzfeldt-Jakob disease
MBM	meat and bone meal
NMR	nuclear magnetic resonance
PBS	phosphate buffer saline
PFA	paraformaldehyde
PIPLC	phosphatidylinositol phospholipase C
PK	protease K
Prion	proteinaceous infectious only
Prnd	Dpl gene
Prnp	PrP gene mouse

PRNP	PrP gene human
PrP	prion protein
^{Ctm}PrP	PrP transmembrane isoform with N-terminus in the cytosol
^{Ntm}PrP	PrP transmembrane isoform with C-terminus in the cytosol
^{Sec}PrP	non transmembrane PrP
PrP^{27-30}	protease resistant core of PrP^{Sc}
PrP^{C}	cellular isoform of the prion protein
PrP^{Res}	PrP isoforms resistant to PK digestion
PrP^{Sc}	disease associate isoform of the prion protein
PrP^{Sen}	PrP isoforms sensitive to PK digestion
PrP^{*}	a) hypothetical metastable PrP intermidiate isoform
	b) fractions of PrP^{Sc} molecules that are infectious
PS	pentosan sulphate
RML	Rocky Mountain Laboratories prion adapted strain
sCJD	sporadic Creutzfeldt-Jakob disease
SOD	superoxide dismutase
SNS	sympathetic nervous system
TfR	Transferrin Receptor
TME	transmissible mink encephalopathy
TSE	transmissible spongiform encephalopathy
vCJD	new variant Creutzfeldt-Jakob disease

Chapter 1: Overview of Transmissible Spongiform Encephalopathies

Transmissible spongiform encephalopathies (TSEs) are progressive neurodegenerative disorders affecting both humans and a variety of animals. They include Creutzfeldt-Jakob disease (CJD), Gerstmann-Sträussler-Scheinker disease (GSS), Fatal Familial Insomnia (FFI), and Kuru in humans, Scrapie in sheep, Bovine Spongiform Encephalopathy (BSE) in cattle, Chronic Wasting Disease (CWD) in deer and elk and Transmissible Encephalopathies in mink (Figure 1.1). The brains of affected individuals are characterised by neuronal loss, astrocytosis, spongiform changes and with or without characteristic amyloid plaques and fibrils consisting of abnormal PrP molecules (Bell and Ironside, 1993; Masters and Richardson, 1978) (Figure 1.2).

A common feature of all TSEs or prion diseases is the aberrant metabolism of the host encoded prion protein (PrP) which can exist in at least two conformations, distinguished by their physicochemical properties. The cellular form, PrP^{C}, is a membrane-bound protein, the function of which still remains unclear. Its structure comprises a C-terminal globular domain, enriched in α helical secondary structure. On the contrary, PrP^{Sc}, the disease associated conformation is rich in β structure and displays detergent insolubility and partial resistance to proteolysis treatment (Pan et al., 1993a). Finally, it has been suggested but not proven unequivocally that PrP^{Sc} is the real infectious agent (Prusiner, 1982).

The aim of this chapter is to provide a broad introduction to human and animal TSEs and a general overview of the biology of the prion protein, with special emphasis on what is known about the nature of the infectious agent. More specific aspects of prion disease, although interesting, will not be covered here since they have been reviewed exhaustively elsewhere (Aguzzi and Heikenwalder, 2005; Collinge, 2001; Prusiner, 1998; Weissmann, 2004).

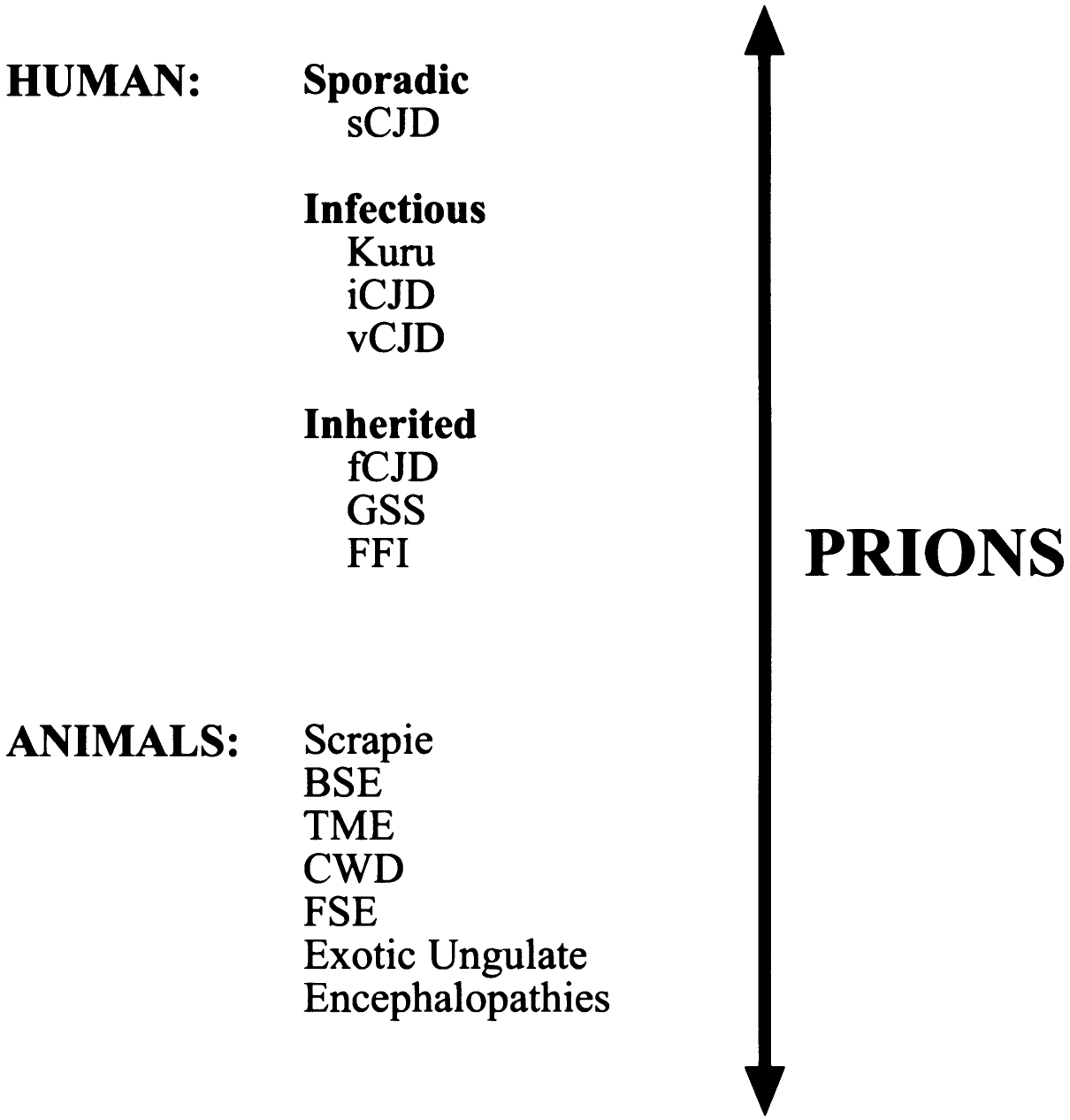

Figure 1.1 Prion diseases affecting humans and animals.
Prion diseases can affect humans and a great variety of animals. In humans, there are at least three possible origins; Sporadic and Inherited cases involve somatic and germ line point mutations in the *PRNP* gene, encoding for the prion protein PrP. Infectious transmission includes contamination through surgical procedures (iCJD), ritualistic cannibalism (Kuru) and more recently infection from bovine prions (vCJD). In animals, prion diseases include Scrapie in sheep and goat, Bovine Spongiform Encephalopathy in cattle, Chronic Wasting Disease in deer and elk, encephalopathy in mink, cats and several exotic ungulates. Abbreviations: Creutzfeldt-Jakob disease (CJD), Gerstmann-Sträussler-Scheinker disease (GSS), Fatal Familial Insomnia (FFI), Bovine Spongiform Encephalopathy (BSE), Chronic Wasting Disease (CWD), Feline Spongiform Encephalopathy (FSE).

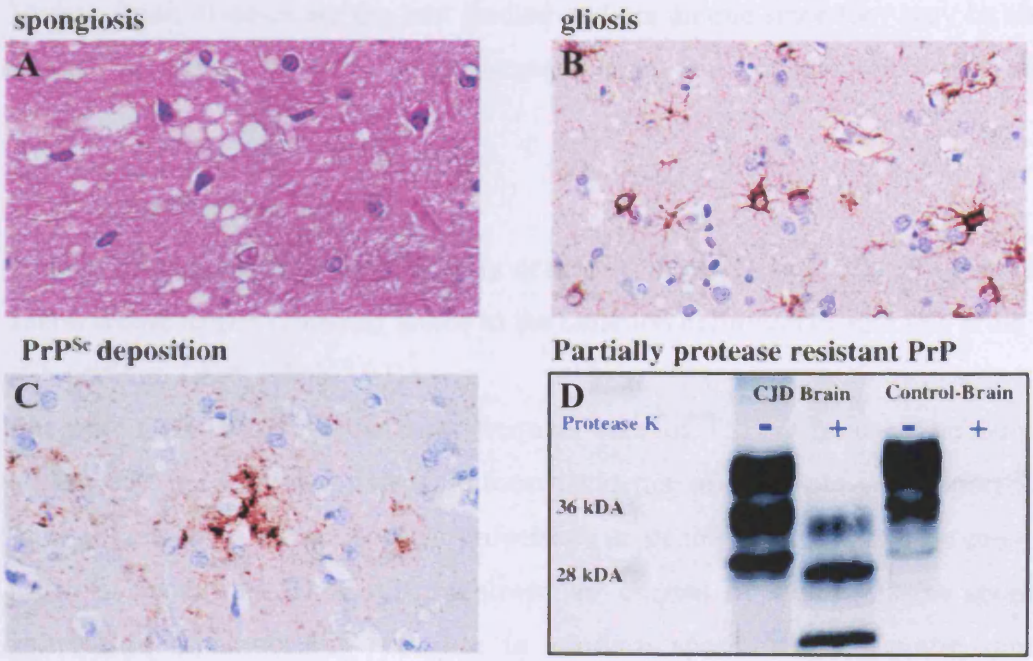

Figure 1.2 Neuropathological and biochemical features of Prion disease. Histopathological changes in the brain of affected patients include: A) fine vacuolation also referred to as spongiosis of the grey matter (H&E staining); B) astrocytic and microglial hyperplasia and hypertrophy (GFAP staining); C) Prion protein deposition either in large amyloid plaques or non-amyloid deposits; D) brain homogenate from infected patients presents the pathological isoform of the prion protein, which shows partial resistance to Protease K treatment. Modified from Glatzel and Aguzzi, 2001.

1.1 Human TSEs

Human Prion diseases are the best studied and are unique since they may be classified on their etiological basis which may be sporadic, inherited or acquired by infection.

1.1.1 Sporadic prion diseases

Human prion diseases were originally described in the early 1920s by Creutzfeld and Jakob whose names remained linked to the common definition of sporadic prion disease (Creutzfeldt, 1920; Jakob, 1921).

Sporadic CJD (sCJD) is the most frequent case of TSE in humans, accounting for almost 85% of total, and with a uniform incidence of $1/10^6$ per year. Sporadic cases were diagnosed when no specific infectious or genetic origin could be proven. The cause of sporadic CJD is still unknown: the current hypothesis is the spontaneous generation of abnormal PrP due to random spontaneous somatic mutations. Homozygosity in position 129, where either methionine (M) or valine (V) may be present, has been identified as a predisposing determinant for sCJD susceptibility (Palmer et al., 1991). The disease is characterised by an onset in middle age with a peak between 60-65 years and a very fast progression to death occurring generally within 6 months (Collinge, 2001).

1.1.2 Infectious prion diseases

Kuru

Kuru, initially believed to be originated by a "slow virus", spread among individuals of the Fore linguistic group living in the highlands of Papua New Guinea (Gajdusek and Zigas, 1957). However, it was later revealed that endocannibalism led to horizontal transmission of the disease: during ritualistic feasts, women and children consumed the brains and internal organs of deceased relatives. The disappearance of the cannibalistic rituals resulted in a drastic decline in Kuru incidence, supporting the proposed mechanism of transmission. The possible origin is believed to be a single case of sporadic CJD and oral transmission was responsible for the prolonged incubation time, approximately 10-15 years with rare cases of up to 40 years. Disease onset and progression were longer compared to sCJD and ataxia was reported in most of the cases.

Analysis of the *PRNP* 129 (M/V) polymorphism in 80 patients and 95 unaffected controls demonstrated that Kuru preferentially affected individuals with the M/M genotype (Lee et al., 2001a).

Iatrogenic transmission

Almost 30 years ago the first case of iatrogenic transmission of CJD was documented: a patient receiving a cornea transplant developed CJD and later was found that also the donor died of the same pathology (Duffy et al., 1974). Altogether, in the past years, hundreds of cases of iatrogenic transmission have been reported. More than half of the total cases of iatrogenic CJD are linked to treatment with human pituitary growth hormone, extracted from cadavers, to treat dwarfism or gonadotrophins to treat infertility in women (Koch et al., 1985; Powell Jackson et al., 1985). A few cases of disease transmission caused by contamination of neurosurgical instruments originally were reported by Jones and Nevin in the early 1950s. Weissmann and colleagues have further shown the intrinsic ability of infectious prions to bind steel, the principal component of surgical instruments, and have developed an effective decontamination procedure (Flechsig et al., 2001; Jackson et al., 2005; Zobeley et al., 1999).

New Variant CJD

Following the BSE crisis in the UK in the late 1980s, a CJD Surveillance Unit was introduced to estimate the possibility of transmission from cows to humans. In 1996, ten patients were originally reported with a pathological phenotype different from all previously CJD reported cases (Will et al., 1996). The disease which became known as variant CJD (vCJD) presented an early onset of symptoms, with an average of 26 years compared to 66 years characteristic of sporadic CJD. These new cases also exhibited prolonged disease duration (13-14 months compared to 5 months for spontaneous CJD (sCJD)). In vCJD, PrP accumulation was also reported to occur in peripheral tissues such as the tonsils, spleen and lymph nodes, which had never been reported for sCJD (Hill et al., 1997b). Post mortem examination revealed the presence of "florid" amyloid plaques, positive for the prion protein, surrounded by a halo of spongiform change (Ironside et al., 1996). Apart from the epidemiological link, there is an abundance of other supporting biochemical and histopathological evidence associating vCJD with

BSE. Firstly, macaque inoculated with BSE show neuropathological features analogous to vCJD cases (Lasmezas et al., 1996). Furthermore both BSE and vCJD share a common glycosylation fingerprint, distinct from all other cases of prion disease (Collinge et al., 1996). Finally BSE and vCJD have the same incubation time and produce a similar pattern of lesions, when introduced into transgenic mice (Bruce et al., 1997). To date, 107 cases of vCJD have been confirmed in the UK by post mortem autopsy and no accurate estimation of future cases can be made. It is however noteworthy that all vCJD cases described so far present M/M homozygosity at the polymorphic codon 129.

Recently a patient who developed vCJD after receiving red blood cells from a donor who subsequently died from variant CJD has raised public concern about the safety of blood and blood derivatives (Ironside and Head, 2004). Blood transmission has been studied in sheep where BSE infectivity by blood transfer was successfully achieved (Houston et al., 2000). Infectivity has also been successfully transmitted to rodents but not to primates, using blood from CJD and Kuru patients. Studies in animal models suggest that most prion infectivity in blood may be cell-associated, with lower levels in the plasma, and there is evidence suggesting that any infectivity present may be reduced during the process of plasma fractionation (Will, 2003). However, the possibility that plasma or blood products can transmit the disease in human cannot be completely excluded or confirmed at present.

1.1.3 Inherited prion disease

Only 10-15% of human prion diseases are genetically inherited as autosomal dominant traits (Hsiao et al., 1989). All cases of familial CJD (fCJD) have been unequivocally linked to mutations in the *PRNP* gene, as all cases of GSS and FFI. One noteworthy mutation is the D178N substitution which shows the ability to give rise to different neuropathological phenotypes according to which polymorphic residue is present in position 129: the presence of a methionine results in FFI presenting as a progressive sleep disorder and affecting more than 30 different families worldwide (Goldfarb et al., 1992). Conversely, when the D178N mutation was found in combination with a valine in position 129, patients present a severe dementia and the pathological features are

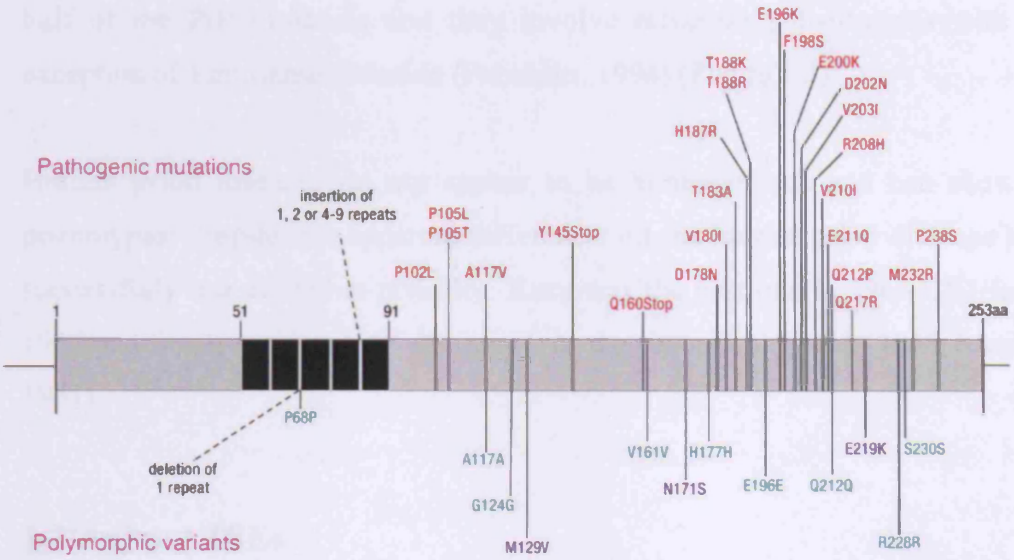

Figure 1.3 Pathogenic *PRNP* mutations and polymorphisms.
The diagram shows a schematic representation of the human prion protein, above which are listed the mutations (missense substitutions and insertions) linked to familial CJD, GSS and FFI. Below are shown the many polymorphisms, including the M129V which has been linked to disease susceptibility and different neuropathological phenotypes. Adapted from Collinge J., 2001.

typical of the cases of familial CJD (Gambetti et al., 1995). More than 20 different *PRNP* mutations have been described to date: they mainly occur within the C–terminal half of the PrP molecule and they involve missense substitutions with the only exception of a nonsense mutation (Pocchiari, 1994) (Figure 1.3).

Human prion diseases do not appear to be homogeneous and can show variable phenotypes; despite this apparent difference, all the human prion diseases have been successfully transmitted to primates: Kuru was the first one in 1966 CJD followed in 1968 and finally GSS in 1981 (Gajdusek et al., 1966; Gibbs et al., 1968; Masters et al., 1981).

1.2 Animal TSEs

1.2.1 Scrapie

Scrapie was originally reported more than 200 years ago and is endemic in many countries (Brown and Bradley, 1998). It is a fatal neurodegenerative condition affecting sheep and goats. Different routes of infection have been suggested for the spreading of the disease and ingestion of infected material seems to be the most likely possibility; however, introduction through skin lacerations or maternal transmission cannot be excluded (Elsen et al., 1999; Pattison et al., 1972).

1.2.2 Chronic Wasting Disease and Mink Transmissible Encephalopathies

Chronic Wasting Disease (CWD) and Transmissible Mink Encephalopathies (TME) affecting wild cervid and mink respectively were reported in the late 1960s in Colorado and 1947 in Minnesota (Marsh and Hadlow, 1992; Williams and Young, 1980). Some polymorphisms in the cervid *PRNP* gene have been described for CWD but not for TME and their relationship with susceptibility is still under investigation. Similarly to Scrapie, the route of infectivity for CWD and TME remain unclear but seem to involve lateral transmission. It has been suggested that TME was generated by ingestion of material contaminated by Scrapie or by exposure to an as-yet uncharacterised prion disease in cattle (Marsh et al., 1991).

1.2.3 Bovine Spongiform Encephalopathy (BSE)

BSE, also known as Mad Cow disease, was recognised in the United Kingdom in 1986, with a peak of around 1200 cases/month in 1993, and was promptly associated with other TSE's, such as Scrapie due to the presence of the typical brain lesions (Anderson et al., 1996; Wells et al., 1987). It is well accepted that BSE reached epidemic proportions due to the wide use of dietary protein supplements, namely meat and bone meal (MBM), containing the scrapie agent. Previously, treatment with lipid solvents were believed to inactivate the infective agent until inactivation procedures were changed in the late 1970s in order to minimise expenses (Ernst and Race, 1993; Prusiner, 1997). The dramatic decline in the number of reported cases reflected the decision to ban the practice of feeding animal remains to cattle in 1988. BSE cases have been described in other European countries such Switzerland, France and Germany, albeit with a total incidence 100 fold lower than in the UK, where it has had a substantial impact on the livestock industry (Detwiler and Rubenstein, 2000). Strain studies in mice aiming to characterise the BSE agent revealed the existence of a single strain of the transmissible agent in contrast with the multiple strains identified for scrapie in sheep (Bruce et al., 1994).

1.3 The Spread of prions

1.3.1 Peripheral invasion

Despite the wealth of experimental studies involving intracranial inoculation, natural TSE infections are most commonly acquired by peripheral exposure to the infectious agent: infection through the food chain was initially responsible for the spread of BSE among cattle resulting the emergence of vCJD in humans (Bruce et al., 1997; Hill et al., 1997a; Wilesmith et al., 1991). Therefore it is crucial to understand how infectivity, once acquired peripherally reaches the CNS. At early stages following peripheral inoculation, laboratory animals accumulate infectivity in lymphoid tissues, long before possible detection in the central nervous system (Farquhar et al., 1994; Kimberlin and Walker, 1979). However, when PrP^{Sc} is introduced into *Prnp*$^{-/-}$ mice via intraperitoneal route no disease is transmitted to the brain, suggesting the requirement for at least one intermediate compartment expressing PrP (Blättler et al., 1997). Lymphoid tissue involvement is not always a prerequisite but may reflect strain specificity like in the

case of BSE and sCJD, where PrP^{Sc} is mainly accumulating in the CNS (Hill et al., 1999b; Somerville et al., 1997). On the other hand, sheep affected by scrapie and vCJD patients presented infectivity in lymphoid tissues, with PrP^{Sc} detected in both follicular dendritic cells (FDC) and tingible body macrophages in the germinal centres (GCs), specialised regions responsible for B cells affinity maturation (Hilton et al., 1998; Vankeulen et al., 1996). A number of different cell populations are involved in the spread of TSE infectivity, as I will discuss below.

B and T lymphocytes

Lymphocytes of the T-cell lineage have been shown to be dispensable for scrapie pathogenesis as early demonstrated by the unaltered incubation time in mice subjected to thymectomy and later confirmed by inoculation of transgenic mice deficient in the T cell compartment (Klein et al., 1997; McFarlin et al., 1971). In contrast, B lymphocyte impairment had a profound effect on neuroinvasion, even if their expression of the prion protein was not an absolute requirement (Klein et al., 1998). However, sub-lethal γ-irradiation, known to kill all active dividing cells like B and T lymphocytes but also monocytes, did not affect scrapie pathogenesis as also B cell restricted PrP expression did not restore spleen replication in a PrP knockout background (Fraser and Farquhar, 1987; Montrasio et al., 2001). This apparent contradiction could be explained by the key role played by B lymphocytes in the secretion of cytokines, like TNF and lymphotoxin α and β, required for the maturation and correct maintenance of many other cell types like follicular dendritic cells and the general micro architecture of secondary lymphoid organs (Cyster et al., 1999; Kosco-Vilbois et al., 1997).

Follicular Dendritic Cells and Complement

Follicular dendritic cells (FDC) were positively identified as PrP expressing cells in tissues from spleen, lymph nodes, and Peyer's patches in both infected and uninfected mice (McBride et al., 1992). Moreover, in infected mice FDCs were found as preferential sites for PrP^{Sc} accumulation (Kitamoto et al., 1991). Their resistance to irradiation and their strict dependency from mature B cells made them an ideal candidate for a critical role in the neuroinvasion process. Independent experiments, based on genetically modified immunodeficient mice, came to the same conclusion: mice lacking mature FDCs did not present spleen infectivity (Brown et al., 1999b; Koni

et al., 1997; Mabbott et al., 2000; Matsumoto et al., 1996; Montrasio et al., 2000). There are however some inconsistencies in these experiments such as the dependency on the particular strain used: RML, in contrast with ME7, seemed to accumulate in the spleen even in the absence of PrP expression on FDCs as long as other cells, like lymphocytes, were PrP positive (Blättler et al., 1997). It was hypothesised that FDCs could uptake PrP^{Sc} after peripheral inoculation in the same way they capture and retain foreign antigens in a complex with complement components. In support of this hypothesis, mice lacking specific components of the complement cascade were partially protected from the scrapie agent, following intraperitoneal exposure (Klein et al., 2001; Mabbott et al., 2001).

Macrophages

Tingible body macrophages are present inside the germinal centres and contain intracellular depositions of PrP^{Sc} in infected animals (Jeffrey et al., 2000). A positive role as a scavenger of infectivity has been proposed for macrophages based on both *in vitro* and *in vivo* data (Beringue et al., 2000; Carp and Callahan, 1982). However, it remains unclear whether macrophages actively clear scrapie infectivity or whether PrP^{Sc} uptake occurs by passive sequestration.

Dendritic cells

Dendritic cells (DCs) are known to patrol the organism in order to collect antigens before delivering them to the lymphoid centres (Banchereau et al., 2000). Different lines of evidence suggest a potential role for dendritic cells for the transport of infectious prions to the germinal centres: DCs have been shown to be chemotactically attracted by the cytotoxic PrP 106-126 fragment and, more relevantly, a subpopulation of DCs is able to transport PrP^{Sc} from the intestine to mesenteric lymph nodes (Huang et al., 2002; Kaneider et al., 2003).

M cells

Prion infectivity can be orally introduced as in the case of BSE and vCJD (Will et al., 1996). Before reaching the Peyers patches, prions have to escape the gut lumen. M cells have been studied in their ability to uptake both foreign antigens and pathogens, translocate across the gut epithelial layer and present them to components of the immune system such as dendritic cells and lymphocytes (Neutra et al., 1996). Recently,

in vitro experiments have demonstrated the possibility that M cells act as a mucosal portal for prion entry upon dietary exposure (Heppner et al., 2001).

1.3.2 The journey from Spleen to Brain

As suggested above, prions replicate in peripheral organs before reaching the CNS, in a way dependent on the presence of at least one intermediate PrP expressing tissue (Blättler et al., 1997; Race et al., 2000). Original experiments have shown that, following intraperitoneal injection, replication occurred specifically in the corresponding segment of the spinal cord, connected through the splanchnic nerves of the sympathetic nervous system (Baldauf et al., 1997). Moreover lymphoid organs are mainly innervated by the sympathetic network (Felten et al., 1988). Recent investigations proved the hypothesis that the sympathetic route serves as a link between the lymphoreticular compartment and the CNS: damaging the sympathetic nervous system (SNS), with chemical or immunological approaches, resulted in reduced prion titres and in some cases prevention of the disease. In the same study, a complementary approach was also taken to show that transgenic mice in which lymphoid organs were hyper-innervated by sympathetic nerves were characterised by reduced incubation time and higher titres of infectivity were found in the spleen (Glatzel et al., 2001). The accumulated evidence implies a possible scenario in which infectivity spreads peripherally in the lymphoreticular system, in a way dependent directly by FDC and with the indirect participation of B lymphocytes and complement components, before reaching the CNS via peripheral SNS innervations (Aguzzi et al., 2001). However many questions remain unanswered, for example, whether FDC are responsible for the direct transfer of infectivity to the SNS terminals or if intermediate cell types are involved, as suggested by the fact that the germinal centres within the lymphoid tissue appear to be poorly innervated.

Once invasion has taken place in the PNS, the infectious agent still has to travel to the CNS. Both axonal and non-axonal transport systems have been proposed: for PrP^{C} a mechanism of fast axonal transport has been reported but for PrP^{Sc} all available data is indirect, estimating a speed of 1-2 mm/day and not compatible with a fast axonal transport (Borchelt et al., 1994; Kimberlin et al., 1983). The finding of PrP^{Sc} presence in the region surrounding the axons of peripheral fibres supports the idea of an alternative,

non-axonal, transport mechanism (Groschup et al., 1999; Hainfellner and Budka, 1999). In the latter case, a domino-like mechanism, requiring expression of PrP, could be envisaged (Glatzel and Aguzzi, 2000). Finally, it is also possible that the two mechanisms could somehow not be mutually exclusive.

Prion replication was historically restricted to CNS and lymphoid tissues (Legname et al., 2004). A recent report had raised the concern about PrP^{Sc} presence in non-lymphoid organs, which were able to accumulate PrP^{Sc} in the presence of chronic inflammation (Heikenwalder et al., 2005). This apparent new tropism of prion replication could be explained on the basis that inflammed organs like the kidney, liver and pancreas present with infiltration of B and T cells together with FDC and tingible body macrophages.

1.4 The nature of the infectious agent

The initial observation that the scrapie agent was resistant to inactivation with conventional procedures which were known to destroy nucleic acids and inactivate viruses offered the first indication that it might differ from any other known pathogen (Alper et al., 1967; Gordon, 1946; Pattison, 1965b). An accumulation of evidence suggested that the main constituent of the infectious agent was proteinaceous in nature. For many years, the true nature of the agent responsible for this group of diseases remained an enigma for the scientific community. The breakthrough was offered by the discovery of the prion protein: researchers were able to identify a single protein, called PrP or the prion protein, by enrichment for infectivity in the brain of a scrapie infected Syrian Hamster (Bolton et al., 1982). The prion protein was initially characterised by its Protease K resistance and was designated PrP^{27-30} based on its apparent molecular weight. Later studies proved that PrP^{27-30} was derived by proteolytic cleavage from a larger protein of 33-35 KDa, named PrP^{Sc} (Oesch et al., 1985). PrP^{Sc} had the ability to co-purify with infectivity and all treatments that destroyed PrP^{Sc} resulted in prion inactivation. Determination of the N-terminal sequence of PrP^{27-30} led to the establishment that the prion protein was encoded by a host gene, named *Prnp* in mice and *PRNP* in humans (Basler et al., 1986). Under physiological conditions, the gene product is a protease sensitive protein known as PrP^{C}, the function of which remains unclear.

1.4.1 The protein only hypothesis

Based on the evidence that prion infectivity always co-purifies with a protein component, and more specifically, with PrP^{Sc}, the Nobel laureate Stanley Prusiner proposed the modern definition of prions: "Small proteinaceous infectious particles that resist inactivation by procedures which modify nucleic acids" (Gabizon et al., 1988; McKinley et al., 1983; Prusiner, 1982; Prusiner, 1989). According to Prusiner's idea, PrP^{Sc} is the infectious agent able to propagate itself by causing the conversion of endogenous PrP^{C}. On one hand, the protein only hypothesis successfully managed to accommodate phenomena such as prion strains and species barrier, without having to evoke nucleic acids. On the other hand, many attempts to disprove Prusiner's hypothesis have previously failed as all attempts to isolate a prion specific nucleic acid were unsuccessful to date.

1.4.1.1 Mechanisms of prion replication

Two models of the conformational conversion of PrP^{C} into PrP^{Sc} have been so far proposed: A) the template-directed refolding; B) the seeding model (Figure 1.4).

Template-directed refolding

The template-directed refolding model makes the assumption of the existence of a high energy barrier between PrP^{C} and PrP^{Sc} conformations (Prusiner, 1991) (Figure 1.4A). PrP^{Sc} is predicted to be more stable but remains kinetically inaccessible. On the other hand, a small population of PrP^{C} could exist in an alternative conformation denoted PrP^{*}, able to bind a still uncharacterised cellular factor called Protein X, whose existence has to date been based on genetic evidence (Cohen et al., 1994; Telling et al., 1995). PrP^{*} describes a metastable intermediate and its existence could only be proved once it has been isolated.

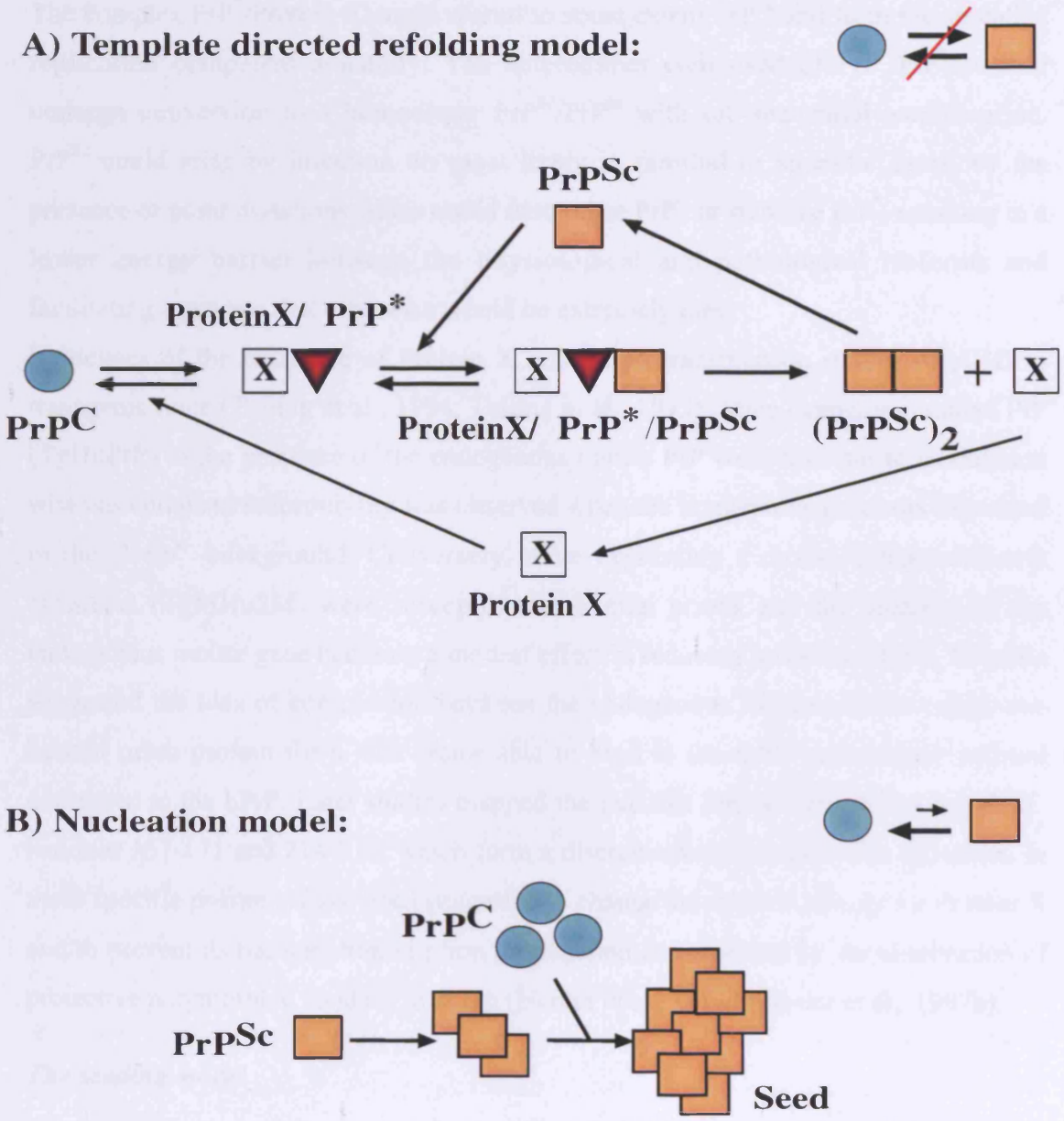

Figure 1.4 Models for the conversion of PrP^C to PrP^{Sc}.
A) Template directed refolding model: PrP^C and PrP^{Sc} are assumed not to be in direct equilibrium due to the presence of a high energy barrier preventing conversion. However PrP^C can exist in an alternative conformation called PrP* which in association with a still uncharacterised molecular chaperone, Protein X, is able to bind PrP^{Sc} and form the replication competent complex. PrP^{Sc} could arise by infection or, most likely in familial or sporadic cases, by the presence of point mutations which could destabilise PrP^C or stabilise PrP*. B) The seeding model postulates the existence of equilibrium between PrP^C and PrP^{Sc}. Such equilibrium is in favor of PrP^C, however PrP^{Sc} can be stabilised only when it forms a crystal-like aggregate, also called "seed". The formation of the initial seed is the rate-limiting step and once formed, monomeric PrP is rapidly incorporated. When the seed reaches a critical size, its fragmentation generates new seeds resulting in the overall cascade of amplification.

The complex PrP^{*}/Protein X could recruit to some extent PrP^{Sc} and form the so-called replication competent assembly. The heterodimer composed of PrP^{*}/PrP^{Sc} would undergo conversion to a homodimer PrP^{Sc}/PrP^{Sc} with sub-sequential amplification. PrP^{Sc} could arise by infection or, most likely in familial or sporadic cases, by the presence of point mutations which could destabilise PrP^{C} or stabilize PrP^{*}, resulting in a lower energy barrier between the physiological and pathological isoforms and facilitating a process that otherwise would be extremely rare.

Evidences of the existence of Protein X arise from transmission studies of sCJD to transgenic mice (Telling et al., 1994; Telling et al., 1995). Mice expressing human PrP (TgHuPrP) in the presence of the endogenous mouse PrP were resistant to inoculation whereas complete susceptibility was observed when the human transgene was expressed in the *Prnp*$^{-/-}$ background. Conversely, mice expressing a mouse-human chimeric construct (TgMHu2M) were susceptible to human prions and the ablation of the endogenous mouse gene had only a modest effect in reducing incubation time. The data suggested the idea of competition between the endogenous mouse and the exogenous human prion protein for a host factor able to bind to the mPrP with higher affinity compared to the hPrP. Later studies mapped the putative interaction site for Protein X: residues 167-171 and 214-218, which form a discontinuous epitope. Point mutations in these specific positions have been suggested to change the relative affinity for Protein X and to prevent its participation in prion propagation as supported by the observation of protective polymorphic residues in sheep (Hunter et al., 1993; Kaneko et al., 1997b).

The seeding model

According to the seeding or nucleation model the limiting step in the conversion mechanism would be the formation of an initial seed formed by PrP^{Sc} molecules (Jarrett and Lansbury, 1993)(Figure 1.4B). PrP^{C} and PrP^{Sc} would be in constant thermodynamic equilibrium, determined by the mass action rule. Such equilibrium favours PrP^{C} and only a small amount of PrP^{Sc} would be present at any given time, due to its intrinsic instability. Only in the rare event of the formation of a highly ordered structure or "seed", PrP^{Sc} would get stabilised. The seed would be able to grow by the addition of new PrP^{Sc} molecules until reaching a critical size. Upon breakage, new seeding nuclei are formed and more PrP^{Sc} molecules could be incorporated. The generation of new seeds would lead to further amplification in the system and a much faster kinetic of production of PrP^{Sc} molecules. The limiting step of the whole process would be the

initial generation of the seed, which is a function of the local PrP^{Sc} concentration and that could spontaneously arise in case of familial prion disease or be exogenously introduced.

Although there is a great deal of evidence in favour of both models, to date, neither has been confirmed or disproved.

1.4.1.2 PrP strains

One of the most challenging aspects of the protein only hypothesis remains the explanation of the existence of different prion strains, as was originally identified in sheep. Prion strains are different in their biological properties: originally, strains were classified not only by incubation time but also by the pattern of neuronal vacuolation and PrP^{Sc} deposition when introduced into inbred mice (Bruce et al., 1992; Dickinson et al., 1968; Fraser and Dickinson, 1973). The observation that the same inbred line was able to propagate different strains with different properties excluded that strain specificity was determined simply by the PrP primary structure. To be defined as a strain the observed biochemical properties had to be transmissible to an experimental animal both of the same and different species. Two hamster adapted scrapie strains, derived from mink and called "hyper" (HY) and "drowsy" (DY) suggested a possible explanation without invoking the requirement of a nucleic acid (Pattison and Millson, 1961). HY and DY produced distinct syndromes in the inoculated recipients and, following limited proteolysis, had different migration patterns on polyacrylamide gels (Bessen and Marsh, 1994). The explanation to the differential protease sensitivity was based on the original assumption of the existence of more than one PrP^{Sc} conformation (Prusiner, 1991). In order to distinguish between the different conformers and to facilitate their classification, limited proteolysis with Protease K had been extensively employed. Because different subtypes show different cleavage sites between amino acids 79 and 103, Protease K digestion produces resistant cores exhibiting slightly different gel mobility (Parchi et al., 2000). More recently, strains have been distinguished not only by molecular weight after Protease K digestion but also regarding the relative ratio of the different glycoforms (Collinge et al., 1996).
In summary, the protein only hypothesis postulates that different strains are the direct consequence of different pathological PrP conformations, as also supported by differential resistance to denaturating agents (Safar et al., 1998).

1.4.1.3 The species barrier

As above mentioned, PrP strains are characterised both by biochemical and pathological features. When laboratory animals are inoculated with infected material of the same species, all animals develop disease within a very narrow period of time. The definition of a species barrier was based on the original observation that, when animals were inoculated with prions from different specie, they did not develop disease with the same efficiency and presented much longer and heterogeneous incubation times (Pattison, 1965a). However, if the first passage occurred, sub-sequential passages resulted in a reduction in the incubation time, a process referred to as "adaptation" (Kimberlin and Walker, 1977). The concept of a species barrier has been studied with the help of transgenic animals and cell-free conversion systems and the unequivocal conclusion was that the PrP primary sequence in both donor and acceptor has to be the same in order to obtain successful and reproducible conversion (Caughey, 2003). PrP^{C} conversion to PrP^{Sc} has been schematised as a two-step event: the binding between the two different isoforms seems to precede the actual change in conformation, as outlined in *in vitro* studies, where heterologous PrP^{Sc} was able to bind efficiently the endogenous PrP^{C} even if there was no successful production of new PrP^{Sc} molecules (Horiuchi et al., 2000). On the same line of evidence, heterozygosity at codon 129 in human has been suggested to elicit a protective role against sCJD which occurs more often in homozygous individuals (Priola, 1999). The species barrier can be overcome by the introduction of a transgene encoding the donor sequence into the recipient mouse (Prusiner et al., 1990). Moreover, transgenic mice overexpressing exclusively the human form were susceptible to CJD and have been extensively used as a model to study transmission of BSE to human (Collinge et al., 1995).

1.4.1.4 Attempts to prove the protein only hypothesis: generation of infectivity in vitro

It is well accepted that PrP^{Sc} is derived from the normal host protein PrP^{C} and the two isoforms, despite sharing the same amino acid sequence, are extremely different in terms of their secondary structure. They also differ in their biochemical properties - PrP^{Sc} is relatively detergent insoluble and displays increased resistance to Protease K

digestion compared to PrP^C. According to the protein only hypothesis, PrP^{Sc} is believed to be able to self impose its own pathological conformation in an autocatalytic manner using the normal host isoform PrP^C as a substrate (Griffith, 1967; Prusiner, 1982). Although the generation of PrP deficient mice has demonstrated the absolute requirement for PrP^C in prion pathogenesis, definitive proof is still missing (Büeler et al., 1993). In order to be proven, the disease must be reproduced in a recipient animal by a molecule totally generated *in vitro* and in the absence of possible nucleic acid contamination which might still leave room for alternative interpretation.
Unlike in the mammalian system, yeast prions closely illustrate the prion hypothesis: the yeast proteins HET-s and Sup35 were successfully converted *in vitro* to their prion state, characterised by an altered and self-propagating conformation, and used to infect other cells (Maddelein et al., 2002; Sparrer et al., 2000; Tanaka et al., 2004).
I will here review some of the many attempts taken to generate infectivity *in vitro*.

More than a decade ago, the first attempt to generate PK resistant PrP, namely PrP^{Res}, mixing equimolar amounts of PrP^C and PrP^{Sc} was unsuccessful (Raeber et al., 1992).
Later, Kocisko and colleagues succeeded in the task of converting radio labelled PrP^C to a PK resistant form by mixing highly enriched protein fractions obtained by immunoprecipitation from infected brain homogenate. This attempt had the disadvantage of using a large molar excess of PrP^{Sc} over PrP^C, preventing not only the detection of infectivity associated with the newly synthesised material but questioning the compatibility with the *in vivo* process where PrP^C is definitely the most abundant specie (Kocisko et al., 1994). *In vitro* studies has shown that PrP^{Res} formation can be efficiently stimulated by chaotropes/detergents, chaperons, sulphated glycans and elevated temperatures (DebBurman et al., 1997; Wong et al., 2001). It is worth mentioning that an *in situ* conversion system, based on brain slices from infected mice, has been developed, allowing the study of conversion in a setting compatible with the tissue cytoarchitecture (Bessen et al., 1997).

In agreement with the seeding model, Saborio and colleagues have developed a new technique, called protein-misfolding cyclic amplification (PMCA), which allows very efficient amplification of the an initial PrP^{Sc} inoculum (Saborio et al., 2001). The technique is based on incubation cycles alternated with sonication steps which produce PrP^{Sc} oligomeric seeds able to catalyse the further conversion of PrP^C molecules, in a

way conceptually analogous to a DNA polymerase chain reaction. PMCA proved able to amplify indefinitely the original inoculum and the *in vitro* produced PrP^{Res} had biochemical properties similar to the ones observed *in vivo*, such as resistance to denaturation and proteolysis, tendency to form aggregates and, more importantly, *in vivo* infectivity (Castilla et al., 2005). However, the approach could not exclude the contribution of other molecules, for example, RNA which had been originally proposed to be involved in the generation of strain diversity and more recently had been demonstrated to stimulate prion protein conversion *in vitro* (Deleault et al., 2003; Weissmann, 1991).

Later, different groups focussed their energy towards the far more challenging task of generating infectivity *de novo*, without the assistance of an original PrP^{Sc} inoculum. Different groups successfully converted recombinant PrP, produced in bacteria, into a β-rich isoform that showed partial Protease K resistance. Moreover, these rearranged molecules were detergent insoluble and resistant to denaturation induced by chemical or physical agents. Some of them also showed the ability to polymerise into structures that resembled the one extracted from the brains of animals affected by prion disease (Liberski et al., 1991). Original experiments aimed to generate PrP^{Res} were performed in the presence of aggressive denaturing agents such as Urea and Guanidine hydrochloride (Hornemann and Glockshuber, 1998; Swietnicki et al., 1997). A further level of complexity was introduced by the observation that recombinant PrP could spontaneously unfold at low pH and in reducing condition to give rise to a still soluble conformation dominated by the presence of a β sheet structure, called PrP^{β} (Jackson et al., 1999). However, using a very elegant setting, Hill and colleagues have shown that *de novo* generated PrP^{β} was still not infectious (Hill et al., 1999a).This could be eventually explained by the possible requirement of still uncharacterised cellular element such as above mentioned Protein X (Telling et al., 1995).

Very recently, a fragment of the prion protein (amino acids 89-230) was successfully folded in amyloid fibrils and, when injected into transgenic animals overexpressing the same fragment, produced a disease with features common to TSE (Legname et al., 2004). As a proof of its infectivity, the disease was transmitted to recipient mice in a second passage. Despite being the closest attempt to confirm all the requirements of the protein only hypothesis, there is still the doubt that the disease might have risen

spontaneously in the transgenic mice used for the study and that inoculation of "synthetic prions" might have simply accelerated a spontaneous event. Based on the different histopathological manifestation of the disease, Legname and collegues considered their result to be the generation of a novel prion strain.

1.4.2 Alternative hypotheses

Despite being the most accepted explanation, the protein only hypothesis was not the only one proposed and had to face high scepticism from the scientific community. TSE's had been suggested to arise by an unconventional virus or a virino infection (Dickinson and Outram, 1988; Gajdusek, 1977; Kimberlin, 1982). PrP localisation on the cell surface suggested its putative role as viral receptor. In PrP knockout mice, the virus could not enter the cell, resulting in resistance to scrapie inoculation (Rohwer, 1991). Co-purification of infectivity with PrP^{Sc} had been proposed to be a result of putative sequence homology between a unidentified viral protein and PrP^{Sc} itself. The resistance of purified infectious preparations to procedures known to hydrolyse nucleic acids argued that either the prion genome was very small or did not even exist whereas a conservative explanation predicted that the putative genome was highly protected (Alper et al., 1967). Original experiments proved that an average of one oligonucleotide, shorter than 80 bases, could be found per ID_{50} unit (Kellings et al., 1992). More recent data, using return refocusing electrophoresis, excluded also the viroid hypothesis. The conclusion of the authors was that the possibility of a prion specific polynucleotide was highly remote (Safar et al., 2005). Among the many suggested hypotheses, it is worth mentioning: a replicating polysaccharide with membranes and infection by a Spiroplasma-like agent (Bastian, 1979; Gibbons and Hunter, 1967).

The Unified theory

Charles Weissmann tried to mediate the conflicting hypotheses by proposing an "unified theory": a PrP conformer, designated PrP^{*}, would be part of the infectious agent in association with a small host encoded RNA molecule, the co-prion; PrP^{*} and the co-prion would replicate independently and the possibility of incorporation of alternative RNA would explain the different phenotypes between prion strains (Weissmann, 1991). A report in which *in vitro* PrP^{Sc} amplification was stimulated by

addition of a RNA fraction from mammalian tissues has recently added new strength to the unified theory (Deleault et al., 2003).

1.5 Biology of the prion protein

1.5.1 PrP Structure

The structures of recombinant PrP, obtained from mouse, hamster and human, have been studied by nuclear magnetic resonance (NMR) and they present the same overall conformation (Hosszu et al., 1999; James et al., 1997; Riek et al., 1996). Mature PrP can be divided into two different regions: an unstructured N-terminal domain and a highly structured C-terminus, both of approximately 100 residues each. The N-terminus contains five tandem repeats of a consensus sequence of eight amino acids (PHGGGWGQ), the expansion of which was originally linked to familial prion disease (Owen et al., 1992). The octapeptide region has been shown to bind copper ions with high affinity (K_d 10^{-14} M), suggesting a physiological role of the prion protein in copper homeostasis (Hornshaw et al., 1995). More recently a second copper binding site has been characterised between residues 96 and 111 (K_d 4 10^{-14} M) (Jackson et al., 2001). The C-terminus contains three α helices and a very short antiparallel β sheet, with a single disulphide bound linking helices 2 and 3, displaying a globular fold like structure (Riek et al., 1996). Rearrangement of the overall secondary structure is necessary to produce PrP^{Sc}, which has higher β sheet content (Pan et al., 1993b). It is noteworthy that most of the PrP sequence is not necessary for prion propagation: the N-terminal deletion up to residue 80 is still replication competent and transgenic animals harbouring a construct lacking amino acids 23-88 and 141-176 (known also as PrP106) are still susceptible to disease (Fischer et al., 1996; Supattapone et al., 1999). Nevertheless, the presence of the N-terminal domain seems to facilitate efficient prion propagation, as shown for the transgenic Δ23-88, which developed the disease albeit with an incubation period three times longer than their wild-type counterparts (Supattapone et al., 2001).

1.5.2 Cellular trafficking of PrP

1.5.2.1 PrP^C Biosynthesis

PrP is a sialoglycoprotein, attached to the cell surface via a glycosylphosphatidylinositol (GPI) anchor and its biogenesis is similar to that of other membrane and secreted proteins (Stahl et al., 1987). PrP is synthesised as a polypeptide chain of 254 residues. The first 23 amino acids provide a signal peptide required for the correct targeting to the rough endoplasmic reticulum (ER); removal of the signal results in failure to reach the plasma membrane and in cytoplasmic accumulation of the prion protein (Lee et al., 2001b). Once inside the ER, PrP is subject to different post-translational modifications: two potential N-linked glycosylation sites (Asn-X-Thr, positions 180 and 196 of mouse PrP) can be modified by addition of mannose–rich oligosaccharides, sensitive to digestion by endoglycosidase H. The ER lumen also provides the correct environment for the formation of a single disulphide bond between cysteines 178 and 213 (Turk et al., 1988). Finally the last 24 residues at the C-terminus are cleaved before the attachment of the GPI moiety to serine 230. In order to reach the cell surface, the prion protein translocates to the Golgi compartment where the oligosaccharides chains undergo complex modifications such as glycan sialylation (Figure 1.5).

1.5.2.2 PrP internalisation

Early experiments showed a constant cycling of the prion molecule between the plasma membrane and the endocytic compartment from which most of PrP^C returns to the cell surface (Shyng et al., 1993). Surface iodination labelling and immunofluorescence microscopy showed a typical transit time of 1 hour. During each passage a small fraction (1-5%) undergoes a proteolytic cleavage near residue 110. After the cleavage, both fragments return to the cell surface but the N-terminal fragment is secreted in the extra cellular space (Harris et al., 1993). PrP trafficking appears to be a complex cellular event and the mechanism of PrP internalisation is still a matter of debate, since caveolae, rafts and clathrin coated pits have all been shown to be involved.

Pioneering experiments using chicken PrP proved that the N-terminus was important for correct internalisation by coated pits as deletion mutants within this domain accumulated at the plasma membrane (Shyng et al., 1995b). Indeed, the same sequence

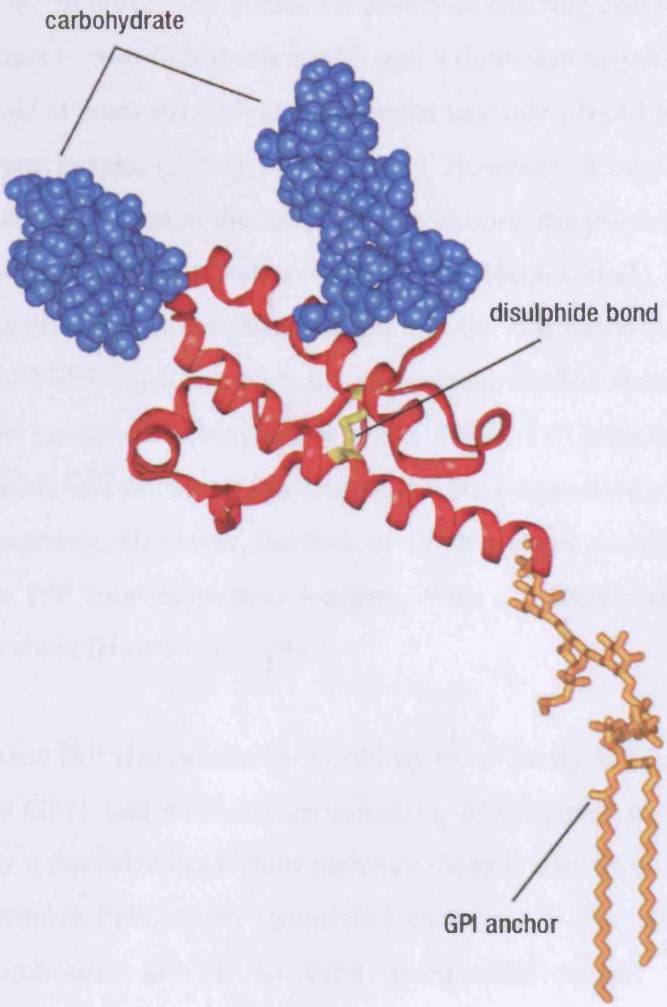

Figure 1.5 Three-dimensional model of human PrP^C.
PrP is composed of an N-terminal unstructured region and, as illustrated, a C-terminal globular domain with an overall α-helical structure (red). During its transit along the secretory pathway, the Prion protein acquires specific features such as two N-linked sugar chains (blue), a disulphide bond (yellow) and a GPI anchor (orange) responsible for its correct localisation at the cell surface Adapted from Collinge J., 2001.

when cloned in front of Thy1, another GPI anchored protein, was sufficient to change its membrane environment and confer the ability of entering coated pits (Sunyach et al., 2003). Experiments with hypertonic buffer and a dominant negative mutant of dynamin I (K44A) provided compelling evidence for the key role played by clathrin coated pits in PrP endocytic uptake (Shyng et al., 1994). However, it has to be mentioned that dynamin can also be found at the neck of caveolae and the previous experiment cannot exclude impairment of internalisation via caveolae (Henley et al., 1998). The generation of GFP tagged PrP allowed a further insight into the internalisation mechanism (Lee et al., 2001b). GFP-PrP localises with the endosomal marker transferrin, the uptake of which involves coated pits (Magalhaes et al., 2002). PrP behaviour is rather unusual compared to most GPI-anchored proteins which are internalised via a clathrin-dynamin independent pathway. Moreover, the lack of a cytoplasmic domain in PrP suggests the existence of a PrP transmembrane receptor, with a clathrin coated pit signal in its cytoplasmic domain (Harris et al., 1996).

On the other hand PrP also possesses the ability to co-purify with caveolar markers such as ganglioside GM1 and antibody crosslinking of GPI proteins is known to trigger endocytosis by a caveolae dependent pathway (Mayor and Riezman, 2004; Vey et al., 1996). Furthermore PrP copper-stimulated endocytosis was selectively blocked by filipin, a compound known to bind membrane sterols and alter caveolar structure/function (Marella et al., 2002).

A possible explanation to the apparent contradiction is that it cannot be excluded that copper-induced and unstimulated/constitutive endocytosis occur by alternative pathways including both caveolae and clathrin coated pits. Understanding the trafficking of the prion protein remains an ambitious goal since the cellular site of interaction/conversion between PrP^{C} and PrP^{Sc} has been proposed to take place on the cell surface or in an internal compartment (Taraboulos et al., 1992).

1.5.2.3 PrP and Rafts

Once on the cell surface, PrP molecules are found within rafts: highly ordered microenvironments, enriched in cholesterol and sphingolipids, and characterised by their insolubility in non-ionic detergents (Naslavsky et al., 1997). Rafts are highly

specialised domains that can selectively include or exclude proteins to variable extents and are believed to form preferential foci for signal transduction events (Simons and Toomre, 2000). PrP association with rafts is an event that occurs early in the secretory pathway and seems to have a role in stabilising its correct folding, as shown by cholesterol depletion experiments (Sarnataro et al., 2004). Rafts may be sites for conversion of PrP^{C} to PrP^{Sc} since exchange of the GPI anchor with the CD4 transmembrane domain not only removes PrP from rafts but also prevents PrP^{Sc} formation (Kaneko et al., 1997a; Taraboulos et al., 1995). The presence of PrP in lipid rafts is not contradictory with its association with coated pits: only a small population of total PrP undergoes endocytosis at a given time and possibly leaves the raft microenvironments before entering the coated pits, as seen in primary neurons and neuroblastoma cells (Sunyach et al., 2003).

1.5.2.4 Organelles involved in PrP trafficking

Intracellular trafficking requires transport between different subcellular compartments. Pioneering observations suggest that the trafficking of caveolae internalised proteins divert from the classic route involving the endosomal/lysosomal network (Anderson, 1998). Insight into the mechanism of vesicle transport has been mainly achieved by the study of the Rab proteins (Zerial and McBride, 2001).

Cellular and ultra-structural analysis reveals the presence of PrP^{C} in the Golgi and in endosomal intracytoplasmic organelles, with no cytoplasmic or synaptic vesicle labeling (Laine et al., 2001). GFP-PrP transits through the Rab5-positive early endosome compartment whereas GFP-GPI does not (Magalhaes et al., 2002). However, PrP^{C} has been reported in caveosomes - endosomes containing caveolin - in non neuronal cell lines (Peters et al., 2003). Knowledge of the routeing of PrP^{C} could be extremely useful in understanding which subcellular compartments are involved in the generation of PrP^{Sc}, since changes in trafficking can delay scrapie onset *in vivo* (Gilch et al., 2001). In parallel, PrP^{Sc} generation was increased in an *in vitro* cell model by transfection of a dominant-negative Rab4 and a constitutive active Rab6a mutant. The former regulates membrane recycling from early endosomes to the plasma membrane whereas the latter stimulates the retrograde trans-Golgi transport. Instead, a mutated version of Rab9 which is normally responsible for cargo sorting from late endosomes to the Golgi apparatus did not alter PrP^{Sc} formation (Beranger et al., 2002). Based on their data, the

authors hypothesised the involvement of retrograde transport of PrP^{Sc} to the ER, where it could seed the conversion of still immature PrP^{C} molecules.

As a final remark, there is a wealth of evidence suggesting that PrP^{C} may use different mechanisms of internalisation, involving both clathrin dependent and independent routes. Conversely, PrP internal trafficking seems less heterogeneous and canonical endosomal organelles play an important role, at least in neuronal cells.

1.5.3 PrP alternative topologies and localisation

1.5.3.1 Transmembrane PrP

In addition to the translocated isoform, denoted ^{Sec}PrP, different transmembrane topologies of the prion protein were originally described using cell free systems in combination with microsomal membrane preparations (Hay et al., 1987). Two transmembrane PrP conformations have been reported so far and they differ in term of whether the C-terminus (^{Ctm}PrP) or the N-terminus (^{Ntm}PrP) of the protein is directed towards the ER lumen. The production of these isoforms is dependent on the putative transmembrane region (amino acids 113-135) and the upstream hydrophilic sequence (104-112), termed STE for Stop Transfer Effector. Usually, ^{Ctm}PrP and ^{Ntm}PrP are only produced in small amounts (less than 10% of the total) during the transit through the endoplasmatic reticulum but the introduction of point mutations was able to alter the relative ratio of the different topologies. Transgenic mice harbouring a ^{Ctm}PrP favouring mutation (20-30% of the total) developed spontaneous neurodegeneration, including ataxia and this was in line with studies reporting increased levels of ^{Ctm}PrP in some cases of inherited prion disease (GSS mutations P105L and A117V) (Hegde et al., 1998). However, both transgenic mice and human cases did not show spontaneous accumulation of PrP^{Sc}. Quite surprisingly, when challenged with exogenous PrP^{Sc}, ^{Ctm}PrP mice not only accumulated PrP^{Sc} but a direct proportional accumulation of ^{Ctm}PrP was observed at the expense of ^{Sec}PrP (Hegde et al., 1999). The observation led the authors to speculate about a possible active role of ^{Ctm}PrP in prion disease pathogenesis. The mechanism by which transmembrane PrP could induce neurotoxicity is still uncharacterised and under investigation.

Most recently a PrP construct carrying the mutations L9R-3AV (3AV is the designed name of the triple mutation A112V/A114V/A117V) produced exclusively ^{Ctm}PrP when

transfected into cell lines. The mutant protein failed to reach the cell surface and was retained in the endoplasmic reticulum (Stewart et al., 2005). However, neurons derived from transgenic mice harbouring the above mutations, accumulated ^{Ctm}PrP in the Golgi apparatus and expressed an equal amount of ^{Sec}PrP (Stewart and Harris, 2005). Tg (L9R-3AV) mice developed a severe neuropathology presenting neurodegeneration in different brain areas, including the cerebellum and hippocampus. Strikingly, disease onset was prolonged in the *Prnp*$^{-/-}$ background compared to the wild type, suggesting that ^{Ctm}PrP caused neurodegeneration via a mechanism dependent on the presence of wild type PrP.

^{Ntm}PrP differs more from the other topologies due to the absence of the GPI moiety and the lack of glycosylation. At the present moment, ^{Ntm}PrP has not been associated with any TSE pathology and there is no conclusive evidence for its existence *in vivo*.

1.5.3.2 Cytoplasmic PrP

Plasma membrane proteins could spontaneously undergo misfolding during their transit to the endoplasmic reticulum and a mechanism known as retrograde transport usually ensures that misfolded, and potentially toxic, species are degraded in the cytoplasm by the proteasome complex (Kopito, 1997). Accumulation of even a small amount of cytosolic PrP (cytPrP), induced by treatment with proteasome inhibitors, was shown to be toxic in cell lines (Ma and Lindquist, 2001). In parallel, transgenic animals overexpressing a cytoplasmic version of PrP, due to the removal of the N-terminal signal peptide, developed ataxia and cerebellar neurodegeneration in a gene dosage dependent manner (Ma et al., 2002). CytPrP generated insoluble aggregates and proved to be partially Protease K resistant, two hallmarks typical of PrP^{Sc}-like conformations (Ma and Lindquist, 2002). Conversely another group has speculated that retrotranslocation could be an artefact due to an excessive increase in PrP messenger rather than a genuine reduction of the proteasome machinery (Drisaldi et al., 2003).

In striking contrast, there are at least two lines of evidence arguing against cytPrP toxicity. Firstly, PrP was found to be expressed in the cytosol of a small population of neurons in the hippocampus, thalamus and somatosensory neurocortex and none of the examined cells appeared either apoptotic or necrotic (Mironov et al., 2003); secondly, cytPrP is able to counteract Bax-mediated apoptosis in human primary neurons and

neuroblastoma cells (Roucou et al., 2005; Roucou et al., 2003). Hopefully, further studies will clarify the true role of cytosolic PrP in pathogenesis.

1.6 PrP Function

Despite its pivotal role in prion disease, after more than ten years since the generation of PrP knockout mice, the function of the prion protein still remains an enigma (Büeler et al., 1992). It was expected that the ablation of the *Prnp* gene could generate useful information regarding the function of PrP. Instead, no obvious phenotype was observed, posing the dilemma of how a protein highly expressed in the brain, where its expression is finely regulated during development, and in many other cell types could be dispensable for the organism. Only later analysis revealed minor alterations in electro physiological and circadian rhythm although these observations could not be completely reproduced by independent analysis (Collinge et al., 1994; Herms et al., 1995; Tobler et al., 1996).

Some of the putative functions attributed to PrP in the past years are outlined below giving emphasis to its suggested role in copper metabolism, signal transduction and pro-and-anti apoptotic functions.

1.6.1 Copper metabolism

The continuous endocytic recycling followed by PrP argues in favour of a role in active uptake of an extracellular ligand. PrP's role in copper uptake and metabolism was initially suggested by its high binding affinity and by the later observation that following exposure to copper (100-500 μM) more than half of the PrP surface pool was internalised by endocytosis (Brown et al., 1997; Pauly and Harris, 1998). The mechanism by which copper stimulates endocytosis is not clear although a recent report has suggested a process involving protein misfolding (Kiachopoulos et al., 2004). PrP binds not only copper but also other metal ions such as zinc, manganese and nickel (Brown et al., 2000; Pan et al., 1992).

Synaptosomal fractions from PrP knockout mice presented a 50% decrease in copper concentration, favouring the possibility of copper re-uptake by PrP in the presynapses (Kretzschmar et al., 2000). Impaired copper uptake could result in reduced activity of

cytosolic super oxide dismutase (SOD1), which requires copper and zinc as coenzymes to elicit its catalytic activity, and *Prnp*$^{-/-}$ mice were more sensitive to oxidative stress as monitored by increased oxidation of proteins and lipids (Herms et al., 1999). Moreover, recombinant PrP, either from mouse or chicken, was found to harbour SOD1 activity *in vitro* (Brown et al., 1999a). All the above evidence seemed to point in favour of an active role of PrP in copper homeostasis. However, other investigators failed to detect any difference in the amount of subcellular copper or in dismutase activity between *Prnp*$^{+/+}$ and *Prnp*$^{-/-}$ mice (Hutter et al., 2003; Waggoner et al., 2000). Therefore, the role of the prion protein in these pathways remains controversial.

1.6.2 Cell survival and apoptosis

A divergent set of evidence has been generated regarding the role of the prion protein in cell survival and cell death. PrP was found to interact directly with the anti-apoptotic protein Bcl-2 and was able to confer partial resistance to apoptosis induced by anisomycin treatment (Chiarini et al., 2002; Kurschner et al., 1995); in line with this, primary neurons derived from *Prnp*$^{-/-}$ mice have been shown to be more prone to neuronal death (Kuwahara et al., 1999). Furthermore, PrP interaction with the cell surface protein STI1 has been shown to activate a protective pathway, related to cAMP and PKA signalling (Zanata et al., 2002).

In clear contradiction to the above data suggesting a neuroprotective role, the work of other groups has pointed towards an active involvement of PrP in cell death. PrP overexpression was reported to increase cell death triggered by staurosporin treatment and caspase 3 activity whereas primary cultured neurons from PrP knockout mice were partially protected (Paitel et al., 2002; Paitel et al., 2004). In a different approach, the prion protein fragment, spanning amino acids 106-126, exhibited the ability to induce apoptosis in rat hippocampal neurons possibly through binding to the low affinity neurotrophin receptor p75 in neuroblastoma cells (Della-Bianca et al., 2001; Forloni et al., 1993). The same peptide led to JNK-Jun pathway activation and consequent cell death in primary cortical neurons (Carimalo et al., 2005).

1.6.3 Signal transduction

Insights suggesting a possible PrP function in signal transduction came from crosslinking experiments using α-PrP antibodies. In a first report the tyrosine kinase Fyn was activated in a PrP dependent manner (Mouillet-Richard et al., 2000). The response was restricted to cells differentiated *in vitro* in the serotonergic or noradrenergic lineages and subsequent studies suggested a role for PrP in the homeostasis of serotonergic neurons (Mouillet-Richard et al., 2005). Since PrP and Fyn lie on opposite faces of the plasma membrane, the transmembrane molecule NCAM, previously purified in association with PrP, could mediate the signal transduction resulting in neuritogenesis (Santuccione et al., 2005; Schmitt-Ulms et al., 2001). Conversely, PrP specific monoclonals rapidly triggered apoptosis in hippocampal and cerebellar neurons *in vivo* (Solforosi et al., 2004).

PrP participation in signal transduction pathways was also suggested by its ability to interact with the adaptor protein Grb2, involved, for example, in the activation of MAP kinases (Spielhaupter and Schatzl, 2001). Finally, PrP has been suggested to participate in lymphocyte activation: this study showed that PrP expression was increased following cell activation and antibodies against PrP suppressed mitogen-induced activation (Cashman et al., 1990).

1.6.4 PrP interacting proteins

The possibility that proteins interacting with PrP may elucidate the physiological function of PrP^{C} or play a role in prion diseases, has led to a quest for prion interacting proteins. Some of the interacting partners may be involved in the conformational transition responsible for the generation of PrP^{Sc} and, therefore, could be potential targets for therapeutic approaches. Many proteins have been isolated in the past for their ability to interact with PrP. Figure 1.6 shows some of the PrP partners which have had their binding sites identified.

Stanley Prusiner originally suggested the existence of a molecular chaperone, known as Protein X, involved in the transconformation process (Telling et al., 1995). Quite interestingly, the heat shock protein 60 (Hsp60) was originally isolated from a HeLa cDNA library as a novel PrP interactor and its bacterial homologue, GroEL, was able to

induce aggregation of recombinant PrP *in vitro* (Edenhofer et al., 1996; Stockel and Hartl, 2001). Wild type PrP and the mutant Q217R bound the ER chaperone Bip, which might play a role in the quality control of newly synthesised molecules (Jin et al., 2000). PrP may not only interact with chaperones but itself possesses chaperoning activity similar to the nucleocapsid protein from HIV-1 and the ability to bind nucleic acids (Gabus et al., 2001). This could be of relevance, since host encoded RNA molecules have recently been shown to be required for *in vitro* conversion between PrP^{C} and PrP^{Sc} (Deleault et al., 2003).

Amongst the most recently identified interactors, tubulin has been proposed to be responsible for the correct transport of PrP along the microtubular track whereas interaction with NRAGE, a cytoplasmic protein believed to facilitate apoptosis, has been suggested to modulate neuronal viability (Bragason and Palsdottir, 2005; Nieznanski et al., 2005). It is noteworthy that both tubulin and NRAGE, like many other isolated partners, do not share the same subcellular compartment with PrP resulting in a difficult interpretation of where the interaction may occur.

1.6.5 PrP: receptor or ligand?

Despite its constant recycling in the endocytic pathway, the main cellular localisation of PrP remains the plasma membrane, arguing in favour of its possible function as a receptor or ligand, as later supported by experimental evidence (Gauczynski et al., 2001; Zanata et al., 2002).

PrP acts as cellular receptor for laminin and mediates neuritogenesis both in PC12 cells and in primary neurons (Graner et al., 2000a; Graner et al., 2000b). The 37 KDa laminin receptor precursor (LRP) was initially identified as a PrP interactor by a yeast two-hybrid screen and its levels were increased in scrapie infected animals compared to uninfected controls (Rieger et al., 1997). Subsequently, a function of the LRP/LR complex was proposed in mediating internalisation of exogenous recombinant PrP (Gauczynski et al., 2001). Glycosamynoglycans (GAGs) show the ability to interact with PrP and the binding affinity is enhanced by the presence of copper ions (Pan et al., 2002). Recently, Heparan Sulphate has also been proposed as a receptor for the uptake of prion rods (Horonchik et al., 2005). In summary, novel approaches need to be undertaken to provide further insight into the role of PrP which, being so

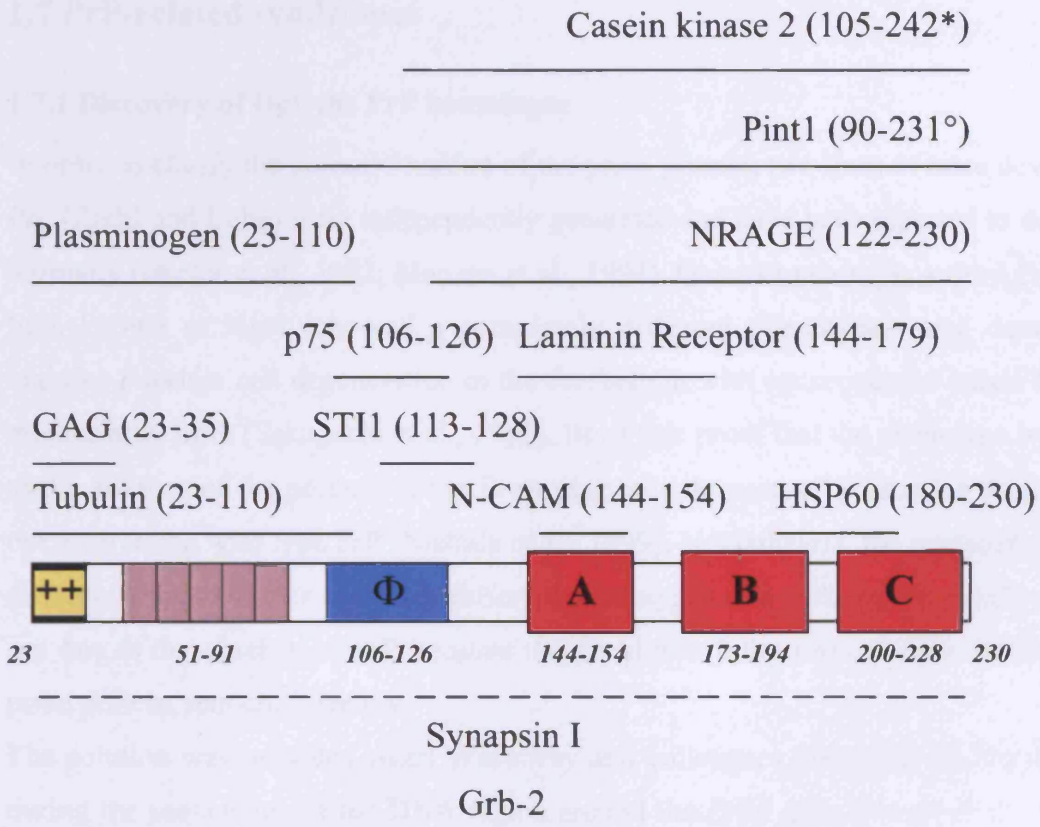

Figure 1.6 Prion interacting molecules.
PrP precursor molecules are processed by cleavage of the N- and C- terminal signal peptides to produce a protein, which contains a positively charged region (yellow), five octarepeats (gray), a highly conserved hydrophobic domain (blue) and three alpha helices (red). Numbers in italics indicate the start and the end of each structural domain. The binding site of each Prion interacting partner is reported in brackets, apart for Synapsin I and Grb-2, which have not been mapped in detail. All numbers refer to human PrP sequence; Pint1 and Casein kinase interacting domains are mapped against mouse (°) and bovine (*) PrP respectively.

evolutionary conserved, must have a clear physiological function apart conferring susceptibility to prion disease.

1.7 PrP-related syndromes

1.7.1 Discovery of Dpl, the PrP homologue

In order to clarify the normal function of the prion protein, two lines of mice devoid of PrP (ZrchI and Edbg) were independently generated and have been reported to develop normally (Büeler et al., 1992; Manson et al., 1994). Quite surprisingly, a third PrP null line, known as Ngsk, showed a completely different phenotype: mice developed massive Purkinje cell degeneration in the cerebellum with consequential ataxia from 6 months after birth (Sakaguchi et al., 1996). Bona fide proof that the phenotype was due to the absence of the product of the *Prnp* gene was the rescue by crossing with a line overexpressing wild type PrP (Nishida et al., 1999). Nevertheless, the explanation why different knockout lines exhibited different phenotypes was still elusive: clearly it was not due to the absence of PrP because the ZrchI and Edbg lines, despite lacking the prion protein, remained healthy.

The solution was provided when Westaway and colleagues identified the *Prnd* gene, during the sequencing of the DNA region around the *Prnp* gene (Moore et al., 1999). The *Prnd* gene lies 16 kb downstream of *Prnp* and contains an open reading frame predicted to encode a protein related to PrP. Two major transcripts (2.7 and 1.7 Kb) have been reported and the product of the gene was named Dpl or Doppel for Downstream prion protein-like gene. The ataxic phenotype was later ascribed to the ectopic expression of Dpl in the Nagasaki line. In wild type mice, Dpl transcripts were undetectable in brain but deletion of the splice acceptor site present in front of *Prnp* exon 3, which was ablated in the strategy used to generate the Ngk line but not in the Zrch or Edbg lines, resulted in an intergenic spicing event between the *Prnp* and *Prnd* genes: the result of which was a chimeric transcript, produced under the control of the *Prnp* promoter and containing the first two non-coding *Prnp* exons linked to the Dpl-encoding *Prnd* exon. This was later confirmed by the generation of other knockout lines (ZrchII and Rcm0) using targeting strategies analogous to the one employed for the generation of the Ngsk line and showing a similar ataxic phenotype. Moreover, introduction of cosmid DNA expressing Dpl was able to further accelerate the ataxic

syndrome in ZrchII mice as a direct consequence of the higher levels of Dpl present in the CNS. On the other hand, a single PrP allele could abrogate Dpl toxicity and extend the lifespan of the mice (Rossi et al., 2001).

More recently a third gene, called *Prnt* has been reported downstream of *Prnd*, confirming the existence of three PrP related open reading frames within 50 Kb (Makrinou et al., 2002).

1.7.1.1 Dpl: Structure and Function

Prnp and *Prnd* do not share homology at the DNA level, suggesting an ancient gene duplication event of an ancestor prion gene. Dpl, like PrP, was characterised as an N-glycosylated protein, anchored to the cell surface by a GPI moiety (Figure 1.7A) (Silverman et al., 2000). Similarity between PrP and Dpl is confined to the C-terminal domain: Dpl lacks the octarepeats and the hydrophobic region present at the N-terminus of PrP. Nevertheless Dpl and PrP share the ability to bind copper and despite being only 25% identical regarding the amino acids composition, the C-terminus of PrP and Dpl are largely superimposable (Qin et al., 2003)(Figure 1.7B).

Mice in which the *Prnd* gene has been interrupted by insertion of a neomycin cassette display normal development but mutant males are infertile due to abnormal gametogenesis, demonstrating an unexpected physiological function of Dpl (Behrens et al., 2002). Dpl was found to be dispensable for prion disease progression as investigated using a neuronal grafts paradigm (Behrens et al., 2001). Furthermore, protein folding intermediates induced by urea treatment, which exist for PrP, cannot be detected for Dpl arguing against the possibility that Dpl can get converted to a pathological conformer (Nicholson et al., 2002).

1.7.1.2 Structural-functional analysis of Dpl toxicity

PrP seems to possess the ability to antagonise Dpl-mediated toxicity since Dpl can trigger cell death only in the absence of PrP. Many models have been proposed to account for this observation: among which, the idea that PrP and Dpl are able to compete for an as-yet unknown common ligand involved in a signal transduction pathway, as suggested by the binding of PrP and Dpl Fab's to cerebellar granule cells (Legname et al., 2002). Recently, Westaway and colleagues have elegantly shown

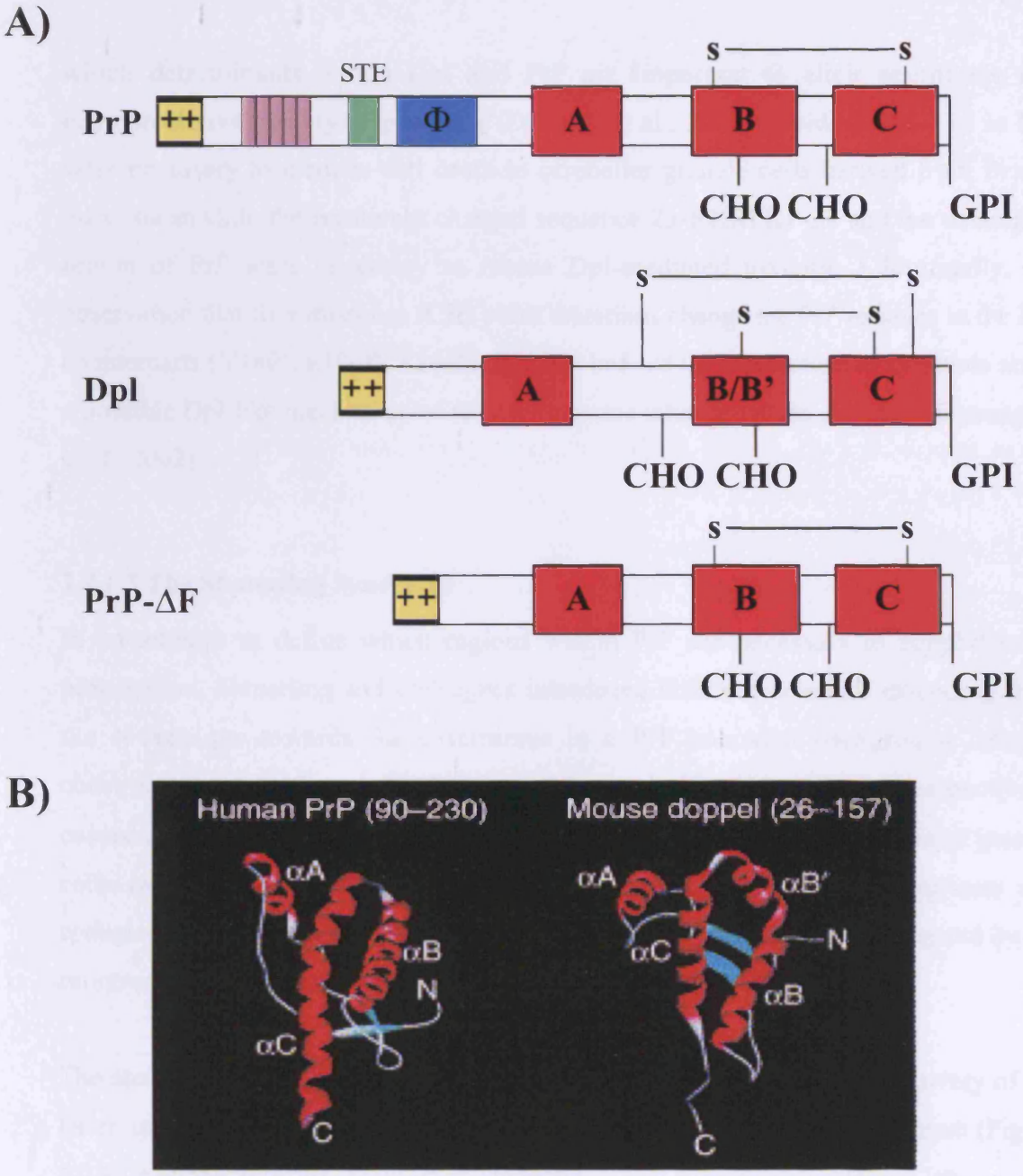

Figure 1.7 Structural comparison of PrP and Dpl.
A) Prion proteins share common features such the presence of three alpha helices (shown in red), glycosylation (CHO) and attachment to the plasma membrane via a glycosylphosphatidylinositol anchor (GPI). At the N-terminus a conserved cluster of basic residues is present (++); conversely, Dpl and the PrP deletion mutant ΔF do not present the octarepeat region (grey boxes), the stop transfer effector region (STE) and the hydrophobic core (Φ), required for the generation of the transmembrane isoforms.
B) NMR structure of human PrP and mouse Dpl. Alpha helices are shown in red and beta strands are represented in cyan. Although the overall 3D structures are quite conserved, Dpl presents an interruption in the second alpha helix (B/B') and a shorter loop spacing between alpha helices B and C. Modified from Westaway and Carlson, 2002.

which determinants within Dpl and PrP are important to elicit neurotoxic and neuroprotective activity respectively (Drisaldi et al., 2004): residues 101-125 in Dpl were necessary to mediate cell death in cerebellar granule cells derived from *Prnp*$^{-/-}$ mice, meanwhile the positively charged sequence 23-KKRPKP-28 and the octarepeat region of PrP were necessary to rescue Dpl-mediated toxicity. Additionally, the observation that four missense fCJD point mutations change the PrP residues in the Dpl counterparts (V180I, E196K, E200K, E211Q) had led the researchers to speculate about a possible Dpl-like mechanism of toxicity in some inherited prion disease (Mastrangelo et al., 2002).

1.7.1.3 The Shmerling Syndrome

In an attempt to define which regions within PrP are necessary to support prion propagation, Shmerling and colleagues introduced different deletions extending from the N-terminus towards the C-terminus in a PrP knockout background. Mutant constructs termed ΔE and ΔF, lacking amino acids 32-121 and 32-134 respectively, caused an ataxic phenotype associated with massive reduction in the number of granule cells in the cerebellum, within three months of birth. Massive astrogliosis and spongiosis were also observed and the toxic phenotype was completely abrogated by the re-introduction of a single copy of wild type PrP (Shmerling et al., 1998).

The analogy between the Shmerling and Dpl Syndromes was, after the discovery of the latter, quite evident since Dpl not only structurally resembles the PrP-ΔF mutant (Figure 3.7A) but the two disorders also share common symptoms including ataxia and cerebellar cells loss. Furthermore, the toxic effect of Dpl and PrP deletions could be rescued by a single copy of full length PrP. The only apparent discrepancy was due to the vectors used to generate the transgenic lines: the "Half Genomic PrP" vector, used to drive the expression of the ΔE and ΔF mutations, was active in granule cells but inactive in Purkinje cells, meanwhile Dpl expression was under control of the complete PrP promoter, known to be transcriptional active mainly in Purkinje cell and much less in granule cells (Fischer et al., 1996). When targeted specifically to Purkinje cells, the PrP-ΔF mutant was able to phenocopy Dpl overexpression and, once more, toxicity was abrogated by the presence of a single copy of wild type PrP (Flechsig et al., 2003).

Finally, ubiquitous expression of Dpl resulted not only in loss of Purkinje but also granule cells (Moore et al., 2001).

1.7.1.4 A possible common toxicity pathway

All the evidence pointed in the direction that both PrP-ΔF and Dpl might cause cell death through the same pathway, either interfering with a survival signal or activating a cell death cascade. A classic dominant negative effect, such as interference of truncated PrP or Dpl in a pathway requiring PrP, cannot be invoked since the pathology develops in the knockout background only. Weissmann and coworkers suggested a possible model: PrP would normally bind an as-yet uncharacterised ligand L_{PrP} via its C-terminal globular domain and elicit a survival signal via its N-terminal flexible tail (Shmerling et al., 1998). The lack of an obvious phenotype in PrP knockout mice would be due to the interaction between L_{PrP} and π, a hypothetical protein with functional properties similar to PrP and able to trigger the same signal cascade. Truncated PrP, and possibly also Dpl, could still bind L_{PrP} but not activate the downstream pathway, behaving like a dominant inhibitor of π. However, the existence of L_{PrP} and π remains speculative since no potential candidate exhibiting such behaviour have been suggested so far.

1.8 The aim of the experimental work

As reviewed above, after many years the physiological function of PrP still remain elusive. The aim of the present work was the identification of novel PrP interacting molecules which would be extremely useful to characterise the molecular pathways in which PrP is involved. On the other hand, the system I have used allowed to screen for candidates which preferentially bind misfolded PrP; such proteins not only could clarify the mechanism responsible for PrP^{Sc} generation but could provide novel therapeutic targets in the cure of prion disease.

Chapter 2: Materials and Methods

2.1 Tissue Culture

2.1.1 Cell lines and media

Mouse Neuroblastoma N2a

Uninfected N2a cells were obtained from the ATCC and cultured according to their recommended guidelines. Chronically infected N2a were kindly provided by Dr. P. Kloehn from the MRC Prion Unit, London. Cells were cultured in OPTIMEM supplemented with 10% FCS - heat inactivated for 30 minutes at 56°C - and penicillin/streptomycin.

Human 293T

Human 293 cells were obtained from the ATCC and cultured according to the suppliers' protocol. Cells were grown in Dulbecco Modified Eagle Medium containing 10% heat inactivated FCS, penicillin/streptomycin and L-glutamine.

Human HCT116

HCTs cells were provided by the CRUK Cell Production Unit. Cells were grown in Dulbecco Modified Eagle Medium, supplemented with 10% heat inactivated FCS, penicillin/streptomycin and L-glutamine.

Stock solution of penicillin (10000 u/ml), streptomycin (10 mg/ml) and L-glutamine (200 mM) were diluted 1:100 and were purchased from GibcoBRL.

2.1.2 Cell maintenance and passaging

All cell lines were grown in a 5% CO_2 incubator at 37°C and were routinely passaged at 1:5 or 1:10, twice a week. 293T and HCTS116 cells were trypsinised with 10X Trypsin (GibcoBRL) diluted to 1X in PBS. Media was removed and cells washed once in PBS before being trypsinised for 5 min at 37°C and resuspended in 10 ml of pre-warmed media.

N2a passaging did not require trypsin but were gently detached by pipetting.

2.1.3 Cell freezing

Confluent cells were gently detached from plates by mild trypsinisation and centrifuged for 5 minutes at 900 rpm. The resulting pellet was then resuspended in 1 ml of freezing buffer (90% FCS, 10% DMSO) at a concentration of 2 10^6 cells/ml and stored at –70°C. The following day, aliquots were transferred to a liquid nitrogen tank for long term storage.

2.1.4 Cell thawing

Frozen vials were quickly transferred from the liquid nitrogen storage to a 37°C water bath. Once completely thawed, the 1 ml aliquot was diluted in 10 ml complete media and spun down for 5 minutes at 900 rpm. The supernatant was then discarded and the pellet resuspended in 10 ml of complete media and transferred to a 10 cm dish to allow recovery.

2.1.5 Standard Lipofectamine 2000 Transfection

Cells were transfected using the Lipofectaminie 2000 reagent (Invitrogen) according to the manufacturers' protocol. Briefly, cells were plated in 10 cm dishes at 70% confluence the day before transfection. 20 μg plasmid DNA and 40 μl Lipofectamine 2000 were diluted into two separate tubes, each containing 1.5 ml serum-free OPTIMEM. The contents of the tubes were mixed together and subsequently incubated at room temperature for 20-30 minutes. In the meantime, cells were washed once with OPTIMEM and incubated in the presence of the complex (3 ml final) for 4-5 hrs at 37°C. The complex was aspirated and after one wash with OPTIMEM, complete media was added. Cells were analysed 48 hours post transfection by Western blot or FACS assay.

2.1.6 siRNA transfection

A pool composed by four siRNAs against the human PIP7 gene was purchased from Dharmacon (catalog # M-013452-00); a non targeting control pool was used to assess specificity (catalog # D-001206-13). Pools were dissolved in RNAase-free water to a

final concentration of 20 μM and stored at -20°C. Human 293T cells were transfected with Lipofectamine 2000 according to manufacturers' conditions. Briefly, cells were plated the day before transfection in order to obtain plate at 70% confluence. 60 μl of Lipofectamine 2000 and 20 μl of siRNA stock pool were dissolved in separate tubes, each one containing 500 μl of serum-free OPTIMEM. After 5 minutes, the contents of the two tubes were gently mixed by pipetting and allowed resting for 30 minutes in order to form the transfection complex. In the meantime, cells were washed once with serum-free OPTIMEM and 3 ml of serum-free OPTIMEM was added; the complex (1 ml) was added to the plate in order to reach a final siRNA concentration of 100 nM. 5 hours later, the complex was removed, cells were washed once and 10 ml of complete media were added. SiRNA efficiency was judged at two different time points: 36 and 60 hours after transfection. The following day, cells were resuspended and splitted into three aliquots: the first one for FACS analysis, the second for Western blot analysis. The last aliquot was re-plated. The next day, further aliquots were taken and the experiment was terminated.

2.1.7 Cell Treatments

2.1.7.1 Pentosan Sulphate and Suramin

Human 293T cells were transfected as described above; 24 hrs later, the media was changed and the following compounds were dissolved in complete media: Suramin (Sigma) 200 μg/ml, Pentosan Sulphate (Fibrase, TEOFARMA) 100 μg/ml. Cells were returned to the incubator for additional 24 hrs before being fixed and processed according to the standard FACS protocol.

2.1.7.2 PIPLC

In order to specifically release all GPI anchored proteins, confluent N2a cells were washed once with PBS. PIPLC (GLYKO) was diluted in serum-free OPTIMEM to a final concentration of 250 mU/ml and added to the culture. Cells were incubated for 2 hours at 37°C, the media was then removed and cells were washed twice with PBS, before fixation in 4% PFA.

2.2 Yeast Physiology

2.2.1 Yeast strain phenotype

S. cerevisiae CDC25-2 cells were ura3, lys2, leu2, trp1, his200, ade2-101, cdc25-2 temperature sensitive. Cells were grown in YPD media at 25°C. Cells were routinely checked for the presence of revertants able to grow at the restrictive temperature of 36°C.

2.2.2 Standard yeast transformation

100 ml of yeast culture in mid-log-phase (OD_{600}=0.4) were spun at 3000 rpm for 5 minutes, washed once in 1 ml water, once in 1 ml of TEL buffer. Cells were resuspended in 1 ml of TEL (50 µl of cell suspension was found suitable for one transformation). DNA to be transformed was prepared in a separate tube (2 µg of vector in a final volume of 8 µl) and mixed with 2 µl of 10 mg /ml salmon sperm DNA, used as carrier, boiled for 5 minutes at 95°C and placed on ice for 5 minute. 50 µl of cell suspension were added to the DNA and gently mixed. 300 µl of TELP buffer were added, samples were vortexed strongly for about 10 seconds then incubated at 25°C for 4 hours. After incubation, heat shock was performed for 15 minutes at 42°C, the tube was spun at room temperature for 2 minutes at 6000 rpm, the supernatant was aspirated and the pellet was resuspended in 1 ml 1 M Sorbitol. 100 µl were plated, and remaining cells were spun down again and resuspended in 100 µl 1 M Sorbitol and plated. Plasmid DNA containing the suitable auxotrophy marker (LEU2 or URA3) allowed selecting transformant in defined synthetic media on the base of nutritional requirements. Plates were incubated at 25°C and colonies were visible after 2-3 days.

2.2.3 Yeast extracts

50 ml of S. cerevisiae culture was grown in the appropriate selection media until OD_{600}=0.5 (5 x 10^8 cells), and centrifuged in Falcon tubes at 3000 rpm for 5 minutes. The pellet was resuspended in 3 ml of buffer A and incubated for 10 minutes at room temperature. After spinning down at 2000 rpm for 2 minutes, the supernatant was aspirated, the pellet resuspended in 2 ml of buffer B and transferred to a 2 ml eppendorf tube. 4 µl of 20 mg/ml Zymolase T-100 solution was added and the sample was

incubated for 10 min at 37°C in a water bath. All the following steps were performed in cold room. Tubes were spun for 1 minute at 4000 rpm; the pellet was washed once in 1 ml of ice cold buffer C, spun 1 min at 4000 rpm and an equal volume of buffer EB was added to the pellet (5 x 10^8 cells yield 80-100 µl pellet). Triton X-100 was then added to a final concentration of 0.25% and cells were lysed on ice for 3 min with occasional vortexing. This resulted in the production of a whole cell extract. In order to separate soluble and insoluble fractions, an additional centrifugation step was performed (10 minutes at 13000 rpm): the supernatant was the soluble fraction and the pellet was the detergent insoluble fraction. The pellet was resuspended in 100 µl of EB buffer.

2.2.4 Library subcloning for rRRS

The original RRS full brain mouse library was a generous gift from Dr Ami Aronheim. In order to perform the screen using the rRRS approach, the whole library was subcloned into the pYESRas(61)ΔF plasmid using the restriction enzymes EcoRI and XhoI.

2.2.5 cDNA library transformation

The above described standard yeast transfection protocol was modified as follows: 1.6 litres of CDC-2 yeast, previously transformed with the plasmid encodying Myr-PrP23-230 as bait, were grown until OD_{600}= 0.4. Cells were washed once in water and once in TEL. A total amount of 160 µg of library DNA was mixed with 120 µl of 10 mg /ml salmon sperm DNA. Yeast were finally plated on 44 plates (YNB/Glucose, - Leu, -Ura) and incubated at 25°C. As negative controls, cells transfected only with the bait or empty pYESRas vector were plated at 36°C. These controls allowed the detection of the presence of revertant or possible contamination during the transfection procedure.

2.2.6 Library screen

Colonies (1 x 10^5) appeared 4-5 days after library transformation. Plates were replica plated on two different YNB/Galactose plates, either with or without methionine. Both sets of plates were incubated at 36°C for an additional 5-7 days. Thereafter, colonies that exhibited efficient growth only on the plate lacking methionine, as compared to the

twin plate containing methionine, were picked to a YNB/Glucose plate lacking ura and leu, using a grid. Candidates were allowed to grow for 2-3 days at 25°C before undergoing an additional replica plating step and being tested a second time for methionine dependent growth. Only colonies which passed both tests were processed for DNA extraction.

2.2.7 Plasmid DNA extraction

Candidate clones were picked and grown overnight in 5 ml YNB media lacking ura. The following day, yeast cells were centrifuged and the pellet washed once in water before resuspension in 100 µl of STET Buffer; 0.2 g of 0.45 mm glass beads (Sigma) were then added and the samples were vortexed vigorously for 10-15 minutes; following the addition of another 100 µl of STET Buffer, samples were boiled at 95°C for 10 min and let cooled on ice. An aliquot of 100 µl was transfered to a new tube, mixed with 50 µl of 7.5 M Ammonium Acetate, incubated for 1 hour at –20°C and centrifuged at full speed. 100 µl of supernatant were placed in a new tube and DNA was precipitated with 200 µl of ice cold 100% Ethanol. After 10 min of refrigerated centrifugation, pellet was washed once with 70% Ethanol and finally resuspended in 20 µl of water. 1 µl was used to transform chemically competent bacteria. Transformation reactions were plated on Ampicillin plates and allow growing overnight. Single colonies were picked and expanded by miniprep. DNA was compared to bait by EcoRI-XhoI restriction digestion.

2.2.8 Candidate identification

Inserts were excised by enzymatic digestion (EcoRI-XhoI) and subcloned into the pGEX vector. Standard sequencing reactions were performed using the following primers:

Forward 5' ggg ctg gca agc cac gtt tgg tg 3'

Reverse 5' ccg gga gct gca tgt gtc aga gg 3'

The resulting sequences were submitted to the BLAST server.

2.2.9 Solutions and Media

YPD MEDIA
Yeast extracts 1.1% w/v
Bacto Peptone 2.2%
D-Glucose 2%
Bacto Agar >20g/500ml

YNB/GALACTOSE MEDIA
Yeast Nitrogen Base 0.32%
Ammonium Sulfate 2.5 g
Galactose 15 g
D-Raffinose 10 g
Glycerol 10 g
Bacto Agar >20g/500ml

YNB/GLUCOSE MEDIA
Yeast Nitrogen Base 0.85g
Ammonium Sulfate 2.5 g
Glucose 10 g
Bacto Agar >20g/500ml

All amino acid solutions were obtained from Sigma. 5 mg/ml stock solutions were prepared - with the exception of methionine which was 20 mg/ml in order to obtain efficient repression of bait expression – and stored at 4°C. All stock solutions were diluted 1:100 before use.

YEAST BUFFER A:
100 mM PIPES/KOH pH9.3
10 mM DTT
0.1% Na-Azide

YEAST BUFFER B

50 mM Kpi pH 7.4
0.6 M Sorbitol
10 mM DTT

YEAST BUFFER C
50 mM HEPES/KOH pH 7.5
100 mM KCl
2.5 mM MgCl
0.4 M Sorbitol

EB BUFFER
50 mM HEPES/KOH pH 7.5
100 mM KCl
2.5 mM MgCl2
1 mM DTT
Protease inhibitor cocktail

TEL BUFFER
10 mM TRIS/HCl pH 7.5
0.1 mM EDTA
100 mM Lithiun Acetate

TELP BUFFER
10% 10X TEL
10% H2O
80% of 50% PEG solution

STET BUFFER
8% Sucrose
50 mM TRIS pH 8.0
50 mM EDTA
5% TRITON X-100

2.3 Molecular Biology

2.3.1 PrP constructs

Bait generation for the Ras Recruitment System

The murine PrP open reading frame, encompassing residues 23 to 230, was amplified by PCR using as a template the previously described Half genomic PrP plasmid (Fischer et al., 1996) and cloned into pYES2 plasmid containing an active form of Ras (amino acids 2-185) lacking its C-terminal CAAX box by BamHI-NotI restriction digestion. Following the above cloning step, the Ras-PrP fusion was subsequently subcloned into pMet25 by HindIII-NotI digestion. Since the original pMet vector contained only a HindIII site in the multiple cloning sites but not a NotI site, a pMet25-M-Chp plasmid was used as backbone, since it provided a unique NotI site at the 3' end of the Chp.
Forward: 5'a ccc ggatcc atg aaa aag cgg cca aag cct gga ggg tgg aac acc 3'
Reverse: 5'aat aat gcggccgc tca ggatct tct ccc gtc gta ata ggc ctg gg 3'
All primers used in this work were manufactured by Sigma-Genosys.

Bait generation for the reverse Ras Recruitment System

PrP23-230 was amplified by PCR using the following primers:
Forward: 5'a ccc aagctt atg aaa aag cgg cca aag cct gga ggg tgg aac acc 3'
Reverse: 5'aat aat gcggccgc tca ggatct tct ccc gtc gta ata ggc ctg gg 3'
For the myristoylated version, an alternative forward primer containing the vSrc signal was used: 5'a ccc aagctt atg *ggg agc agc aag agc aag ccc aag gac ccc agc cag cgc* aaa aag cgg cca aag cct gga ggg tgg 3'
Following enzymatic digestion by HindIII-NotI, the fragments were inserted into the pYEplac181 plasmid, previously modified with a Met3 promoter, chosen for its higher regulation stringency compared to the Met25.

GFP-PrP fusion constructs

Fusions between the green fluorescence protein (GFP) and PrP wild type, ΔE, ΔF and ΔSP were a generous gift from Dr Vilma R. Martins and have been previously fully characterised (Lee et al., 2001b).

Full length PrP

Full length PrP was provided by Prof A. Negro and Dr C. Sorgato (Massimino et al., 2004).

Endocytosis impaired PrP mutant

The 3F4 mouse PrP construct and the NGAG mutant were kindly provided by Professor Roger Morris (Sunyach et al., 2003).

2.3.2 PIP7 constructs

Full length PIP7

The pBK hnRNP M4 construct was kindly provided by Dr. O. Bajenova and Professor P. Thomas and has been previously described (Bajenova et al., 2003; Bajenova et al., 2001).

PIP7 fusion constructs

The PIP7 fragment was excised from the library vector by EcoRI-XhoI enzymatic digestion and subcloned in pGEX. To generate constructs expressing exclusively the Tandem Repeat region or the RRM3 domain fused either to GFP or GST, polymerase chain reaction was performed using pGEX-PIP7 as template in combination with the following primers:

Tandem Repeats:

Forward: taa taa aga att cag gag cgc atg ggc gca ggc tta gg

Reverse: taa tcg gaa ttc tta ggc ctt cct ggc tac tcc agg tgc

RRM3:

Forward: taa taa aga att cag ggt gga gcc gga ggt gct agc

Reverse: taa tcg gaa ttc tta agc att tct atc aat tcg aac atc

Amplification products were cloned in the EcoRI site of pEGFP-C3 vector (Clontech) or pGEX (Amersham-Biosciences) to generate GFP and GST fusions respectively.

2.3.3 Miscellaneous constructs:

The GFP-GPI plasmid was kindly provided by Dr. Chiara Zurzolo.

2.3.4 Cloning

2.3.4.1 DNA restriction digestion

One unit of restriction enzyme digests 1 µg DNA in one hour at 37 °C. Restriction digests contained 2 µg DNA, 2 µl 10X recommended buffer and 5 units of restriction endonuclease (NEB). Water was added to 20 µl. After 2 hours at 37 °C the reactions were stopped with 5 µl loading buffer and loaded onto an agarose gel.

2.3.4.2 Gel electrophoresis for separation of DNA fragments

Agarose gel electrophoresis was carried out in horizontal gel chambers. Depending on the size of the DNA fragments agarose concentrations between 0.8% and 2 % were used. The agarose was dissolved in 1X TAE Buffer (w/v) in a microwave and ethidiumbromide was added to a final concentration of 10 µl/g agarose. The gel was poured into a gel chamber and left to polymerise. DNA fragments were loaded in the wells and separated at voltages between 60 and 125V depending on gel size and percentage. Bands were visualized by a UV transilluminator.

2.3.4.3 Purification of DNA fragments with a GFX PCR DNA and Gel Band Purification Kit

The band of interest was cut out from the gel with a sterile scalpel, transferred to an eppendorf tube and 500 µl of Capture buffer were added and the tube was incubated at 60°C until the agarose was completely dissolved. For purification of PCR products, instead, 300 µl of Capture buffer were added. All following steps are the same for PCR products and purifcation from agarose gels. The sample was then transferred to a GFX column and incubated for one minute at room temperature. Afterwards it was centrifuged for 30 seconds at 13000 rpm in a microcentrifuge. The flow-through was discarded and the column washed with 500 µl of wash buffer and centrifuged again at 14000 rpm for 30 seconds. Finally the GFX column was transferred to an eppendorf

tube and the DNA was eluted by spinning 50 µl water through the column at 13000 rpm for 1 min.

2.3.4.4 Dephosphorylation of Vector DNA

To avoid possible religation of vector DNA the the 5'-ends of the purified digested vectors were dephosphorylated with 1 µl alkaline phosphatase , 2 µl of NEB 3 buffer in a final volume of 20 µl for 1 hour at 37 degrees. Dephosphorylated DNA was subsequently purified on a DNA purification column.

2.3.4.5 Ligation of DNA fragments

Ligations were carried out overnight at 16°C. For each reaction 1 µl of T4 ligase, 2 µl T4-ligase buffer and vector and insert DNA in a ratio of 3:1 were used in the final volume of 20 µl.

2.3.4.6. Preparation of chemically competent E. coli

Bacteria were allowed to grow overnight in 5 ml of LB media at 37°C with vigorous shaking. The following day 2 ml were used to inoculate 500 ml of LB media and the bacterial culture was allowed to reach OD_{600}=0.5. The culture was then divided into two sterile centrifuge beakers and incubated on ice for 30 minutes, before spinning 12 minutes at 2500 rpm. Supernatant was discarded and each pellet was resuspended in 20 ml RF-1 buffer and transfered to a 50 ml Falcon tube. After 15 minutes on ice, cells were spun for 12 minutes at 2500 rpm, the supernatant discarded and each pellet resuspended in 3.5 ml of RF-2 Buffer. Aliquots were immediately stored at –80°C. All operations were performed in sterile conditions and using sterile equipment.

2.3.4.7 Transformation of E. coli

An aliquot of 100 µl competent XL-1 Blue cells was thawed on ice and mixed with 0.5 µg DNA. The mixture was incubated on ice for 30 minutes, heated to 42°C for 1 minute and transferred back on ice for further 5–10 minutes. 500 µl of LB were added and the transformation mixture was incubated for 1 hour at 37°C. 150- 200 µl were spread on a

plate containing the appropriate antibiotic (Ampicillin or Kanamycin 100µg/ml) and incubated overnight at 37 °C.

2.3.4.8 Isolation of Plasmid DNA with Qiaprep Spin Miniprep Kit

5 ml of an overnight bacterial culture were centrifuged for 5 min at 3500 rpm and the supernatant discarded. The pellet was resuspended in 250 µl of buffer P1 and 250 µl of buffer P2 (lysis buffer) and incubated for 5 min at room temperature to allow lysis. The reaction was stopped with 350 µl of neutralization buffer N3 and the solution was spun for 10 min at 13000 rpm in a microcentrifuge. The supernatant was applied to the column for binding of the DNA, centrifuged for 1 min at 13000rpm and washed with 250 µl buffer PE and recentrifuged. After discarding the flow through the columns were centrifuged again to remove the last remaining wash buffer. The column was then placed into an eppendorf tube and 50 µl of H_2O were added. For the elution of the DNA the columns were centrifuged at 13000 rpm for 1 min again and the eluted DNA was stored at -20°C.

2.3.4.9 Isolation of Plasmid DNA in a preparative scale with Qiagen Maxiprep Kit

Bacteria containing the plasmid of interest were cultured overnight in 200 ml and harvested by centrifugation for 15 min at 3500 rpm. The pellet was resuspended in 10 ml buffer P1 and 10 ml buffer P2 were added for alkaline bacterial lysis and the sample was incubated for 10 min at room temperature. After lysis the reaction was neutralized with 10 ml of chilled buffer P3, incubated on ice for 20 min and centrifuged for 30 min at 4000 rpm. The supernatant was applied to columns which had been equilibrated with 10 ml buffer QBT. The DNA bound to the column was washed twice with 30 ml buffer QC and finally eluted by applying 15 ml elution buffer QF. The DNA was precipitated with 10.5 ml isopropanol and the tube centrifuged for 30 min at 15000 g. The DNA pellet was dried and diluted in a suitable volume of H_2O to achieve a final concentration of 1 µg/µl.

2.3.4.10 DNA isolation from mouse tail biopsy

500 µl of Tail Buffer were added to a 5 mm tail biopsy and incubated overnight at 55°C. The sample was placed on Eppendorf Mixer for 5 minutes. Following addition of 250 µl of 5M NaCl, samples were mixed for further 5 minutes and spun for 10 minutes full speed on a bench centrifuge. 500 µl of supernatant were transferred to a new tube and mixed with an equal volume of isopropanol. In order to precipitate the DNA, tubes were centrifuged for 10 minutes at full speed and the pellet, once washed with 70% Ethanol, was resuspended in 200 µl H_20. 1-2 µl were used for each genotyping reaction.

2.3.4.11 Genotyping mouse genomic DNA by PCR

LacZ primers were used for genotyping the XE413 and NPX275 mice.
Forward CGT CAC ACT ACG TCT GAA CG
Reverse CGA CCA GAT GAT CAC ACT CG
The product was a band of 500 bp.

2.3.4.12 DNA sequencing

For a typical sequencing reaction: 8 µl of BDT v3.1 (BigDye terminator kit from Applied Biosystems UK, shipped stock was diluted 1:16), 3.2 pmoles of primer, 200 ng DNA, water up to a final volume of 20 µl.
The reaction was placed in a thermal cycler and the following program was performed:
STEP1 go to 96°C (2.5°/sec)
STEP2 denaturation 96°C for 1.00 minute
STEP3 denaturation 96°C for 10 seconds
STEP4 go to annealing temp (1.0°/sec)
STEP5 annealing (temperature varied according to the primer melting temperature)
STEP6 go to extension temp 60°C (1.0°/sec)
STEP7 annealing 60°C for 4.00 minutes
STEP8 Cycling go to STEP3 X 24
STEP9 cooling 4°C forever
Reactions were purified using DyeEx Spin Columns (QIAGEN). DNA sequencing was performed on an Applied Biosystems 3730 DNA Analyser, a capillary sequencing platform.

2.3.4.13 Solutions

DNA Loading buffer:
50 mM Bromophenolblue
1 mM EDTA (pH 8.0)
50 % (w/v) Glycerol

50X TAE buffer:
242 g Tris
57.1 ml glacial Acetic acid
100 ml 0.5M EDTA
H_20 up to 1 litre (final pH 7.8)

LB-Medium:
10 g NaCl
10 g tryptone
5 g yeast extract
pH adjusted to pH 7.4 with NaOH
H_20 to 1 litre

LB-Agar:
LB Medium as above described
20 g Agar before autoclaving

RF-1 Buffer:
12 g Rubidium-chloride
9 g Manganese-chloride x $2H_2O$
2.94 g Potassium-Acetate
1.5 g Calcium-chloride x $2H_2O$
150 g Glycerol
pH adjusted to 5.8 with Acetic Acid.
H_2O up to 1 litre

RF-2 Buffer:

2.09 g MOPS

1.2 g Rubidium Chloride

11.0 g Calcium-chloride x 2H2O

150 g Glycerol

pH adjusted to 6.8 with Sodium-Hydroxide

H_2O to 1 litre

RF-1 and RF-2 solutions were passed through a 0.22 μ filter and stored at 4°C.

2.4 Production of mouse monoclonal antibodies

All procedures described below have been performed by the CRUK Antibody Unit.

2.4.1 Immunisation Schedule

Recombinant GST-PIP7 fusion protein was produced as described in section 2.X. In order to generate PIP7 specific antibodies, GST was removed by digestion with Thrombin protease according to the manufacturer instruction. 20 μg of antigen were injected as immunogen per animal. Each injection volume did not exceed 0.1 ml at each of the 2 sites/mouse. All injections were made subcutaneously. A total of 4 Cd-1 females (HARLAN) were immunised according the following schedule:

DAY	OPERATION
0	Pre-bleed and Primary immunisation in Complete Freunds
21	First boost in Incomplete Freunds
31	First test bleed
49	Second boost in Incomplete Freunds
59	Second test bleed

77	Third boost in Incomplete Freunds
87	Final Bleed

All test bleeds were analyzed by Western Blot and ELISA confirming the mounting immune response and positive mice were identified.

2.4.2 Splenocytes isolation

The spleen was aseptically removed and placed into a 10 cm^2 tissue culture dish containing 10 ml of pre-warmed DMEM medium with no serum. Any possible contamination by connective tissue was trimmed off and discarded. Using sterile scissors, several small holes were cut in the spleen. Using a 1.0 ml syringe and a 19 gauge needle, media was aspirated and flushed inside the spleen until most of the cells were released into the dish. Any cell clumps were disrupted by pipetting. Cells were then transferred to a sterile centrifuge tube. The culture dish was washed once with an additional 10 ml of pre-warmed medium lacking serum which was passed once through a 0.2 micron filter and combined with the first 10 ml. Cell clumps were allowed to attach and the supernatant, containing the splenocytes, was transfered to a fresh tube.

2.4.3 Splenocytes fusion

Splenocytes were washed twice in serum-free DMEM and spun at 400 g. 20 ml of mouse myeloma cells were washed once and combined with the splenocytes solution. After a further centrifugation step at 800 g for 5 minutes, the medium was removed and the pellet was resuspended in 0.5 ml of 50% PEG solution in medium. PEG was slowly added to the pellet while cells were resuspended by gentle stirring with a pipette. Cells were allowed to rest for a minute. A 10 ml pipette was filled with pre-warmed media lacking serum and 1 ml was added to the cell suspension during the subsequent minute with continuous stirring. After the addition of the remaining 9 ml, cells were centrifuged at 400 g for 5 minutes. After discarding the supernatant, cells were resuspended into 10 ml of medium supplemented with 20% FCS and 1X Azaserine Hypoxantine (final

working concentration 5.7 μM Azaserine, 100 μM Hypoxanthine). The cell suspension was mixed with 100 ml of the same medium: 100 μl cells were aliquoted in 10 wells of a 96 well plate and placed in a 37°C incubator. Clones were visible after 4-5 day.

2.4.4 ELISA

Antigen specific ELISA

The following procedure was used to screen test bleeds and hybridoma clones.

Plates were coated with the antigen used for immunisation (C-terminal portion of PIP7) at a final concentration of 3 μg/ml in PBS and left overnight at 4°C. The next day, ELISA plates were washed once with PBS-T and rinsed 5 times with sterile water. To avoid non specific binding, plates were incubated overnight at 4°C with 20% w/v non fat dry milk in PBS. The following day, the blocking solution was removed and wells were washed once with sterile water. For test bleeds, 10 μl was added to the first well and serial dilutions were made. For hybridoma fusion, 90 μl of cell supernatants were used. The plates were incubated overnight at 4°C or, alternatively, for 2 hours at room temperature. Supernatant/bleed was removed and the following washes were performed: 1X PBS-T, 5X water. Anti-mouse secondary antibody, HRP conjugated, was diluted 1:2000 in PBS-T and incubated on the plates for 1 hour at room temperature. 3 washing steps in PBS-T were finally performed. For the detection, the OPD peroxidase substrate (Sigma) was used according to the manufacturer's guidelines. Briefly, one urea tablet was mixed with 20 ml of water and once fully dissolved an OPD hydrogen peroxide tablet was added. 75 μl of the resulting solution was added to each well. Reactions were stopped by adding 50 μl of 2 M HCl. Plates were read using a microplate reader set to 490 nm.

Subclassing ELISA

Positive clones were transferred from a 96 to a 24 well plate containing DMEM/20% FCS and IL6. After one week, the supernatant was tested in order to determine the antibody subclass. Affinity purified anti subclass antibodies were kept as stock solutions at 1 mg/ml and diluted to 5 μg/ml in PBS prior to use. Aliquots of 50 μl of the diluted anti subclass antibody were added to each well overnight at 4°C. The next day, plates

were washed 3 times with PBS and blocked with 200 µl 2% non fat dry milk in PBS for 2 hours. A final wash with PBS-T was performed at the end of the blocking step. 50 µl of test sample were taken from hybridoma culture and added in duplicate into each well containing the different antibody subclasses and incubated for 2 hours at room temperature. Three washes with PBS-T were performed before the addition of 50 µl of 1:1000 dilution of goat anti-mouse Fab-peroxidase conjugated in PBS-T. Plates were incubated for 2 hours at room temperature and washed three times in PBS-T. Substrate for detection was prepared as described for the standard ELISA protocol. Photographs of the plate were taken using a Polaroid camera. The procedure was repeated at least once in order to have unambiguous result.

2.4.5 Antibody purification

2.4.5.1 Purification of Mouse IgG1 antibody

2 litres of filtered supernatant were buffered with 1 litre of 3M Ammonium Sulphate pH 9.0; the final pH was adjusted to 9.0 with 10 M NaOH before loading onto a 25 ml Protein A column (5ml/minute). Bound antibodies were eluted with 0.1M Citrate pH 4.0; after elution, the solution was immediately neutralized using 10 M NaOH and antibodies were desalted in PBS.

2.4.5.2 Purification of Mouse IgG3 antibody

1 litre of filtered supernatant was buffered with 100 ml of 1M TRIS pH 8.0; the final pH was carefully adjusted to 8.0 with 10M NaOH before loading on a 25 ml Protein A column (5ml/minute). Bound antibodies were eluted with Gentle Elution Buffer (PIERCE); antibodies were first desalted in 0.1M TRIS and subsequently in PBS.

2.4.5.3 Desalting Purified Antibody

A G25 (Amersham) column was equilibrated with 4 volumes of PBS before applying the purified Ab solution. The column was loaded with antibody solution (20% column volume) and elution was obtained by the addition of 1 volume of PBS.

2.4.5.4 Antibody storage

All antibodies were sterile filtered and stored at 4°C. For long term storage, aliquots were frozen at –80°C.

2.5 Protein Biochemistry

2.5.1 Protein preparations

Cell lysate

Growth media was removed and cells were washed once in PBS. Cells were lysed directly on the plate by addiction of Lysis Buffer (500µl/10 cm dish). Total lysate was transferred to an eppendorf tube and left on ice for 10 minutes. Lysate was spun at 1000 g for 5 minutes in a refrigerated bench centrifuge, in order to eliminate the cell debris. Protein concentrations were determined by Bradford assay.

Total brain homogenate

Mouse brains, from mice older than 2 months of age, were mechanically homogenized in PBS in order to obtain a 10% w/v preparation. The solution was then subjected to a centrifugation step of 5 minutes at 1000 g in a refrigerated centrifuge. Protein concentrations were determined by Bradford assay.

Brain membrane enrichment protocol

Total mouse brain was homogenized in Buffer A with a teflon/glass potter (20 strokes) to reach a final concentration of 40 mg/ml. The homogenized tissue was centrifuged at 1000 g for 5 min. The supernatant was collected, transferred to a new tube and centrifuged at full speed for 15 min. The pellet containing a crude membrane fraction was resuspended in Buffer A. Bradford assay was performed to estimate the protein concentration.

2.5.2 Bradford assay

Protein concentrations were determined using the Bio-Rad Protein Assay, based on absorbance shift in Coomassie Brilliant Blue G-250 (CBBG) when bound to arginine and aromatic residues. The anionic (bound form) has a maximum absorbance at 595 nm whereas the cationic form (unbound form) has an absorbance maximum at 470 nm. The 5X stock solution was diluted in H_2O and 1 ml was aliquoted in polystyrene cuvettes of 1 cm path lenght. 2 µl of protein lysate was dissolved in each cuvette. Concentrations were obtained by linear interpolation with a calibration curve of known concentrations, prepared using bovine albumin as a standard.

2.5.3 Production of recombinat GST fusion proteins

pGEX plasmids containing the PIP7 cDNAs were trasformed in E. coli; a single colony was picked and inoculated in 100 ml of LB/Ampicillin and allowed to grow overnight at 37°C. The next day, the culture was diluted 1:10 in fresh LB/Ampicillin and allowed to grow until OD_{600}=0.5. At this step, one aliquot of uninduced bacteria was taken for later analysis. In order to stimulate recombinat protein production, IPTG was added to a final concentration of 0.4 mM. Bacteria were allowed to grow for an additional 4 hours with vigorous shaking at 30°C. The culture was spun down at 5000 rpm for 10 minutes at 4°C.

All the following steps were performed in cold room: the bacterial pellet was resuspended in 10 ml of NETN buffer. Lysozyme was added at the final concentration of 100 µg/ml and bacteria were incubated on ice for 30 minutes with occasional mixing. The solution was then sonicated with 10-20 pulses (power 50%, duty 50%) and spun at 10000 g for 10 minutes at 4°C. The supernatant contained the total bacterial lysate.

2.5.4 Purification or recombinant proteins

In order to purify recombinant fusion proteins from the whole bacterial lysate, the supernatant was incubated with glutatione sepharose beads (Amersham Biosciences) for 1 hour at 4°C (1 µl of dry beads binds 5-10 µg of GST). Beads were washed 3 times with NETN buffer and bound proteins were eluted by adding a freshly prepared solution of glutathione (20 mM in 100 mM TRIS pH8, 120 mM NaCl). Several small elutions were found to be more efficient than a single elution step. Beads were rotated for 10

minutes at 4°C per elution. Supernatant pools were dialyzed in PBS for 24 hours in order to remove excess glutatione. For long term storage, glycerol was added to 10% final volume and samples were stored at –20°C.

2.5.5 GTS pull down assaye

50 µg of purified GST-fusion protein were coupled to 30 µl of glutathione sepharose beads and rocked at 4°C for 2-3 hours. Beads were washed three times in NETN buffer and incubated overnight at 4°C with 1.2 mg of 10% (w/v) mouse brain homogenate diluted in IP buffer of the specified pH. The following day, beads were washed three times in IP buffer, resuspended in sample buffer and processed by Western blot.

2.5.6 Protease K digestion

A stock solution of 40 mg/ml Protease K (Sigma) was made and stored in 100 µl aliquots at –20°C. Digestion reactions were performed at the final specified concentration of 50 µg/ml for brain homogenate and 30 µg/ml for mammalian cell lysate, 5 µg/ml for yeast lysate. When Protease K digestion was performed after a GST pull down experiment, 100 µl of *Prnp*$^{-/-}$ brain homogenate (1.5 mg/ml) was added in order to avoid overdigestion. If not otherwise specified, digestion reactions were performed at 37°C for 1 hour in a thermomixer. Digestions were terminated by addition of PMSF (2mM final) and incubation on ice (30 minutes), before addition of the SDS sample buffer.

2.5.7 Immunoprecipitation

1 mg of total brain homogenate or N2a cell lysate was diluted in a final volume of 1 ml with IP Buffer. 10 µg of antibody were added and the tube was placed with gentle rocking at 4°C for 4 hours or overnight. At the end of the incubation step, 20 µl of sheep anti-mouse magnetic beads (DYNAL) were added per reaction and further incubated for 2 hours at 4°C. Beads were finally washed three times in IP Buffer (1 ml/wash) before addition of 30 µl of sample buffer. Samples were boiled for 10 minutes at 95°C and processed according the standard Western Blot protocol.

2.5.8 SDS-PAGE

SDS-PAGE was performed on 1.5 mm Biorad mini gels or 1.5 mm Biorad vertical gels. Table 2.1 shows the composition of the resolving gel for either 2 small gels (left column) or 1 big gel (right column). The percentage of the resolving gels is given in the head of the table. According to the molecular weight of the protein of interest, 8% to 15% polyacrylamide gels were used. The resolving gel was overlaid with isopropanol to ensure a smooth gel interface. Before adding the stacking gel, the isopropanol was removed and the gel surface rinsed with water. Table 2.2 shows the compositon of the stacking gel. TEMED and APS cause were added immediately prior before pouring the gel.

Table 2.1 Composition of resolving gel for SDS-PAGE and required volume of TEMED and APS. The volume of TEMED and APS is independent of the gel-percentage and therefore given only once for each size of gel.

Percentage	8%		10%		12%		15%	
Buffer1 (ml)	3.75	7.5	3.75	7.5	3.75	7.5	3.75	7.5
AcrylBis	3	6	3.75	7.5	4.5	9	5.6	11.2
H_2O	8.25	16.5	7.5	15	6.75	13.5	6.7	11.4
TEMED	25µl (small) 50µl (large)							
APS	75µl (small) 150µl (large)							

After pouring the stacking gel the comb was inserted immediately and the gel was left for polymerisation. The comb was removed from the polymerised gel and the slots were rinsed with water. To obtain an even loading of samples, the required amount of sample was added to 4X sample buffer and filled up to the final volume with lysis buffer. The solution was boiled at 95°C for 5 min and then loaded onto the gel. As a standard for the molecular weight a prestained marker (New England Biolabs) was used. Gel electrophoresis was performed in a gel tank filled with 1X Running Buffer and under the constant amperage of 45 mA for 2-3 hrs. Total proteins were transferred to a nitrocellulose membrane (Schleicher and Schuell) using semi-dry apparatus (SemiPhor, HOEFER) for 1 hour applying a current of 0.8 mA/cm^2 of membrane.

Table 2.2 Composition of stacking-gel for SDS-PAGE

	Small	Big
Buffer2 (ml)	2	4
AcrylBis	0.6	1.2
H_2O	5.4	10.8
TEMED	25µl	50µl
APS	75µl	150µl

2.5.9 Western blot

After transfer from the gel to the membrane the transfer efficiency was confirmed by staining all proteins with Ponceau red (Sigma). The membrane was incubated 5 min in the Ponceau solution. The excess of Ponceau was rinsed away with water and the membrane was blocked in blocking buffer on a shaker for 1 hour at room temperature or at 4°C overnight to avoid unspecific binding of the antibodies. The membrane was subsequently incubated with the primary antibody against the protein of interest for 1 hour at room temperature. All primary antibodies (1 mg/ml) were diluted 1:1000 in blocking buffer. Following the incubation with the primary antibody the membrane was washed 3 times for 10 min each at room temperature in washing buffer to remove unbound antibody. The secondary antibody was chosen depending on the nature of the primary antibody. For mouse monoclonal primary antibodies the secondary one was a peroxidase conjugated anti-mouse IgG, for rabbit polyclonal antibodies the secondary antibody was a peroxidase-conjugated anti-rabbit-IgG. Both secondary antibodies (Sigma) were used in dilution of 1:3000 in blocking buffer and the membranes were incubated for 30 min at room temperature. Blots were washed 3 times in washing buffer as described above and proteins were visualized using an ECL kit (Amersham-Pharmacia) according to manufacturers' instruction: the two solutions of the kit were mixed in 1:1 ratio and the membrane was incubated for 1 min in the solution. Different exposures were taken using Kodak MBX autoradiography films and an automatic fixer/developer (IGP $Compact_2$).

2.5.10 Buffers and Solutions

Lysis Buffer:
150 mM NaCl
25 mM Tris pH8
0.5% TRITON X-100
0.5% DOC
Protease inhibitors

IP Buffer:
150 mM NaCl
0.5% NP-40
Either 50 mM Tris / MOPS / Na-Acetate
pH adjusted as required by the experiment.
Protease inhibitors

NETN buffer:
100 mM Nacl
20 mM Tris pH8
1 mM EDTA
0.5% NP-40
Protease inhibitors

Buffer A:
0.32 M Sucrose
0.1 mM PMSF
1 mM MgCl2
10 mM Hepes
1 mM $NaHCO_3$
Protease inhibitors

PROTEIN GEL SAMPLE BUFFER (4X):

4 ml SDS 10%

1.6 ml Tris pH 6.8

2 ml glycerol

1.9 ml H2O

0.5 ml B-mercaptoethanol

Bromophenol blue

BUFFER 1

544.95 g Tris

pH adjusted to 8.8

H_2O up to 3 litres

Solution was autoclaved and stored at 4°C.

SDS was added to a final concentration of 0.4% before use.

BUFFER 2

181.65 g Tris

pH adjusted to 6.8

H_2O up to 3 litres

Solution was autoclaved and stored at 4°C.

SDS is added to a final concentration of 0.4% before use.

10X SDS-PAGE RUNNING BUFFER

240 g Tris

1120 g Glycine

200 ml SDS 20% solution

H_2O up to 8 litres

10X TRANSFER BUFFER:

29 g Glycine

58 g Tris-base

3.7 g SDS

H_2O up to 1 litre

1X TRANSFER BUFFER:
100 ml 10X transfer buffer
200 ml Methanol
700 ml H_2O

PBST
400ml PBS
400ml Tween20

WB BLOCKING BUFFER:
5% w/v non fat dry milk in PBST

2.6 Microscopy and Cell imaging techniques

2.6.1 FACS

Cell Fixation

Cells were washed once with ice cold PBS and resuspended by gentle pipetting in PBS. Cells were centrifuged at 900 rpm for 3 minutes at room temperature, supernatant was discarded and the pellet gently resuspended in 4% PFA/PBS and left on ice for 15 minutes for fixation. Cells were washed once in PBS and resuspended in 2 ml of FACS Buffer (2%FCS in endotoxin free PBS).

Antibody Staining

An aliquot of $0.5x10^6$ cells was transferred into FACS tubes (FALCON) for staining. When internal staining was performed, the FIX and PERM Kit was used (CALTAG Laboratories) following manufacturer's guidelines. Otherwise cells were incubated with 100 µl of primary antibody solution in FACS buffer (ICSM18 and different PIP7 antibodies were used at a final concentration of 10 µg/ml whereas undiluted hybridoma supernatant was used for TfR staining) on ice for 30 minutes. Cells were washed once in FACS buffer, spun at 900 rpm for 2 minutes and resuspended in 100 µl of labelled secondary antibody (10 µg/ml). Following an incubation step of 30 minutes on ice, the pellet was washed once and resuspended in 300 µl of FACS buffer.

Data acquisition and analysis

All samples were analysed with a FACS Calibur device. Forward and side scatter were adjusted in order to avoid collection of cell debris or cell clumps. Unless stated otherwise, 25000 events were collected for each sample. Statistical analysis was performed using the FLOJO software.

2.6.2 FRET

Antibody labelling

A prepacked aliquot of Cy3 monofunctional dye (Amersham Bioscience) was firstly dissolved in 20 µl of DMF. Four hundred and fifty µl of sterile filtered αPIP7 4G4 antibody (1mg/ml) were mixed with 50 µl Bicine (1 M, pH 8.0) in a small glass container covered in aluminium foil to protect from light exposure. The container was placed on a magnetic stirrer and the Cy3 solution was carefully added dropwise. The coupling reaction took approximately 1 hour at room temperature. To separate the labelled antibody from the free unincorporated dye, the reaction was run through on a 10 ml disposable chromatography column (BIORAD) according to the manufacturer's protocol. Briefly: the column was washed three times with PBS; the coupling reaction containing the Cy3-Ab was loaded on the column, followed by 3 ml of PBS. A fraction of 1.5 ml was collected in an eppendorf tube. Spectroscopic analysis was performed in order to determine the Dye/Antibody ratio. Labelled antibody was sterile filtered and kept at 4°C for a maximum of 2 weeks.

Immunofluorescence for FRET

The complete procedure was performed at room temperature. Mouse N2a cells were plated on glass coverslips and transfected with mouse GFP-PrP or with GFP as a negative control. 48 hours post transfection, cells were washed twice with PBS and fixed for 10 minutes with 4% PFA/PBS. After two additional washes in PBS, cells were permeabilised with a 0.2% TritonX100/PBS solution for 5 minutes. A fresh solution of 1mg/ml of Na-Borohydrate/PBS was then added and left for 5 minutes in order to quench any remaining PFA and any cellular autofluorescence. Two PBS washes were

performed before a blocking step of 5 minutes with a 1% BSA/PBS solution. Cells were incubated for 1 hour with the previously labelled α-PIP7-Cy3 antibody at the final concentration of 10 μg/ml. After 2 washes in PBS, coverslips were mounted using MOWIOL/DABCO and allowed to dry overnight at 37°C. Slides were stored at 4°C in the dark.

Fluorescence Resonance Energy Transfer (FRET) by Fluorescent Lifetime Imaging Microscopy (FLIM) in Frequency Domain

A detailed description of the FRET monitored by FLIM can be found elsewhere (Larijani et al., 2003). Lifetime detection was monitored in the frequency (phase) domain. Phase methods provide an average lifetime where sinusoidally modulated light is used to excite the sample. The measurement of the phase shift and the relative modulation depth of the emitted fluorescence compared to the excitation lead to the two lifetime values Tau-phase (τ_p) and Tau-modulation (τ_m). The average fluorescence lifetime, $< \tau >$, is defined by the average $(\tau_m+\tau_p)/2$. I monitor the decrease in lifetime of donor (EGFP) in the presence of the acceptor (Cy3 dye). All images were taken using a Zeiss Plan-APOCHROMAT 100x/1.4 numerical aperture, phase 3 oil objective, with images recorded at a modulation frequency of 80.218 MHz. GFP-PrP was excited using the 488 nm line of an Argon/Krypton laser and the resultant fluorescence separated using a dichroic beamsplitter (Q505 LP; Chroma Technology Corp.). FRET acquisition and analysis was performed by Dr Veronique Calleja, Cell Biophysics Laboratory, CRUK.

2.6.3 Immunofluorescence

PIP7 immunofluorescent staining

Cells were washed twice with PBS and fixed with 4% PFA for 10 minutes at room temperature. For nuclear PIP7 staining, cells were permeabilised with 0.5%Triton/PBS for 5 minutes whereas for surface labelling cells were left untreated. Cells were blocked with 10% FCS/PBS (supplemented with 0.1% Triton for nuclear labellings) for 30 minutes at room temperature prior to antibody incubation. All PIP7 antibodies were diluted to 10 μg/ml in the appropriate blocking solution for 1 hour at room temperature,

washed 3 x 5 minutes with block and incubated with Cy3 conjugated goat anti mouse IgG (H&L) for 30 minutes at room temperature in the dark. Cells were finally washed 3 x 5 minutes with PBS prior to nuclear staining with Dapi and mounting in Mowiol. Cells were visualised on a Zeiss Axioplan 2 upright microscope using AxioVision 4.1 imaging software. This experiment was performed in collaboration with Dr Nnennaya Kanu.

Confocal analysis of PrP-PIP7

Confocal analysis was performed by Dr Axel Behrens using a Zeiss Axioplan Upright 2 and Zeiss Axiovert 200 Inverted microscopes.

2.6.4 Immunohistochemistry

The described procedures were performed by the CRUK Histopathology Unit

2.6.4.1 Immunohistochemical staining on paraffin sections

Brain samples were fixed overnight in 10% NBF (100 ml 37% formaldehyde, 4 g NaH_2PO_4, 6.5 g Na_2HPO_4 in 1L H_2O) transferred into 70% Ethanol and embedded in paraffin block. Four microns sections were cut from each block and placed on glass charged slides. Slides were subjected to a standard de-waxing protocol as follows: 2 x 10 minutes in Xylene, 2 minutes sequentially in 100%, 95%, 90%, 80%, 70%, 50%, 25% ethanol and 5 minutes in PBS. After antigen retrieval (12 minutes in a microwave in 0.1M Sodium Citrate pH6), slides were blocked for 30 minutes. For PIP7 staining, the 4C2 antibody (1 mg/ml) was used at the final dilution 1:250 in combination with a mouse on mouse kit (DAKO ARK).

2.6.4.2 LacZ staining to monitor β-galactosidase activity

Brain samples from adult mice were fixed in LacZ fix solution (0.2% glutaraldehyde, 5mM EGTA, 2mM $MgCl_2$ in PBS) for 20 minutes. Following 3 washes of 5 minutes each in wash solution (2mM $MgCl_2$, 0.02% NP-40 in PBS), slides were incubated at 37°C in staining buffer (1 mg/ml X-Gal, 2.12 mg/ml Potassium Ferrocyanide, 1.64 mg/ml Potassium Ferrycianide dissolved in wash solution). Stainings were stopped by repetitive washes in PBS and samples were stored at 4°C.

2.7 Scrapie analysis

2.7.1 Scrapie Cell Assay

Five thousands chronically infected cells (iPK1 clone, a generous gift from Dr. Peter Klohn, MRC Prion Unit, London) were plated on a 96 wells plate in the presence of the different α-PIP7 monoclonal antibodies; α-PrP specific antibody ICSM18 and an isotype control were also included, in order to assess treatment specificity. After 4 days, cells were passaged at 1:8 dilutions and allowed to grow for 3 additional day, in the continuous presence of the antibodies. In order to establish the number of PrP^{Sc} positive cells, an aliquot of 1000 cells was supplemented with 24000 non infected cells and plated in each of 7 wells (containing 200 µl PBS) of an ELISPOT plate (Multi Screen Immobilon-P 96-well Filtration Plates, sterile, Millipore, previously activated with 70% ethanol) and washed twice with PBS by suction. After 1 hour at 50°C, 50 µl of PK (0.5 µg/ml) were added to each well, and incubated for 90 min at 37°C. The samples were washed with PBS, exposed to 2 mM PMSF for 10 min, and washed again with PBS. After incubation with 160 µl of 3 M guanidinium thiocyanate, 10 mM Tris·HCl (pH 8.0) for 10 min, the filters were washed four times with PBS and incubated with 160 µl of Superblock for 45 min. 50 µl ICSM18 (0.6 µg/ml, in TBST/1% non fat milk) was added; after 1 hour the supernatant was removed, and the wells were washed 7 times with TBST. 50 µl of alkaline phosphatase-conjugated anti-IgG1 (Southern Biotechnology Associates; 1:4,500 in TBST/1% milk powder) was added for 1 hour. Wells were washed 8 times with TBST, and 50 µl of alkaline phosphatase conjugate substrate (prepared as recommended by Bio-Rad) was added for 8 min and followed by 2 washes with water. Plates were stored in the dark at –20°C. PrP^{Sc}-positive cells were counted using the Zeiss KS ELISPOT system (Stemi 2000-C stereo microscope equipped with a Hitachi HV-C20A color camera and a KL 1500 LCD scanner and WELLSCAN software from Imaging Associates, Bicester, U.K.). The settings were optimized to give a maximal ratio of counts for PrP^{Sc}-positive samples relative to negative control samples, while keeping the sample counts as high as possible. The described procedure was performed by Dr. P. Klohn at the Institute of Neurology, London.

2.7.2 Neuronal Graft

Neuronal ectoderm was obtained from E13.5 embryos (derived from XE413 x NPX275 crosses). The detailed procedure has been described elsewhere (Behrens et al., 2001). Stereotactic injection of neuroectoderm was performed by Dr. Sebastian Brandner with the help of Heike Naumann at the MRC Prion Unit, London.

2.8 Reagents

2.8.1 Antibodies

Clone name	Antigen	Origin/Supplier
Primary Abs		
actin	actin	Sigma
PIP7 4C2	hnRNP M4	CRUK Monoclonal Service
PIP7 4G4	hnRNP M4	CRUK Monoclonal Service
PIP7 4G5	hnRNP M4	CRUK Monoclonal Service
PIP7 5H1	hnRNP M4	CRUK Monoclonal Service
PIP7 1B8	hnRNP M4	CRUK Monoclonal Service
OX26	Transferrin Receptor	CRUK Monoclonal Service
HPC1	Syntaxin1	Molecular Neuro PathoBiology Lab CRUK
ICSM18	PrP	MRC Prion Unit

6H4	PrP	Prionics
Secondary Ab		
HRP goat anti Mouse	-	Sigma
APC Rat anti Mouse IgG_1	-	BD Pharmigen
R-PE Goat anti Mouse IgG_3	-	SouthernBiotec
Alexa 488 Goat anti Mouse IgG	-	Molecular Probes
Cy3 Goat anti Mouse IgG	-	Jackson Laboratories

Chapter 3: Identification of proteins interacting with misfolded PrP

3.1 INTRODUCTION

There is a wealth of evidence that the critical event in the occurrence of transmissible spongiform encephalopathies is the generation of PrP^{Sc}, described as the neuropathological isoform of the normally host encoded protein PrP^{C}. Its original isolation in association with infectivity, the cloning of the cognate cDNA and the finding that it is encoded by a host gene are just few of the milestones in modern prion biology (Basler et al., 1986; Bolton et al., 1982; Chesebro et al., 1985).

The transition appears to be mainly conformational since no differences in primary amino acids sequence or post-translational modification have been found. The two isoforms differ in both secondary structure and biochemical properties (Figure 3.1A). PrP^{C} is mainly composed of α helical structures, in contrast with the rich β content of the abnormal isoform (Caughey et al., 1991). PrP^{Sc} is insoluble in non-denaturing detergents and has the property to form highly ordered amyloid aggregates like fibrils and plaques. Moreover it is partially resistant to protease digestion whereas PrP^{C} is completely sensitive (McKinley et al., 1983). Protease K digestion has been extensively used in laboratory research to discriminate between the two species and, more importantly, it has proved one of the most valuable tools in the diagnosis of prion disease, such as BSE in cattle.

Different *in vitro* conditions have been established in order to confer to recombinant PrP some of the PrP^{Sc}-like properties, namely increased β sheet content, tendency to form aggregates and partial PK resistance (Jackson et al., 1999; Lee and Eisenberg, 2003). The transition from a predominantly α helical secondary structure to a β rich one is believed to be the first step in the conversion reaction and may proceed through one or more folding intermediates, called PrP^{β} (Swietnicki et al., 1997).

A)

Secondary structure	alpha	beta	beta
Protease K sensitivity	sensitive	partially resistant	resistant
Solubility	soluble	insoluble	insoluble
Aggregate formation	-	+	+
Infectivity	-	-/+	+++

B) **Working hypothesis:**

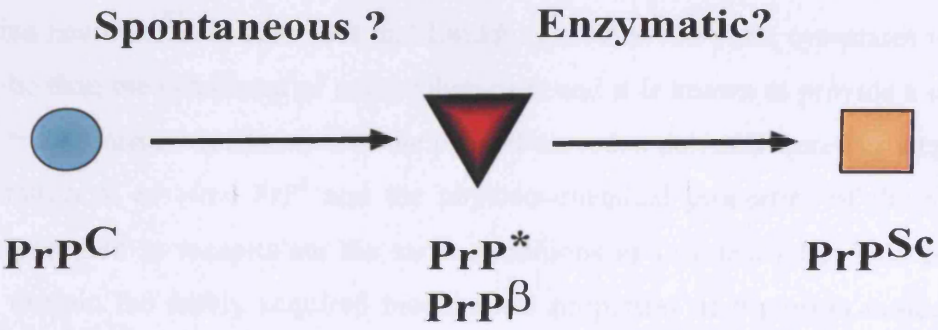

Figure 3.1 Alternative PrP conformations.
A) Secondary structure and biochemical features of different PrP isoforms. PrP^{C} denotes the cellular isoform of the prion protein characterised as being mainly composed of alpha helices, detergent soluble and sensitive to Protease K digestion. PrP^{Sc} is the abnormal, pathogenic isoform and is enriched in beta sheets, mainly detergent insoluble and resistant to limiting proteolysis. Many attempts to generate infectivity in vitro have successfully produced different PrP conformations, here summarised as PrP^{β}, exhibiting an increased content in β structures, increased insolubility and tendency to form aggregates. PrP* has been originally used to describe a metastable conformation of PrP^{C} when bound to Protein X (Cohen et al, 1994). B) According to my working hypothesis, misfolding of PrP^{C} is required in order to produce the structural rearrangement resulting in the generation of PrP^{Sc}. Such a process could require both spontaneous and enzymatic steps and the identification of binding proteins specific for intermediate conformations could be very valuable for therapeutic approaches.

The *in vivo* existence of PrP^{β} is mainly speculative but PrP^{β} could partially overlap with PrP^{*}, a metastable intermediate supposed to arise during the conversion from PrP^{C} to PrP^{Sc} (Cohen et al., 1994).

According to my current working hypothesis, the series of events resulting in the final appearance of PrP^{Sc} could in principle involve either spontaneous biophysical or enzymatic steps (Figure 3.1B).

In support of this idea, despite presenting many of the properties typical of PrP^{Sc}, none of the β isoforms produced *in vitro* has been shown so far to be infectious suggesting that some of the PrP^{Sc} properties could arise spontaneously *in vitro* by physico–chemical manipulation but possibly one or more unidentified auxiliary molecules are required to confer infectivity (Hill et al., 1999a). This hypothesis is supported by recent results obtained with the protein misfolding cyclic amplification (PMCA): successful *in vitro* amplification of infectivity has been achieved but only when complete brain homogenate is used (Castilla et al., 2005).

Recently, Linquist and colleagues have shown that PrP, when expressed in a heterologous system like the yeast cytoplasm, becomes detergent insoluble and partially PK resistant. The same group have also shown that whenever glycosylation and oxidation of the sulphydryl bond were prevented, PrP adopted PrP^{Sc}-like properties in mammalian neuroblastoma cells (Ma and Lindquist, 1999). The yeast cytoplasm is far more acidic than the cytoplasm of mammalian cells and it is known to provide a more reducing environment. Modification of the pH and the redox potential were key steps in the generation of *in vitro* PrP^{β} and the physico–chemical properties of the yeast cytoplasm seemed to recapitulate the same conditions as in a test tube. This could partially explain the newly acquired biochemical properties of the prion molecule: actually in S. cerevisiae, prions can occur spontaneously, albeit at low rates, perhaps providing an optimal physiological environment to study PrP conversion.

The focus of the experiments described in this chapter was to attempt to establish a novel screening strategy with the aim of isolating novel PrP interacting molecules. Conventional two-hybrid systems, although extremely versatile and powerful, are

known to have some intrinsic limitations and has been already successfully and extensively employed for searching for prion interacting molecules: Bcl-2 (Kurschner et al., 1995), Hsp60 (Edenhofer et al., 1996), the 37KDa laminin receptor precursor (Rieger et al., 1997), synapsin 1b, Grb2 and Pintl (Spielhaupter and Schatzl, 2001). With the only exception of the laminin receptor precursor, which had been studied in great detail, physiological relevance for the remaining interactions is yet to be demonstrated. One of the main criticisms of this kind of approach is that the cytoplasm is not the natural environment for the prion protein and many of the isolated interactors were exclusively cytoplasmic, such as Grb2. Moreover, no data was obtained regarding the conformation adopted by PrP in these screens.

Increasing evidence suggests that *in vivo* PrP has to undergo a partial misfolding and this provides the rational of my experimental design. My approach was to exploit the newly acquired properties of the prion protein, when expressed in the cytoplasm of S. cerevisiae, to screen a cDNA library in order to find candidate proteins that preferentially interact with misfolded PrP, either PrP^{β} or PrP^{*}.

Proteomic approaches have shown that proteins act in complexes in order to fulfil their physiological functions (Gavin and Superti-Furga, 2003). The identification of new PrP interacting molecules would be extremely helpful for the clarification of the involvement of PrP in specific cellular pathways and could lead to the elucidation of its biological function. From this point of view, it is very difficult to conceive that the structural conversion resulting in the production of PrP^{Sc} is an event occurring independently from the cellular context. If host encoded proteins were involved in PrP^{Sc} generation, their identification could be beneficial to the development of new therapeutic approaches to a disease that so far has no effective treatment.

3.2 RESULTS

3.2.1 The Ras Recruitment System (RRS)

In order to screen for potential interactors with misfolded PrP, I took advantage of the Ras Recruitment System (RRS) developed by Aronheim and colleagues (Figure 3.2) (Broder et al., 1998). The RRS is based on the absolute requirement of both Ras

localisation and activity at the plasma membrane in order to provide a growth signal. This is usually achieved by a farnesyl moiety present at the C-terminus of the protein (Rine and Kim, 1990). The yeast strain Cdc25-2 is viable at the permissive temperature of 25°C but cannot grow when shifted to the restrictive temperature of 36°C because of a temperature sensitive mutation in the Cdc25 guanyl nucleotide exchange factor. The expression of a constitutively active form of mammalian Ras (RasV12) lacking the consensus sequence for farnesylation and fused to the bait of interest is unable to rescue the Cdc25-2 mutation on its own. However, after successful protein-protein interaction between the bait and a member of the library, anchored at the plasma membrane by a specific localisation signal like the vSrc myristoylation sequence, RasV12 would be able to complement the Cdc25-2 mutation and finally confer cell growth even at the restrictive temperature. The system has been demonstrated to possess extreme versatility and capability to avoid false positives: the bait is under the control of the Met25 promoter that can be repressed by presence of methionine in the growth media, whereas the target library is under the control of a Galactose inducible promoter. Because PrP is highly expressed in the brain which is also the preferential site of prion accumulation and pathogenesis, I decided to screen a cDNA library obtained from adult mouse brain.

In a first experimental approach, the sequence encoding the mature form of mouse PrP aa23-aa230, missing both N- and C-terminal signal peptides, was originally fused in frame to the C-terminus of a constitutive active form of Ras. The resulting chimeric protein was expressed in a tightly regulated manner and as expected, no fusion protein was expressed in the presence of methionine. Quite surprisingly, the chimeric Ras-PrP protein was not insoluble, as predicted, since it was found in the detergent soluble fraction (data not shown). Moreover, it was totally sensitive to PK digestion, suggesting that the presence of Ras might confer higher solubility and protease sensitivity compared to the prion protein alone.

Unfortunately, RasV12-PrP was sufficient to rescue the Cdc25 mutation even in the absence of cDNA library expression, compromising the correct interpretation of the screen. One possible cause could be attributed to the presence of a highly conserved hydrophobic domain mapped between aa106-aa126 of PrP (Hay et al., 1987). This stretch of hydrophobic residues, responsible of the transmembrane isoforms of the prion

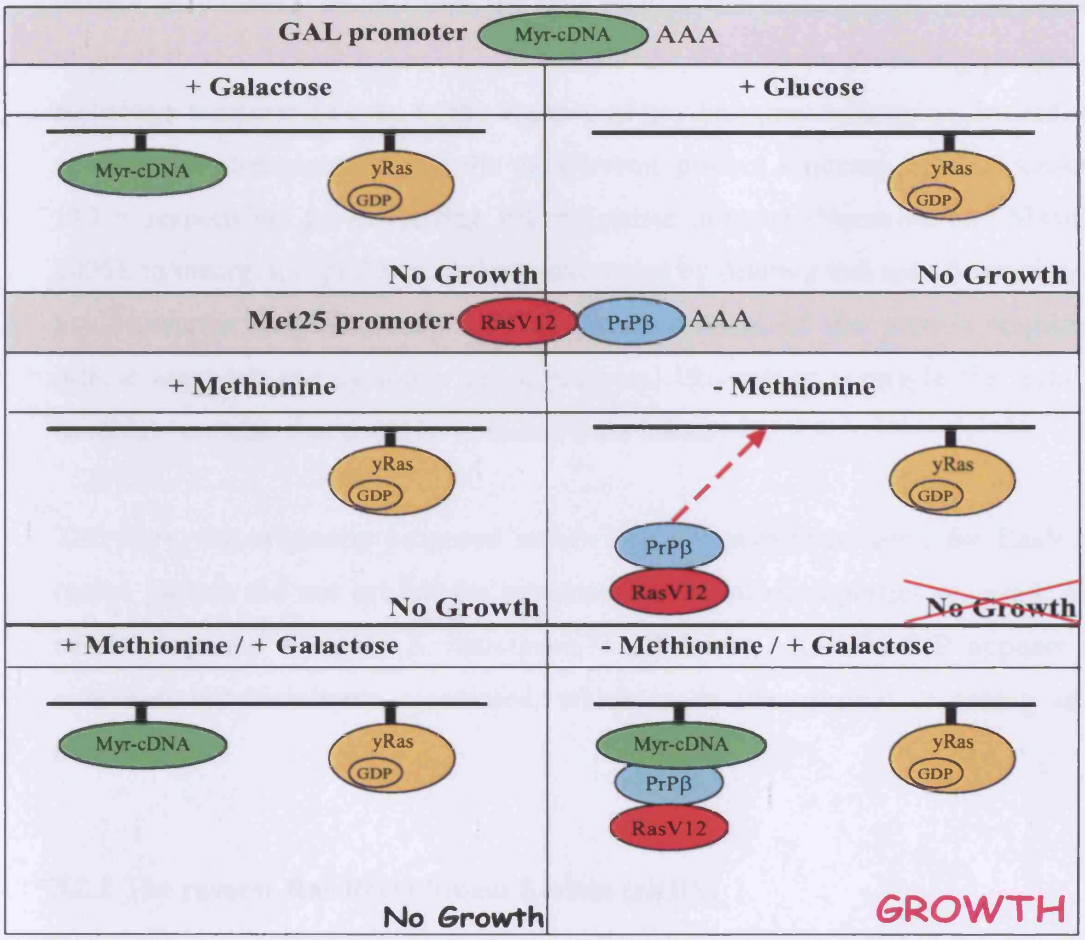

Figure 3.2 The Ras Recruitment System (RRS).
Schematic representation of the Ras Recruitment system (RRS) for screening for proteins interacting preferentially with misfolded PrP. A myristoylated cDNA library is localised on the inner layer of the plasma membrane of a Cdc25-2 yeast strain. The yeast Ras (yRas) is present in the inactive GDP-bound form due to the absence of a functional exchange factor Cdc25 at the restrictive temperature. The bait, PrP23-230, is fused to a cytoplasmic version of a constitutive active form of Ras. Only upon successful interaction between the bait and a member of the library, RasV12 is translocated to the plasma membrane and confers cell growth at the restrictive temperature. Unfortunately, expression of the fusion protein RasV12-PrPβ was sufficient to confer growth at the restrictive temperature even without library expression. This was explained to be the result of a possible weak interaction between the hydrophobic region present in PrP and the plasma membrane (red dotted arrow).

protein, may weakly interact with the lipid bilayer: this domain alone could potentially target PrP, and therefore RasV12, to the plasma membrane, providing growth at the restrictive temperature even in the absence of any bait-pray interaction. Indeed, recent studies have demonstrated that the palindromic protein sequence 112-AGAAAAGA-119 is responsible for conferring PK resistance in yeast (Norstrom and Mastrianni, 2005). In theory, this problem could be overcome by deleting this specific portion of the bait, however deletions may also eliminate regions of the protein required for interaction with one or more target proteins, limiting in principle the number of candidate proteins that could be obtained from the screen.

Therefore, the originally proposed screen was not performed since the RasV12-PrP fusion protein did not exhibit the expected biochemical properties required, namely insolubility and Protease K resistance. Furthermore, RasV12-PrP appears to be constitutively membrane associated, which made the original screening strategy impossible.

3.2.2 The reverse Ras Recruitment System (rRRS)

Although very powerful, the RRS is not suitable for studying interactions with integral plasma membrane proteins or proteins that may weakly associate with the plasma membrane, such as PrP. In order to overcome this specific problem, a novel approach has been developed: the reverse RRS (rRRS, Figure 3.3). The new technique was specifically designed to screen for candidates using membrane proteins like receptors or ion channels as bait thereby localising them to the plasma membrane and preserving their functional environment, conformation and binding specificity (Hubsman et al., 2001). The rRRS was therefore a more suitable system to screen for potential PrP interactors. To allow the screen to be performed in this way, the reagents previously described needed to be modified. The original full mouse brain cDNA library was subcloned at the C-terminus of a cassette encoding oncogenic RasV12 lacking both a membrane localisation sequence and stop codon.

It is well established that the rRRS is associated with a higher background level of false positives that the original RRS. This is due to the fact that any member of the cDNA library, either directly encoding a membrane protein or proteins that associate with any

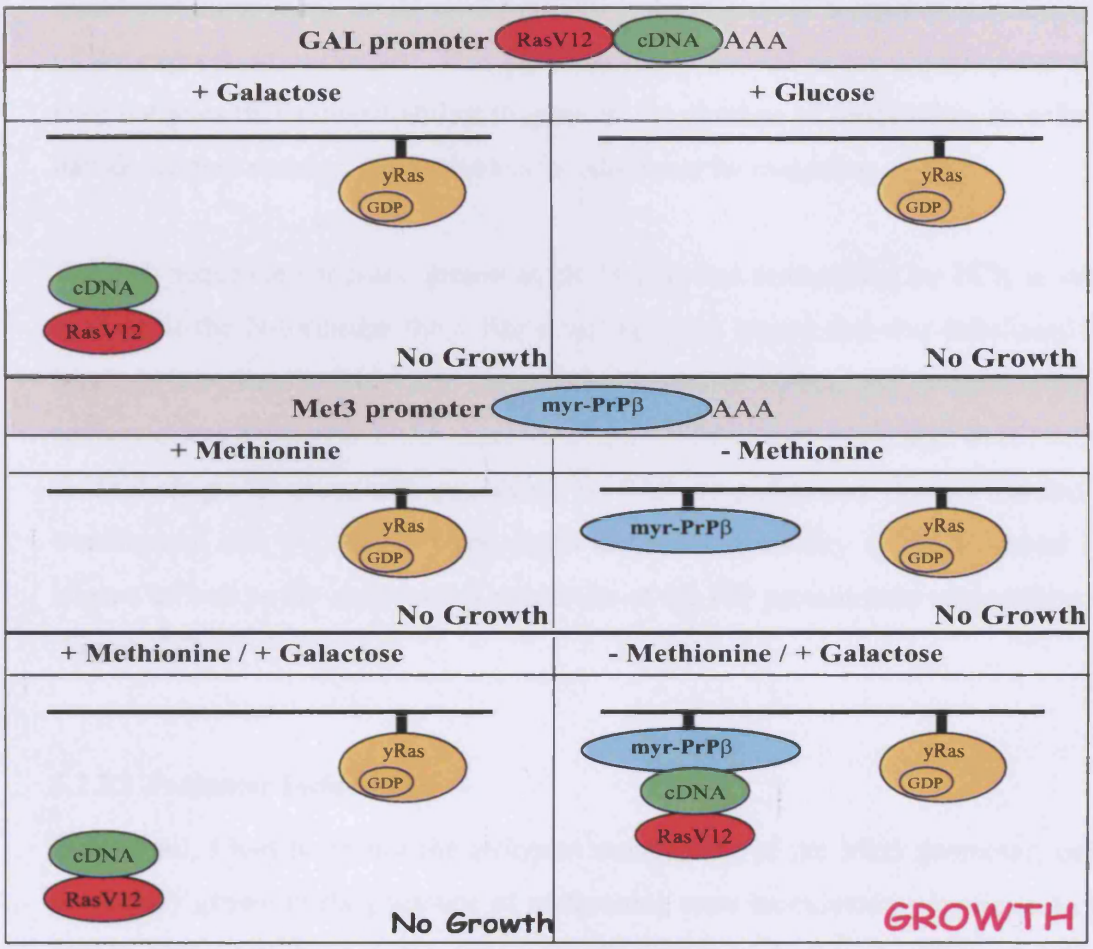

Figure 3.3 The reverse Ras Recruitment System (rRRS).
The conventional Ras Recruitment System was found to be unsuitable for transmembrane or membrane associated proteins. To overcome this limitation, the reverse RRS has been established. The protein of interest, PrP23-230, is now anchored to the inner layer of the cell membrane via the vSrc myristoylation signal and is not sufficient to confer cell growth at the restrictive temperature. The cDNA library is fused to a cytoplasmic and constitutively active form of Ras. After protein-protein interaction, RasV12 is translocated to the plasma membrane, complements the Cdc25-2 mutation and allows growth at the restrictive temperature. Any cDNA directly encoding for membrane proteins or for proteins associating with membrane components would bypass the requirement of bait-pray interaction. These candidates could be identified for their ability to grow in a bait independent fashion and would be excluded from further analysis. Clones presenting the ability to rescue the Ccd25-2 mutation were expanded and the identity of the cDNAs established by sequencing.

membrane component, could confer growth at the restrictive temperature independently of the expression of the bait. This problem can be solved in my experimental setting: only colonies that showed ability to grow in the absence of methionine, therefore in a bait-dependent manner, were selected for additional investigation.

The PrP sequence encoding amino acids 23-230 was reamplified by PCR in order to include at the N-terminus the v-Src myristoylation signal and was subcloned into a Met3 driven plasmid (MyrPrP). An alternative version lacking the membrane targeting sequence was generated at the same time as a control. Both constructs were sequenced to exclude point mutations generated by PCR amplification. The constructs were transformed into a Cdc25-2 yeast strain and the inducibility of the promoter I have chosen as well as the biochemical properties of the PrP protein were subject to analysis (Figure 3.4).

3.2.2.1 Promoter Inducibility

First of all, I had to ensure the stringent inducibility of the Met3 promoter; colonies previously grown in the presence of methionine were inoculated in duplicate in liquid media, with or without methionine, and allowed to grow for an additional 12 hours, before protein extraction and analysis by SDS PAGE (Figure 3.4A). No bait protein was detected when cells were grown in media containing methionine. Conversely, repression by methionine was promptly released after 12 hours. Promoter stringency and inducibility were therefore confirmed in my experimental set-up. This offered the ideal requisite to successfully perform the screen, since colonies would be chosen for their ability to grow in a bait dependent fashion.

3.2.2.2 Insolubility

Figure 3.4A shows that, after release of repression, MyrPrP preferentially partitioned into the detergent insoluble fraction, although some was still detected in the supernatant. This could in theory be explained by the presence of the myristoylation moiety but PrP was able to localise to the pellet fraction even in the absence of the specific myristoylation signal. This supports the hypothesis of PrP intrinsically association with

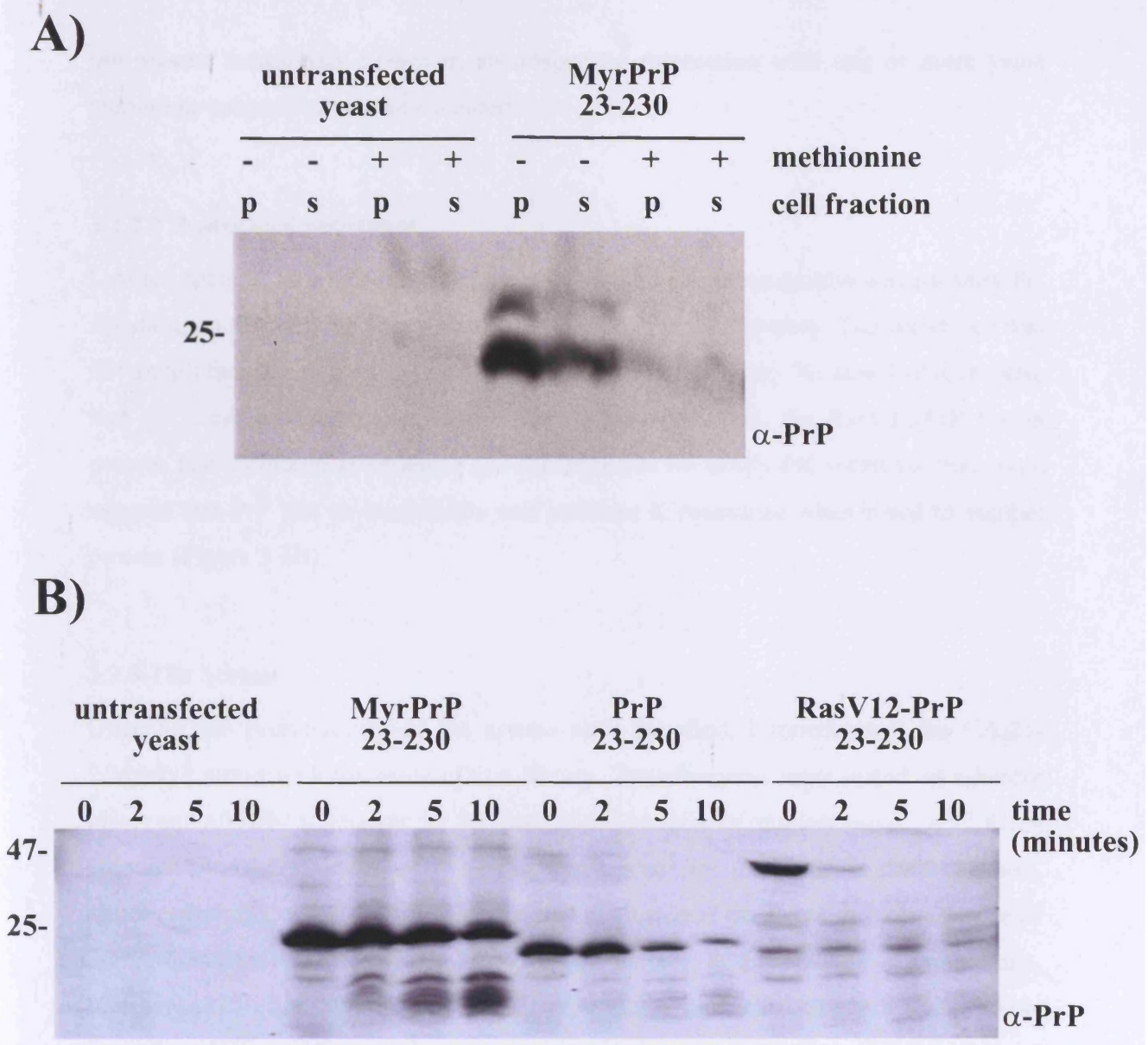

Figure 3.4 Biochemical properties of the Prion protein expressed in the yeast cytoplasm. A) Inducibility/Insolubility. The myristoylated PrP construct was transformed in the CDC25-2 strain and subject to analysis by Western blot using the α-PrP antibody ICSM18. The protein was expressed only after release from methionine inhibition and preferentially partitioned in the detergent insoluble fraction (p:pellet; s:supernatant). B) Partial Protease K resistance. Yeast extracts were subjected to limited proteolysis with PK (5 μg/ml) for the indicated times. Both versions of the prion protein, with and without the myristoylation modification, showed partial resistance to digestion whereas the fusion protein RasV12-PrP, originally designed for the RRS, was totally sensitive to proteolysis.

the plasma membrane, however, an unspecific interaction with one or more yeast membrane proteins cannot be excluded.

3.2.2.3 Protease K resistance

Limited proteolysis was performed and revealed that the prion protein was partially PK resistant, confirming the data obtained by the Lindquist laboratory. The resistance was not an artefact due to the presence of the myristoylation moiety because PrP alone also had the same biochemical property. As a positive control, the RasV12-PrP fusion protein that I initially intended to use confirmed to be totally PK sensitive; this could suggest that PrP lost its insolubility and protease K resistance when fused to another protein (Figure 3.4B).

3.2.3 The Screen

Once all the prerequisites of the screen were satisfied, I transformed the Cdc25-2/MyrPrP strain with the brain cDNA library. Transformants were plated on Glucose plates and allowed to recover for 5-7 days at the permissive temperature of 24°C. Once colonies were fully visible, cells were replica plated onto Galactose-containing plates, either containing or lacking methionine, and incubated at the restrictive temperature of 36°C. Transformants exhibiting efficient growth only in the absence of methionine, therefore only when PrP was expressed, were picked and recovered on glucose plates for a few days at 24°C. Selected colonies were replica plated for a second time and retested for their methionine-dependent growth. Only colonies able to undergo the two consecutives rounds of selection were considered "bona fide" candidates. The detailed screening procedure is described in the Materials and Methods section. Colonies able to rescue the Ccd25 phenotype were picked from plates and expanded in liquid culture. Plasmid cDNAs, encoding the target candidates, were extracted from yeast clones and sequenced. The nucleotides sequences were then compared with all the known sequences present in the database (http://www.ncbi.nlm.nih.gov/BLAST/) in order to identify the potential candidates.

3.2.4 Candidates evaluation

As a result from the screen, proteins were cloned and the working name "PIP" was chosen (Prion Interacting Proteins) (Table 3.1). Some information concerning the identity of some of the candidates, their sub cellular localisation and possible links with the prion protein are detailed below.

Table 3.1 Identification of the cDNAs retrieved from the rRRS screen.
Plasmids were extracted from yeast colonies and subject to DNA sequencing; sequences were submitted to the BLAST server and, when possible, matched to already known proteins.

PIP1	* Not cloned, possibly due to plasmid integration in the yeast genome.
PIP2	Mus Musculus DnaJ (Hsp40) homolog, subfamily B, member 6, (in frame) Score = 577 bits (291), Expect = 3e-161 Identities = 446/482 (92%), Gaps = 10/482 (2%) UniProtKB/Swiss-Prot entry Q54946
PIP3	Mus Musculus Poly(rC)-binding protein 2 (in frame), putative hnRNP X Score = 555 bits (280), Expect = 1e-154 Identities = 442/480 (92%), Gaps = 11/480 (2%) UniProtKB/Swiss-Prot entry Q61990
PIP4	Mus Musculus Enolase 2 (gamma Enolase) (out of frame) Score = 371 bits (187), Expect = 2e-99 Identities = 249/263 (94%), Gaps = 6/263 (2%) UniProtKB/Swiss-Prot entry P17183
PIP5	Mus Musculus HCM7087 gene (out of frame), virtual transcript Score = 321 bits (162), Expect = 3e-84 Identities = 297/340 (87%), Gaps = 7/340 (2%)
PIP6	Mus Musculus Ran (in frame) Score = 345 bits (174), Expect = 3e-91 Identities = 279/307 (90%), Gaps = 8/307 (2%) UniProtKB/Swiss-Prot entry P62827
PIP7	Mus Musculus hnRNP M4 (in frame) Score = 507 bits (256), Expect = 3e-140 Identities = 386/414 (93%), Gaps = 15/414 (3%) UniProtKB/Swiss-Prot entry Q9D0E1

Despite many attempts to rescue the plasmid encoding the first candidate, PIP1, I did not manage to rescue it. I believe the library plasmid had integrated irreversibly into the yeast genome, preventing any possible identification.

PIP2 was known as DnajB6, the mouse homologue of the bacterial chaperone groP. Hsp40 family members are known to function in concert with other molecular chaperones of the Hsp60 and Hsp70 families (Michels et al., 1997; Ohtsuka, 1993).

PIP4 encoded the neuronal specific isoform of the enzyme Enolase 2 which has neurotrophic and neuroprotective properties on central nervous system (CNS) neurons. It has enzymatic activity and produces phosphoenolpyruvate in glycolysis (Kaghad et al., 1990).

PIP5 was a novel gene; the sequence was annotated in the database by genomic survey and the existence of a genuine transcript has not yet been confirmed.

However, both PIP4 and PIP5 were out of frame. This had been previously reported in other screens and the explanation lies in the way the cDNA library was generated: a standard oligo dT primer, modified with an XhoI site at the 3' end was annealed to the polyA tail of a total mRNA preparation. After the generation of a double strand cDNA a blunt-end linker containing an EcoRI site was randomly inserted at the 5' end. The insertion of the linker was a random, therefore only approximately 1 out of 3 cDNAs is actually in frame.

PIP6 was positively identified as Ran, a well known member of small GTPases proteins, involved in the nucleocytoplasmic transport (Wennerberg et al., 2005).

Quite interestingly PIP3 and PIP7 were part of the RNA binding protein super family: hnRNPs (Krecic and Swanson, 1999; Weighardt et al., 1996).

At this point, on the preliminary analysis of the identified cDNAs, it was quite difficult to distinguish between potential candidates and false positive, known to occur quite often in this kind of screen. Many of the isolated proteins are known to be cytoplasmic or nuclear, making it difficult to suggest how they could interact in a physiological context with PrP. There was however one interesting exception: reading the literature related to the PIP7 candidate, I found different reports confirming its localisation both in the nucleus and on the cell surface (Bajenova et al., 2001; Blanck et al., 1994).

Being in a subcellular compartment that would allow physical interaction, I established a GST pull down assay to quickly evaluate if the yeast interaction between PIP7 and PrP was real. The PIP7 cDNA was subcloned into a pGEX vector and recombinant fusion protein was produced in E. coli. GST alone and GST-PIP7 were coupled to glutathione sepharose beads and mixed with total mouse brain homogenate. Three bands, corresponding to di-, mono- and un-glycosylated PrP respectively, were enriched specifically by the GST-PIP7 fusion protein and not by GST (Figure 3.5A).

3.2.5 PIP7

PIP7 encodes the mouse ortholog of the human heterogeneous RNA binding protein M4. It was originally characterised as part of a cluster of four nuclear proteins (M1-M4) of 64.000-68.000 Da by Two Dimensional Electrophoresis. Transcripts newly synthesized by RNA polymerase II are directly bound by the heterogeneous nuclear ribonucleoproteins (hnRNPs) which package them in a transcript specific manner and are involved in important RNA processes such as splicing, polyadenylation and nuclear-cytoplasm transport as a direct consequence of their binding. The exact molecular function of most members of the hnRNP family proteins has not been extensively studied. As a potential indication of their role in RNA editing, M family proteins are known to bind with high affinity to poly G and poly U homopolimers *in vitro* (Datar et al., 1993).

The primary sequence of PIP7 is composed of 728 amino acids and on Western blot the protein appeared to migrate as a doublet of 64 and 68 KDa. The shorter isoform, lacking 29 amino acids in the region between the RNA binding domain 1 and 2, is believed to arise by alternative splicing of exon 6. Structural analysis revealed the presence of three RNA binding domains, also called RRM (amino acids 69-147, 202-279, 651-727) and four putative transmembrane helices (amino acids 158-178, 293-313, 322-342, 627-647) (Figure 3.5B).

The novel function of hnRNP M4 as a receptor was originally reported more than ten years ago (Blanck et al., 1994). A cDNA encoding a novel gene, called NAGR1, was cloned in the attempt to identify the receptor for human thyroglobulin hormone. Due to

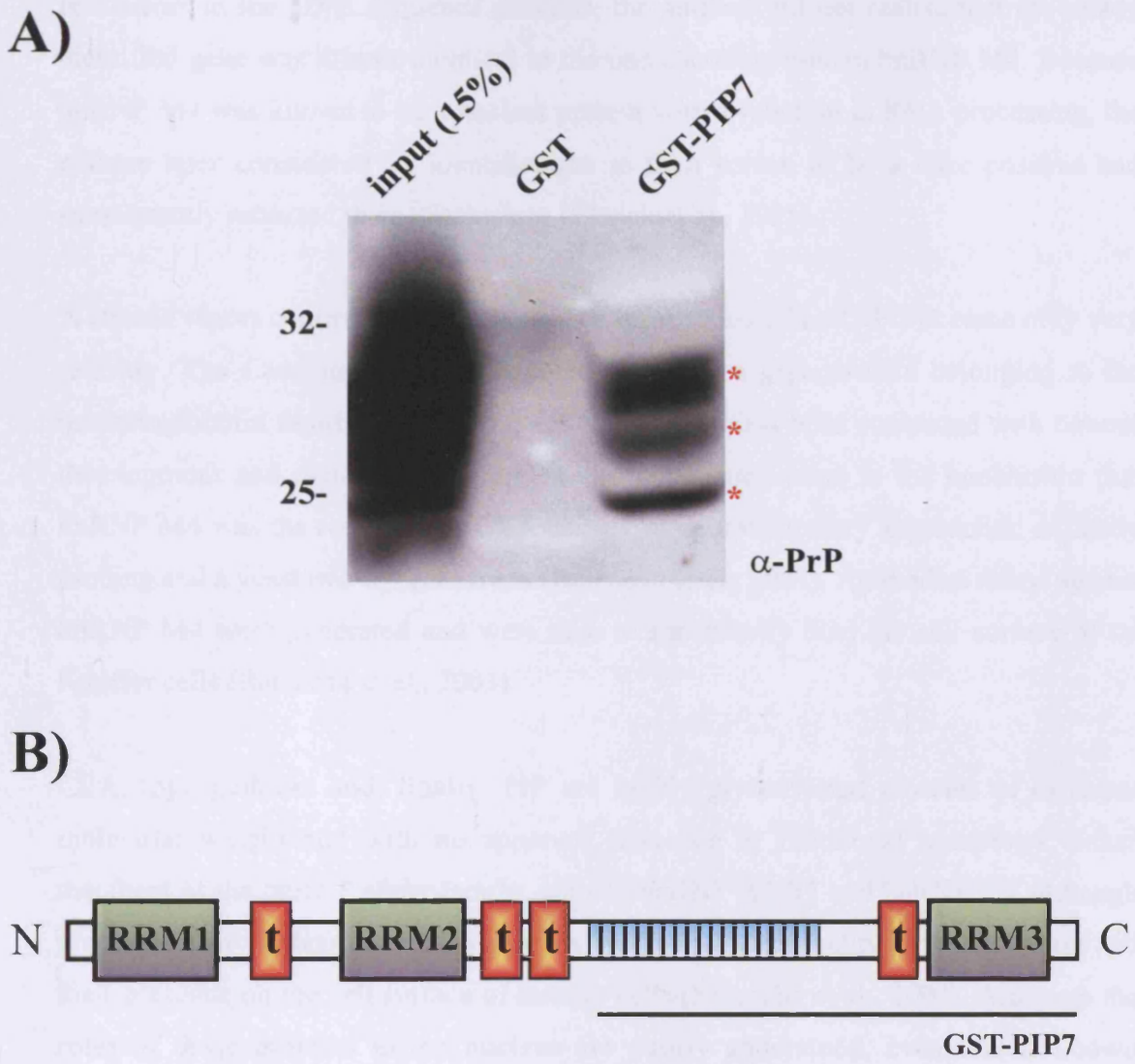

Figure 3.5 hnRNP M4 (PIP7), a novel PrP interacting protein.
A) The PIP7-PrP interaction was confirmed by *in vitro* GST pull down. Total brain homogenate obtained from adult mouse was incubated with glutathione beads coated with GST or GST-PIP7 proteins. After extensive washing, beads were boiled and processed by standard SDS PAGE. α-PrP antibody ICSM18 was used for the detection. All three PrP isoforms, corresponding to di-, mono-, and unglycosylated PrP (red marks) were specifically enriched by GST-PIP7 and not by GST alone. In the first lane, total lysate was loaded (15%) to facilitate comparison. B) Structural features of hnRNP M4. The protein presents three putative RNA binding domains (green boxes) and a region encompassing 27 repeats of a methionine-arginine-glycine rich sequence (blue squares). At least two different isoforms are present, arising from the alternative splicing of 29 amino acids between RRM1 and RRM2. Four transmembrane helices (red boxes) were predicted on the basis of a hydropathy plot, suggesting a putative topology with both the N- and C-terminus in the intracellular space. A black bar indicates the partial cDNA retrieved from the yeast library. The fragment was sufficient to confirm PrP interaction and was injected into mice in order to produce a panel of monoclonal antibodies.

few errors in the DNA sequence analysis, the authors did not realise that the newly identified gene was almost identical to the one encoding human hnRNP M4. Because hnRNP M4 was known to be a nuclear protein with a function in RNA processing, the authors later considered its identification in their screen to be a false positive and subsequently retracted their conclusions (Blanck et al., 1995).

A second report confirming the cell surface localisation of hnRNP M4 came only very recently. The Carcinoembryonic Antigen (CEA) is a glycoprotein belonging to the immunoglobulin family. The overexpression of CEA has been correlated with tumour development and metastasis. Bajenova and colleagues came to the conclusion that hnRNP M4 was the receptor for CEA using two complementary approaches; antibody probing and a yeast two-hybrid screen (Bajenova et al., 2001). Antibodies raised against hnRNP M4 were generated and were able to specifically bind the cell surface of rat Kupffer cells (Bajenova et al., 2003).

CEA, thyroglobulin and, finally, PrP are highly glycosylated proteins of different molecular weight and with no apparent sequence or functional homology. Other members of the hnRNP super family, namely hnRNP A2/B1 and hnRNP C1, although predominantly nuclear have been recently studied for their ability to bind albumin and their presence on the cell surface of tumour cells (Fritzsche et al., 2004). Although the roles of these proteins in the nucleus are poorly understood, even less is known regarding their apparent surface function. This dual localisation could hence reflect a hallmark of different members of this family.

3.2.5.1 Generation and characterisation of PIP7 monoclonal antibodies.

In order to better characterise the molecular basis of the PrP-PIP7 interaction, I decided to generate a panel of monoclonal antibodies (mAb), to use as a tool for my future experiments. Mice were immunised using specifically the PIP7 fragment present in the original yeast clone. The complete procedure is described in details in the materials section. As a result, a panel consisting of 5 mAbs was produced by the CRUK internal Monoclonal Service. First of all, the subclass of each antibody was determined by ELISA: with the only exception of clone 4G4 which is an IgG3, all the remaining

monoclonal antibodies belong to IgG1 subclass. Subsequently, the monoclonals were fully characterised using the different approaches detailed below:

3.2.5.2 Western Blot analysis

Because antibodies were raised against the last 300 amino acids at the C-terminus of PIP7, encompassing both the Tandem Repeats region (TR) and the RRM3 domain, I overexpressed the single regions, fused to a green fluorescence protein (GFP), in human 293T cells: the aim of the experiment was to map the binding region of each mAb. The GFP-TR and GFP-RRM3 constructs did not have any overlapping sequence, allowing a clear interpretation of the result. GFP alone was included in the experiment to provide a suitable negative control. Protein extracts were loaded in parallel and each sample was probed with the specific α-PIP7 mAb or a GFP-specific antibody. Western blot analysis using a GFP antibody revealed correct expression of GFP fusion proteins of the expected molecular weight (Figure 3.6). All antibodies detected endogenous levels of the PIP7 proteins at the expected molecular weight of 64 and 68 KDa. Four of the clones, specifically recognised the Tandem Repeats region. This region presents repetitions of the same amino acids sequence and this could eventually explain its higher immunogenicity. No data were obtained for the 9H1 clone which failed to recognise both the endogenous and the over expressed PIP7 fragments.

3.2.5.3 FACS

Since one of the possible place of interaction with PrP is the cell surface, I wanted to check if was possible to monitor the PIP7 surface levels as have been previously reported (Bajenova et al., 2003). I investigated whether my panel of mAb were able to detect and confirm the presence of PIP7 on the surface of mouse neuroblastoma N2a cells, the most used cell line for studying the cell biology of PrP and prion replication. Untransfected N2a cells were fixed, following an optional step of permeabilisation in order to discriminate between the specific surface pool and the total population, known to be mainly nuclear. The FLOWJO analysis is shown in Figure 3.7: all antibodies, including the 9H1 clone, were able to detect PIP7 on the cell surface. The signal was specific compared to the background obtained when the primary antibody was omitted. Although similar levels of staining were observed on the cell surface, the antibodies

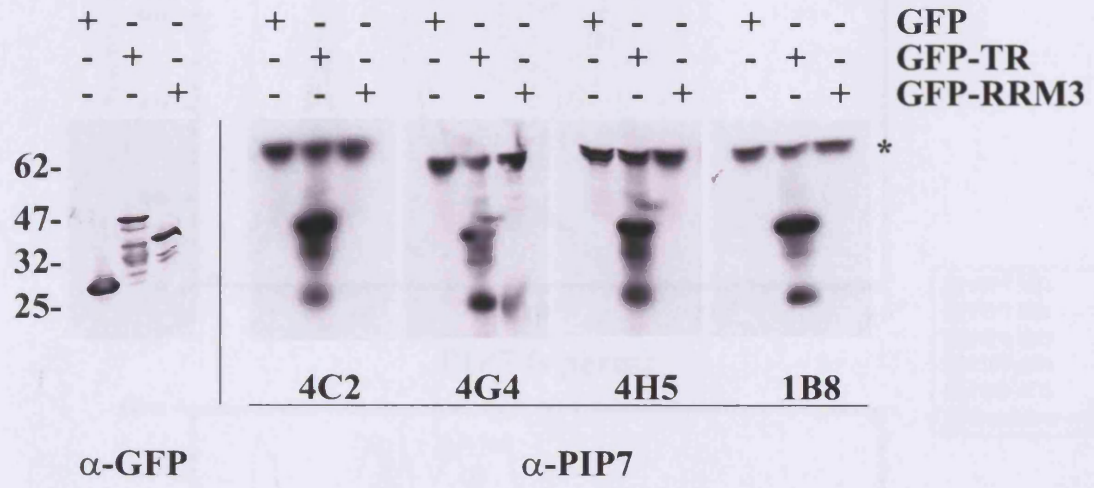

Figure 3.6 PIP7 monoclonal antibodies recognize the Tandem Repeats region. In order to provide a further characterization of the PIP7 monoclonal antibodies, the original yeast clone used as an immunogen was divided into two non overlapping fragments, the Tandem Repeats region and the RRM3 domain, and expressed as fusion proteins with the Green Fluorescence Protein (GFP) in human 293T cells. All PIP7 antibodies were able to detect endogenous levels of protein (asterisk) and preferentially recognised the Tandem Repeat region but not the RRM3 domain. No data were produced by the 9H1 clone which failed to detect both endogenous and ectopically overexpressed PIP7 protein. As a positive control, extracts were probed with a GFP specific antibody (left side), which detected fusion proteins of the expected molecular weight.

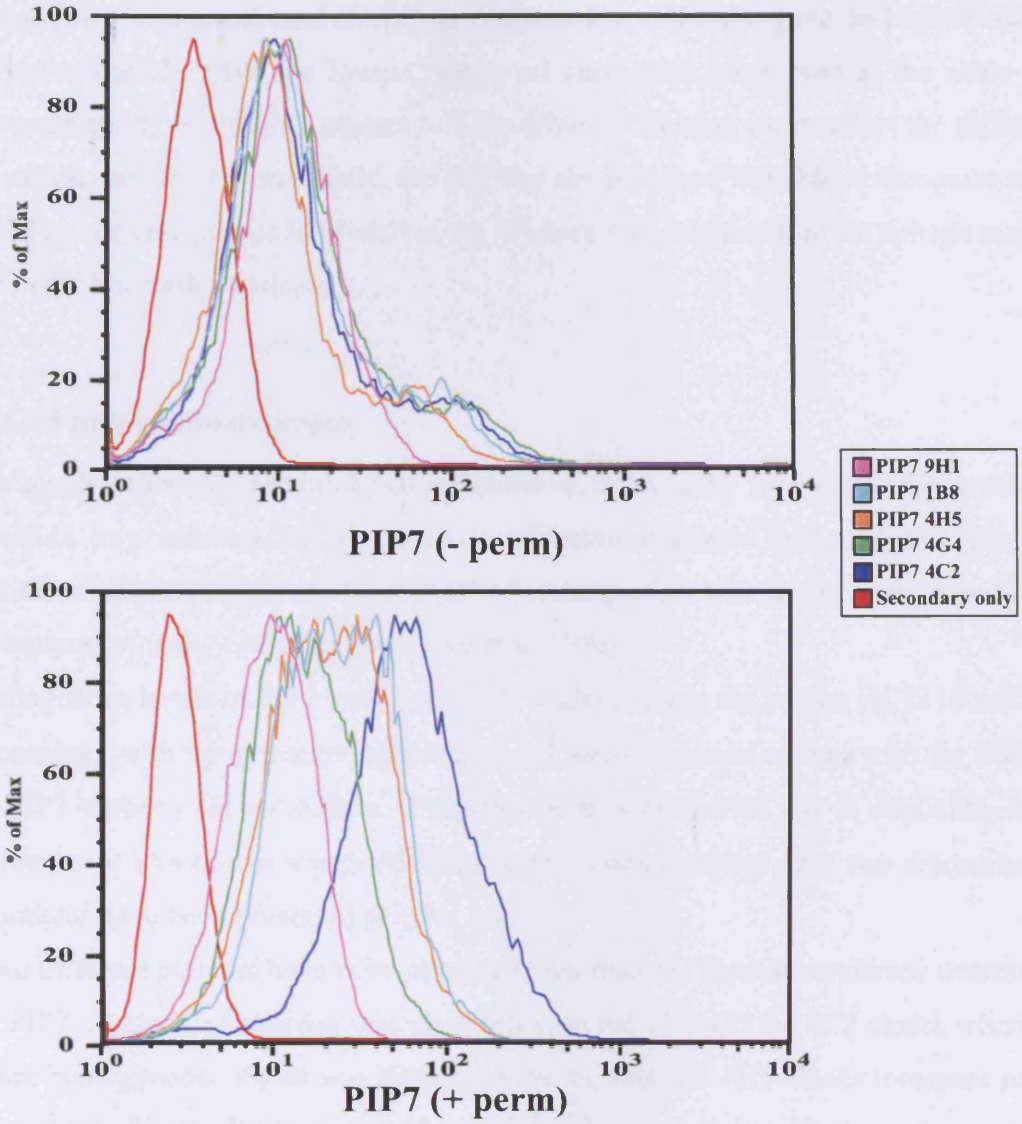

Figure 3.7 Specificity of PIP7 monoclonal antibodies shown by FACS analysis. Human 293T cells were fixed and stained with the generated PIP7 antibodies. An optional step of permeabilisation was included in order to discriminate between the surface pool (top panel) and the total PIP7 population (bottom panel). All PIP7 antibodies gave comparable signal for the surface pool. A different situation emerged when the total population was examined. The 4C2 clone gave the highest staining whereas the 9H1 the lowest. All antibodies have been used at the same final concentration (20 μg/ml).

recognised the internal pool to varying degrees. The 4C2 clone gave the highest staining whereas the H1 gave the lowest. Since all antibodies were used at the same final concentration, the relative intensity of the different staining must reflect the difference in affinity of the clones. Finally, the fact that the H1 clone was able to recognise native PIP7 on the cell surface but failed in the Western blot suggests that the epitope may not be linear but conformational.

3.2.5.4 Immunofluorescence

Although extremely powerful and quantitative, analysis by flow cytometry would not provide any information about co-localisation between the candidate proteins. Moreover, PIP7 protein has been reported to be present both in the nucleus and in the cytoplasm of many cell lines (Bajenova et al., 2003).

Endogenous levels of PIP7 were subject to analysis using the human HCT116 cell line. In analogy with the previous experiment, cell were fixed and stained with the different α-PIP7 monoclonal antibodies. The experiment was carried out in duplicate, in the presence or absence of a permebilising agent. For simplicity only two representative examples have been presented (Figure 3.8).

Two different patterns have been observed regarding the plasma membrane distribution of PIP7. A speckled staining was observed with the 1B8 and the 4C2 clones whereas a more homogeneous signal was detected with the 9HI and 4H5 clones (compare panels A and B). Since all staining were performed in parallel, with the same antibody concentration, the observed difference may reflect differential affinity or specificity of each mAb. All antibodies recognised the nuclear PIP7 pool with the exception of the 9H1 clone, which in the previous FACS analysis showed preferential specificity for the membrane pool only. No cytoplasmic stained was observed in any of the samples and the signal obtained in each staining was specific, because the signal was not present when the primary antibody was omitted (panel C)

3.2.5.5 Immunohistochemistry

Since PIP7 was cloned from a full brain cDNA library, I attempted to test the spatial distribution of the protein in adult brain by immunohistochemistry. Section were

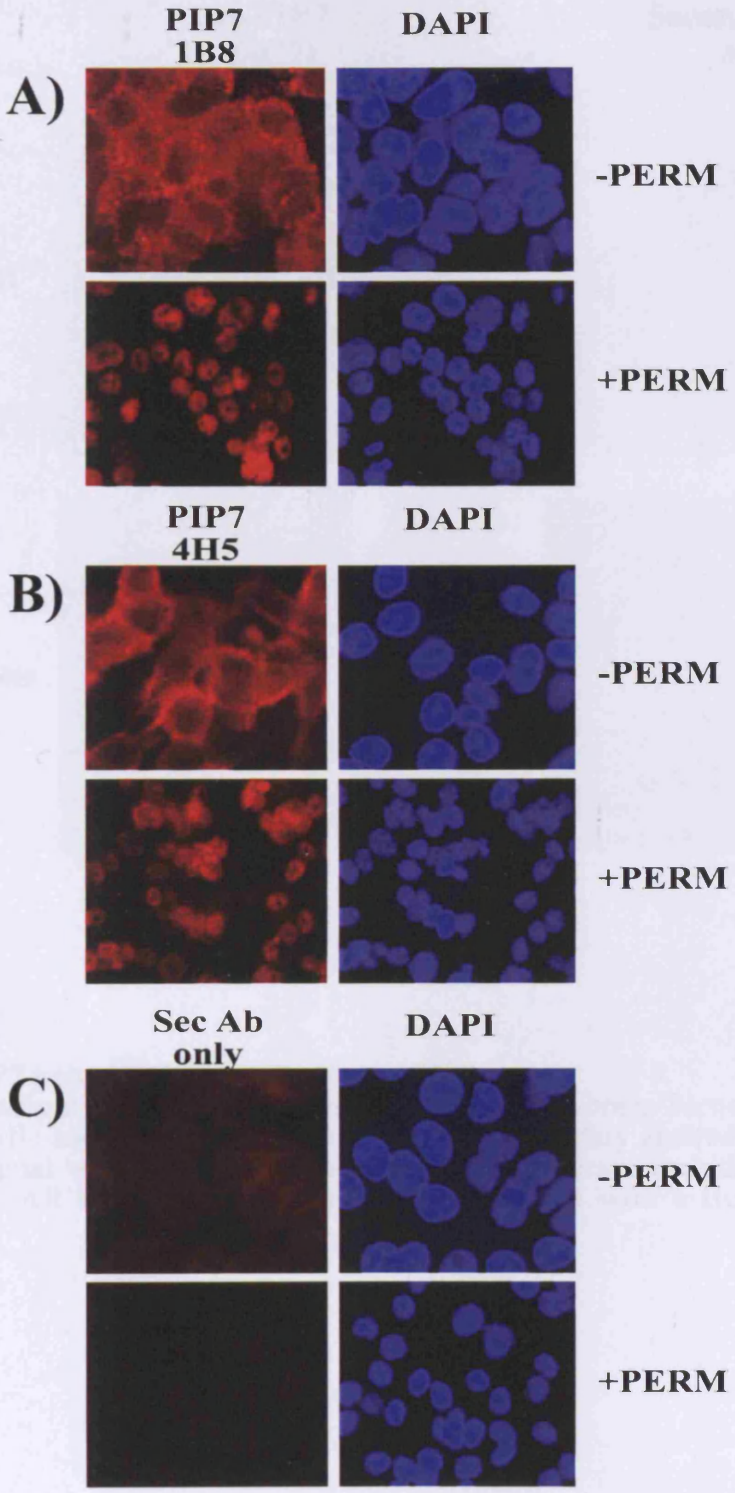

Figure 3.8 Surface and nuclear localisation of PIP7 in human HCT116 cells. Immunofluorescent staining of endogenous PIP7 on the surface and inside the nucleus of the cell line HCT116. The figure illustrates the two different staining patterns observed on the surface of the cells. Clones 1B8 and 4C2 gave a speckled surface pattern whereas 9H1 and 4H5 exhibited a more continous and intense staining. All four antibodies appeared to detect the nuclear pool to comparable extents.

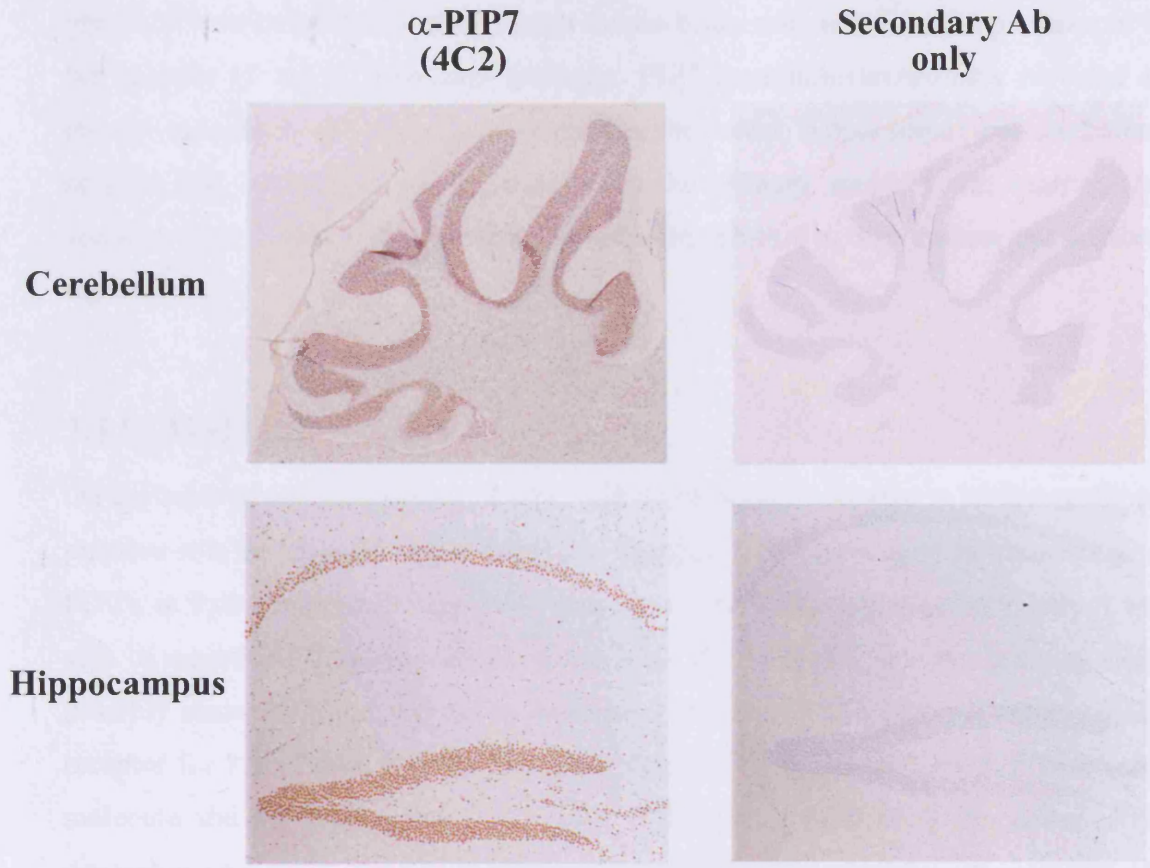

Figure 3.9 PIP7 pattern of expression in the CNS.
Consecutive sections were obtained from a wild type mouse brain. Sections were stained with the PIP7 specific antibody 4C2 (left panel) or with secondary antibody only (right panel). A specific signal was observed in most areas of the brain including cerebellum and hippocampus. All sections were lightly counterstained with a Hematoxilin solution.

prepared from paraffin embedded adult mouse brain and stained in the presence or in the absence of the 4C2 primary antibody. PIP7 immunohistochemistry revealed an intense staining in all brain regions including the cortex, hippocampus and cerebellum (Figure 3.9). No signal was detected when the primary antibody was omitted. All sections were lightly stained with a Hematoxilin solution to discriminate the different regions.

3.3 SUMMARY

On the basis of the preliminary *in vitro* pull down result, I decided to further study the putative role of hnRNP M4, (which, for simplicity will from now be referred to as PIP7), in Prion biology. I based my decision on the following reasons. Firstly, I was able to reproduce the yeast interaction *in vitro*. Furthermore, the two proteins could possibly share the same cellular compartment, making PIP7 a putative novel cellular receptor for PrP. Taken together, I believe that PIP7 is a genuine new PrP interacting molecule and not a false positive. Further experiments will clarify the nature of the interaction and could greatly contribute to the characterisation of the still unknown role of PrP in cell physiology. Most importantly, since PIP7 had been identified for its ability to bind misfolded PrP, I believe it should also be evaluated for a role also in prion pathology and as a potential therapeutic target in the treatment of the diseases. The panel of monoclonal antibodies I have generated and preliminarily characterised will provide a very valuable tool for my future analysis.

Chapter 4: Characterisation of the PrP-PIP7 interaction

4.1 INTRODUCTION

The original proposition of one or more prion protein receptors was initially suggested more than 10 years ago (Shyng et al., 1994). The nature of the prion protein, which is devoid of any cytoplasmic tail, suggested it might associate with one or more transmembrane proteins, able to recruit the endocytic machinery. The most studied PrP receptor is the 37/67 KDa laminin receptor (LRP/LR). It was originally discovered in a screen performed in S. cerevisiae (Rieger et al., 1997). PrP and LRP interacted both *in vitro* and *in vivo* (Gauczynski et al., 2001). Recombinant PrP is able to bind mammalian cells in a LRP dependent manner, as shown by antibody competition experiments. Moreover the LRP complex is responsible for the internalisation of up to 50% of the PrP molecules bound to the cell surface, indicating the need for other components to mediate PrP cell entry. Alternatively, other pathway besides clathrin coated pits could also be involved (Marella et al., 2002).Two different regions within the prion molecule are responsible for the interaction, amino acids 53-93 and 144-179, whereas the region proximal to the LRP transmembrane domain (161-179) binds PrP directly.

In Chapter 3 I described a novel screening procedure I have used with the intent to find novel PrP interacting proteins (PIPs). I have successfully identified a potential candidate, PIP7, and confirmed its ability to interact *in vitro* with the prion protein. The experiments described in this chapter attempt to understand the biology of the PrP-PIP7 interaction, using a series of complementary approaches. Particular attention has been focused on the protein pool of PIP7 present on the cell surface, which is the most likely place of interaction.

In order to dissect the molecular mechanism of interaction, different PrP mutants have been used. Every construct used has been extensively characterised and its behavior in the cell context is well understood. Since the suggested role for PIP7 was a novel PrP receptor, different chemical treatments were applied to stimulate PrP endocytosis and the fate of the PIP7 protein was monitored.

4.2 RESULTS

4.2.1 Biochemistry of the PIP7-PrP interaction.

4.2.1.1 PrP-PIP7 co-immunoprecipitation studies

A GST pull down is a powerful and flexible system to confirm novel protein-protein interaction but has the disadvantage of using a fusion between the sequence of interest and the Glutathione-S-Transferase tag. Such recombinant proteins might not reflect the original biochemical properties of the native protein and the exposure of hydrophobic patches due to incorrect folding could be responsible for aspecific protein associations. From this point of view, the use of GST alone is not a sufficient negative control to exclude partial misfolding in the PIP7 sequence resulting possibly in a non physiological interaction.

Despite the association inferred from the screen and the positive interaction in the pull down assay, I wanted to investigate whether PrP-PIP7 interaction could take place in a more physiological environment. To do so, I performed a standard co-immunoprecipitation assay (Figure 4.1A). Total lysate was obtained from uninfected N2a cells and incubated with the α-PrP specific antibody 6H4 or, as a negative control, with an isotype control. The α-PrP antibody was able to enrich for the prion protein as shown in the lower panel of the figure and to selectively co-immunoprecipitate PIP7 (upper panel). Conversely, the isotype control antibody neither enriched PrP nor was able to co-immunoprecipitate PIP7, confirming the specificity of the observed interaction.

In a parallel experiment, I tested different α-PIP7 mAbs for their ability to enrich PIP7 from total brain homogenate. The antibodies were able to immunoprecipitate PIP7 albeit to different extents and, since they were used at the same final concentration (10 μg/ml), the difference should reflect their different relative affinities: PIP7 enrichment by the 4H5 clone was undetectable when compared to the 4C2 and 4G4 clones, with the latter providing the highest enrichment in PIP7 levels. When the same membrane was probed with a α-PrP antibody, only the 4G4 clone was able to co-immunoprecipitate

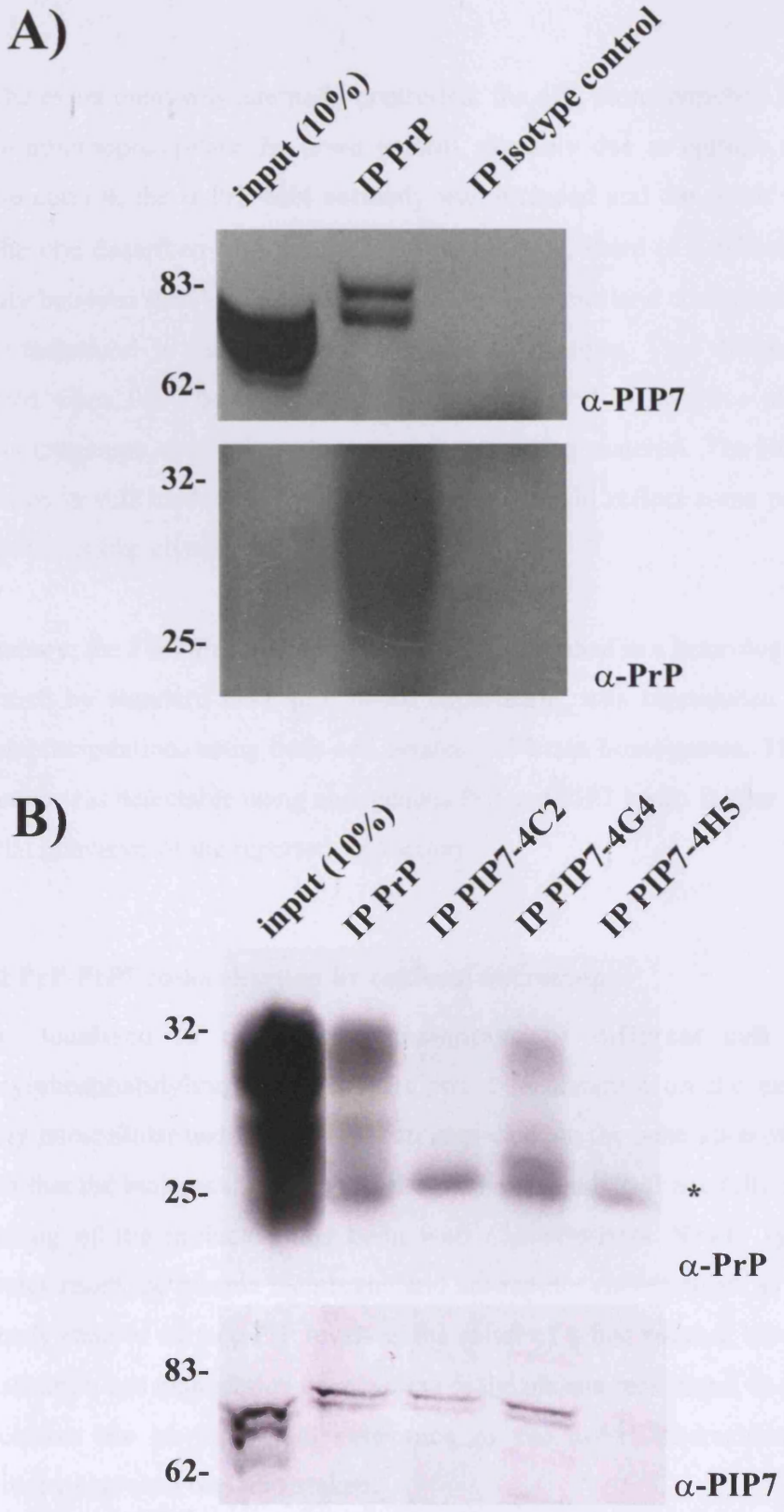

Figure 4.1 PrP-PIP7 interaction by co-immunoprecipitation.
A) PrP was immunoprecipitated from N2a cell lysates using the 6H4 antibody. Western blot analysis reveals enrichment in PrP levels and concomitantly, co-immunoprecipitation of PIP7 protein. The control antibody neither immunoprecipitated PrP nor enriched PIP7. B) Total brain homogenate from adult mouse was used for PIP7 immunoprecipitation. The 4G4 clone was not only able to immunoprecipitate PIP7 but also allowed co-immunoprecipitation of the prion protein. As a positive control, the 6H4 antibody was included in parallel and enriched both PrP and PIP7 levels. The position of the light chain of the antibodies is annotated by the asterisk.

PrP. The experiment was internally controlled: the 4C2 clone enriched in PIP7 but did not co-immunoprecipitate the prion protein, possibly due to epitope masking. As a positive control, the α-PrP 6H4 antibody was included and the result was consistent with the one described in Figure 4.1A. Interestingly, there is a difference in the gel mobility between the PIP7 isoforms present in the input lane compared to the slightly higher migration in the co-immunoprecipitated sample. This difference was also observed when PIP7 was directly immunoprecipitated irrespective of whether total brain homogenate or cell lysate were used as starting material. The reason of such a difference is still matter of investigation since it could reflect some post-traslational modifications like glycosylation or phosphorylation.

In summary, the PIP7-PrP interaction, originally described in a heterologous system and confirmed by standard GST pull down experiment, was reproduced *in vivo* by co-immunoprecipitation, using both cell lysates and brain homogenate. The fact that the interaction was detectable using endogenous PrP and PIP7 levels further strengthens the potential relevance of the reported interaction.

4.2.1.2 PrP-PIP7 co-localisation by confocal microscopy

PrP is localised to the plasma membrane of different cell types by its glycosylphosphatidylinositol moiety. Correct localisation on the cell surface and possibly intracellular trafficking has been implicated in the generation of PrP^{Sc}. Despite the fact that the biological function of the prion protein is still not fully understood, the trafficking of the molecule has been well characterised. Newly synthesised PrP molecules reach the plasma membrane and are rapidly endocytosed: as a consequence the steady state of surface PrP levels is the result of a fine balance between transport, internalisation and degradation or recycling to the plasma membrane. In order to further characterise the physiological relevance of the novel interaction described, a microscopy approach was undertaken.

Mouse neuroblastoma cells were transfected with a GFP-PrP fusion construct that had been shown to be functional in respect of its correct localisation and prompt internalisation in response to copper stimulation (Lee et al., 2001b). Forty-eight hours after transfection, cells were fixed and stained with a fluorescence conjugated α-PIP7-

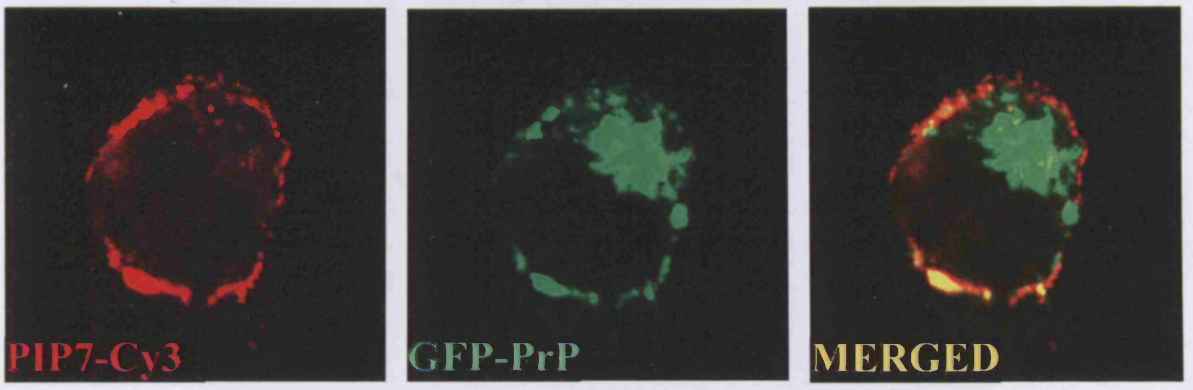

Figure 4.2 Co-localisation of PIP7 and PrP on the surface of N2a cells. Mouse N2a cells were transiently transfected with GFP-PrP, fixed and stained with a directly labeled α-PIP7 antibody (4G4-Cy3). Samples were analysed by confocal microscopy. PIP7 (left panel) and PrP (middle panel) were both present on the cell surface. In the right side panel the overlay of both signals indicated co-localisation.

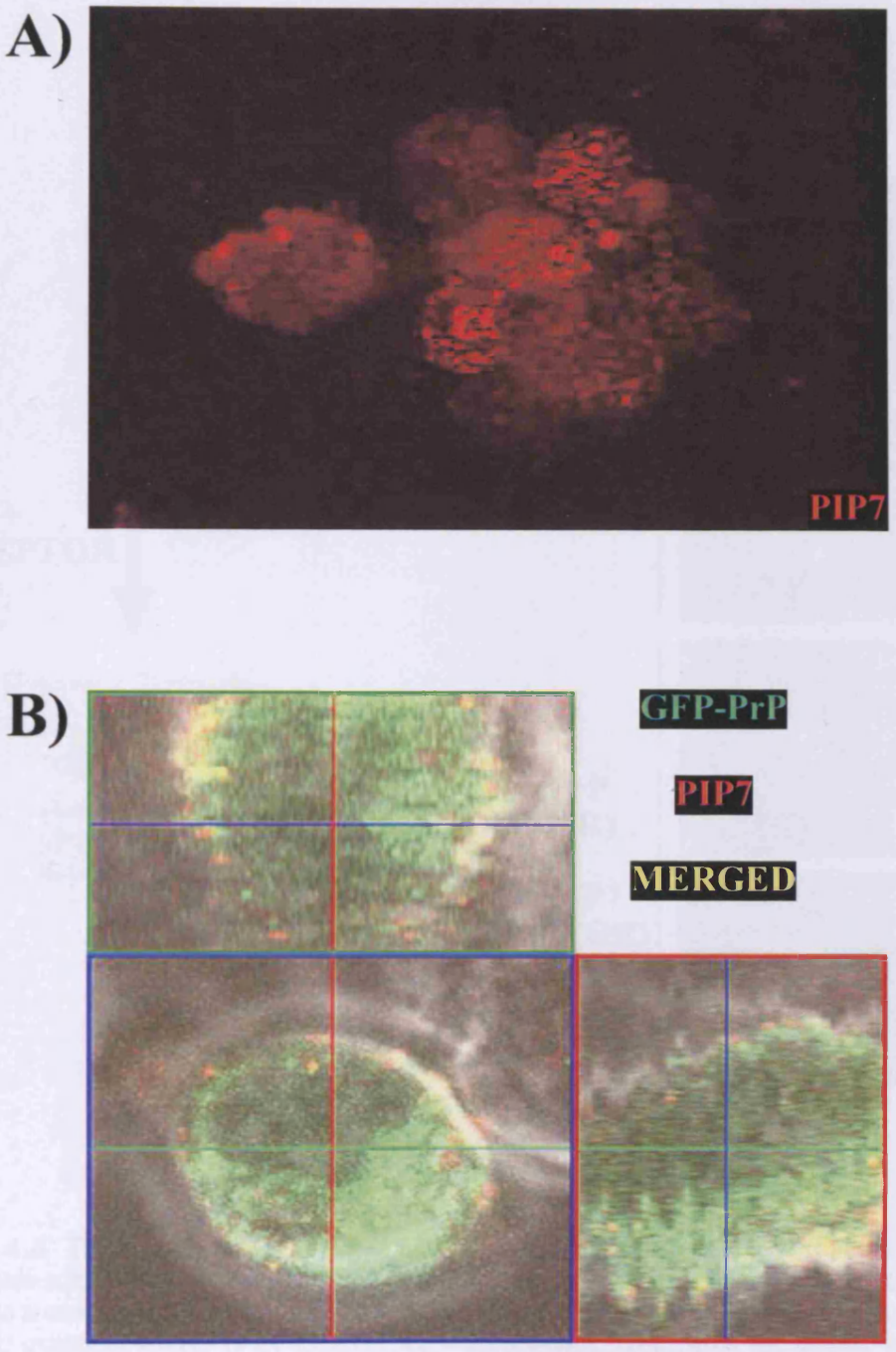

Figure 4.3 PrP-PIP7 co-localisation in the endocytic compartment.
A) Live N2a cells were incubated with PIP7 labelled antibodies at 4°C and shifted at 37°C before confocal analysis; the experiment showed the fast kinetic of endocytosis of the PIP7 protein when analysed. B) The experiment described in A) was repeated with GFP-PrP transfected cells. PrP-PIP7 co-localisation was observed on the cell surface and in vesicular compartment underneath the plasma membrane.

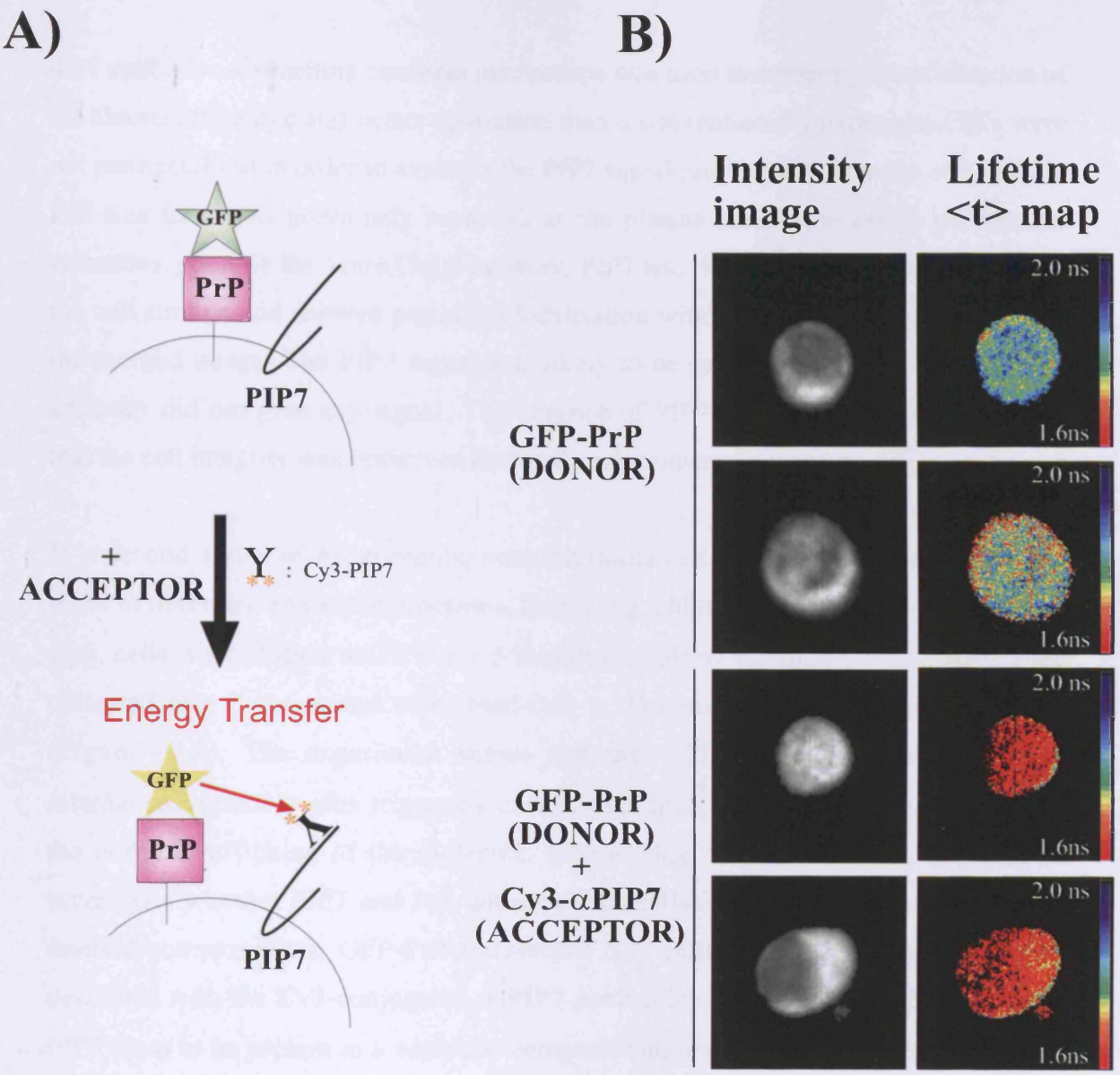

Figure 4.4 Direct interaction of PrP and PIP7 monitored by FRET/FLIM. A) Diagram schematising fluorescence lifetime imaging microscopy: FRET involves the transfer of energy from an excited donor molecule to a nearby spectrally overlapping acceptor. One method to quantify FRET is by measuring fluorescence lifetime of the donor, which is reduced as energy is transferred to the acceptor molecule. B) Epifluorescence Frequency Domain FLIM images of N2a cells transfected with GFP-PrP (donor) alone or in the presence of the acceptor PIP7 antibody (Cy3-αPIP7) as indicated. The left panels represent the intensity image of the donor fusion construct GFP-PrP whereas the right panels represent the calculated average lifetime maps of GFP-PrP alone or in presence of the acceptor PIP7 antibody. The lifetimes are shown on a pseudo-coloured scale from 1.6 ns (red) to 2.0 ns (blue).

4G4 antibody. A scanning confocal microscope was used to achieve greater emission of the fluorescence dye and better resolution than a conventional microscope. Cells were not permeabilised in order to evaluate the PIP7 signal present only from the cell surface. PrP was found, as previously reported, at the plasma membrane and in perinuclear structures, possible the Trans Golgi network. PIP7 was, instead, localised exclusively on the cell surface and showed partial co-localisation with the prion protein, as shown in the merged image. The PIP7 signal was likely to be specific since an isotype control antibody did not give any signal. The absence of PIP7 nuclear staining demonstrates that the cell integrity was preserved during the experimental procedure (Figure 4.2).

In a second series of experiments, neuroblastoma cells were preincubated at 4°C in order to minimize endocytic processes. Following addition of the α-PIP7 labelled with Cy3, cells were shifted to 37°C for 5 minutes, to allow internalisation. Images were collected in a Z series and assembled into a 3D reconstruction of a group of cells (Figure 4.3A). The experiment shows that the α-PIP7 antibodies can be rapidly internalised, possibly after triggering endocytosis upon protein clustering or following the normal trafficking of the molecule. Considering the above results, I wanted to investigate whether PIP7 and PrP not only co-localise on the cell surface but also in internal compartments. GFP-PrP transfected N2a cells were labelled, as previously described with the Cy3-conjugated α-PIP7 mAb prior to live imaging. Both PrP and PIP7 seem to be present in a vesicular compartment, underneath the plasma membrane (Figure 4.3B). At the present moment, it is difficult to conclude whether the observed vesicles are endosomes in the process of being internalised or recycling to the plasma membrane. Because of the short time frame of the experiment, they are more likely to reflect internalising vesicles. Further studies using specific vesicle markers should allow the complete dissection of the nature of the PrP-PIP7 association in the internal compartment.

4.2.1.3 In *vivo* interaction measured by FRET

Interactions between proteins in living cells are extremely dynamic, and techniques that simply co-localise putative partners offer only limited information about these interactions. Fluorescence Resonance Energy Transfer (FRET) measures distance-dependent interactions between the electronic excited states of two fluorescent

molecules. If the two molecules of interest are interacting in an *in vivo* context, excitation energy would be transferred from the donor molecule to the acceptor. The efficiency of FRET is inversely proportional to the intermolecular distance, therefore the phenomenon would only be observed if the donor and the acceptor are in close enough spatial proximity to allow physical interaction.

Since PrP and PIP7 have the ability to interact, as shown by co-immunoprecipitation, and they co-localise in the same cellular compartment, as observed by confocal microscopy, they were suitable candidates for an energy transfer approach, keeping in mind that protein-protein interaction is a requisite necessary but not sufficient to produce FRET. N2a cells were transfected with GFP-PrP, which would provide the donor molecule. Forty-eight hours post transfection, cells were fixed and, after permeabilisation, were incubated with the Cy3-conjugated α-PIP7 mAb, as an acceptor. The obvious choice for this experiment was the 4G4 clone, which in the co-immunoprecipitation experiment proved to be the only antibody compatible with the PrP-PIP7 interaction. A scheme of the experiment is represented on the left side and the result is presented on the right (Figure 4.4A and 4.4B respectively). There was a significant decrease in the donor lifetime, following the phenomenon of energy transfer, in the presence of the acceptor molecule. The experimental setting used did not permit determination of the exact location of the interaction; the FRET was measured as a mean intensity of the whole cell image. Further studies using a microscope with higher resolution would allow the discrimination of the specific sub cellular compartments involved in the energy transfer (e.g. endosomes); the FRET is so far the first piece of evidence for the *in vivo* protein-protein interaction between the prion protein and PIP7, in the presence of an intact cellular environment.

4.2.1.4 Determination of the PrP minimal binding region in PIP7.

The cDNA clone retrieved from the brain library consisted of the C-terminus of the PIP7 protein where two distinct structural domains are present: an unusual motif rich in glycines and methionines (approximately 200 amino acids long) and a RNA binding domain (90 amino acids). I wanted to narrow down the PrP interaction domain to one of

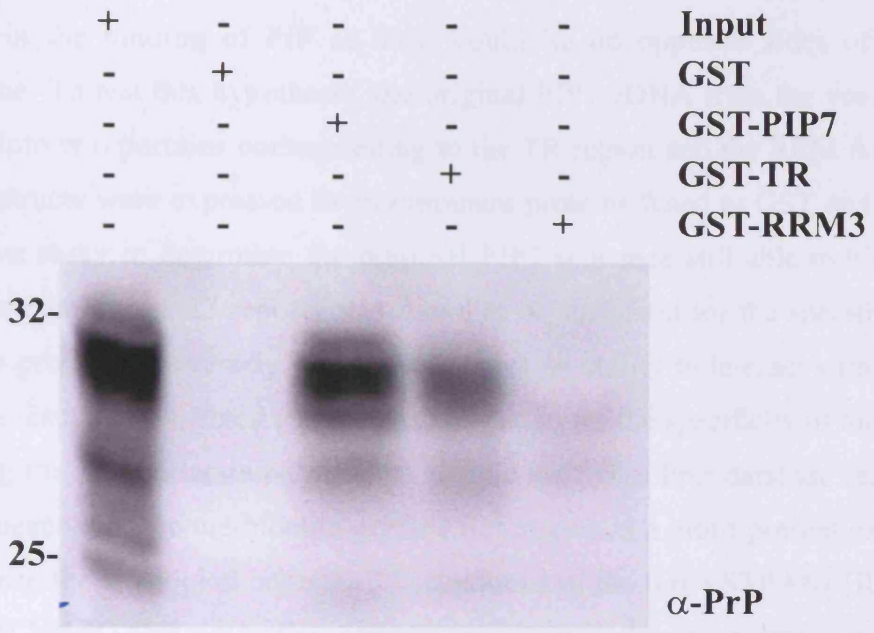

Figure 4.5 Determination of the PrP binding domain in the PIP7 protein. The PIP7 fragment present in the yeast clone contained two distinct domains: a region presenting 27 repetitions of a sequence rich in methionine-arginine-glycine (TR) and a RNA binding domain (RRM3). The single domains were expressed as GST fusion proteins and subject to pull down assay. The result shows that the Tandem Repeats region is sufficient to interact with PrP.

the above mentioned regions. *In Silico* analysis predicted a possible transmembrane helix between the Tandem Repeats region (TR) and the RRM3 domain in PIP7; if the prediction was correct, there could be no direct cooperation between the two different regions in the binding of PrP as they would lie on opposite sides of the plasma membrane. To test this hypothesis, the original PIP7 cDNA from the yeast clone was divided into two portions corresponding to the TR region and the RRM domain alone. The constructs were expressed as recombinant proteins fused to GST and subject to a pull down assay to determine the minimal PIP7 sequence still able to bind PrP. The region containing the 27 repeats was found to be sufficient for the specific binding to the prion protein. Conversely, the RRM3 shows no ability to interact with PrP (Figure 4.5). The results also offered a possible explanation for the specificity of the interaction; searching for RRM containing proteins against the Swiss Prot database retrieved 4522 entries meanwhile the methionine-glycine rich region is a motif present exclusively in PIP7. Since the TR region contains 27 repetitions of the [GEVSTPAN]-[ILMV]-[DE]-[RH]-[MLVI]-[GAV] no further attempt to minimise the interacting region has been made but future experiments based on peptide competion will confirm the present observation.

4.2.1.5 PrP-PIP7 requirements for binding

The PIP7 protein had been reported in the literature as a receptor for thyroglobulin and CEA. I tried to use this previous knowledge towards the elucidation of the mechanism of its novel interaction with PrP.

The synthesis of the thyroid hormone involves several steps, including secretion by thyrocytes and maturation in the follicular lumen of the thyroid (Malthiery and Lissitzky, 1987). Since studies had revealed a period of 48 hrs in order to achieve complete maturation, it had been proposed that thyroglobulin is internalised by thyrocytes. However, the hormone has to escape degradation by lysosomes and this had been proposed to occur through a mechanism called "receptor mediated exocytosis". A protein located on human chromosome 19 had been cloned as a monomer of the N-acetylglucosamine-specific receptor for the thyroid hormone and further analysis had demonstrated that the sequence was identical to the one of human hnRNP M4 (Blanck et al., 1994; Blanck et al., 1995). Interestingly, the interaction between thyroglobulin and its N-acetylglucosamine-specific receptor was reported to be both calcium and pH

dependent. In light of this information, the influence of these criteria on the PIP7-PrP interaction was investigated using the previously established GST pull down assay.

Calcium dependency

PIP7, as mentioned before, acts as receptor for the Carcino Embryonic Antigen (CEA) and for thyroglobulin. In both cases, investigators had reported a strict requirement for calcium ions in the ligand-receptor interaction.

PIP7 did not present any apparent sequence homology with C-type lectins, cation dependent receptors containing carbohydrate recognition domains (CRD), consisting of two anti-parallel beta strands and two alpha helices but the TR region contains negative charged amino acids that have been suggested as a potential coordination site for calcium ions. Moreover, the interaction between PrP and PIP7 was originally described in the yeast cytoplasm, where neither of them could have been glycosylated, suggesting that the presence of sugar chains was in principle not an absolute requirement for the interaction. However, I wanted to test whether the presence of calcium could contribute in establishing the binding.

The standard protocol for purification of fusion proteins included 1mM EDTA in the buffer used, a concentration sufficient to chelate endogenous concentrations of calcium and magnesium. Nevertheless, it could not be excluded an inhibitory effect when the putative coordination site of the repeat regions were loaded with exogenous calcium. The GST pull down was performed in the presence of an end-point concentration of 10 mM $CaCl_2$ which resulted in a detectable decrease in the amount of PrP bound, compared to the untreated situation or when the experiment was performed in presence of 10 mM EDTA. When calcium and EDTA were added together, the chelating agent was able to block the inhibitory effect of calcium and the PrP-PIP interaction had the same efficiency as the untreated sample (Figure 4.6). Taken together, the presence of calcium ions was not only necessary to establish but partially prevented the PIP7-PrP interaction.

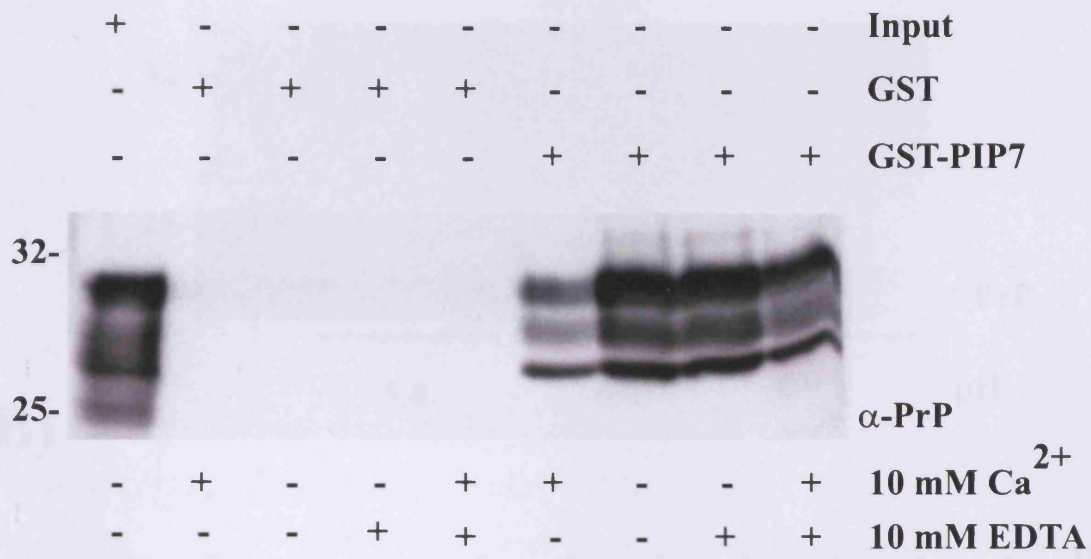

Figure 4.6 The role of calcium ions in PrP-PIP7 interaction.
The standard pull down assay was performed in the presence of exogenous calcium ions and/or EDTA. A significant reduction in the amount of PrP bound to PIP7 was observed when calcium was added to the buffer. EDTA alone had no apparent effects and was able to restore initial binding intensity, when added in combination with calcium.

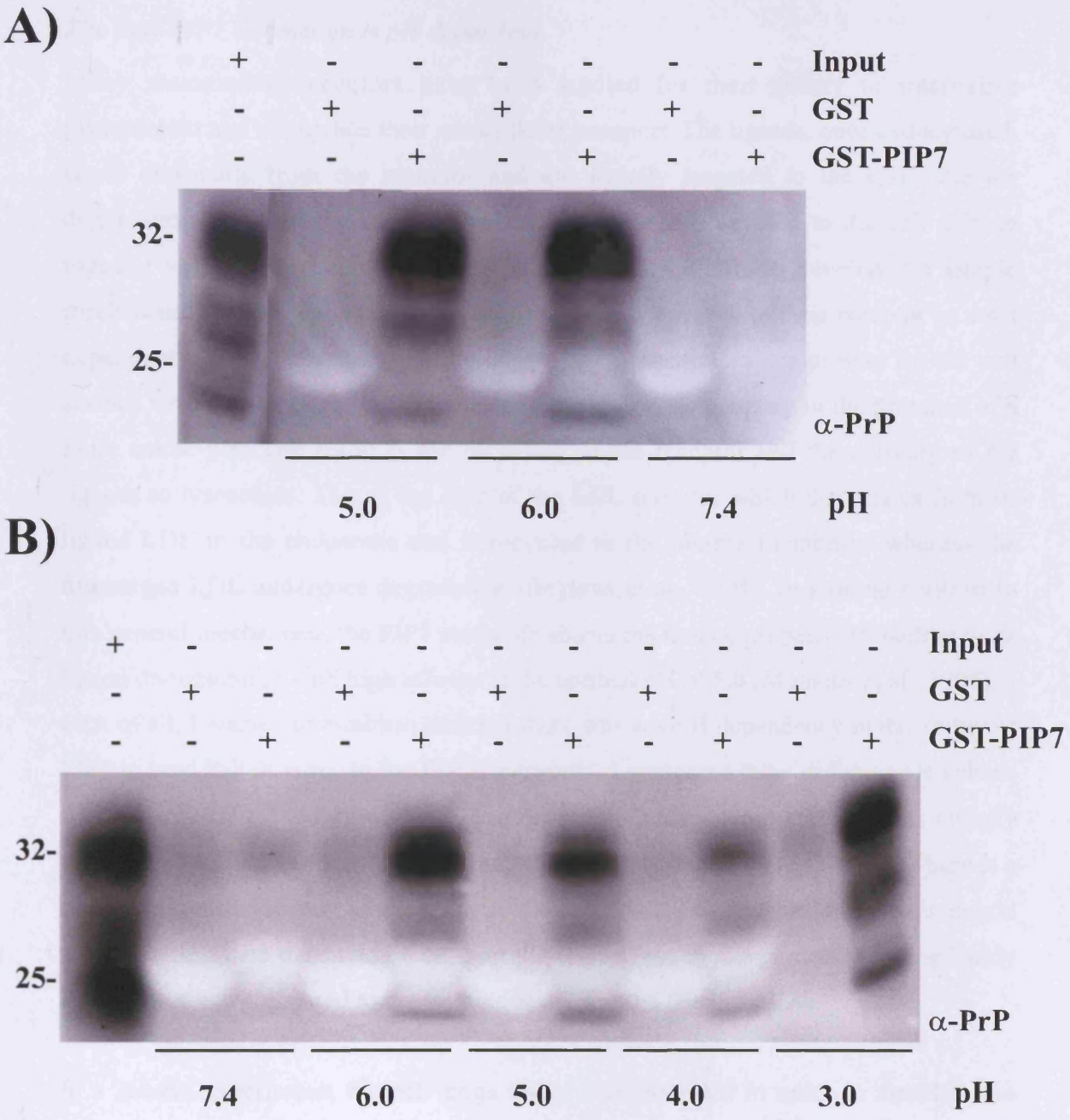

Figure 4.7 pH dependency of the PrP-PIP7 interaction.
Mouse total brain homogenate was equilibrated at the specified pH and subject to GST pull down with GST alone or with GST-PIP7; two independent experiments are here presented: A) PrP-PIP7 interaction was more easily detectable at pH values lower than the physiological 7.4, at which value the interaction is only barely detectable. B) The experiment described above was repeated testing an extended range of pH values. Interaction was stronger at the mild acidic value of 6.0 and at the most extreme value of 3.0. Despite of the pH used in the experiment, the interaction was exclusively specific to PIP7, since no binding was detected with GST alone.

The PrP-PIP7 interaction is pH dependent.

Many mammalian receptors have been studied for their ability to internalise glycoprotein and to regulate their intracellular transport. The ligands, once endocytosed, could dissociate from the receptor and are usually targeted to the lysosome for degradation or, as in the case of Tranferrin molecules, recycled to the cell surface together with their receptors (Alberts et al., 1994). Cells have developed a simple mechanism to recycle the receptors: many ligands interact with their receptor in a pH dependent manner. Optimal binding occurs at the neutral values present on the cell surface whereas the complex dissociates in the endocytic pathway in the presence of a more acidic pH. The result is the recycling of the receptor and the delivery of the ligands to lysosomes. This is the case of the LDL receptor which dissociates from its ligand LDL in the endosome and is recycled to the plasma membrane whereas the discharged LDL undergoes degradation (Beglova et al., 2004). In striking contrast to this general mechanism, the PIP7 molecule shows the unique property of binding to its ligand thyroglobulin with high affinity at the optimal pH of 5.0 (Miquelis et al., 1987).
First of all, I wanted to establish whether there was any pH dependency in the ability of PIP7 to bind PrP *in vitro*. In the first experiment, I compared three different pH values, which might reflect the physiological environments encountered by PrP on its journey from the plasma membrane (pH 7.4) to the lysosomal compartment (pH 5.0). There is a clear preference for interaction at an acidic pH: the binding at pH 7.4, which should mainly recapitulate the situation on the cell surface, was in this particular setting barely detectable when compared to the binding at pH 6 and 5 (Figure 4.7A).

In a second experiment, the pH range tested was extended in order to establish the optimal value for the interaction. The range spanned from the physiological value of pH 7.4 to the extreme acidic value of pH 3.0 (Figure 4.7B). The binding was stronger at a mild acidic value (6.0) and decreased proportionally to a minimum value (4.0). The interaction between GST and Glutathione beads was stable and comparable in the range from pH 7.4 to 4.0, as revealed by Ponceau staining of the membrane, and allowing a direct correlation between the binding strength and the pH value. Most surprisingly, the PrP enrichment was even more pronounced at the lowest value tested (3.0), originally included in the test as an end point value at which no interaction was expected to be detected. The result obtained at pH 3 is even more striking because the Ponceau analysis

revealed that only approximately 20% of fusion proteins were present on the sepharose beads at the end of the washing procedure, possibly due to the instability of the GST-glutathione interaction in such extreme condition. Nevertheless, even if the beads presented on their surface a smaller amount of fusion proteins compared to all the other samples, the maximal interaction between PrP and PIP7 was observed at this pH. However, it is difficult to find a rational explanation since no cellular compartment shows such acidic conditions.

In both experiments GST alone was not sufficient to bind PrP at any pH tested. In light of this evidence, it is possible to conclude that, in the *in vitro* GST pull down assay, the interaction preferentially occurs at an acidic pH. However *in vivo* data are required to confirm the significance of these findings in a more physiological setting.

4.2.2 Reciprocal co-regulation of PrP-PIP7 surface levels.

4.2.2.1 PrP overexpression leads to PIP7 surface accumulation.

During the microscopy assay described above (Figure 4.2), I noticed that the strongest PIP7 immunostaining was observed preferentially in the cells showing the highest PrP-GFP expression, I therefore further investigated a possible direct correlation between PrP and PIP7 surface levels.

Human 293T cells were transfected, as described, with the GFP-PrP construct used in the co-localisation study and analysed by surface flow cytometry; a GFP plasmid was used as a negative control to exclude any artefact due to the transfection protocol used and to judge the specific effect of PrP overexpression. The transfection efficiency was estimated at around 50% by microscopic observation. Figure 4.8 panel A) shows the appearance of a discrete population of cells expressing high levels of PrP whereas in panel D) an increase in PIP7 surface levels (marked by a red arrows) is observed specifically in the GFP-PrP transfected cells. Subsequential analysis, with FLOWJO software, allowed the distinction between transfected (GFP positive) and untransfected (GFP negative) cells to be made. PrP and PIP7 levels were unaltered in the GFP negative subset (panels B and E) despite of which plasmid was used for the transfection.

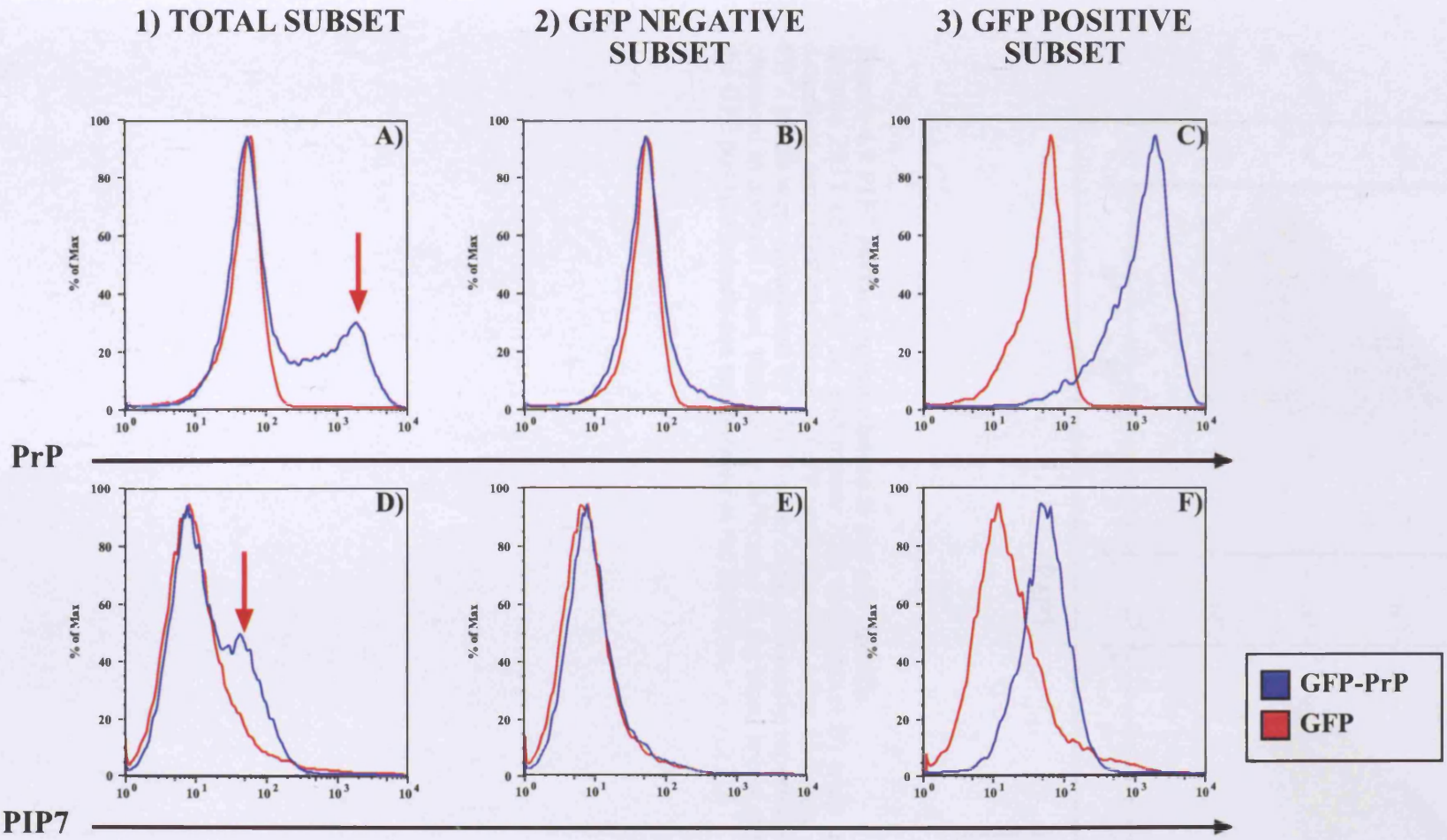

Figure 4.8 PrP overexpression leads to PIP7 surface accumulation.
Human 293T cells were transiently transfected with a GFP-PrP fusion construct (blue line) or GFP alone (red line), as negative control. Forty-eight hours after transfection, cells were fixed and stained with PrP and PIP7 antibodies and surface protein levels were monitored using a FACScalibur device. Total subset cells are represented (1) or specifically transfected (2) or untransfected (3) populations by gating according to the presence or absence of the GFP signal. PIP7 levels were specifically increased in cells transfected with the PrP encoding plasmid and not the empty vector (compare C and F).

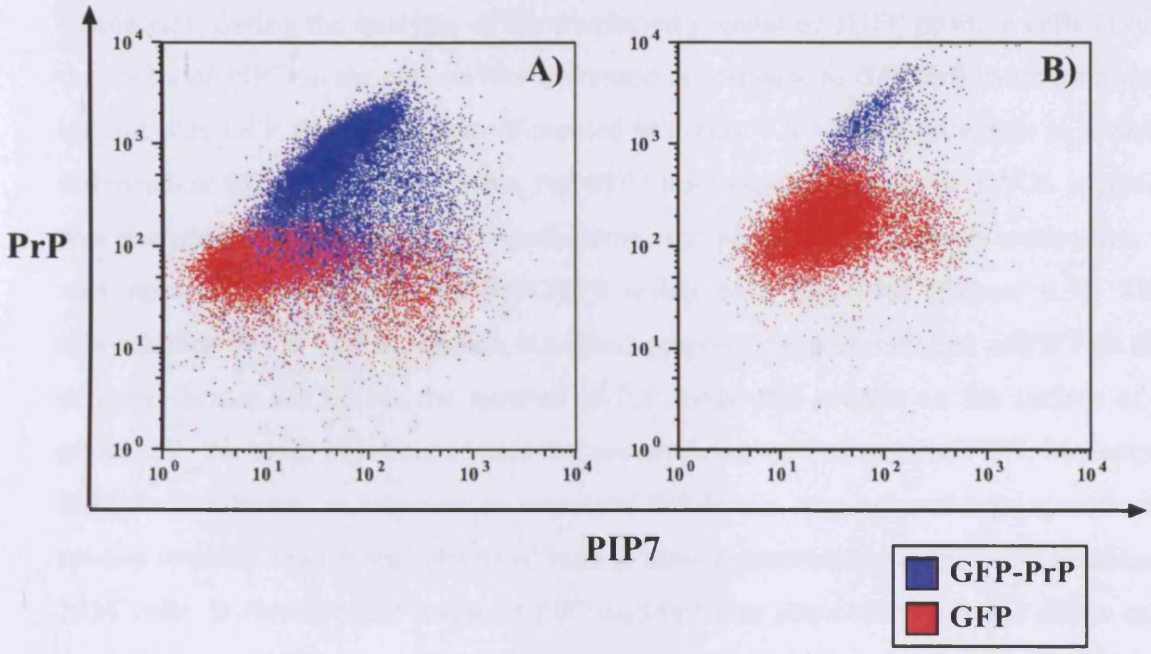

Figure 4.9 PIP7 surface accumulation is not cell specific.
Human 293T cells (panel A) and mouse N2a cells (panel B) were transfected, as previously described, with GFP-PrP (blue) or GFP (red) plasmid. After 48 hours, cells were fixed and PrP-PIP7 levels were monitored by FACS assay. The previously reported surface accumulation was observed in both cell lines, despite the difference in the basal levels of the studied proteins. Only the GFP positive subsets are represented in the Dot Plot.

In contrast, during the analysis of the tranfected population (GFP positive cells only), the levels of PIP7 on the cell surface increased in response to GFP-PrP overexpression but not with GFP alone. The data illustrated in Figure 4.8 were reproducible in several independent experiments. Since the PrP-PIP7 immunostaining for the FACS analysis was performed within the same sample using isotype specific secondary antibodies, it was possible to visualise the PrP-PIP7 levels in a Dot Plot (Figure 4.9). The consequence of PrP overexpression is a direct proportional accumulation of PIP7 on the cell membrane: the higher the number of PrP molecules present on the surface of a given cell, the more pronounced was the accumulation of endogenous PIP7. Moreover PIP7 accumulation, in response to increased PrP levels, was not cell type specific or species specific since it was observed both in mouse neuroblastoma cells and in human 293T cells. Different basal levels of PIP7 and PrP was also observed in the above cell lines: PrP and PIP7 appeared to be more highly expressed in N2a compared to 293T, although this observation could in principle reflect as well differences in the antibody affinities between mouse and human proteins.

4.2.2.2 PrP structural requirements for PIP7 accumulation

In order to better characterise the direct proportionality observed, different PrP mutants were tested in the FACS assay with the aim to understand which features of the prion protein are required for PIP7 accumulation.

Different PrP N-terminal deletion mutants have been generated in the past with the purpose of defining the minimal region able to support scrapie pathogenesis. Transgenic mice harbouring two of the constructs, named ΔE and ΔF (respectively missing residues 32-123 and 32-134 respectively), surprisingly developed ataxia and neurodegeneration of cerebellar cells. When expressed in N2a cells, they were shown to be correctly processed and reach the cell surface (Shmerling et al., 1998).

When used in the above FACS assay, both ΔE and ΔF were able to accumulate PIP7, as had been observed for the full length PrP (Figure 4.10 and data not shown). In the same experiment, cells transfected with the wild type construct presented an approximately 3 fold increase in surface levels of PrP meanwhile cells transfected with the ΔE mutant resulted in a 4.5 fold increase, possibly due to less efficient internalisation of the mutant molecule (Lee et al., 2001b).

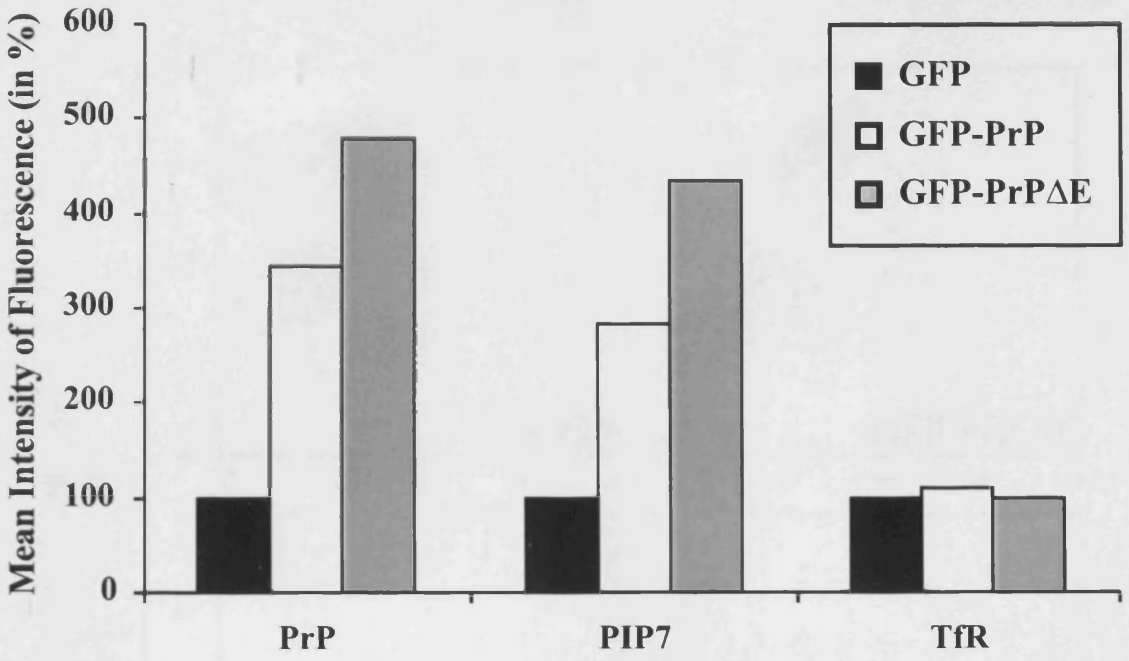

Figure 4.10 Specific effect of PrP overexpression on PIP7 surface levels. Human 293T cells were transfected with an empty GFP vector or with constructs encoding GFP-PrP wild type or the N-terminal deletion ΔE. Forty-eight hours post transfection, samples were fixed and stained with the above-indicated antibodies. PrP levels were greatly increased by ectopic overexpression; this resulted in a concomitant accumulation on the cell surface of endogenous PIP7. The levels of Transferrin Receptor (TfR) did not change, arguing that PIP7 surface accumulation was a specific result of PrP overexpression. The mutant construct ΔE has been reported to show abnormal endocytic behavior as reflected here by the higher surface levels achieved post-transfection; as a consequence, also PIP7 levels were higher.

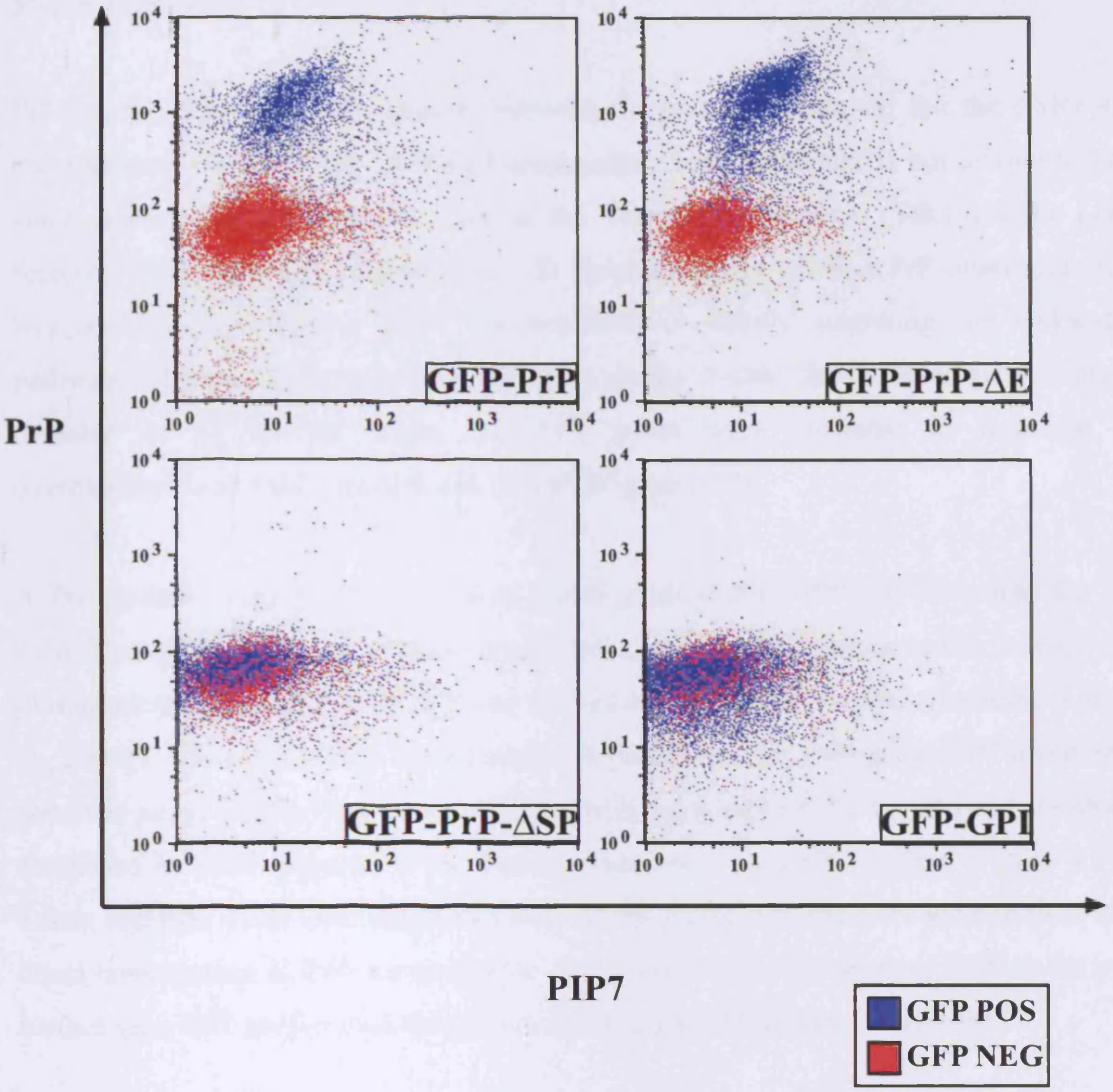

Figure 4.11 PrP structural requirements for PIP7 surface accumulation. Transiently transfected 293T cells expressing wild type GFP-PrP, mutants GFP-PrP-ΔE, PrP-ΔSP or GFP-GPI were fixed and analysed by FACS. In order to provide an internal control, transfected cells, (blue) and untransfected cells (red) were compared for each construct. Full length GFP-PrP and the N-terminal deletion construct ΔE generated a proportional increase in PIP7 surface levels. Conversely, the increase was not observed either when a PrP mutant lacking the signal peptide was expressed or when a minimal GFP construct was targeted to the plasma membrane via a GPI moiety.

Alteration in PrP levels resulted in a proportional increase in PIP7 levels (2.8 and 4.3 fold respectively).

PrP has the ability to cycle rapidly between the plasma membrane and the endocytic compartment via a clathrin mediated mechanism. Such behaviour is not unique to PrP since other membrane proteins such as the Transferrin Receptor (TfR) and the LDL receptor share the same characteristic. In order to assess whether PrP overexpression was specifically affecting PIP7 accumulation or simply saturating the endocytic pathway, I monitored the levels of TfR as a suitable control: the observed accumulation revealed to be specific since the TfR levels were unaltered in response to overexpression of wild type and mutant PrP (Figure 4.10).

A PrP mutant, lacking the N-terminal signal peptide (GFP-PrP-ΔSP) required for the correct translocation to the endoplasmatic reticulum has been shown to fail to reach the plasma membrane and has been found to localise exclusively in the cytoplasm (Lee et al., 2001b). When cells were transfected with this mutant no increase in PIP7 levels was observed as no difference was observed in cells transfected with the minimal construct composed by GFP targeted to the plasma membrane by a GPI anchor (Figure 4.11). Taken together, these data suggested that: a) the increase in the PIP7 surface pool is a direct consequence of PrP accumulation on the cell surface b) targeting GFP to the cell surface via a GPI anchor moiety was not sufficient to accumulate surface PIP7.

To further confirm that PrP alone, and not the GFP moiety of the fusion protein was responsible of the observed PIP7 behaviour, I transfected a vector encoding untagged PrP or a empty control vector into human 293T cells. The result obtained with the GFP-PrP construct was successfully reproduced, as overexpression of untagged PrP caused PIP7 surface accumulation, suggesting there was no contribution of the GFP tag which theoretically could alter PrP structure by steric hindrance and be in part responsible for the stabilisation of the PrP-PIP7 interaction (Figure 4.12).

4.2.2.3 Reduction of PIP7 surface levels by treatments aimed to reduce PrP levels

To further dissect the biology of the novel interaction I applied different drug treatments.

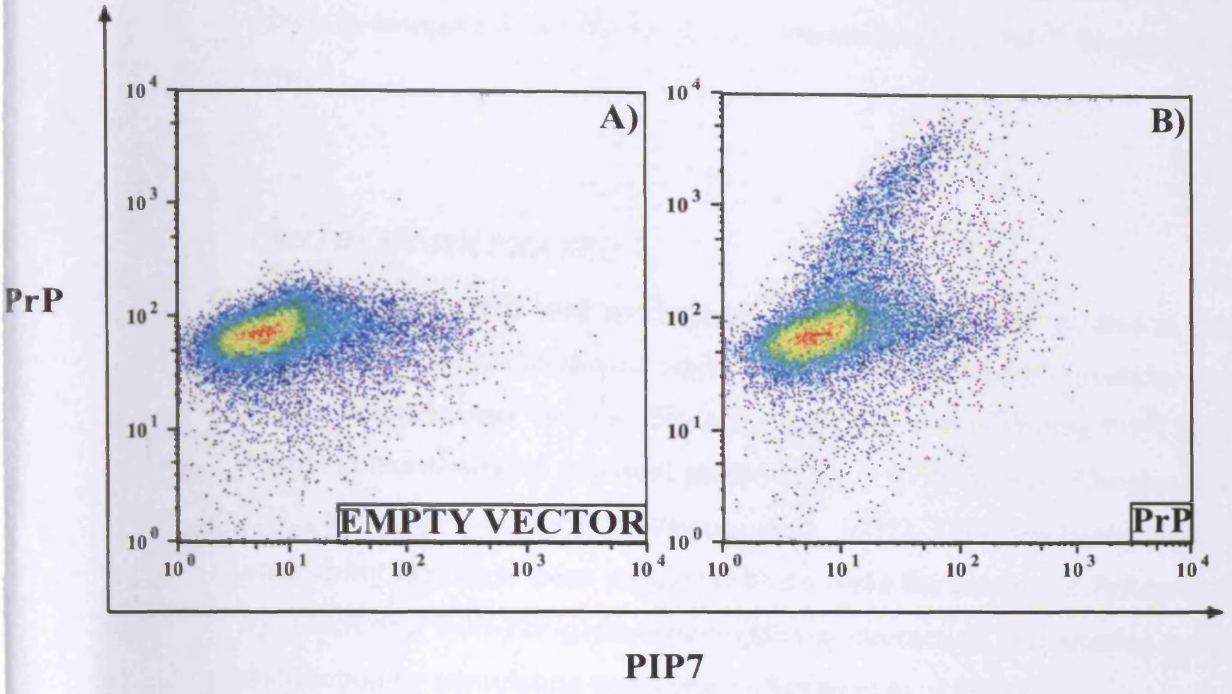

Figure 4.12 PrP overexpression, like GFP-PrP, increases PIP7 levels. Human 293T cells were transfected with an empty vector (A) or with vector encoding untagged PrP (B). After fixation, samples were stained with PrP and PIP7 antibodies and processed by flow cytometry. PIP7 accumulation was observed only as direct consequence of PrP overexpression. The result argued against any possible contribution of the GFP tag in stabilising PIP7 surface levels.

The choice of treatments was based on prion literature and more emphasis has been given to compounds which have been shown to affect PrP^{Sc} biogenesis *in vitro* or *in vivo*.

PENTOSAN SULPHATE

Polyanionic glycans, such as Pentosan Sulphate, have been studied in the past twenty years as a potential therapeutic agent against prion disease progression. Originally used against conventional viruses, they proved effective in inhibiting PrP^{Sc} accumulation *in vitro* and demonstrated potential prophylactic activity *in vivo* (Caughey and Raymond, 1993; Farquhar et al., 1999; Ladogana et al., 1992). Their mechanism of action remains unclear but they have been suggested to decrease the amount of PrP on the cell surface by interfering with PrP-glycosaminoglycans interaction and altering its physiological distribution by stimulating endocytosis (Shyng et al., 1995a).
In the next set of experiments, the aim was to alter the newly established surface steady-state, characterised by high levels of exogenous PrP and endogenous PIP7, by stimulating PrP endocytosis and follow the fate of PIP7 molecules. I decided to use GFP-PrP since, as previously shown, the fusion protein appeared to be functional and allowed easy discrimination between transfected and untransfected cells. GFP-PrP-ΔE was included in the panel as the minimal mutant that was still able to produce PIP7 surface accumulation. Finally, the GFP-PrP-ΔSP mutant, unable to produce PIP7 surface accumulation, was used as a negative control (Figure 4.13).

The experimental protocol included transfection of the above constructs and subsequent treatment with Pentosan Sulphate (100 μg/ml) for 24 hrs. Samples were fixed and double stained with α-PrP and α-PIP7 monoclonal antibodies. In line with previous experiments, PIP7 accumulation was observed in the samples transfected with wild type PrP and the ΔE mutant but not with the ΔSP. Pentosan Sulphate treatment has been shown to lower PrP levels by triggering endocytosis and was able to decrease PrP levels by approximately 50% (Figure 4.14). This led to a parallel decrease in PIP7 levels to a comparable extent (70%). PrP-ΔE still retained the ability to get internalised in response to PS stimulation and a proportional PIP7 decrease was also observed.

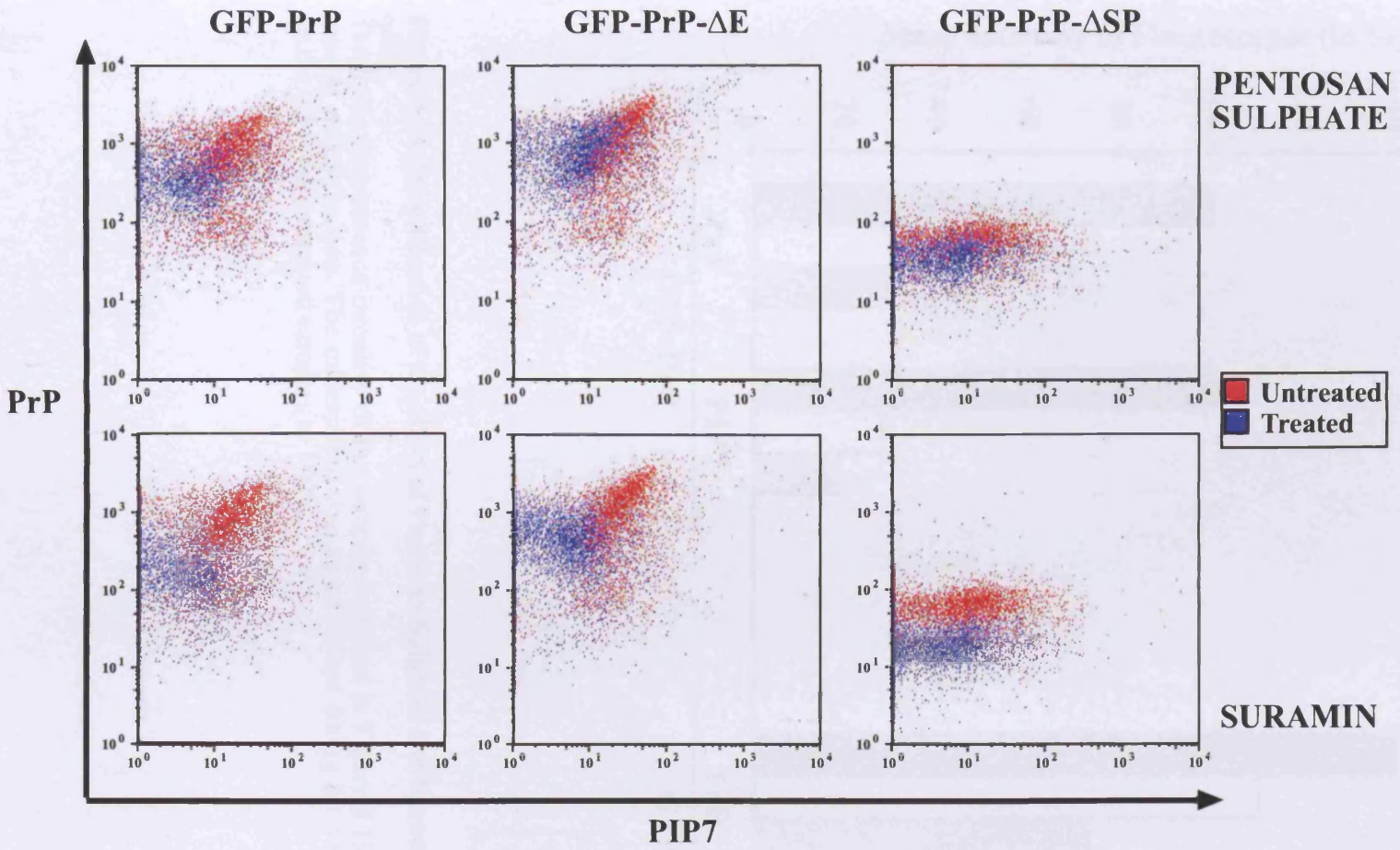

Figure 4.13 Decrease in PIP7 surface levels after treatments intended to reduce PrP levels.
Human 293T cells were transfect with GFP fusion constructs encoding wild type PrP or mutant versions of the protein. After 24 hours, Pentosan Sulfate (100 μg/ml) or Suramin (200 μg/ml) were added to the media and cells were examined the following day for the amount of PrP and PIP7 present on their surface. Both treatments produced a decrease in PrP surface levels; which was mirrored by PIP7 reduction. Cells transfected withPrP ΔSP did not accumulate either exogenous PrP or PIP7 on their surface but the endogenous levels were responsive to the applied treatments. Only GFP positive populations are shown in the analysis.

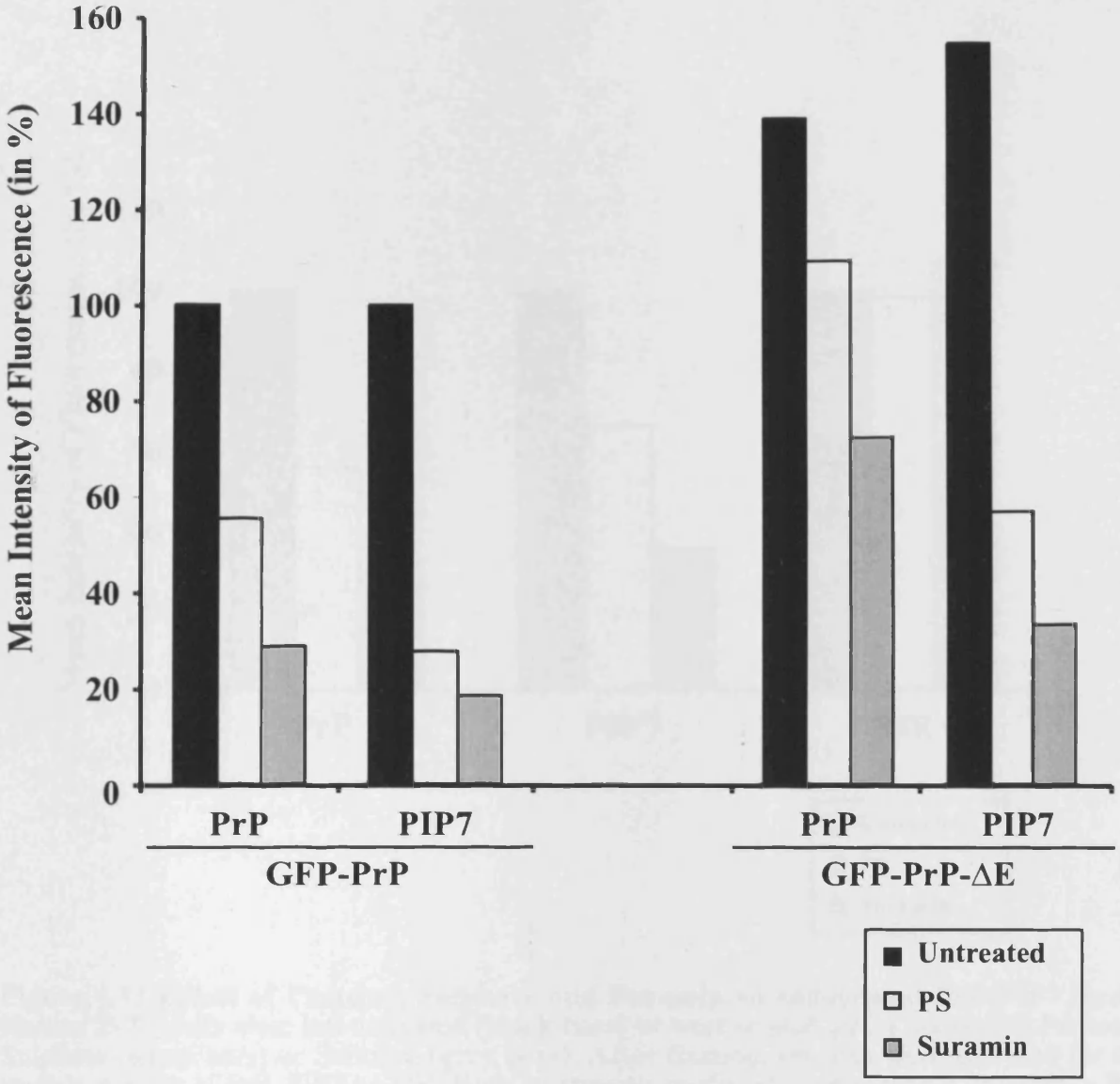

Figure 4.14 Quantification of the effect of Pentosan Sulphate and Suramin on PrP transfected cells.
The mean fluorescence intensity of the samples analysed in Figure 4.13 was plotted for more precise quantification. The experiment was standardised fixing the values of PrP and PIP7 on the GFP-PrP untreated samples to 100%.

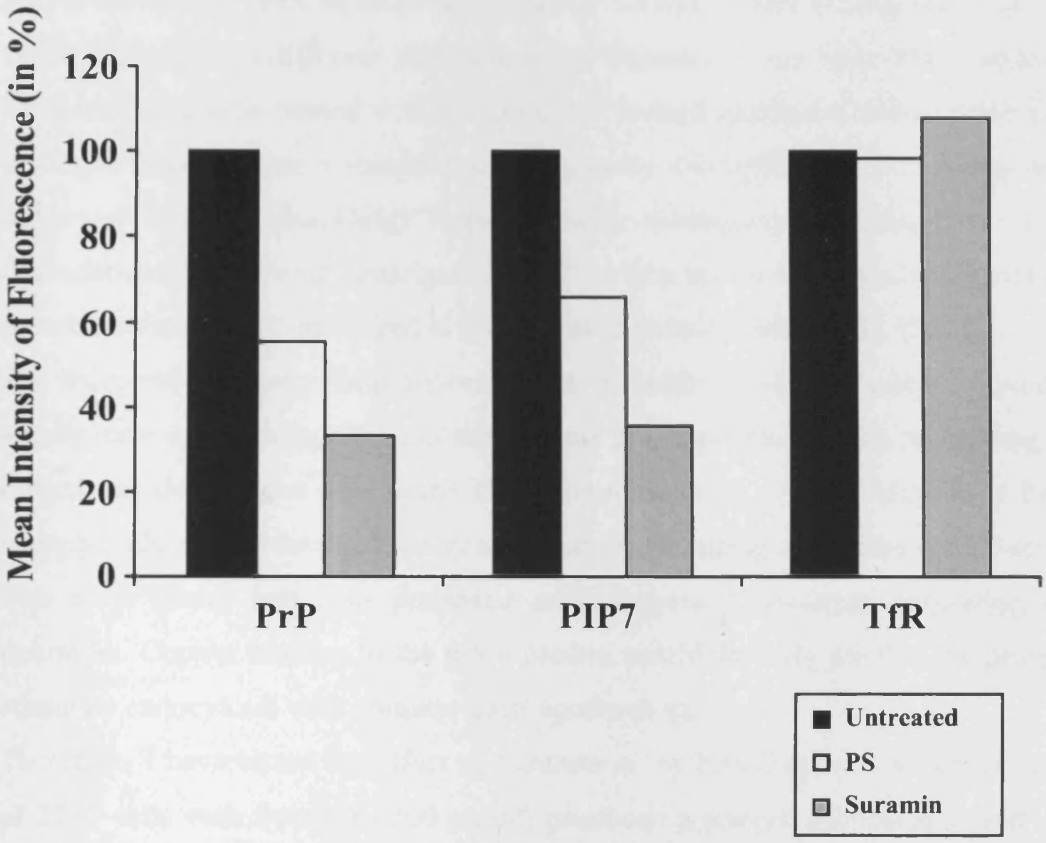

Figure 4.15 Effect of Pentosan Sulphate and Suramin on endogenous PrP-PIP7 levels. Human 293T cells were left untreated (black bars) or were treated for 24 hours with Pentosan Sulphate (white bars) or Suramin (grey bars). After fixation, samples were analysed for the surface content of PrP, PIP7 or TfR. Both treatments produced a reproducible decrease in PrP surface levels and in parallel also the PIP7 surface pool was reduced. The treatments did not produce significant changes in the levels of TfR.

SURAMIN

Suramin was originally developed to treat trypanosomiasis but proved to have a partial anti-prion effect when injected in a hamster scrapie model (Ladogana et al., 1992). More recently two different mechanisms of Suramin action have been proposed. In neuroblastoma cells treated with Suramin, PrP formed aggregates and partitioned in the insoluble fraction when a standard solubility assay was performed. PrP aggregation was observed in the Trans-Golgi Network, with subsequent targeting for lysosomal degradation. As a direct consequence, PrP surface levels were drastically reduced in Suramin treated cells, compared to the untreated sample (Gilch et al., 2001).

An independent study demonstrated that Suramin could not only stimulate PrP aggregation in the intracellular compartments but could also induce misfolding of PrP directly at the plasma membrane (Kiachopoulos et al., 2004). Misfolded PrP was subsequently rapidly internalised by a mechanism requiring its unstructured N-terminus. The same group had also proposed an analogous mechanism following copper treatment. Copper binding to the prion protein would partially misfold the protein and stimulate endocytosis with consequential uptake of the ions.

Therefore, I have tested the effect of Suramin in my FACS assay. Overnight treatment of 293T cells with Suramin (200 μg/ml) produced a marked decreased in PrP surface levels with an analogous decrease in the PIP7 pool (Figure 4.13 and 4.14). Suramin proved even more effective than PS. PrP levels showed a reduction of more than 70% in cells transfected with wild type PrP and 40% in cells receiving the ΔE construct. Conversely, a PIP7 decrease in the order of 75 and 80% was observed for both constructs.

In summary, a direct proportionality was again observed, regardless of which treatment was used: PIP7 surface levels were reduced in response to decrease of surface PrP. Treatments produced the same effect not only in transfected cells but also on endogenous protein levels, arguing against any transfection artifact and most importantly the drugs effect was specific for PrP and PIP7 since the TfR levels were unaltered (Figure 4.15).

PIPLC

Treatments with the phosphatidyilinositol specific phospholipase C (PIPLC) have been shown to release the prion protein from the cell surface (Borchelt et al., 1990). Neuroblastoma N2a cells were chosen for this particular experiment because of their higher amount of surface PrP compared to 293T. Untransfected cells were treated with PIPLC (250 mU/ml) for 2 hrs at 37°C and PrP-PIP7 surface levels were analysed by FACS. Upon treatment, almost all the PrP (>80%) present at the plasma membrane had been removed. When cells were stained with the 4G4 specific α-PIP7 antibody, a concomitant decrease in surface PIP7 levels was observed (30%). Once again the TfR was used as a control to assess specificity and its levels remained unchanged following the enzymatic treatment (Figure 4.16).

4.2.2.4 PIP7 accumulation is independent on PrP endocytosis.

Previous experiments have shown that PIP7 accumulation is dependent on correct localisation of PrP on the cell surface. Once PrP reaches the plasma membrane, molecules get rapidly internalised and, via a recycling compartment, mainly redirected back to the cell surface, with a small percentage targeted to lysosomes. PIP7 accumulation seemed to be the direct consequence of protein-protein interaction occurring primarily on the cell surface. An alternative scenario would be the increased recycling from the acidic compartment back to the cell surface, as originally proposed for the thyroglobulin receptor and suggested by the data I presented showing the higher interaction affinity at acidic pH (Blanck et al., 1994). Cells ectopically expressing the prion protein would not only have increased surface levels but possibly also an increased amount in the endocytic/recycling pathway. The N-terminus of the prion protein contains a characteristic motif rich in positively charged amino acids (KKRPKP) suggested to mediate interaction with sulphated proteoglycans, molecules known to stimulate PrP^C endocytosis (Pan et al., 2002). Substitution of three basic residues generating KQHPHP (a mutant which for simplicity is referred to as NGAG) had the dramatic result of completely abolishing PrP endocytosis (Sunyach et al., 2003).

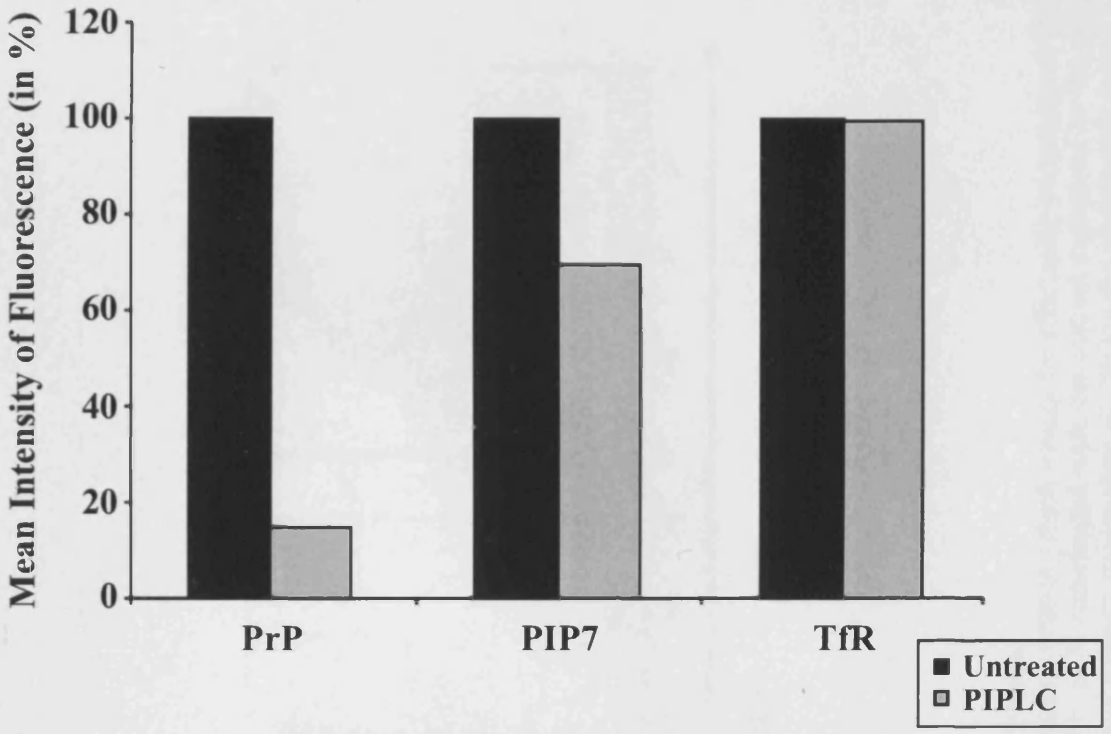

Figure 4.16 PIPLC treatment of N2a cells.
Mouse neuroblastoma N2a cells were treated with 250 mU/ml of PIPLC for 2 hours at 37°C (grey bars) or left untreated (black bars). Following fixation, cells were stained for PrP, PIP7 and TfR. The figure shows only relative amounts present on the cell surface after treatment.

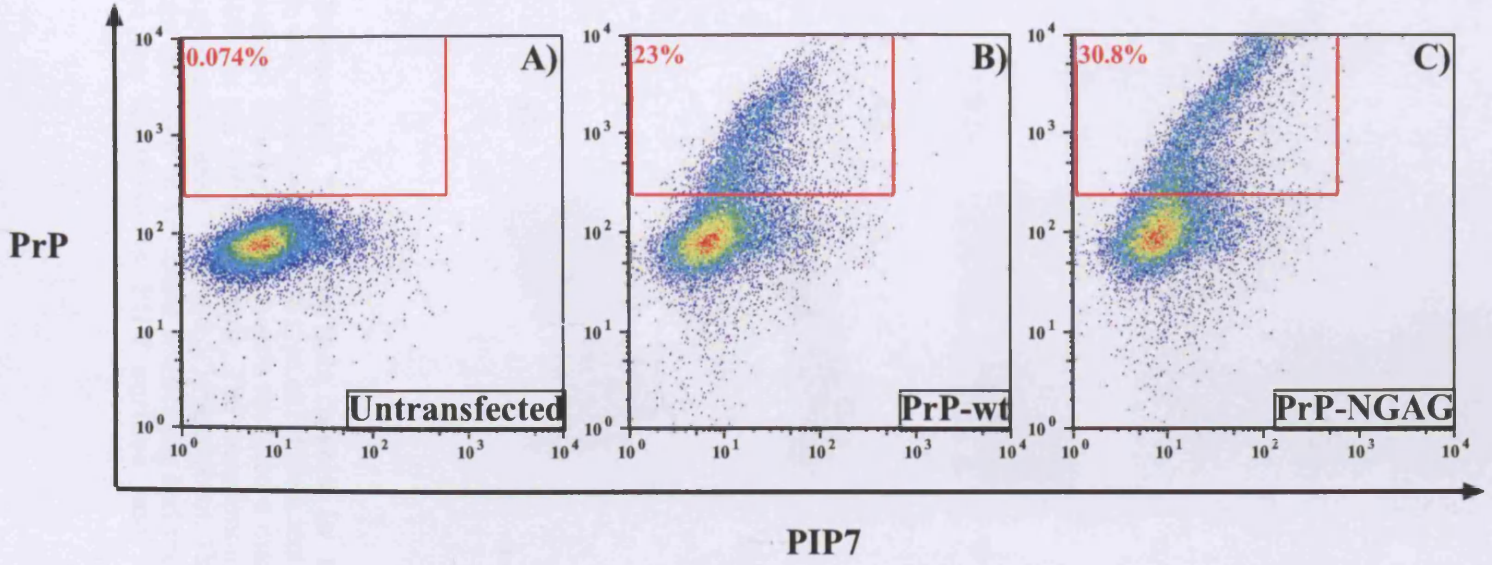

Figure 4.17 PIP7 surface accumulation does not require PrP endocytosis.
Human 293T cells were transfected with a PrP wild type construct or with a mutant which cannot be efficiently endocytosed (NGAG). Double staining analysis by FACS reveals higher PrP levels detected in cells transfected with the mutant compared to the wild type; however the proportional accumulation of PIP7 is still observed suggesting a direct stabilisation of PIP7on the plasma membrane, without the necessity to transit through the endocytic compartment. Percentages indicate the proportion of cells present in the selected area.

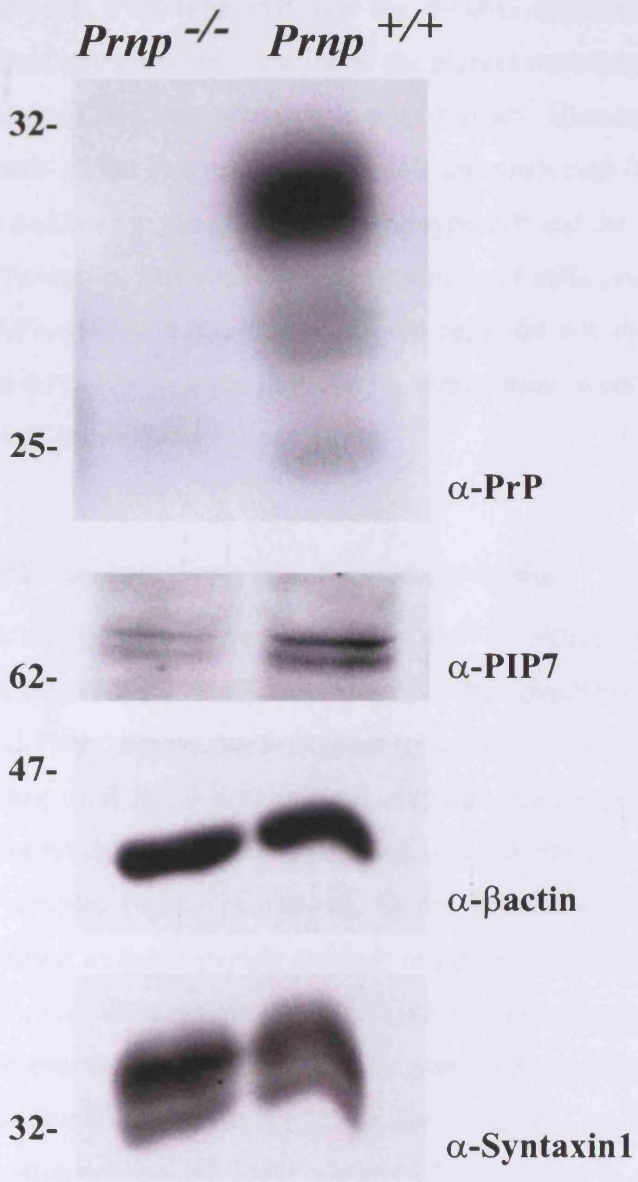

Figure 4.18 Decreased PIP7 surface levels in the brain of *Prnp*$^{-/-}$ mice. Brain homogenate was obtained from wild type or PrP deficient mice and subjected to a membrane enrichment procedure. Western blot analysis revealed a marked decrease in the PIP7 levels, approximately 50%, in the PrP null sample. The same amount of total proteins was loaded in each lane (100 μg) as confirmed by the actin immunoblot. The levels of Syntaxin1, an integral membrane protein involved in vesicular trafficking and membrane fusions, were unaltered, suggesting that the decrease in PIP7 surface pool was a specific consequence.

A comparison between wild type PrP and the NGAG mutant, which cannot be efficiently internalised and therefore recycled to the plasma membrane, would allow the discrimination between the two alternative possibilities. Human 293T cells were transfected with each of the two constructs or left untransfected (Figure 4.17). PIP7 accumulation occurred both in the presence of wild type PrP and the NGAG mutant: the latter was more efficient as estimated by the percentage of cells present in the marked area (23% and 30.8% respectively). Untransfected cells did not show any variations. The results confirmed the hypothesis that PIP7 accumulation occurs independently of the mechanism of PrP endocytosis and recycling.

4.2.2.5 Reduced PIP7 surface levels in PrP knockout brain.

Since PIP7 levels seemed to be influenced by PrP overexpression, I decided to investigate whether *in vivo* PIP7 levels were altered in the complete absence of the prion protein. *Prnp*$^{+/+}$ and *Prnp*$^{-/-}$ brains were obtained from adult mice, sex and age matched. A first attempt using total brain homogenate, without any subsequent cellular sub-fractionation, did not reveal any significant difference in the level of PIP7 between wild type and mutant samples (data not shown). In the second attempt, samples were processed, as described in the materials section, in order to enrich a crude membrane preparation. In this case, Western blot analysis revealed a consistent decrease in PIP7 membrane levels, estimated at around 50% when compared to wild type (Figure 4.18). The decreased was specific because the levels for syntaxin1, an integral membrane associated protein, were unchanged. Equal amount of protein was loaded in each lane as judged by Ponceau staining of the membrane and later confirmed by the α–βactin immunoblot. A reasonable explanation for the apparent discrepancy observed between the two performed experiments might be the presence in the total brain homogenate of the intracellular PIP7 pool which makes up the majority of the total population and might obscure any difference present at the plasma membrane where PIP7 levels are comparatively low. Such a difference at the plasma membrane could only be appreciated after separation of soluble and membrane-bound fractions.

4.2.2.6 PrP response to PIP7 surface levels alteration

So far, manipulations aimed at increasing or reducing the levels of surface PrP have resulted in an accumulation or reduction of endogenous PIP7 levels, respectively. Since the PIP7 knockout was not available to perform an *in vivo* analysis such as the one performed using the PrP knockout, I took an alternative approach to better understand the possible role of PIP7 in the biology of the prion protein. In the experiments presented below, PIP7 levels were altered either by overexpression or siRNA-mediated knock-down and the PrP surface population was monitored.

PIP7 overexpression

Considering the accumulation of endogenous PIP7 following PrP overexpression, I decided to investigate if the increase of PIP7 levels had any effect on the steady state of endogenous PrP. Human 293T cells were transfected with an empty vector or with a plasmid encoding the PIP7 short isoform. Forty-eight hours post transfection, cells were fixed and subjected to surface FACS analysis (Figure 4.19). Specifically in the PIP7 transfected sample but not in the control one, a PIP7 increase of 28.6% correlated with a PrP decrease of 20.9%. The result was considered specific in the light of the TfR, which remained unaltered (+1.0%). The experiment was repeated twice and the result was reproducible.

PIP7 siRNA

Following the result obtained by increasing PIP7 levels on the plasma membrane, I decided to try a complementary approach using gene silencing by RNA interference. A pool of four different siRNA oligos directed against human PIP7 (locus ID 4670) and a non targeting control pool were transfected in 293T cells. Samples were collected at two different time points (36 and 60 hours post transfection) and subjected to analysis by Western blot (for total levels) and by FACS (surface levels only, Figure 4.20). The cell lysates analysed for total PIP7 levels revealed a reduction in response to the PIP7-specific pool at both time points, with higher knock-down efficiency after 36 hours compared to 60 hours post transfection. The reduction was specific since the levels of β-actin, considered here both as a control for equal loading and specificity of the siRNA

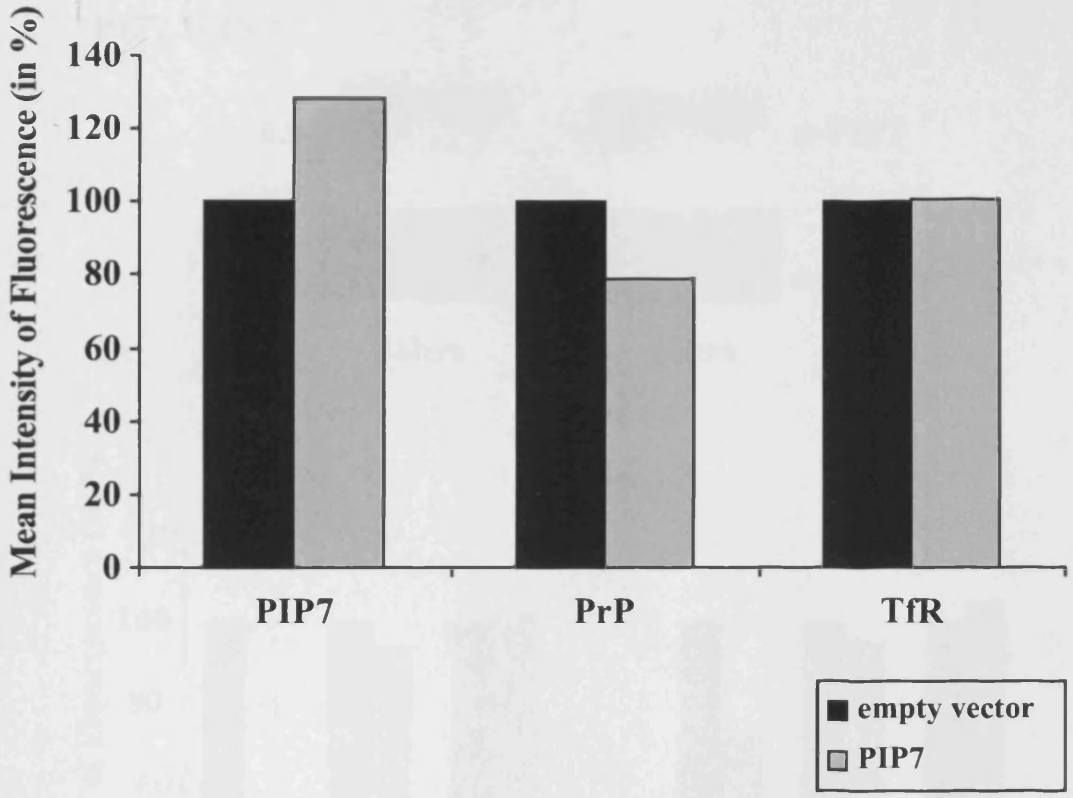

Figure 4.19 PIP7 overexpression in human 293T cells leads to a proportional decrease in PrP surface levels.
Human 293T cells were transfected with plasmids encoding the PIP7 Short isoform or an empty vector. Cells were collected 48 hours post transfection and surface FACS staining was performed. Analysis revealed an increase in PIP7 levels (+28.6%) whereas PrP levels exhibited a corresponding descrease (-20.9%). The TfR surface pool, included as a control for specificity, remained relatively unaltered (+1.0%).

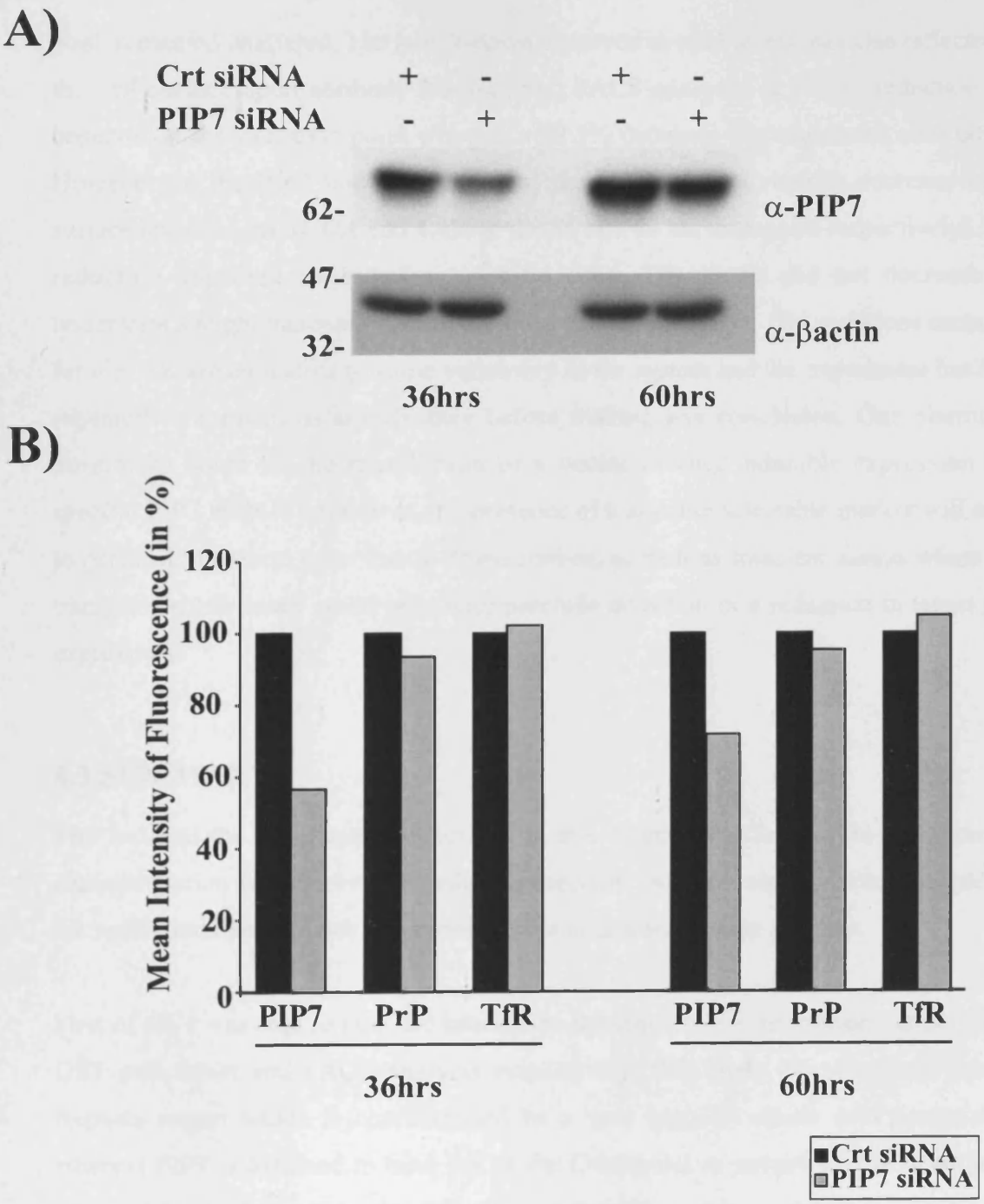

Figure 4.20 Effect of PIP7 siRNA on PrP.
Human 293T cells were transfected with a PIP7 specific siRNA pool or with a control pool. Samples were collected 36 and 60 hours post transfection respectively, and subject to analysis by Western blot or FACS. A) The effect on total PIP7 levels was more pronounced at the first time point compared to the later time point; the same amount of protein (100 μg) was loaded for each sample as confirm by the actin immunoblot. B) Surface protein levels monitored by FACS assay. The surface PIP7 pool was reduced by 43.5% after 36 hours and 28.3% after 60 hours. PrP levels were slightly reduced as well (-6.6% and -4.6%) whereas TfR levels showed a small increase (+2% and +4.6%).

pool, remained unaltered. The knock-down observed in total levels was also reflected on the cell surface upon antibody labeling and FACS analysis. A 43.5% reduction was observed at the first time point whereas a 28.3% decrease was registered after 60 hrs. However, in the PIP7 knock-down cells, there was only a slightly decrease in the surface levels of PrP (6.6% and 4.6% at the 36 and 60 hrs time point respectively). This reduction appeared nevertheless specific since TfR levels did not decrease but underwent a slight increase (+2% and +4.6% correspondingly). The variations measured for the TfR are indicative of some variability in the system and the experiment has to be repeated to confirm its significance before making any conclusion. One alternative possibility could be the transfection of a vector driving inducible expression of a specific PIP7 siRNA. Moreover, the presence of a suitable selectable marker will allow to perform long-term gene knock-down studies, as well as transient assays where low transfection efficiency could otherwise preclude detection of a reduction in target gene expression.

4.3 SUMMARY

The focus of the experiments described in this chapter was to provide a preliminary characterisation for the novel described interaction. Different aspects have emerged and the results obtained provide the starting point to develop further analysis.

First of all, I was able to map the interaction domain of each interaction partner, using GST pull down and FACS analysis respectively: PrP binds the so called Tandem Repeats region which is characterised by a very atypical amino acid composition whereas PIP7 is assumed to bind PrP at the C-terminal as judged by PIP7s ability to accumulate in response to the PrP-ΔE and PrP-ΔF mutant, lacking the flexible N-terminal domain.

In vitro studies have allowed me to identify the optimal binding conditions. PIP7 was known to interact with CEA and Thyroglobulin in a calcium-dependent manner. The PrP-PIP7 interaction, quite strikingly, was partially inhibited by the presence of exogenous calcium. Moreover the two partners seem to associate strongly at acidic pH values, in analogy with the optimal binding condition reported for the PIP7-Thyroglobulin interaction.

Co-localisation between PrP and PIP7 was observed on the cell surface and in a not yet defined vesicular compartment, possibly endosomes, as observed by co focal microscopy. The interaction was confirmed by standard immunoprecipitation and by Fluorescence Resonance Energy Transfer, a very sensitive technique which allowed me to monitor the protein-protein interaction in a cellular context without alteration or disruption of the physiological environment.

Finally, the increased PIP7 surface levels in response to PrP overexpression was correlated with the observation of reduced PIP7 membrane levels in the brain of *Prnp*$^{-/-}$ mice.

Chapter 5: Investigation of the possible involvement of PIP7 in prion disease

5.1 INTRODUCTION

Although many proteins have been shown to interact with the physiological isoform of the prion protein PrP^{C}, to date only plasminogen has been suggested as specific ligand for PrP^{Sc} (Fischer et al., 2000; Maissen et al., 2001). Possibly the best studied prion interacting protein is the laminin receptor (LRP/LR). Preliminary studies have suggested its involvement not only in PrP^{C} metabolism but also in prion propagation. Treatments with specific LRP/LR antibodies or antisense RNA were able to clear PrP^{Sc} from infected neuronal cells (Leucht et al., 2003). Since the conversion between the physiological and the pathological conformation of PrP is believed to take place either directly at the plasma membrane or in the endocytic pathway, it is highly likely that PrP^{Sc} formation was impaired due to fewer PrP^{C} molecules being internalised. Recently, a transgenic mouse line, ectopically expressing antisense LRP RNA in the brain under control of a neuronal promoter, was generated (Leucht et al., 2004). A significant reduction of LRP/LR protein levels was observed in different brain regions. These mice might act as powerful tools to investigate the role of the laminin receptor in scrapie pathogenesis *in vivo*.

In the present chapter, I will extend my analysis of PrP-PIP7 interaction specifically to different aspects of prion disease. I will divide this chapter into two parts: the biochemical characterisation of PrP^{Sc}-PIP7 binding and the attempt to interfere with prion disease progression by modulating PIP7. The former approach was based on the previously described GST pull down whereas the latter used two different but complementary approaches. In a cell based assay, α-PIP7 mAbs were tested for their ability to clear PrP^{Sc}. Alternatively, the *in vivo* requirements of PIP7 for prion infection and replication was assessed by a neurografting approach, where $PIP7^{-/-}$ cells were grafted in a $Prnp^{-/-}$ recipient mouse and challenged with RML prion-infected homogenate.

5.2 RESULTS

5.2.1 Scrapie binding assays

5.2.1.1 PIP7 does not bind PrP^{Res}

The flexibility of the GST binding assay allowed the relative affinity of PIP7 for the physiological conformation of PrP or for the pathological form to be tested. In the previous chapter, I observed an interaction between PIP7 and PrP^{C}; the term PrP^{C} is commonly used to refer to the normal structure of the prion protein, as found in uninfected mice. In the literature, PrP^{Sen} is an alternative designation for PrP^{C} and is exclusively based on the ability to be digested by PK treatment, irrespective of the actual conformation of the protein. Conversely, the definition of PrP^{Sc} as the scrapie specific isoform has to be clarified due to the existence of protease resistant PrP conformations that may or may not be infectious. The more general definition PrP^{Res} encompasses all forms of PrP that resist digestion by PK.

Using uninfected and infected brain homogenate as a source of PrP^{C} and PrP^{Sc} and following limited PK treatment, I attempted to characterise the biochemical properties of the PrP pool bound to PIP7. Total homogenate was prepared from the brain of terminally sick mice, previously intracranially inoculated with RML, or from healthy littermate controls. The experiment was performed as previously described, at pH 6, with the optional step of PK digestion after the last wash, at the standard concentration of 50 μg/ml. As shown in the previous chapter preferential binding between PrP and PIP7 was observed at low pH values; since pH 6 was not the standard value used for PK digestion in the literature, a preliminary experiment was performed in order to test whether PK activity would be preserved. After one hour incubation at 37°C, the N-terminus of PrP was removed giving rise to a subset of bands characterised by lower molecular weight and indicative of $PrP^{27\text{-}30}$, the PK resistant core of PrP^{Sc}, suggesting that PK is fully functional at pH 6.0.(Figure 5.1).
In the absence of protease treatment, GST-PIP7, but not GST alone, was able to enrich for PrP both from uninfected healthy brain and terminally sick brain homogenate.

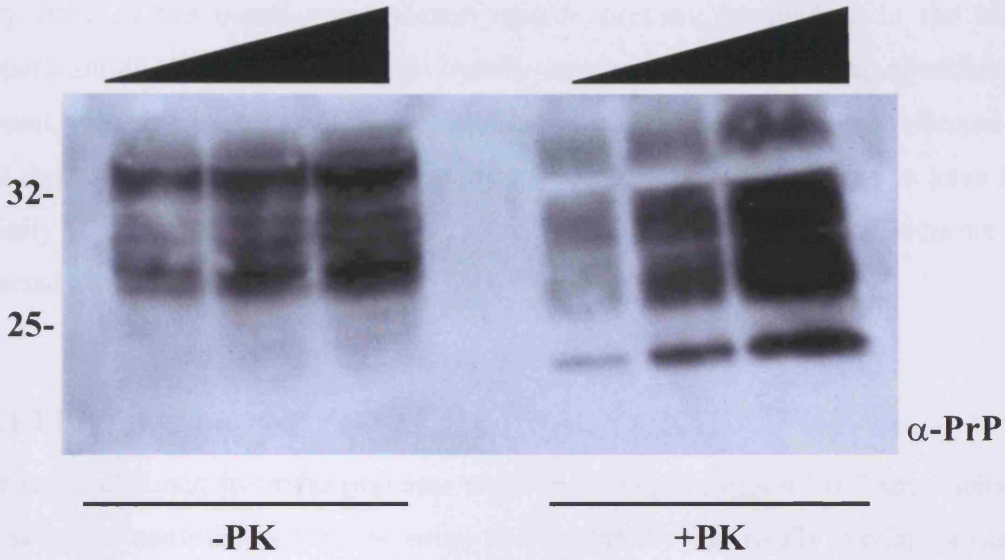

Figure 5.1 Test of Protease K activity at pH 6.0.
Total brain homogenate from terminally sick mice, previously inoculated intracerebrally with RML prions, was equilibrated at pH6.0 and digested with Protease K (50 μg/ml) for 1 hour at 37°C. Increasing amount of proteins, corresponding to 50-100-200 μg, were loaded on a SDS polyacrilamide gel and probed for PrP using ICSM18. The shift observed in the PrP molecular weight in the PK treated samples compared to the untreated ones confirmed the ability of Protease K to cleave the N-terminus of PrP^{Sc} and give rise to a resistant core, known as PrP^{27-30}, even at pH 6.0.

Following the treatment with PK, PrP^{27-30} was detected in the input lane but not in any of the samples subjected to pull down. Quite remarkably, there seemed to be a selective specificity in the binding of different glycosylated isoforms: in wild type brain, as shown in the input lane, the predominant isoforms are the di- and un-glycosylated, with very little of the mono-glycosylated version present; meanwhile in the infected preparation all three isoforms were equally represented. If no binding specificity was present, the same isoforms ratio observed in the input should have been reflected in the pull down. This was the case for the wild type brain but PIP7 proved to have higher affinity for di-glycosylated PrP and lower affinity for the remaining isoforms in the infected sample (Figure 5.2).

5.2.1.2 PIP7 does not bind PrP^{27-30}

The result obtained from the previous experiment might suggest PIP7 specificity for a PK sensitive conformation of the prion protein PrP^{Sen}, that might overlap or not with PrP^{C}. Nevertheless, it was not possible at this stage to exclude whether PrP^{C} and PrP^{Sc} have different binding affinity for the PIP7 receptor. In this possible scenario, PrP^{Sen} might have a higher affinity and could engage PIP7 in the binding and prevent the interaction with PrP^{Res}, characterised by having a lower affinity for the receptor. In order to test this hypothesis, infected brain homogenate was digested with Protease K, before performing the pull down assay, in order to eliminate any PK-sensitive conformations (PrP^{Sen}) and to have a pure preparation of PrP^{27-30}: this would provide a homogeneous population that could be unequivocally tested for its binding ability towards PIP7. This hypothesis is supported by previous data suggesting that the N-terminal region, cleaved upon protease treatment, was not required for the interaction with PIP7 as the PrP-ΔE mutant despite lacking the N-terminus was still able to accumulate PIP7 on the cell surface.

On the left side of Figure 5.3, PrP was specifically pulled down by PIP7 in absence of protease treatment. However, when the sample was pre-treated with PK, as shown in the right panel, no PrP^{27-30} was detected either bound to GST or to GST-PIP7. Therefore I conclude that PrP^{Res} was not able to bind PIP7 under these experimental conditions.

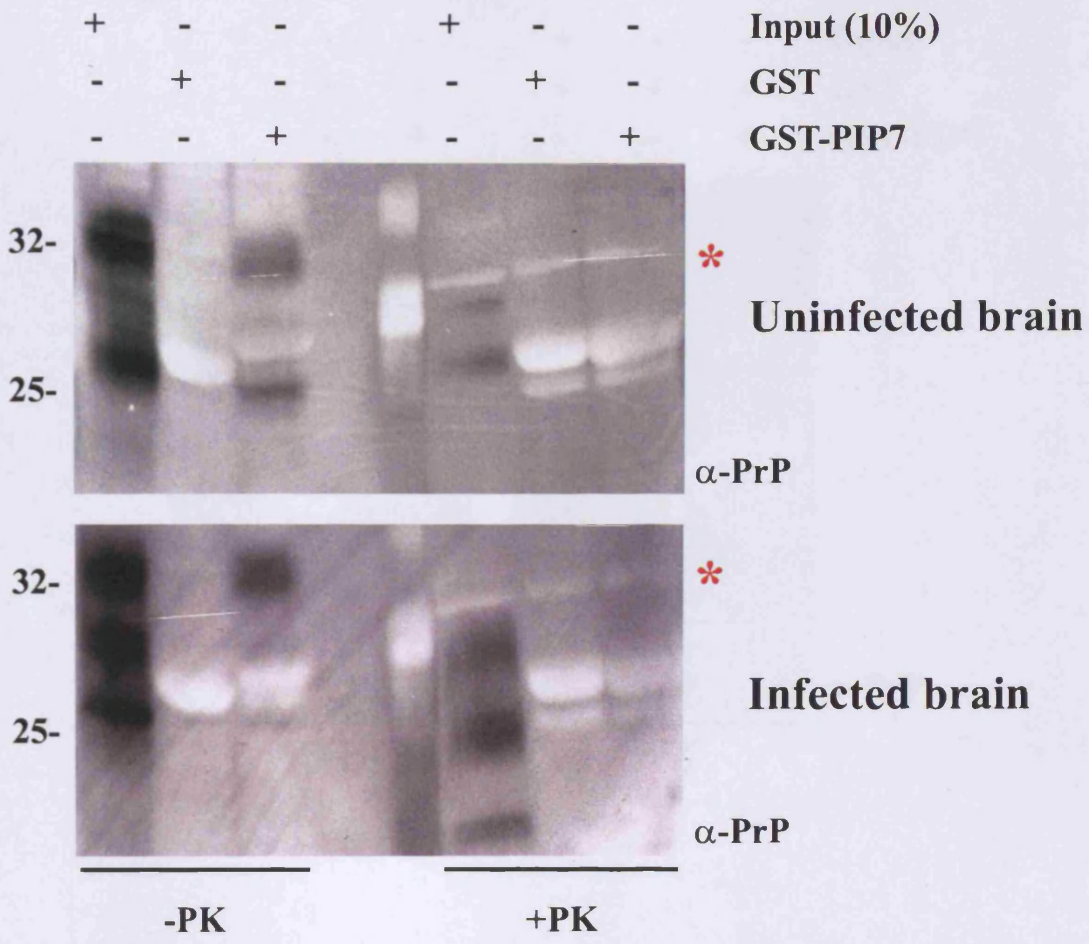

Figure 5.2 PIP7 does not bind PrP^{Sc}.
Brain homogenate (10% w/v) was obtained from healthy or scrapie infected mice. GST pull downs were performed in duplicate: after the final wash, one aliquot was treated with Protease K (50 μg/ml, 1 hour at 37°C) and one left on ice. The reaction was blocked by addition of PMSF to a final concentration of 1 mM for 30 minutes on ice. Loading buffer was added to the samples which were analyzed by SDS-PAGE. Following Western blot analysis with the specific α-PrP antibody ICSM18, PrP-PIP7 interaction was detected in both infected and uninfected samples prior to proteolysis treatment. After treatment PrP^{27-30} was detected only in the infected cell lysate but was not detected in the sample subjected to pull down. The position of Protease K is marked in red (*). Total cell lysate corresponding to 10% of the amount used for the pull down was loaded as input.

5.2.2 Testing the role of PIP7 in prion disease *in vivo*

It is widely accepted that one or more cellular proteins might play a role in the transconformation process leading to the formation of PrP^{Sc} (Kaneko et al., 1997b). One of the most ambitious experiments in the prion field is the generation of animals lacking a specific protein, which has been demonstrated to interact with PrP, and the subsequential delay, or ultimately failure, to develop the disease after inoculation. This has only been shown for mice devoid of the prion protein itself which remains completely free of scrapie symptoms (Büeler et al., 1993). The postulated auxiliary factor Protein X is without doubt the most suitable candidate for this kind of approach but its existence remains speculative (Telling et al., 1995). One molecule that has been investigated for its involvement in prion replication is the neural cell adhesion molecule (NCAM) purified in a high molecular complex containing PrP. However the observation that $NCAM^{-/-}$ mice succumbed to prion disease suggested its dispensability in PrP^{Sc} formation (Schmitt-Ulms et al., 2001).

On the basis of this I attempted to address whether PrP^{Sc} formation and scrapie pathogenesis could be affected in response to disruption of the PIP7 gene.

5.2.2.1 Overview of Gene trap

Gene trap technology was originally designed to provide functional information for novel genes (Gossler et al., 1989). The approach is based on the availability of murine embryonic stem cells (ES) and a specific class of reporter plasmids, containing a splice acceptor site upstream of a chimeric β-geo cassette, encoding both β-galactosidase and neomycin resistance activity but lacking a promoter. When the vector is integrated downstream of a functional promoter, the construct allows the expression of the reporter gene as a fusion transcript with the endogenous exon located upstream of the integration site (Figure 5.4). The integration occurs randomly but can be easily determined by 5'RACE (Townley et al., 1997). The expression of the trapped gene should faithfully recapitulate the endogenous pattern and can be monitored by X-gal staining. This for example is quite helpful in the examination of the pattern of expression during development. More importantly, the function of the trapped gene is often disrupted after the insertion, providing a loss of function phenotype.

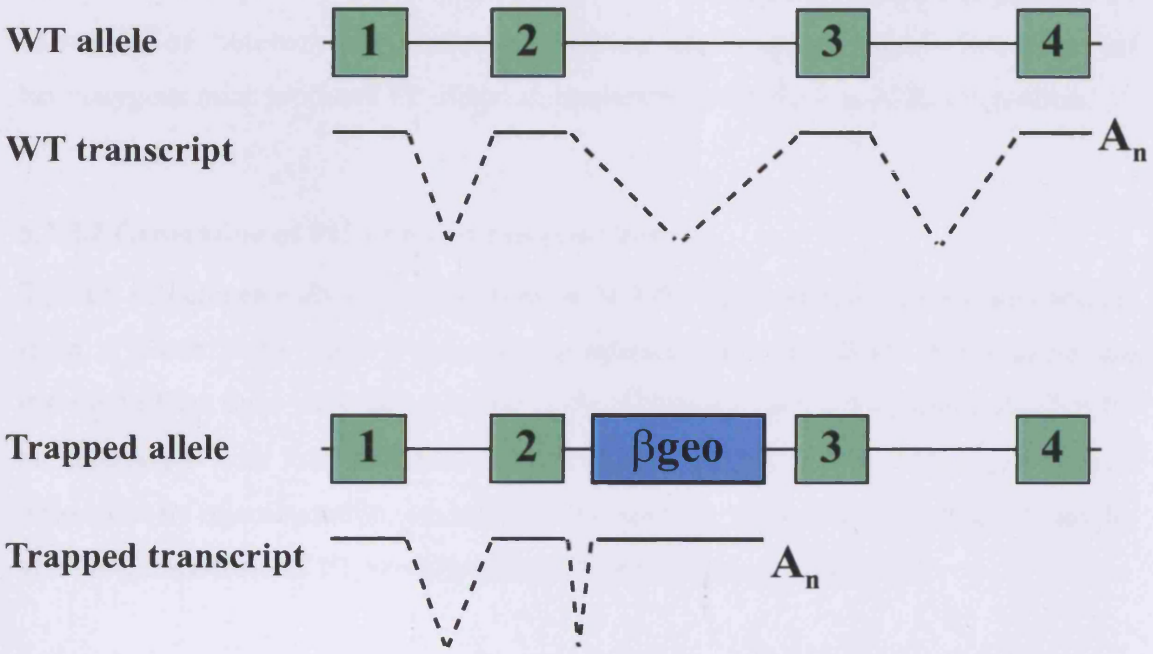

Figure 5.4 Schematic description of the Gene Trap technique.
A gene-trap vector, contains a splice-acceptor sequence upstream of a reporter gene (β-*geo* is a fusion between β-galactosidase and neomycin phosphotransferase II) but no endogenous promoter. The vector inserts randomly into genes, resulting in a fusion transcript containing sequences from exons upstream of the insertion joined to the β-*geo* marker but missing the sequences from exons downstream of the integration site. The identity of the trapped gene can easily be determined by 5' rapid amplification of cDNA ends (5'RACE) followed by automated DNA sequencing.

The mutated ES cell clones can be indefinitely maintained *in vitro* in a multipotent state and with a stable karyotype. They can be differentiated into various cell lineages or reintroduced into blastocysts where they contribute to all cell types, including the germ line (Baker et al., 1997). The chimeric mouse can subsequently be used to produce F1 offspring of heterozygous animals carrying the trapped allele. Intercross of heterozygous mice produces F2 offspring homozygous for the loss of function allele.

5.2.2.2 Generation of PIP7 targeted mouse lines

Two ES cell clones harbouring insertions in the PIP7 open reading frame were obtained from a Gene Trap library (http://baygenomics.ucsf.edu/). Both clones presented insertion of the βgeo cassette upstream of the Tandem Repeats domain responsible for the interaction with PrP. The XE413 and NPX275 ES cell clones were expanded and introduced by microinjection into recipient blastocysts. Chimeras were obtained and, by germ line transmission, F1 heterozygous mice were produced ($PIP7^{+/-}$).

I performed an X-gal staining on heterozygous mice for each of the two lines, with the aim to compare the staining pattern with the PIP7 immunohistochemistry (see Figure 3.9). A wild type sample was included in the panel as a control for staining specificity. Neither the wild type brain nor the NPX275 clone showed clear staining whereas the XE413 clone presented a pattern compatible with the previously observed PIP7 distribution in the cerebellum (Figure 5.5).

There could be a number of explanations for the observed phenotype: chimeric proteins could either exhibit a folding which might inhibit the β-galactosidase enzymatic activity or be unstable and promptly degradated. It is known that insertions capturing the N-terminal signals sequence of a secreted or membrane protein are inactive (Skarnes et al., 1995). Nevertheless, PIP7 is not exclusively localised on the cell surface since most of it is found in the nucleus. It is more likely that the two clones are encoding fusion proteins with different stability. To test the hypothesis, total brain homogenate was prepared from each of the lines and blotted with a specific α-β-galactosidase antibody.

Wild Type

NPX275

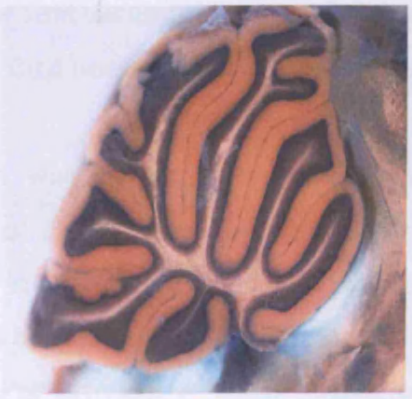

XE413

Figure 5.5 Monitoring LacZ activity in wild type and PIP7 trapped alleles by X-gal staining. X-gal staining was performed on wild type (negative control) and PIP7 mutant mice. For simplicity, only the cerebellum is shown. The XE413 clone produced strong straining whereas the NPX275 clone remained unstained. As expected, no staining was found in the wild type sample.

A band at 175 KDa was observed in the XE413 lysate but no specific band was detected in the NPX275 lysate (data not shown). It was possible to conclude that the lack of β-galactosidase activity in the NPX275 was due to protein instability.
F1 mice positive for the insertion were intercrossed and the F2 offspring analyzed for the presence of knockout animals. None of the two lines, NPX275 and XE413, were able to produce null offspring, even in sub-mendelian ratio. After a preliminary analysis, it seemed that PIP7 disruption resulted in embryonic lethality.

5.2.2.3 Neurograft of PIP7 mutant neuroectoderm

An alternative strategy to investigate the dependence of prion disease on the presence of PIP7 was provided by a neurografting approach. Embryonic lethality of knockout mice can be quite common but neuronal tissue can nevertheless be obtained by grafting immature neuroectodermal cells from genetically modified embryos into an adult recipient host (Isenmann et al., 1996). The host mouse is healthy and permits the study of the properties of the neuronal tissue derived from the donor. However, in this case, it relies on a double assumption: a) knockout embryos must reach E13.5 since neuroectoderm cannot be grafted before that stage; b) PIP7 function must not be required for growth and differentiation in adult neural tissue, after transplantation. In order to test the first assumption, I established time mating by intercrossing the two previously described lines (NPX275 x XE413) and embryos were extracted at E13.5.

Neuroectoderm was surgically removed from 41 embryos and grafted in the caudoputamen of *Prnp*$^{-/-}$ recipient mice. The use of a *Prnp*$^{-/-}$ background for the recipient mice was decided for two reasons: a) animals can remain healthy for prolonged times because prions cannot successfully replicate in the host; b) the absence of endogenous PrP provides a "clear" background where PrP^{Res} accumulation can be easily detected in the tissue originated from the graft. At the same time, total protein lysate was prepared from the same set of embryos and analysed by immunoblot. Figure 5.6 presents the comparison between a mutant and a control. The double mutant presented PIP7 levels which were almost undetectable when compared to the wild-type control, suggesting that the compound mutants were still viable at the stage required for neuroectoderm transplant. The same amount of total proteins was loaded, as checked by both Ponceau staining and α-βactin immunoblot.

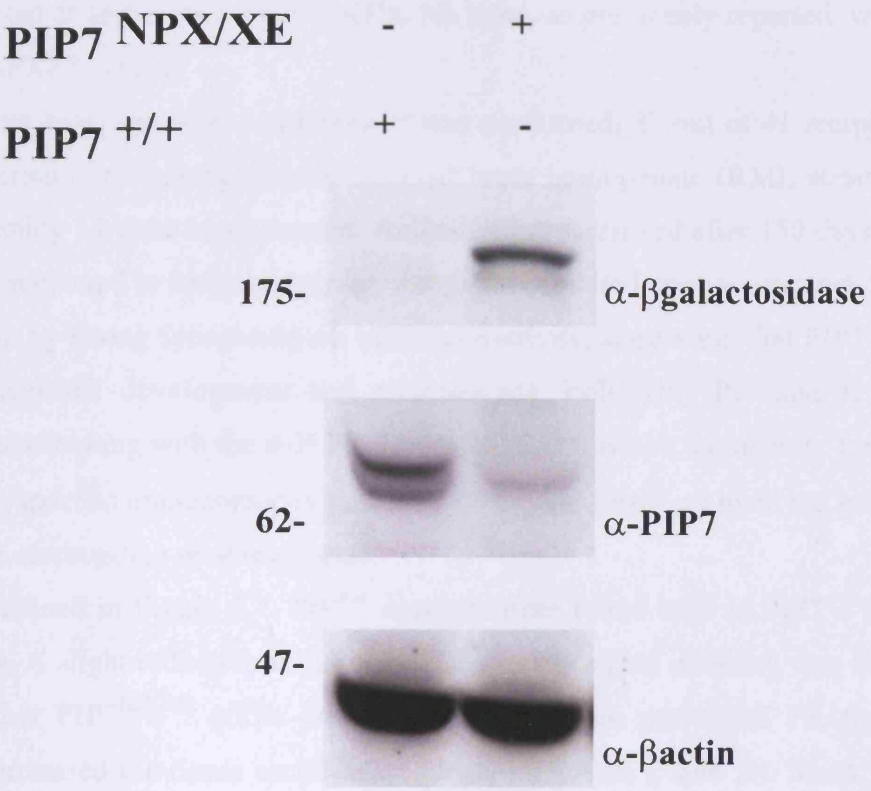

Figure 5.6 Decreased PIP7 levels in embryos obtained from NPX/XE intercross. After surgical removal of the neuroectoderm, embryos were analysed by immunoblot in order to confirm the absence of PIP7. In the NPX/XE mutant total PIP7 levels were largely decreased. Equal protein loading was confirmed by actin immunoblot. The β-galactosidase positive band at 175 KDa reflected the presence of the XE fusion protein whereas no band was detected for the NPX allele.

The reduction of PIP7 protein levels observed in Western blot analysis was estimated to be at least 80%. A LacZ positive band, corresponding to the XE413 trapped allele was detected at approximately 175 KDa. No band, as previously reported, was detected for the NPX275 allele.

Twenty-two days after implantation was performed, 27 out of 41 recipient mice were intracranially challenged with infected brain homogenate (RML strain) whereas the remaining 14 were mock treated. Animals were sacrificed after 150 days and the brains were subjected to immunostaining. All grafts exhibited normal neuronal development as shown by strong synaptophysin immunoreactivity, suggesting that PIP7 is not required for neuronal development and maintenance. Following Protease K digestion and immunostaining with the α-PrP antibody ICSM35, which has affinity for both PrP^{C} and PrP^{Sc}, specific immunoreactivity due to PrP^{Res} was observed in all the grafts but in none of the surrounding recipient tissue.

As outlined in Figure 5.7, PrP^{Res} deposits were found both in $PIP7^{+/+}$ and $PIP7^{NPX/XE}$ grafts. A slight reduction in the ICSM35-specific signal intensity was not reproducible in other $PIP7^{NPX/XE}$ grafts and may be due to the prolonged PK treatment which compromised the tissue architecture (compare panels C and D). Mock infected grafts did not show immunoreactivity after Protease K digestion. Moreover, other hallmarks of prion disease including spongiosis and gliosis were readily detectable in RML-inoculated $PIP7^{NPX/XE}$ grafts. Immunostaining with the 4G4 antibody revealed that, although decreased, PIP7 specific signal was still detectable in the mutant mice, as better seen with higher magnification of the selected area (panels G and H, dotted lines have been placed on the boundaries between the host and the grafted tissue). Thus, a significant reduction of PIP7 protein levels did not have any appreciable effect on PrP^{Sc} generation and neuronal degeneration, at least in the neuroectodermal graft paradigm.

5.2.3 Attempt to cure chronically infected cells with PIP7 antibodies

Several cell lines can be infected by prions and they retain the ability to accumulate PrP^{Sc} after multiple passages (Markovits et al., 1981; Race et al., 1988). These lines are mainly derived from neuronal tissue such as mouse neuroblastoma N2a (Butler et al., 1988), mouse hypothalamic GT1 (Schätzl et al., 1997) rat pheochromocytoma PC12 (Rubenstein et al., 1984) and also a rabbit epithelial line has been reported (Vilette et al., 2001).

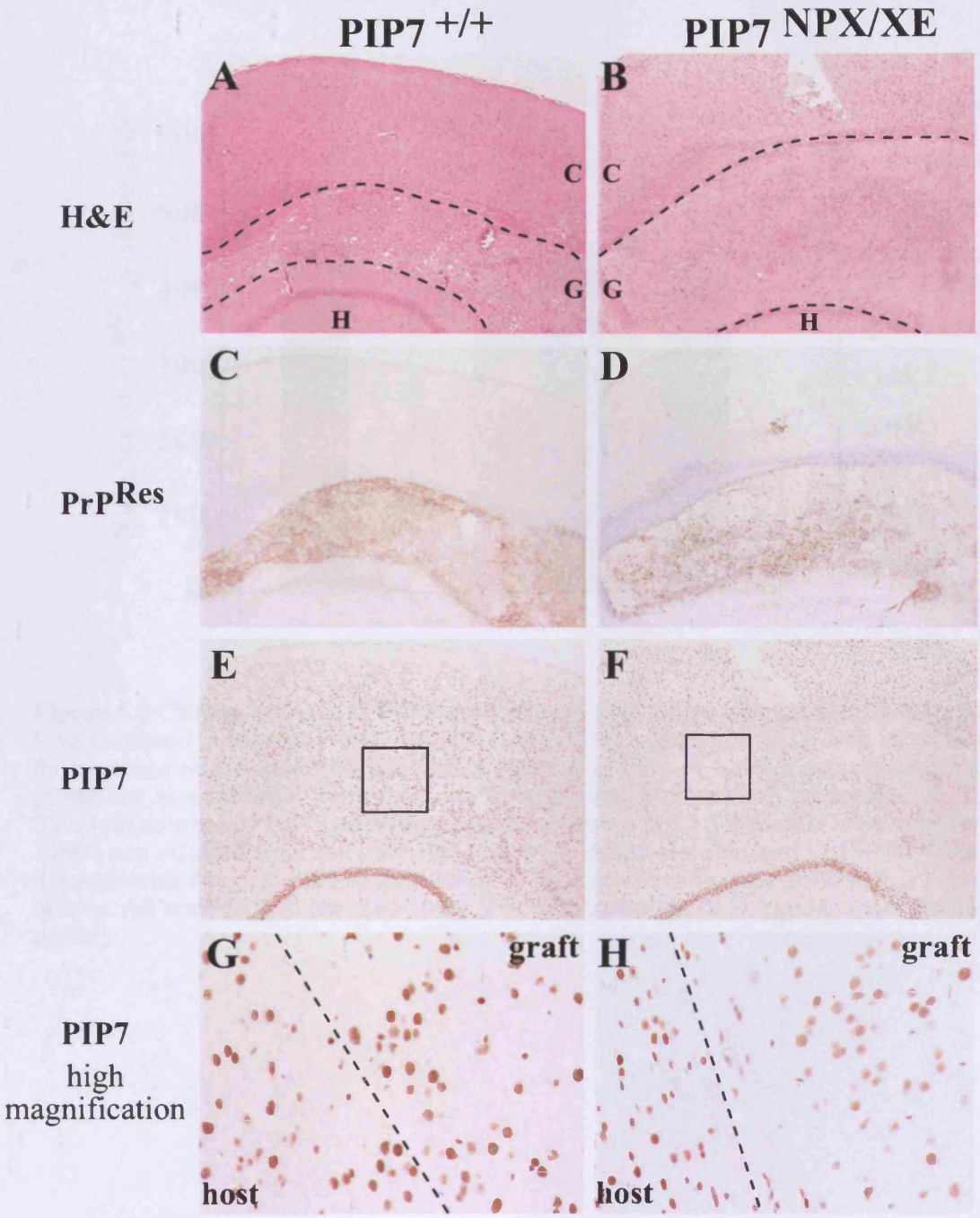

Figure 5.7 Scrapie accumulation in neuronal grafts with reduced amounts of PIP7. Time mating was set up between the XE413 and NPX275 line previously described. Neuroectoderm was extracted from embryos (E13.5) and grafted in *Prnp*$^{-/-}$ recipient mice. Twenty-two days after transplantation, mice were stereotactically injected with RML and histological analysis of the graft was carried out 150 days after inoculation. Hematoxylin & Eosin staining allowed the boundaries between the host and the graft tissue to be distinguished (A and B); PrP^{Res} was detected after Protease K treatment (50 μg/ml for 4 hours at 37°C) in both wild type and mutant samples (C and D); immunostaining with the 4C2 revealed reduced expression of PIP7 protein in mutant grafts (E and F, higher magnification G and H). Abbreviations: C:Cortex, G:Graft, H:Hippocampus.

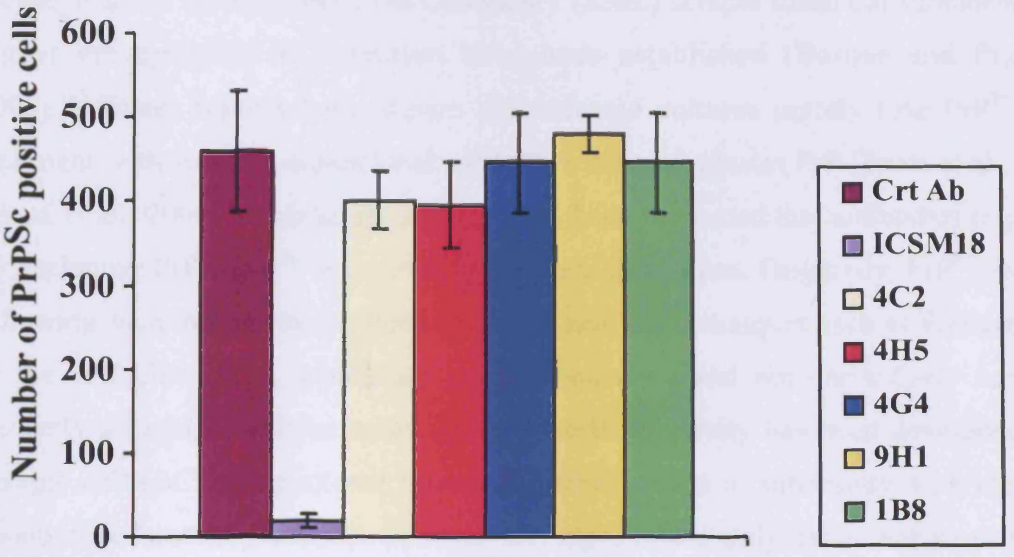

Figure 5.8 Curing activity of PIP7 monoclonal antibodies on chronically infected N2A cells
Five thousand chronically infected IPK1 cells were plated into each well of a 96 well plate in the presence of the specified antibodies. After four days of incubation, cells were split 1:8 and grown for an additional three days, in the continous presence of the antibodies. To determine the exact number of PrP^{Sc} positive cells, a sample of 1000 IPK1 cells were supplemented with 24000 non infected cells and immobilized onto 7 wells of a standard ELISPOT plate. Cells were digested with 1 mg/ml PK (90 minutes at 37°C) before reading the plate with a Zeiss KS Elispot system. All antibodies were used at the final concentration of 50 µg/ml, apart from ICSM18 (10 µg/ml).

Only a small percentage of murine neuroblastoma N2a cells can be infected with the mouse-adapted Rocky Mountains Laboratory (RML) scrapie strain but subclones with higher susceptibility to infection have been established (Bosque and Prusiner, 2000).Different reports have shown that infected cultures rapidly lose PrP^{Sc} upon treatment with specific monoclonal antibodies directed against PrP (Enari et al., 2001; Peretz et al., 2001; White et al., 2003). It has been suggested that antibodies might act by occluding PrP^{C}, PrP^{Sc} or eventually both conformations. Originally, PrP^{Sc} decrease following such treatments has been tested by standard techniques such as Western blots or the cell blot assay, which are semi-quantitative and not particularly accurate. Recently a highly sensitive assay based on cell infectivity has been developed. The Scrapie cell (SC) assay allows the rapid quantification of infectivity with the same sensitivity of a standard mouse bioassay and more importantly has an enhanced signal-to-noise ratio (Klohn et al., 2003).

In order to test a possible role of PIP7 in scrapie propagation the full panel of α-PIP7 mAbs was tested for the ability to cure chronically infected N2a cells. For this particular experiment the highly susceptible clone iPK1 has been used and standard concentration of 50 μg/ml of antibody was used (Klohn et al., 2003). The specific PrP antibody ICSM18 (10 μg/ml) was used in the experiment, as a positive control, having been demonstrated to eradicate prion infectivity both *in vitro* and *in vivo* (White et al., 2003). After one week of treatment, cells were analysed for the presence of PrP^{Sc} by standard SC assay. Treatment with ICSM18 (10 μg/ml) successfully abolished more than 95% of the positive cells when compared to the sample treated with an irrelevant isotype control antibody (Figure 5.8). The treatment with the α-PIP7 monoclonals did not produce a decrease comparable with the one obtained by the α-PrP antibody. Thus α-PIP7 mAbs do not alter PrP^{Sc} levels in chronically-infected N2a cells.

5.3 SUMMARY

In the previous chapter, I attempted a general characterisation of PrP/PIP7 biology using uninfected cell lines hence looking only at the presence of PrP^{C}. The aim of the studies presented in the current chapter was to clarify whether PIP7 has the ability to interact with the disease-associated isoform PrP^{Sc} and participate in scrapie pathogenesis.

From the first set of experiments, it emerged that PIP7 specifically interacts with a PK sensitive PrP subset. PIP7 seems to have no affinity for PrP^{Sc} or PrP^{27-30} as shown in GST pull down assays.

In the second part of the chapter, I have used an *in vivo* and *in vitro* approach respectively to address the potential role of PIP7 in prion disease. I have generated transgenic mice harbouring gene trapped alleles of the PIP7 open reading frame. It has to be mentioned that frequently the trapped allele is not a null allele, but rather a hypomorphic allele. This scenario could occur if the targeted genomic locus undergoes splice-around events, such as when the spliceosome machinery ignores the splice acceptor site present in the vector. Splice-around events can occur in a time- and space restricted manner, resulting in a hypomorphic allele. I believe this is the most probable explanation for the different levels of PIP7 expression observed in the mutant embryos and in the corresponding grafted tissue (compare Figure 5.6 and 5.7). As a consequence, using the neurograft paradigm, I was only able to show that a 50% reduction in PIP7 levels did not have significant effect on prion replication.

Finally, I tested the α-PIP7 mAbs in a cell-based assay for their ability to clear PrP^{Sc}. None of the specific monoclonals produced a significant reduction in total PrP^{Sc} levels, compared to the mock treated cells. I am planning to test the α-PIP7 antibodies for their prophylactic activity: *de novo* infection will be performed in the presence of the monoclonals and infection efficiency will be monitored by SC assay.

The generation of a conditional mouse for PIP7 would be the most suitable approach to clarify its function. This will allow a definitive answer to the role of PIP7 role in prion disease and the study of not only its requirement in replication within the CNS but also via peripheral inoculation, its possible role in neuroinvasion.

Chapter 6: Discussion

6.1 Overview

Prion diseases are a related group of transmissible neurodegenerative conditions affecting humans and a variety of animals. One of the typical features of TSEs is the deposition, mainly in the brain but also in other tissues, of PrP^{Sc} which is the abnormal isoform of the host protein PrP^{C} (Budka et al., 1995). PrP^{Sc} not only has the ability to co-purify with infectivity but is the most prominent component of infectious preparations, providing a reliable marker (Prusiner and Scott, 1997). Although much knowledge has been acquired in past years, basic questions such as the physiological role of PrP and the mechanism by which prions cause brain damage remain unanswered.

6.2 A novel screen for PrP interacting proteins

Many attempts have been taken in the past to identify PrP-interacting proteins in order to elucidate the cellular pathways in which PrP is involved. The aim of the present study was to isolate new interacting partners for the prion protein.

The yeast two-hybrid system is a simple and reliable tool to isolate novel protein-protein interactions (Fields and Song, 1989) and has allowed the identification of interesting PrP partners, as reviewed in the introduction chapter. However, with very few exceptions, the majority of candidates show cellular localisations which are not in line with the trafficking of the prion protein, questioning their relevance. A possible explanation for such results was provided by a recent study showing that proteins of membrane origin were generally under-represented using this kind of approach, possibly because of their incorrect folding in the yeast nucleus, where the yeast two-hybrid takes place (Uetz et al., 2000). The Ras Recruitment System attempts to circumvent this limitation by studying protein-protein interactions in the yeast cytoplasm but still does not allow the use of membrane proteins as bait due to their intrinsic ability to translocate to the plasma membrane independently of protein-protein

interactions (Broder et al., 1998). This was the case for PrP, which was probably able to associate with the plasma membrane even in the absence of its GPI anchor thereby invalidating the screen.

Subsequently, I opted for the reverse Ras Recruitment System in which PrP was located in its natural membrane environment which was supposed to conserve its functional conformation (Hubsman et al., 2001). A second important reason why I performed the rRRS as opposed to the conventional yeast two-hybrid was the observation that, when expressed in the yeast cytoplasm, PrP adopts a misfolded conformation characterised by increased detergent insolubility and partial resistance to proteolysis, two hallmarks of PrP^{Sc} (Ma and Lindquist, 1999). There is no definitive explanation as to why PrP presents such PrP^{Sc}-like properties in this environment. It is conceivable that the acidic and reducing environment found in the yeast cytosol stimulates partial PrP misfolding, as suggested by *in vitro* conversion experiments using recombinant PrP (Jackson et al., 1999). Alternatively, a contribution of some yeast enzymatic factors cannot be excluded.

My approach differs from the classic yeast two-hybrid by exploiting two novel aspects offered by the rRRS. Firstly, PrP was expressed in a more physiological membrane-bound environment and I believe this may play a key role in the identification of candidates which might have failed to be isolated in the past. Secondly, the rRRS takes place in the yeast cytoplasm where PrP seems to acquire biochemical properties typical of PrP^{β}, as I was able to reproduce, whereas there is no information available in the literature about the conformation adopted by PrP in the yeast two-hybrid system. My experimental conditions could in theory allow the isolation of proteins not only able to interact with PrP^{C} but also with PrP^{β}. The outcome of such a screen could not only increase the knowledge about the still unknown functions of PrP but also identify possible candidates which may be involved in the transconformation process. Such proteins, once isolated and characterised, could provide novel therapeutic targets for a pathology that up to now has no effective cure.

6.3 PIP7 isolation and evaluation

As a result of the screen, I cloned a number of potential PrP interacting proteins and I have initially chosen to focus on the hnRNP M4 clone, which I referred to as PIP7,

firstly because of its reported localisation at the plasma membrane where most PrP molecules are present at any given time (Stahl et al., 1987). Moreover, PIP7 has been reported to act as a surface receptor for the Carcinoembryonic antigen in rats and thyroglobulin in humans (Bajenova et al., 2001; Blanck et al., 1994). These lines of evidence raised my interest regarding the possible interaction between PrP and PIP7 and I successfully confirmed the interaction *in vitro* by GST pull down assay and *in vivo* by co-immunoprecipitation studies. With the aid of a panel of monoclonal antibodies I was able to confirm the presence of the PIP7 protein on the cell surface of different cell lines including mouse neuroblastoma N2a cells which are widely used to study the biology of Prion disease.

The PrP interacting domain within PIP7 encompasses a region with a very atypical amino acid composition. The identified Tandem Repeats region includes 27 repetitions of the consensus sequence [GEVSTPAN]-[ILMV]-[DE]-[RH]-[MLVI]-[GAV]. This feature is unique to PIP7 since it is not found in any other protein described in the databases. This region had been suggested as a potential coordination site for calcium ions but in the present case the PrP-PIP7 interaction was partially inhibited by the addition of exogenous calcium.

An indication of which region in PrP was responsible for the interaction with PIP7 was provided by the structure/function analysis by FACS. The accumulation of endogenous PIP7 following PrP overexpression allowed the determination of which portion of PrP was responsible for the interaction. Although I did not identify any PrP mutant, with the exception of the ΔSP which remains in the cytoplasm, unable to produce PIP7 accumulation, I was able to show that the PrP-ΔF mutant, lacking amino acids 32 to 134, was still able to increase endogenous PIP7 surface levels. Assuming that accumulation was a direct consequence of protein-protein interaction, the PIP7 binding site is likely to be in the C-terminal globular domain of the prion protein with no apparent contribution from the N-terminal flexible region.

6.4 Biology of the PIP7-PrP surface interaction

The increase in the levels of the PIP7 surface population following PrP overexpression offered a new perspective to the present study. Overexpression of membrane proteins

could in theory saturate either the lipid environment or the endocytic machinery, resulting in non-specific accumulation of membrane proteins simply by impairing their normal trafficking. To assess the specificity of my observations, I followed the fate of the Transferrin Receptor which is known to be excluded from the raft environment and to become endocytosed by a mechanism based on clathrin coated pits (Shogomori and Futerman, 2001). Recent studies have shown that endogenous PrP expressed on primary neurons has to exit lipid rafts before undergoing coated pit-mediated endocytosis (Sunyach et al., 2003). Furhtermore, TfR and PrP have been characterised for their analogous kinetics of endocytosis and recycling and for their co-localisation during the internalisation process. On the basis of these data, I believe TfR provided a suitable and stringent control for my experiments.

Cells expressing a cytoplasmic version of the prion protein did not accumulate either PrP or PIP7 on their surface, suggesting that PIP7 stabilisation required the presence of PrP specifically on the cell surface. More interestingly, the stabilisation of PIP7 levels required PrP overexpression on the surface of the same cell (an *in cis* event); when cells were transfected with the GFP-PrP construct, only the GFP positive subpopulation displayed an increase in both PrP and consequently PIP7 surface levels; this argued against an *in trans* event because no PIP7 increase was observed in the GFP negative subset despite the intimate contact with PrP overexpressing cells. The finding suggests but does not prove that the PrP-PIP7 interaction cannot be established *in trans* between molecules present on neighbouring cells. This hypothesis can ultimately be confirmed by expressing a PrP mutant devoid of its C-terminal signal peptide. Such a mutant would lack the GPI anchor, resulting in its secretion in the extracellular space, and should not stabilise PIP7 levels exclusively in transfected cells.

An *in trans* effect would be suggestive of a cell surface mechanism whereas the observed *in cis* mechanism of stabilisation could involve either the plasma membrane or the internal endocytic pathway or a contribution from both compartments at the same time. I specifically tested the requirement for effective PrP endocytosis/recycling on PIP7 stabilisation using the NGAG mutant, which suggested that PIP7 surface accumulation does not require PrP endocytosis.

Another interesting question I would like to address is whether PIP7 surface accumulation depends on correct PrP raft localisation: either transfection with the previously described chimeric PrP-CD4 construct, which localises exclusively to

clathrin coated pits, or treatment with drugs such as filipin or methyl-β-cyclodextrin, which compromise raft integrity, will be able to clarify this issue.

Evidence supporting PrP-PIP7 co-endocytosis

Microscopic analysis in living cells suggested a possible association between the studied proteins not only on the cell surface but also in the endocytic pathway. I proceeded to address whether PIP7 internalisation correlated with PrP endocytosis. To do so, I used chemical or enzymatic treatments able to alter PrP surface levels either by stimulating its endocytosis or by releasing it to the extracellular space by cleavage of the GPI anchor. A summary of the results obtained from my *in vitro* studies is outlined in Figure 6.1. Pentosan Sulphate has been reported to act exclusively by stimulating endocytosis whereas the mechanism of action of Suramin is subject to alternative interpretations since it has been reported to affect PrP trafficking both in the secretory and the endocytic pathways (Gilch et al., 2001; Kiachopoulos et al., 2004; Shyng et al., 1995a). The PIP7 decrease in the Suramin treated sample could therefore reflect the result of a reduction in PrP exocytosis or an increase in PrP endocytosis. Although a direct effect of Suramin on PIP7 cannot be excluded, regardless of the mechanism by which PrP surface levels are lowered, a decrease in the PIP7 surface population was always observed whereas the levels of the TfR remained unaltered. The above data is suggestive of a possible PrP-PIP7 association during the endocytic process since a PrP reduction was always followed by PIP7.

Although the membrane topology of PIP7 remains unclear, *in silico* analysis has failed to predict any GPI modification. Therefore, in light of the result of the PIPLC experiment, where PIP7 levels were reduced after PrP release from the plasma membrane, it is possible to argue that PIP7 not only could undergo endocytosis independently of the presence of PrP but also that its internalisation is stimulated by releasing PrP from the membrane environment. From this point of view, it is foreseeable that the presence of PrP could affect the kinetics of PIP7 internalisation as further supported by the trapping of endogenous PIP7 on the cell surface following PrP overexpression.

The PrP surface pool was specifically reduced in response to PIP7 overexpression. This result can be explained by the heterogeneous nature of the surface lipid environment. PrP is known to localise in lipid rafts and its internalisation implies its exit from such

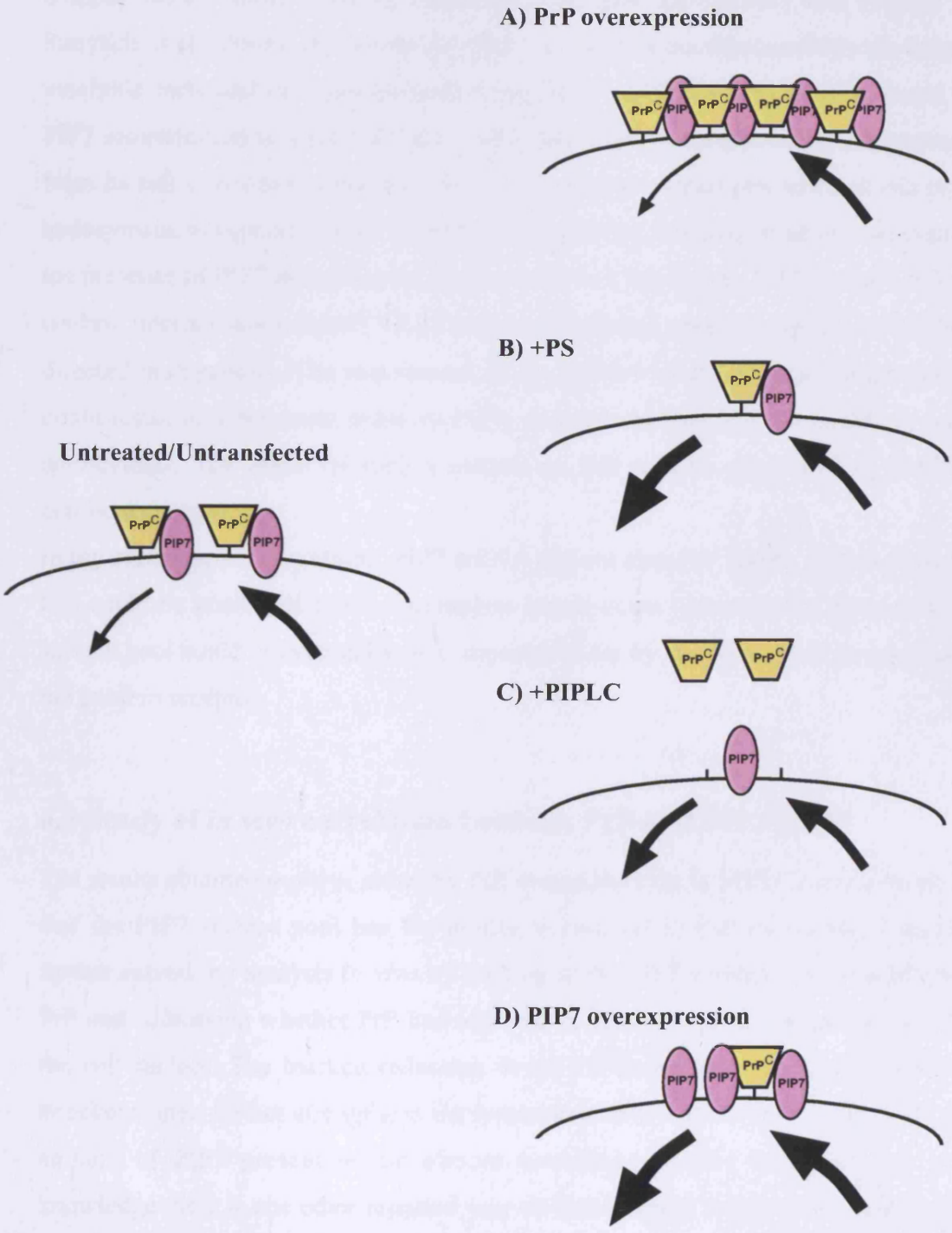

Figure 6.1 Reciprocal effect of PrP-PIP7 equilibrium on the cell surface Data obtained from previously described *in vitro* experiments are here summarised. In the untransfected/untreated situation, there is a steady state between the exocitosys and endocytosis of PrP and PIP7. Such equilibrium could be altered by overexpression of each component (A and D) or with chemical and enzymatic treatments (B and C). PrP increase correlates with PIP7 accumulation whereas PrP decrease produces the same effect on PIP7. On the contrary, PIP7 overexpression is able to reduce endogenous PrP levels. Arrows refer to PIP7 kinetics only.

compartments before entering clathrin-coated pits (Gorodinsky and Harris, 1995; Sunyach et al., 2003). Assuming that PrP can exist in equilibrium between detergent-insoluble rafts and detergent-soluble compartments, PrP overexpression could cause PIP7 sequestration to lipid rafts and, conversely, PIP7 overexpression could extract PrP from its raft environment and relocate it into clathrin-coated pits where it can undergo endocytosis. In support of this hypothesis, I performed a sucrose gradient and confirmed the presence of PIP7 in lipids rafts (data not shown). Moreover, PIP7 presents a putative clathrin internalisation motif (YXXΦ) whose function I am planning to confirm by site-directed mutagenesis. The impairment of recognition by the adaptor complexes (APs) could result in a dominant negative PIP7, still able to bind PrP but unable to undergo endocytosis. The effect of such a mutant on PrP will be monitored by FACS and confocal microscopy.

In my experimental conditions, PIP7 siRNA did not alter PrP levels. Although in theory this could be attributed to the incomplete knock-down obtained, the ablation of PIP7 surface pool could in eventually be compensated for by alternative PrP partners such as the laminin receptor.

6.5 Study of *in vivo* correlation between PrP and PIP7 levels

The results obtained *in vitro*, either by PrP overexpression or PIPLC treatment, revealed that the PIP7 surface pool has the ability to respond to PrP variations. I wanted to further extend my analysis *in vivo* by looking at the PIP7 levels in the total absence of PrP and addressing whether PrP had any role in determining the residency of PIP7 on the cell surface. The marked reduction in the PIP7 membrane subpopulation in PrP knockout mice further strengthens the hypothesis of a role for PrP in establishing the amount of PIP7 present at the plasma membrane (Figure 6.2A and B). To my knowledge there is one other reported case of an identified PrP interactor whose levels appear to be altered in response to the ablation of the *Prnp* gene. NCAM, originally identified by chemical cross-linking experiments, has been recently shown to directly interact with PrP and the targeting of NCAM to lipids rafts was reduced specifically in $Prnp^{-/-}$ brain. The authors suggested that PrP would facilitate NCAM recruitment to lipid rafts with subsequent Fyn kinase activation and stimulation of neurite outgrowth (Santuccione et al., 2005; Schmitt-Ulms et al., 2001).

6.5.1 PIP7-PrP as a potential signal transduction complex

NCAM and PIP7 present quite remarkable analogies since both appear to be regulated by PrP levels. PrP has been previously implicated in signal transduction but, due to the absence of a cytoplasmic domain, it is difficult to conceive any mechanism not relying on as-yet unidentified transmembrane molecules (Mouillet-Richard et al., 2000; Solforosi et al., 2004). NCAM has been suggested to provide such a link between PrP in the extracellular space and the signal transduction machinery present in the cytoplasm (Santuccione et al., 2005). Hypothetically, PIP7 could also play an analogous role, as suggested by published data. In fact, CEA stimulation of *in vitro* cultures of rat Kupffer cells results in the production of IL-1α, IL-6, IL10 and TNF-αcytokines as a consequence of a signalling cascade depending on tyrosine phosphorylation (Gangopadhyay et al., 1997). A later study revealed that PIP7 itself, known to be the CEA receptor, is phosphorylated on tyrosine residues following CEA binding (Laguinge et al., 2005). I performed a preliminary experiment where N2a cells were treated with the α-PIP7 specific mAbs or with control antibodies. An increase in total tyrosine phosphorylation was observed exclusively in the samples treated with the 4H5 and 1B8 mAbs (data not shown). PIP7 contains five tyrosine residues and the NetPhos server predicts two possible tyrosine phosphorylation sites (amino acids 63 and 99). These residues are located before the first transmembrane helix and are predicted to be located in the cytoplasm. Further work is required to study the effect of tyrosine phosphorylation on PIP7 endocytosis and signal transduction ability, to further clarificaty its function.

6.5.2 Possible involvement of PIP7 in the Shmerling Syndrome

Shmerling and colleagues originally proposed the idea of an interaction between PrP and a putative ligand (L_{PrP}), which elicits an essential signal, and also hypothesised the existence of a PrP-like molecule (π) with lower binding affinity able to fulfil the same function as PrP. According to this hypothesis, PrP-ΔF could interact with L_{PrP}, displacing π without eliciting the survival signal. PrP could compete with its truncated counterpart and restore the signal, providing an explanation why PrP-ΔF is toxic only in the PrP knockout background. PrP would be able to engage L_{PrP} with the C-terminal domain whereas the N-terminal flexible region would somehow be involved in eliciting

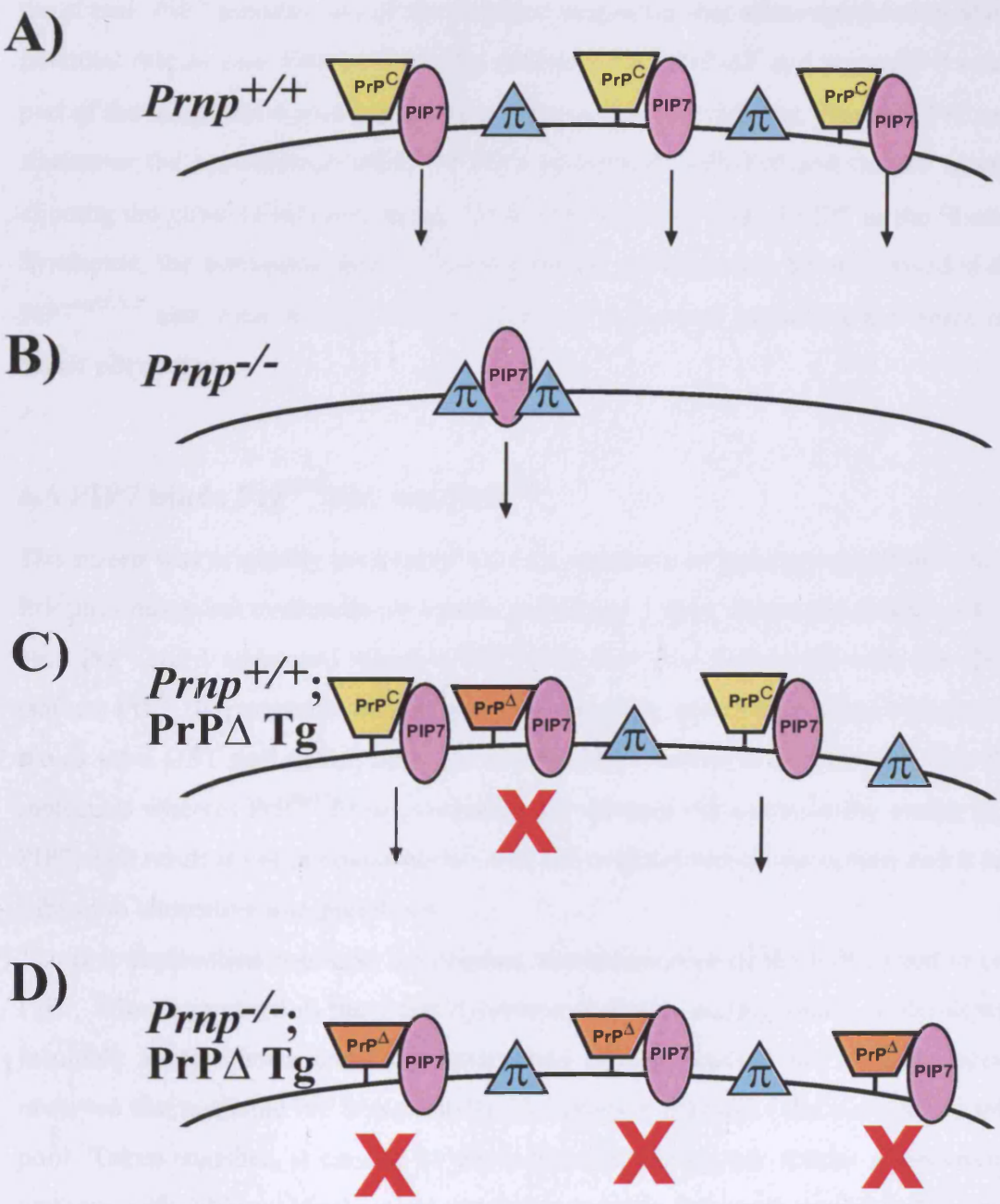

Figure 6.2 *In vivo* PrP-PIP7 correlation and putative involvement in the Shmerling Syndrome
PrP-PIP7 correlation was observed *in vivo* where decreased PIP7 levels were found in the membrane fraction of PrP knockout brain compared to wild type control (A and B). According to the model proposed by Shmerling and colleagues, the interaction between full length PrP and a putative ligand is required to transduce a survival signal. In the absence of PrP, the signal can be elicited by π, a molecule with structural similarities to PrP. However, PrP-ΔF is able to engage the ligand, after displacing π, without producing the required signal cascade. Since PIP7 role in signal transduction has been previously suggested, ongoing experiments will be able to address the PIP7 role in the Shmerling Syndrome (C and D). Black arrows represent ability to transduce the hypothesised survival signal whereas red crosses indicate the impairment of the signal cascade.

the signal. PIP7 possess two of the required properties that allow speculation about its potential role as L_{PrP}. Firstly, it has the ability to bind PrP-ΔF and secondly it could be part of the suggested signalling pathway required for cell viability. Figure 6.2 (C and D) illustrates the hypothetical effect of PIP7 interaction with PrP and the ΔF mutant in eliciting the putative survival signal. To test the possible role of PIP7 in the Shmerling Syndrome, the transgenic line harbouring the ΔF mutation are being crossed with the $PIP7^{NPX/XE}$ and mice will be analysed for any difference regarding the onset of the ataxic phenotype.

6.6 PIP7 binds PrP^{Sen} but not PrP^{Res}

The screen was originally performed with the intention of gaining insight not only into PrP physiology but eventually also prion pathology. I have shown the ability of PIP7 to bind PrP^{C} and I addressed whether PIP7 was also able to interact with the aberrant isoform PrP^{Sc}. Experiments with Protease K digestion, performed either before or after the *in vitro* GST pull down, have shown that PIP7 interacts exclusively with PrP^{Sen} molecules whereas PrP^{Res} from terminally sick animals did not have the ability to bind PIP7. The result is not in contradiction with the original aim of the screen and it can be subject to alternative interpretations.

The first explanation concerns the original characterisation of the bait I used to isolate PIP7. When expressed in the yeast cytoplasm PrP was mainly found in the detergent insoluble fraction but a small percentage was also detected in the soluble fraction. I observed that insoluble PrP was partially PK resistant although I did not test the soluble pool. Taken together, it cannot be excluded that during my screen alternative PrP isoforms with different biochemical properties, namely detergent insoluble-PK resistant species as well as detergent soluble-PK sensitive isoforms were present at the same time. Taking this into consideration, it is at present not possible to determine which PrP isoform interacted with PIP7 to rescue the Cdc25-2 mutation.

The second possible explanation is based on my original working hypothesis: to screen for interactors that preferentially recognize misfolded PrP which not necessarily has to be PK resistant or overlap with PrP^{Sc}. The screen took place in an environment that was only mildly acidic compared to the more extreme conditions used to generate PK resistant PrP *in vitro*; such conditions involved complete denaturation and secondary

structure rearrangement by using chaotropic and reducing agents, such as GdnHCl and DTT and the far more extreme pH value of 4.0.
I believe both explanations must be taken into consideration to determine the validity of the screen, which successfully identified a new PrP interacting partner.

Possible explanations for the pH dependency

PIP7 has the ability to interact *in vivo* with PrP^C but in the GST pull down assay the interaction showed a strict preference for acidic conditions whereas at the physiological pH of 7.4 the interaction was much weaker. The interaction was stable and reproducible in the pH range 6 to 5 and minimal binding was observed at pH 4.0. The explanation of such behaviour is still under investigation but a reasonable hypothesis could be the preference for a specific PrP misfolded intermediate, reported to be present exclusively at pH values between 6.0 and 4.0 (Swietnicki et al., 1997). Acidic conditions and the presence of strong denaturants have the ability to trigger a conformational change in human PrP (90-231) and mouse PrP (121-231) towards a β-sheet rich intermediate, unveiling the intrinsic pH dependency of the C-terminal globular domain (Hornemann and Glockshuber, 1998). Acidic conditions influence protein conformation primarily by altering the protonation state of residues such as glutamic/aspartic acid, lysine, arginine and histidine. Previously established salt bridges could be disrupted and new ones could be formed, resulting in a different folding. However, since PrP rearrangement occurs even at mildly acidic values, histidines are believed to become protonated most readily. This hypothesis finds experimental evidence in molecular dynamics studies, showing that protonation of His187 alone could result in protein transition with a rapid decrease in α helical content and parallel increase in β structures (Langella et al., 2004). In the His187Arg substitution, associated with GSS, the presence of a constitutive positive charge is believed to destabilise PrP resulting in a β-rich conformation. (Cervenakova et al., 1999).
However, the effect of pH cannot be restricted to PrP only. The pH has also the ability to change the binding properties of PIP7, since it has been reported to bind human thyroglobulin specifically in acidic conditions. However, no other information is available at present regarding the influence of pH on the PIP7 protein.

In summary, two different components might be responsible for the pH dependency of the studied interaction since the acidic conditions could alter either the conformation of PrP, PIP7 or both. This could affect their relative affinity for each other and at this point neither possibility can be excluded.

6.7 Potential role of PIP7 in prion disease

The possible involvement of PIP7 in prion replication has been tested using two complementary approaches. The *in vivo* assay using mutated PIP7 grafted tissue excluded its absolute requirement for PrP^{Sc} replication. However, the tested tissue still contained a small amount of PIP7, making it difficult to unambiguously rule out a function of PIP7 in scrapie pathogenesis. However, the lack of effect obtained in the Scrapie Cell assay after one week of treatment with a panel of the α-PIP7 mAbs further argues against a role of PIP7 in prion diseases.

6.8 Concluding remarks and future directions

The aim of this work was to identify novel prion interacting molecules and, based on the preliminary characterisation, PIP7 fulfils the original idea. The link between PrP and PIP7 had been demonstrated both *in vitro* and *in vivo.*

Many possible functions have been attributed to the prion protein in the past (Lasmezas, 2003). PrP does not seem to possess a biological activity that can be easily identified although it may be able to modulate the function of other proteins. A possible scenario, compatible both with the data I have acquired on PIP7 and the NCAM studies, proposes that PrP is able to play the role of a docking molecule able to anchor other molecules to specific lipid microenvironments. The reasons behind this could be multiple: PrP could favour the interaction of the target protein with alternative partners by localisation in specific lipid microdomains, such as lipids rafts which have been shown to be involved in signal transduction (Lucero and Robbins, 2004). Otherwise, PrP could prevent its partner's interaction with other molecules simply by sequestration. In both cases, the surface concentration of such molecules would be strictly regulated by PrP levels and turnover as suggested by my *in vitro* and *in vivo* analysis. However, this hypothesis requires more experiments in order to be confirmed and the isolation of other membrane

molecules showing an analogous mechanism of regulation to PIP7 and NCAM would certainly strengthen the case.

PIP7 is an interesting molecule which is able to play very diverse functions in light of its dual localisation both inside the nucleus and on the cell surface (Bajenova et al., 2001; Datar et al., 1993). Many attempts have been previously taken to find proteins interacting with PrP, mainly with the aim to clarify its enigmatic physiological role. I originally performed a screen in order to identify PrP partners with a well understood biology. However, the biology of PIP7 seems as unclear as that of PrP, allowing only speculative conclusions to be drawn.

PIP7 seems to fulfil the original idea of a PrP receptor as stated by David Harris of a cell surface molecule with the ability to bind and regulate PrP levels (Shyng et al., 1995b). It is possible that more than one PrP receptor exists and this would not be in contradiction with the proposed function of the laminin receptor (Gauczynski et al., 2001). My data suggests an intimate relationship between PrP and PIP7 since modulating the amount of either one reflects the levels of the other. Further experiments have to be done to confirm the effective role of PIP7 as a PrP receptor. The results of the present study and of future efforts would be extremely beneficial to clarify both PrP and PIP7 biology.

References

Aguzzi, A., and Heikenwalder, M. (2005). Prions, cytokines, and chemokines: a meeting in lymphoid organs. Immunity *22*, 145-154.
Aguzzi, A., Montrasio, F., and Kaeser, P. S. (2001). Prions: health scare and biological challenge. Nat Rev Mol Cell Biol *2*, 118-126.
Alberts, B., Bray, D., Lewis, J., Raff, M., Roberts, K., and Watson, J. D. (1994). Molecular Biology of the Cell. 623-624.
Alper, T., Cramp, W. A., Haig, D. A., and Clarke, M. C. (1967). Does the agent of scrapie replicate without nucleic acid? Nature *214*, 764-766.
Anderson, R. G. (1998). The caveolae membrane system. Annu Rev Biochem *67*, 199-225.
Anderson, R. M., Donnelly, C. A., Ferguson, N. M., Woolhouse, M. E., Watt, C. J., Udy, H. J., MaWhinney, S., Dunstan, S. P., Southwood, T. R., Wilesmith, J. W., *et al.* (1996). Transmission dynamics and epidemiology of BSE in British cattle. Nature *382*, 779-788.
Bajenova, O., Stolper, E., Gapon, S., Sundina, N., Zimmer, R., and Thomas, P. (2003). Surface expression of heterogeneous nuclear RNA binding protein M4 on Kupffer cell relates to its function as a carcinoembryonic antigen receptor. Exp Cell Res *291*, 228-241.
Bajenova, O. V., Zimmer, R., Stolper, E., Salisbury-Rowswell, J., Nanji, A., and Thomas, P. (2001). Heterogeneous RNA-binding protein M4 is a receptor for carcinoembryonic antigen in Kupffer cells. J Biol Chem *276*, 31067-31073.
Baker, R. K., Haendel, M. A., Swanson, B. J., Shambaugh, J. C., Micales, B. K., and Lyons, G. E. (1997). In vitro preselection of gene-trapped embryonic stem cell clones for characterizing novel developmentally regulated genes in the mouse. Dev Biol *185*, 201-214.
Baldauf, E., Beekes, M., and Diringer, H. (1997). Evidence for an alternative direct route of access for the scrapie agent to the brain bypassing the spinal cord. J Gen Virol *78*, 1187-1197.
Banchereau, J., Briere, F., Caux, C., Davoust, J., Lebecque, S., Liu, Y. J., Pulendran, B., and Palucka, K. (2000). Immunobiology of dendritic cells. Annu Rev Immunol *18*, 767-811.
Basler, K., Oesch, B., Scott, M., Westaway, D., Walchli, M., Groth, D. F., McKinley, M. P., Prusiner, S. B., and Weissmann, C. (1986). Scrapie and cellular PrP isoforms are encoded by the same chromosomal gene. Cell *46*, 417-428.
Bastian, F. O. (1979). Spiroplasma-like inclusions in Creutzfeldt-Jakob disease. Arch Pathol Lab Med *103*, 665-669.
Beglova, N., Jeon, H., Fisher, C., and Blacklow, S. C. (2004). Cooperation between fixed and low pH-inducible interfaces controls lipoprotein release by the LDL receptor. Mol Cell *16*, 281-292.
Behrens, A., Brandner, S., Genoud, N., and Aguzzi, A. (2001). Normal neurogenesis and scrapie pathogenesis in neural grafts lacking the prion protein homologue Doppel. EMBO Rep *2*, 347-352.

Behrens, A., Genoud, N., Naumann, H., Rulicke, T., Janett, F., Heppner, F. L., Ledermann, B., and Aguzzi, A. (2002). Absence of the prion protein homologue Doppel causes male sterility. Embo J *21*, 3652-3658.
Bell, J. E., and Ironside, J. W. (1993). Neuropathology of spongiform encephalopathies in humans. Br Med Bull *49*, 738-777.
Beranger, F., Mange, A., Goud, B., and Lehmann, S. (2002). Stimulation of PrP(C) retrograde transport toward the endoplasmic reticulum increases accumulation of PrP(Sc) in prion-infected cells. J Biol Chem *277*, 38972-38977.
Beringue, V., Demoy, M., Lasmezas, C. I., Gouritin, B., Weingarten, C., Deslys, J. P., Andreux, J. P., Couvreur, P., and Dormont, D. (2000). Role of spleen macrophages in the clearance of scrapie agent early in pathogenesis. J Pathol *190*, 495-502.
Bessen, R. A., and Marsh, R. F. (1994). Distinct PrP properties suggest the molecular basis of strain variation in transmissible mink encephalopathy. J Virol *68*, 7859-7868.
Bessen, R. A., Raymond, G. J., and Caughey, B. (1997). In situ formation of protease-resistant prion protein in transmissible spongiform encephalopathy-infected brain slices. J Biol Chem *272*, 15227-15231.
Blanck, O., Perrin, C., Mziaut, H., Darbon, H., Mattei, M. G., and Miquelis, R. (1994). Molecular cloning, cDNA analysis, and localization of a monomer of the N-acetylglucosamine-specific receptor of the thyroid, NAGR1, to chromosome 19p13.3-13.2. Genomics *21*, 18-26.
Blanck, O., Perrin, C., Mziaut, H., Darbon, H., Mattei, M. G., and Miquelis, R. (1995). Molecular cloning, cDNA analysis, and localization of a monomer of the N-acetylglucosamine-specific receptor of the thyroid, NAGR1, to chromosome 19p13.3-13.2. Genomics *27*, 561.
Blättler, T., Brandner, S., Raeber, A. J., Klein, M. A., Voigtländer, T., Weissmann, C., and Aguzzi, A. (1997). PrP-expressing tissue required for transfer of scrapie infectivity from spleen to brain. Nature *389*, 69-73.
Bolton, D. C., McKinley, M. P., and Prusiner, S. B. (1982). Identification of a protein that purifies with the scrapie prion. Science *218*, 1309-1311.
Borchelt, D. R., Koliatsos, V. E., Guarnieri, M., Pardo, C. A., Sisodia, S. S., and Price, D. L. (1994). Rapid anterograde axonal transport of the cellular prion glycoprotein in the peripheral and central nervous systems. J Biol Chem *269*, 14711-14714.
Borchelt, D. R., Scott, M., Taraboulos, A., Stahl, N., and Prusiner, S. B. (1990). Scrapie and cellular prion proteins differ in their kinetics of synthesis and topology in cultured cells. J Cell Biol *110*, 743-752.
Bosque, P. J., and Prusiner, S. B. (2000). Cultured cell sublines highly susceptible to prion infection. J Virol *74*, 4377-4386.
Bragason, B. T., and Palsdottir, A. (2005). Interaction of PrP with NRAGE, a protein involved in neuronal apoptosis. Mol Cell Neurosci *29*, 232-244.
Broder, Y. C., Katz, S., and Aronheim, A. (1998). The ras recruitment system, a novel approach to the study of protein-protein interactions. Curr Biol *8*, 1121-1124.
Brown, D. R., Hafiz, F., Glasssmith, L. L., Wong, B. S., Jones, I. M., Clive, C., and Haswell, S. J. (2000). Consequences of manganese replacement of copper for prion protein function and proteinase resistance. Embo J *19*, 1180-1186.
Brown, D. R., Qin, K., Herms, J. W., Madlung, A., Manson, J., Strome, R., Fraser, P. E., Kruck, T., von Bohlen, A., Schulz-Schaeffer, W., *et al.* (1997). The cellular prion protein binds copper in vivo. Nature *390*, 684-687.
Brown, D. R., Wong, B. S., Hafiz, F., Clive, C., Haswell, S. J., and Jones, I. M. (1999a). Normal prion protein has an activity like that of superoxide dismutase [published erratum appears in Biochem J 2000 Feb 1;345 Pt 3:767]. Biochem J *344 Pt 1*, 1-5.

Brown, K. L., Stewart, K., Ritchie, D. L., Mabbott, N. A., Williams, A., Fraser, H., Morrison, W. I., and Bruce, M. E. (1999b). Scrapie replication in lymphoid tissues depends on prion protein- expressing follicular dendritic cells. Nat Med *5*, 1308-1312.
Brown, P., and Bradley, R. (1998). 1755 and all that: a historical primer of transmissible spongiform encephalopathy. Bmj *317*, 1688-1692.
Bruce, M., Chree, A., McConnell, I., Foster, J., Pearson, G., and Fraser, H. (1994). Transmission of bovine spongiform encephalopathy and scrapie to mice: strain variation and the species barrier. Philos Trans R Soc Lond B Biol Sci *343*, 405-411.
Bruce, M. E., Fraser, H., McBride, P. A., Scott, J. R., and Dickinson, A. G. (1992). The basis of strain variation in scrapie, In Prion Diseases of Humans and Animals, S. B. Prusiner, J. Collinge, J. Powell, and B. Anderton, eds. (New York, London: Ellis Horwood), pp. 497-508.
Bruce, M. E., Will, R. G., Ironside, J. W., McConnell, I., Drummond, D., Suttie, A., McCardle, L., Chree, A., Hope, J., Birkett, C., *et al.* (1997). Transmissions to mice indicate that 'new variant' CJD is caused by the BSE agent [see comments]. Nature *389*, 498-501.
Budka, H., Aguzzi, A., Brown, P., Brucher, J. M., Bugiani, O., Gullotta, F., Haltia, M., Hauw, J. J., Ironside, J. W., Jellinger, K., and et al. (1995). Neuropathological diagnostic criteria for Creutzfeldt-Jakob disease (CJD) and other human spongiform encephalopathies (prion diseases). Brain Pathol *5*, 459-466.
Butler, D. A., Scott, M. R., Bockman, J. M., Borchelt, D. R., Taraboulos, A., Hsiao, K. K., Kingsbury, D. T., and Prusiner, S. B. (1988). Scrapie-infected murine neuroblastoma cells produce protease-resistant prion proteins. J Virol *62*, 1558-1564.
Büeler, H., Fischer, M., Lang, Y., Bluethmann, H., Lipp, H., DeArmond, S., Prusiner, S., Aguet, M., and Weissmann, C. (1992). Normal development and behaviour of mice lacking the neuronal cell-surface PrP protein. Nature *356*, 577-582.
Büeler, H. R., Aguzzi, A., Sailer, A., Greiner, R. A., Autenried, P., Aguet, M., and Weissmann, C. (1993). Mice devoid of PrP are resistant to scrapie. Cell *73*, 1339-1347.
Carimalo, J., Cronier, S., Petit, G., Peyrin, J. M., Boukhtouche, F., Arbez, N., Lemaigre-Dubreuil, Y., Brugg, B., and Miquel, M. C. (2005). Activation of the JNK-c-Jun pathway during the early phase of neuronal apoptosis induced by PrP106-126 and prion infection. Eur J Neurosci *21*, 2311-2319.
Carp, R. I., and Callahan, S. M. (1982). Effect of mouse peritoneal macrophages on scrapie infectivity during extended in vitro incubation. Intervirology *17*, 201-207.
Cashman, N. R., Loertscher, R., Nalbantoglu, J., Shaw, I., Kascsak, R. J., Bolton, D. C., and Bendheim, P. E. (1990). Cellular isoform of the scrapie agent protein participates in lymphocyte activation. Cell *61*, 185-192.
Castilla, J., Saa, P., Hetz, C., and Soto, C. (2005). In vitro generation of infectious scrapie prions. Cell *121*, 195-206.
Caughey, B. (2003). Prion protein conversions: insight into mechanisms, TSE transmission barriers and strains. Br Med Bull *66*, 109-120.
Caughey, B., and Raymond, G. J. (1993). Sulfated polyanion inhibition of scrapie-associated PrP accumulation in cultured cells. J Virol *67*, 643-650.
Caughey, B. W., Dong, A., Bhat, K. S., Ernst, D., Hayes, S. F., and Caughey, W. S. (1991). Secondary structure analysis of the scrapie-associated protein PrP 27-30 in water by infrared spectroscopy [published erratum appears in Biochemistry 1991 Oct 29;30(43):10600]. Biochemistry *30*, 7672-7680.
Cervenakova, L., Buetefisch, C., Lee, H. S., Taller, I., Stone, G., Gibbs, C. J., Jr., Brown, P., Hallett, M., and Goldfarb, L. G. (1999). Novel PRNP sequence variant associated with familial encephalopathy. Am J Med Genet *88*, 653-656.

Chesebro, B., Race, R., Wehrly, K., Nishio, J., Bloom, M., Lechner, D., Bergstrom, S., Robbins, K., Mayer, L., and Keith, J. M. (1985). Identification of scrapie prion protein-specific mRNA in scrapie-infected and uninfected brain. Nature *315*, 331-333.
Chiarini, L. B., Freitas, A. R., Zanata, S. M., Brentani, R. R., Martins, V. R., and Linden, R. (2002). Cellular prion protein transduces neuroprotective signals. Embo J *21*, 3317-3326.
Cohen, F. E., Pan, K. M., Huang, Z., Baldwin, M., Fletterick, R. J., and Prusiner, S. B. (1994). Structural clues to prion replication. Science *264*, 530-531.
Collinge, J. (2001). Prion diseases of humans and animals: their causes and molecular basis. Annu Rev Neurosci *24*, 519-550.
Collinge, J., Palmer, M. S., Sidle, K. C., Hill, A. F., Gowland, I., Meads, J., Asante, E., Bradley, R., Doey, L. J., and Lantos, P. L. (1995). Unaltered susceptibility to BSE in transgenic mice expressing human prion protein. Nature *378*, 779-783.
Collinge, J., Sidle, K. C., Meads, J., Ironside, J., and Hill, A. F. (1996). Molecular analysis of prion strain variation and the aetiology of 'new variant' CJD. Nature *383*, 685-690.
Collinge, J., Whittington, M. A., Sidle, K. C., Smith, C. J., Palmer, M. S., Clarke, A. R., and Jefferys, J. G. (1994). Prion protein is necessary for normal synaptic function. Nature *370*, 295-297.
Creutzfeldt, H. G. (1920). Über eine eigenartige herdförmige Erkrankung des Zentralnervensystems. Z ges Neurol Psychiatr *57*, 1-19.
Cyster, J. G., Ngo, V. N., Ekland, E. H., Gunn, M. D., Sedgwick, J. D., and Ansel, K. M. (1999). Chemokines and B-cell homing to follicles. Curr Top Microbiol Immunol *246*, 87-92; discussion 93.
Datar, K. V., Dreyfuss, G., and Swanson, M. S. (1993). The human hnRNP M proteins: identification of a methionine/arginine-rich repeat motif in ribonucleoproteins. Nucleic Acids Res *21*, 439-446.
DebBurman, S. K., Raymond, G. J., Caughey, B., and Lindquist, S. (1997). Chaperone-supervised conversion of prion protein to its protease- resistant form. Proc Natl Acad Sci U S A *94*, 13938-13943.
Deleault, N. R., Lucassen, R. W., and Supattapone, S. (2003). RNA molecules stimulate prion protein conversion. Nature *425*, 717-720.
Della-Bianca, V., Rossi, F., Armato, U., Dal-Pra, I., Costantini, C., Perini, G., Politi, V., and Della Valle, G. (2001). Neurotrophin p75 receptor is involved in neuronal damage by prion peptide-(106-126). J Biol Chem *276*, 38929-38933.
Detwiler, L. A., and Rubenstein, R. (2000). Bovine spongiform encephalopathy: an overview. Asaio J *46*, S73-79.
Dickinson, A. G., Meikle, V. M., and Fraser, H. (1968). Identification of a gene which controls the incubation period of some strains of scrapie agent in mice. J Comp Pathol *78*, 293-299.
Dickinson, A. G., and Outram, G. W. (1988). Genetic aspects of unconventional virus infections: the basis of the virino hypothesis. Ciba Found Symp *135*, 63-83.
Drisaldi, B., Coomaraswamy, J., Mastrangelo, P., Strome, B., Yang, J., Watts, J. C., Chishti, M. A., Marvi, M., Windl, O., Ahrens, R., *et al.* (2004). Genetic mapping of activity determinants within cellular prion proteins: N-terminal modules in PrPC offset pro-apoptotic activity of the Doppel helix B/B' region. J Biol Chem *279*, 55443-55454.
Drisaldi, B., Stewart, R. S., Adles, C., Stewart, L. R., Quaglio, E., Biasini, E., Fioriti, L., Chiesa, R., and Harris, D. A. (2003). Mutant PrP is delayed in its exit from the endoplasmic reticulum, but neither wild-type nor mutant PrP undergoes retrotranslocation prior to proteasomal degradation. J Biol Chem *278*, 21732-21743.

Duffy, P., Wolf, J., Collins, G., DeVoe, A. G., Streeten, B., and Cowen, D. (1974). Possible person-to-person transmission of Creutzfeldt-Jakob disease. N Engl J Med *290*, 692-693.
Edenhofer, F., Rieger, R., Famulok, M., Wendler, W., Weiss, S., and Winnacker, E. L. (1996). Prion Protein Prpc Interacts With Molecular Chaperones of the Hsp60 Family. Journal of Virology *70*, 4724-4728.
Elsen, J. M., Amigues, Y., Schelcher, F., Ducrocq, V., Andreoletti, O., Eychenne, F., Khang, J. V., Poivey, J. P., Lantier, F., and Laplanche, J. L. (1999). Genetic susceptibility and transmission factors in scrapie: detailed analysis of an epidemic in a closed flock of Romanov. Arch Virol *144*, 431-445.
Enari, M., Flechsig, E., and Weissmann, C. (2001). Scrapie prion protein accumulation by scrapie-infected neuroblastoma cells abrogated by exposure to a prion protein antibody. Proc Natl Acad Sci U S A *98*, 9295-9299.
Ernst, D. R., and Race, R. E. (1993). Comparative analysis of scrapie agent inactivation methods. J Virol Methods *41*, 193-201.
Farquhar, C., Dickinson, A., and Bruce, M. (1999). Prophylactic potential of pentosan polysulphate in transmissible spongiform encephalopathies [letter]. Lancet *353*, 117.
Farquhar, C. F., Dornan, J., Somerville, R. A., Tunstall, A. M., and Hope, J. (1994). Effect of Sinc genotype, agent isolate and route of infection on the accumulation of protease-resistant PrP in non-central nervous system tissues during the development of murine scrapie. J Gen Virol *75*, 495-504.
Felten, S. Y., Felten, D. L., Bellinger, D. L., Carlson, S. L., Ackerman, K. D., Madden, K. S., Olschowka, J. A., and Livnat, S. (1988). Noradrenergic sympathetic innervation of lymphoid organs. Prog Allergy *43*, 14-36.
Fields, S., and Song, O. (1989). A novel genetic system to detect protein-protein interactions. Nature *340*, 245-246.
Fischer, M., Rülicke, T., Raeber, A., Sailer, A., Moser, M., Oesch, B., Brandner, S., Aguzzi, A., and Weissmann, C. (1996). Prion protein (PrP) with amino-proximal deletions restoring susceptibility of PrP knockout mice to scrapie. EMBO J *15*, 1255-1264.
Fischer, M. B., Roeckl, C., Parizek, P., Schwarz, H. P., and Aguzzi, A. (2000). Binding of disease-associated prion protein to plasminogen. Nature *408*, 479-483.
Flechsig, E., Hegyi, I., Enari, M., Schwarz, P., Collinge, J., and Weissmann, C. (2001). Transmission of scrapie by steel-surface-bound prions. Mol Med *7*, 679-684.
Flechsig, E., Hegyi, I., Leimeroth, R., Zuniga, A., Rossi, D., Cozzio, A., Schwarz, P., Rulicke, T., Gotz, J., Aguzzi, A., and Weissmann, C. (2003). Expression of truncated PrP targeted to Purkinje cells of PrP knockout mice causes Purkinje cell death and ataxia. Embo J *22*, 3095-3101.
Forloni, G., Angeretti, N., Chiesa, R., Monzani, E., Salmona, M., Bugiani, O., and Tagliavini, F. (1993). Neurotoxicity of a prion protein fragment. Nature *362*, 543-546.
Fraser, H., and Dickinson, A. G. (1973). Scrapie in mice. Agent-strain differences in the distribution and intensity of grey matter vacuolation. J Comp Pathol *83*, 29-40.
Fraser, H., and Farquhar, C. F. (1987). Ionising radiation has no influence on scrapie incubation period in mice. Vet Microbiol *13*, 211-223.
Fritzsche, T., Schnolzer, M., Fiedler, S., Weigand, M., Wiessler, M., and Frei, E. (2004). Isolation and identification of heterogeneous nuclear ribonucleoproteins (hnRNP) from purified plasma membranes of human tumour cell lines as albumin-binding proteins. Biochem Pharmacol *67*, 655-665.

Gabizon, R., McKinley, M. P., Groth, D., and Prusiner, S. B. (1988). Immunoaffinity purification and neutralization of scrapie prion infectivity. ProcNatlAcadSciUSA *85*, 6617-6621.
Gabus, C., Derrington, E., Leblanc, P., Chnaiderman, J., Dormont, D., Swietnicki, W., Morillas, M., Surewicz, W. K., Marc, D., Nandi, P., and Darlix, J. L. (2001). The prion protein has RNA binding and chaperoning properties characteristic of nucleocapsid protein NCP7 of HIV-1. J Biol Chem *276*, 19301-19309.
Gajdusek, D. C. (1977). Unconventional viruses and the origin and disappearance of kuru. Science *197*, 943-960.
Gajdusek, D. C., Gibbs, C. J., and Alpers, M. (1966). Experimental transmission of a Kuru-like syndrome to chimpanzees. Nature *209*, 794-796.
Gajdusek, D. C., and Zigas, V. (1957). Degenerative disease of the central nervous system in New Guinea; the endemic occurrence of kuru in the native population. N Engl J Med *257*, 974-978.
Gambetti, P., Parchi, P., Petersen, R. B., Chen, S. G., and Lugaresi, E. (1995). Fatal familial insomnia and familial Creutzfeldt-Jakob disease: clinical, pathological and molecular features. Brain Pathol *5*, 43-51.
Gangopadhyay, A., Lazure, D. A., and Thomas, P. (1997). Carcinoembryonic antigen induces signal transduction in Kupffer cells. Cancer Lett *118*, 1-6.
Gauczynski, S., Peyrin, J. M., Haik, S., Leucht, C., Hundt, C., Rieger, R., Krasemann, S., Deslys, J. P., Dormont, D., Lasmezas, C. I., and Weiss, S. (2001). The 37-kDa/67-kDa laminin receptor acts as the cell-surface receptor for the cellular prion protein. Embo J *20*, 5863-5875.
Gavin, A. C., and Superti-Furga, G. (2003). Protein complexes and proteome organization from yeast to man. Curr Opin Chem Biol *7*, 21-27.
Gibbons, R. A., and Hunter, G. D. (1967). Nature of the scrapie agent. Nature *215*, 1041-1043.
Gibbs, C. J., Jr., Gajdusek, D. C., Asher, D. M., Alpers, M. P., Beck, E., Daniel, P. M., and Matthews, W. B. (1968). Creutzfeldt-Jakob disease (spongiform encephalopathy): transmission to the chimpanzee. Science *161*, 388-389.
Gilch, S., Winklhofer, K. F., Groschup, M. H., Nunziante, M., Lucassen, R., Spielhaupter, C., Muranyi, W., Riesner, D., Tatzelt, J., and Schatzl, H. M. (2001). Intracellular re-routing of prion protein prevents propagation of PrP(Sc) and delays onset of prion disease. Embo J *20*, 3957-3966.
Glatzel, M., and Aguzzi, A. (2000). Peripheral pathogenesis of prion diseases [In Process Citation]. Microbes Infect *2*, 613-619.
Glatzel, M., Heppner, F. L., Albers, K. M., and Aguzzi, A. (2001). Sympathetic innervation of lymphoreticular organs is rate limiting for prion neuroinvasion. Neuron *31*, 25-34.
Goldfarb, L. G., Petersen, R. B., Tabaton, M., Brown, P., LeBlanc, A. C., Montagna, P., Cortelli, P., Julien, J., Vital, C., Pendelbury, W. W., and et al. (1992). Fatal familial insomnia and familial Creutzfeldt-Jakob disease: disease phenotype determined by a DNA polymorphism. Science *258*, 806-808.
Gordon, W. S. (1946). Advances in veterinary research. Vet Rec *58*, 516-520.
Gorodinsky, A., and Harris, D. A. (1995). Glycolipid-anchored proteins in neuroblastoma cells form detergent-resistant complexes without caveolin. J Cell Biol *129*, 619-627.
Gossler, A., Joyner, A. L., Rossant, J., and Skarnes, W. C. (1989). Mouse embryonic stem cells and reporter constructs to detect developmentally regulated genes. Science *244*, 463-465.

Graner, E., Mercadante, A. F., Zanata, S. M., Forlenza, O. V., Cabral, A. L., Veiga, S. S., Juliano, M. A., Roesler, R., Walz, R., Minetti, A., *et al.* (2000a). Cellular prion protein binds laminin and mediates neuritogenesis. Brain Res Mol Brain Res *76*, 85-92.
Graner, E., Mercadante, A. F., Zanata, S. M., Martins, V. R., Jay, D. G., and Brentani, R. R. (2000b). Laminin-induced PC-12 cell differentiation is inhibited following laser inactivation of cellular prion protein. FEBS Lett *482*, 257-260.
Griffith, J. S. (1967). Self-replication and scrapie. Nature *215*, 1043-1044.
Groschup, M. H., Beekes, M., McBride, P. A., Hardt, M., Hainfellner, J. A., and Budka, H. (1999). Deposition of disease-associated prion protein involves the peripheral nervous system in experimental scrapie. Acta Neuropathol (Berl) *98*, 453-457.
Hainfellner, J. A., and Budka, H. (1999). Disease associated prion protein may deposit in the peripheral nervous system in human transmissible spongiform encephalopathies. Acta Neuropathol (Berl) *98*, 458-460.
Harris, D. A., Gorodinsky, A., Lehmann, S., Moulder, K., and Shyng, S. L. (1996). Cell biology of the prion protein. Curr Top Microbiol Immunol *207*, 77-93.
Harris, D. A., Huber, M. T., van Dijken, P., Shyng, S. L., Chait, B. T., and Wang, R. (1993). Processing of a cellular prion protein: identification of N- and C-terminal cleavage sites. Biochemistry *32*, 1009-1016.
Hay, B., Barry, R. A., Lieberburg, I., Prusiner, S. B., and Lingappa, V. R. (1987). Biogenesis and transmembrane orientation of the cellular isoform of the scrapie prion protein [published errratum appears in Mol Cell Biol 1987 May;7(5):2035]. Mol Cell Biol *7*, 914-920.
Hegde, R. S., Mastrianni, J. A., Scott, M. R., DeFea, K. A., Tremblay, P., Torchia, M., DeArmond, S. J., Prusiner, S. B., and Lingappa, V. R. (1998). A transmembrane form of the prion protein in neurodegenerative disease. Science *279*, 827-834.
Hegde, R. S., Tremblay, P., Groth, D., DeArmond, S. J., Prusiner, S. B., and Lingappa, V. R. (1999). Transmissible and genetic prion diseases share a common pathway of neurodegeneration [see comments]. Nature *402*, 822-826.
Heikenwalder, M., Zeller, N., Seeger, H., Prinz, M., Klohn, P. C., Schwarz, P., Ruddle, N. H., Weissmann, C., and Aguzzi, A. (2005). Chronic lymphocytic inflammation specifies the organ tropism of prions. Science *307*, 1107-1110.
Henley, J. R., Krueger, E. W., Oswald, B. J., and McNiven, M. A. (1998). Dynamin-mediated internalization of caveolae. J Cell Biol *141*, 85-99.
Heppner, F. L., Christ, A. D., Klein, M. A., Prinz, M., Fried, M., Kraehenbuhl, J. P., and Aguzzi, A. (2001). Transepithelial prion transport by M cells. Nat Med *7*, 976-977.
Herms, J., Tings, T., Gall, S., Madlung, A., Giese, A., Siebert, H., Schurmann, P., Windl, O., Brose, N., and Kretzschmar, H. (1999). Evidence of presynaptic location and function of the prion protein. J Neurosci *19*, 8866-8875.
Herms, J. W., Kretzchmar, H. A., Titz, S., and Keller, B. U. (1995). Patch-clamp analysis of synaptic transmission to cerebellar purkinje cells of prion protein knockout mice. Eur J Neurosci *7*, 2508-2512.
Hill, A. F., Antoniou, M., and Collinge, J. (1999a). Protease-resistant prion protein produced in vitro lacks detectable infectivity. J Gen Virol *80*, 11-14.
Hill, A. F., Butterworth, R. J., Joiner, S., Jackson, G., Rossor, M. N., Thomas, D. J., Frosh, A., Tolley, N., Bell, J. E., Spencer, M., *et al.* (1999b). Investigation of variant Creutzfeldt-Jakob disease and other human prion diseases with tonsil biopsy samples [see comments]. Lancet *353*, 183-189.
Hill, A. F., Desbruslais, M., Joiner, S., Sidle, K. C., Gowland, I., Collinge, J., Doey, L. J., and Lantos, P. (1997a). The same prion strain causes vCJD and BSE [letter] [see comments]. Nature *389*, 448-450.

Hill, A. F., Zeidler, M., Ironside, J., and Collinge, J. (1997b). Diagnosis of new variant Creutzfeldt-Jakob disease by tonsil biopsy. Lancet *349*, 99.
Hilton, D. A., Fathers, E., Edwards, P., Ironside, J. W., and Zajicek, J. (1998). Prion immunoreactivity in appendix before clinical onset of variant Creutzfeldt-Jakob disease [letter]. Lancet *352*, 703-704.
Horiuchi, M., Priola, S. A., Chabry, J., and Caughey, B. (2000). Interactions between heterologous forms of prion protein: binding, inhibition of conversion, and species barriers [In Process Citation]. Proc Natl Acad Sci U S A *97*, 5836-5841.
Hornemann, S., and Glockshuber, R. (1998). A scrapie-like unfolding intermediate of the prion protein domain PrP(121-231) induced by acidic pH. Proc Natl Acad Sci U S A *95*, 6010-6014.
Hornshaw, M. P., McDermott, J. R., and Candy, J. M. (1995). Copper binding to the N-terminal tandem repeat regions of mammalian and avian prion protein. Biochem Biophys Res Commun *207*, 621-629.
Horonchik, L., Tzaban, S., Ben-Zaken, O., Yedidia, Y., Rouvinski, A., Papy-Garcia, D., Barritault, D., Vlodavsky, I., and Taraboulos, A. (2005). Heparan sulfate is a cellular receptor for purified infectious prions. J Biol Chem *280*, 17062-17067.
Hosszu, L. L., Baxter, N. J., Jackson, G. S., Power, A., Clarke, A. R., Waltho, J. P., Craven, C. J., and Collinge, J. (1999). Structural mobility of the human prion protein probed by backbone hydrogen exchange. Nat Struct Biol *6*, 740-743.
Houston, F., Foster, J. D., Chong, A., Hunter, N., and Bostock, C. J. (2000). Transmission of BSE by blood transfusion in sheep. Lancet *356*, 999-1000.
Hsiao, K., Baker, H. F., Crow, T. J., Poulter, M., Owen, F., Terwilliger, J. D., Westaway, D., Ott, J., and Prusiner, S. B. (1989). Linkage of a prion protein missense variant to Gerstmann-Straussler syndrome. Nature *338*, 342-345.
Huang, F. P., Farquhar, C. F., Mabbott, N. A., Bruce, M. E., and MacPherson, G. G. (2002). Migrating intestinal dendritic cells transport PrP(Sc) from the gut. J Gen Virol *83*, 267-271.
Hubsman, M., Yudkovsky, G., and Aronheim, A. (2001). A novel approach for the identification of protein-protein interaction with integral membrane proteins. Nucleic Acids Res *29*, E18.
Hunter, N., Goldmann, W., Benson, G., Foster, J. D., and Hope, J. (1993). Swaledale sheep affected by natural scrapie differ significantly in PrP genotype frequencies from healthy sheep and those selected for reduced incidence of scrapie. J Gen Virol *74*, 1025-1031.
Hutter, G., Heppner, F. L., and Aguzzi, A. (2003). No superoxide dismutase activity of cellular prion protein in vivo. Biol Chem *384*, 1279-1285.
Ironside, J. W., and Head, M. W. (2004). Variant Creutzfeldt-Jakob disease: risk of transmission by blood and blood products. Haemophilia *10 Suppl 4*, 64-69.
Ironside, J. W., Sutherland, K., Bell, J. E., McCardle, L., Barrie, C., Estebeiro, K., Zeidler, M., and Will, R. G. (1996). A new variant of Creutzfeldt-Jakob disease: neuropathological and clinical features. Cold Spring Harb Symp Quant Biol *61*, 523-530.
Isenmann, S., Brandner, S., and Aguzzi, A. (1996). Neuroectodermal grafting: a new tool for the study of neurodegenerative diseases. Histol Histopathol *11*, 1063-1073.
Jackson, G. S., Hosszu, L. L., Power, A., Hill, A. F., Kenney, J., Saibil, H., Craven, C. J., Waltho, J. P., Clarke, A. R., and Collinge, J. (1999). Reversible conversion of monomeric human prion protein between native and fibrilogenic conformations. Science *283*, 1935-1937.

Jackson, G. S., McKintosh, E., Flechsig, E., Prodromidou, K., Hirsch, P., Linehan, J., Brandner, S., Clarke, A. R., Weissmann, C., and Collinge, J. (2005). An enzyme-detergent method for effective prion decontamination of surgical steel. J Gen Virol *86*, 869-878.
Jackson, G. S., Murray, I., Hosszu, L. L., Gibbs, N., Waltho, J. P., Clarke, A. R., and Collinge, J. (2001). Location and properties of metal-binding sites on the human prion protein. Proc Natl Acad Sci U S A *98*, 8531-8535.
Jakob, A. (1921). Über eigenartige Erkrankungen des Zentralnervensystems mit bemerkenswertem anatomischem Befunde. (Spastische Pseudosklerose-Encephalomyelopathie mit disseminierten Degenerationsherden). Z ges Neurol Psychiatr *64*, 147-228.
James, T. L., Liu, H., Ulyanov, N. B., Farr-Jones, S., Zhang, H., Donne, D. G., Kaneko, K., Groth, D., Mehlhorn, I., Prusiner, S. B., and Cohen, F. E. (1997). Solution structure of a 142-residue recombinant prion protein corresponding to the infectious fragment of the scrapie isoform. Proc Natl Acad Sci U S A *94*, 10086-10091.
Jarrett, J. T., and Lansbury, P. T., Jr. (1993). Seeding "one-dimensional crystallization" of amyloid: a pathogenic mechanism in Alzheimer's disease and scrapie? Cell *73*, 1055-1058.
Jeffrey, M., McGovern, G., Goodsir, C. M., Brown, K. L., and Bruce, M. E. (2000). Sites of prion protein accumulation in scrapie-infected mouse spleen revealed by immuno-electron microscopy. J Pathol *191*, 323-332.
Jin, T., Gu, Y., Zanusso, G., Sy, M., Kumar, A., Cohen, M., Gambetti, P., and Singh, N. (2000). The chaperone protein BiP binds to a mutant prion protein and mediates its degradation by the proteasome. J Biol Chem *275*, 38699-38704.
Kaghad, M., Dumont, X., Chalon, P., Lelias, J. M., Lamande, N., Lucas, M., Lazar, M., and Caput, D. (1990). Nucleotide sequences of cDNAs alpha and gamma enolase mRNAs from mouse brain. Nucleic Acids Res *18*, 3638.
Kaneider, N. C., Kaser, A., Dunzendorfer, S., Tilg, H., and Wiedermann, C. J. (2003). Sphingosine kinase-dependent migration of immature dendritic cells in response to neurotoxic prion protein fragment. J Virol *77*, 5535-5539.
Kaneko, K., Vey, M., Scott, M., Pilkuhn, S., Cohen, F. E., and Prusiner, S. B. (1997a). COOH-terminal sequence of the cellular prion protein directs subcellular trafficking and controls conversion into the scrapie isoform. Proc Natl Acad Sci U S A *94*, 2333-2338.
Kaneko, K., Zulianello, L., Scott, M., Cooper, C. M., Wallace, A. C., James, T. L., Cohen, F. E., and Prusiner, S. B. (1997b). Evidence for protein X binding to a discontinuous epitope on the cellular prion protein during scrapie prion propagation. Proc Natl Acad Sci U S A *94*, 10069-10074.
Kellings, K., Meyer, N., Mirenda, C., Prusiner, S. B., and Riesner, D. (1992). Further analysis of nucleic acids in purified scrapie prion preparations by improved return refocusing gel electrophoresis. J Gen Virol *73*, 1025-1029.
Kiachopoulos, S., Heske, J., Tatzelt, J., and Winklhofer, K. F. (2004). Misfolding of the prion protein at the plasma membrane induces endocytosis, intracellular retention and degradation. Traffic *5*, 426-436.
Kimberlin, R. H. (1982). Scrapie agent: prions or virinos? Nature *297*, 107-108.
Kimberlin, R. H., Hall, S. M., and Walker, C. A. (1983). Pathogenesis of mouse scrapie. Evidence for direct neural spread of infection to the CNS after injection of sciatic nerve. J Neurol Sci *61*, 315-325.
Kimberlin, R. H., and Walker, C. (1977). Characteristics of a short incubation model of scrapie in the golden hamster. J Gen Virol *34*, 295-304.

Kimberlin, R. H., and Walker, C. A. (1979). Pathogenesis of mouse scrapie: dynamics of agent replication in spleen, spinal cord and brain after infection by different routes. J Comp Pathol *89*, 551-562.
Kitamoto, T., Muramoto, T., Mohri, S., Doh ura, K., and Tateishi, J. (1991). Abnormal isoform of prion protein accumulates in follicular dendritic cells in mice with Creutzfeldt-Jakob disease. JVirol *65*, 6292-6295.
Klein, M. A., Frigg, R., Flechsig, E., Raeber, A. J., Kalinke, U., Bluethmann, H., Bootz, F., Suter, M., Zinkernagel, R. M., and Aguzzi, A. (1997). A crucial role for B cells in neuroinvasive scrapie. Nature *390*, 687-690.
Klein, M. A., Frigg, R., Raeber, A. J., Flechsig, E., Hegyi, I., Zinkernagel, R. M., Weissmann, C., and Aguzzi, A. (1998). PrP expression in B lymphocytes is not required for prion neuroinvasion. Nat Med *4*, 1429-1433.
Klein, M. A., Kaeser, P. S., Schwarz, P., Weyd, H., Xenarios, I., Zinkernagel, R. M., Carroll, M. C., Verbeek, J. S., Botto, M., Walport, M. J., *et al.* (2001). Complement facilitates early prion pathogenesis. Nat Med *7*, 488-492.
Klohn, P. C., Stoltze, L., Flechsig, E., Enari, M., and Weissmann, C. (2003). A quantitative, highly sensitive cell-based infectivity assay for mouse scrapie prions. Proc Natl Acad Sci U S A *100*, 11666-11671.
Koch, T. K., Berg, B. O., De Armond, S. J., and Gravina, R. F. (1985). Creutzfeldt-Jakob disease in a young adult with idiopathic hypopituitarism. Possible relation to the administration of cadaveric human growth hormone. N Engl J Med *313*, 731-733.
Kocisko, D. A., Come, J. H., Priola, S. A., Chesebro, B., Raymond, G. J., Lansbury, P. T., and Caughey, B. (1994). Cell-free formation of protease-resistant prion protein [see comments]. Nature *370*, 471-474.
Koni, P. A., Sacca, R., Lawton, P., Browning, J. L., Ruddle, N. H., and Flavell, R. A. (1997). Distinct roles in lymphoid organogenesis for lymphotoxins alpha and beta revealed in lymphotoxin beta-deficient mice. Immunity *6*, 491-500.
Kopito, R. R. (1997). ER quality control: the cytoplasmic connection. Cell *88*, 427-430.
Kosco-Vilbois, M. H., Zentgraf, H., Gerdes, J., and Bonnefoy, J. Y. (1997). To 'B' or not to 'B' a germinal center? Immunol Today *18*, 225-230.
Krecic, A. M., and Swanson, M. S. (1999). hnRNP complexes: composition, structure, and function. Curr Opin Cell Biol *11*, 363-371.
Kretzschmar, H. A., Tings, T., Madlung, A., Giese, A., and Herms, J. (2000). Function of PrP(C) as a copper-binding protein at the synapse. Arch Virol Suppl, 239-249.
Kurschner, C., Morgan, J. I., Yehiely, F., Bamborough, P., Da Costa, M., Perry, B. J., Thinakaran, G., Cohen, F. E., Carlson, G. A., and Prusiner, S. B. (1995). The cellular prion protein (PrP) selectively binds to Bcl-2 in the yeast two-hybrid system Identification of candidate proteins binding to prion protein. Brain Res Mol Brain Res *30*, 165-168.
Kuwahara, C., Takeuchi, A. M., Nishimura, T., Haraguchi, K., Kubosaki, A., Matsumoto, Y., Saeki, K., Yokoyama, T., Itohara, S., and Onodera, T. (1999). Prions prevent neuronal cell-line death. Nature *400*, 225-226.
Ladogana, A., Casaccia, P., Ingrosso, L., Cibati, M., Salvatore, M., Xi, Y. G., Masullo, C., and Pocchiari, M. (1992). Sulphate polyanions prolong the incubation period of scrapie-infected hamsters. J Gen Virol *73*, 661-665.
Laguinge, L., Bajenova, O., Bowden, E., Sayyah, J., Thomas, P., and Juhl, H. (2005). Surface expression and CEA binding of hnRNP M4 protein in HT29 colon cancer cells. Anticancer Res *25*, 23-31.

Laine, J., Marc, M. E., Sy, M. S., and Axelrad, H. (2001). Cellular and subcellular morphological localization of normal prion protein in rodent cerebellum. Eur J Neurosci *14*, 47-56.
Langella, E., Improta, R., and Barone, V. (2004). Checking the pH-induced conformational transition of prion protein by molecular dynamics simulations: effect of protonation of histidine residues. Biophys J *87*, 3623-3632.
Larijani, B., Allen-Baume, V., Morgan, C. P., Li, M., and Cockcroft, S. (2003). EGF regulation of PITP dynamics is blocked by inhibitors of phospholipase C and of the Ras-MAP kinase pathway. Curr Biol *13*, 78-84.
Lasmezas, C. I. (2003). Putative functions of PrP(C). Br Med Bull *66*, 61-70.
Lasmezas, C. I., Deslys, J. P., Demaimay, R., Adjou, K. T., Lamoury, F., Dormont, D., Robain, O., Ironside, J., and Hauw, J. J. (1996). Bse Transmission to Macaques. Nature *381*, 743-744.
Lee, H. S., Brown, P., Cervenakova, L., Garruto, R. M., Alpers, M. P., Gajdusek, D. C., and Goldfarb, L. G. (2001a). Increased susceptibility to Kuru of carriers of the PRNP 129 methionine/methionine genotype. J Infect Dis *183*, 192-196.
Lee, K. S., Magalhaes, A. C., Zanata, S. M., Brentani, R. R., Martins, V. R., and Prado, M. A. (2001b). Internalization of mammalian fluorescent cellular prion protein and N-terminal deletion mutants in living cells. J Neurochem *79*, 79-87.
Lee, S., and Eisenberg, D. (2003). Seeded conversion of recombinant prion protein to a disulfide-bonded oligomer by a reduction-oxidation process. Nat Struct Biol *10*, 725-730.
Legname, G., Baskakov, I. V., Nguyen, H. O., Riesner, D., Cohen, F. E., DeArmond, S. J., and Prusiner, S. B. (2004). Synthetic mammalian prions. Science *305*, 673-676.
Legname, G., Nelken, P., Guan, Z., Kanyo, Z. F., DeArmond, S. J., and Prusiner, S. B. (2002). Prion and doppel proteins bind to granule cells of the cerebellum. Proc Natl Acad Sci U S A *99*, 16285-16290.
Leucht, C., Simoneau, S., Rey, C., Vana, K., Rieger, R., Lasmezas, C. I., and Weiss, S. (2003). The 37 kDa/67 kDa laminin receptor is required for PrP(Sc) propagation in scrapie-infected neuronal cells. EMBO Rep *4*, 290-295.
Leucht, C., Vana, K., Renner-Muller, I., Dormont, D., Lasmezas, C. I., Wolf, E., and Weiss, S. (2004). Knock-down of the 37-kDa/67-kDa laminin receptor in mouse brain by transgenic expression of specific antisense LRP RNA. Transgenic Res *13*, 81-85.
Liberski, P. P., Brown, P., Xiao, S. Y., and Gajdusek, D. C. (1991). The ultrastructural diversity of scrapie-associated fibrils isolated from experimental scrapie and Creutzfeldt-Jakob disease. J Comp Pathol *105*, 377-386.
Lucero, H. A., and Robbins, P. W. (2004). Lipid rafts-protein association and the regulation of protein activity. Arch Biochem Biophys *426*, 208-224.
Ma, J., and Lindquist, S. (1999). De novo generation of a PrPSc-like conformation in living cells. Nat Cell Biol *1*, 358-361.
Ma, J., and Lindquist, S. (2001). Wild-type PrP and a mutant associated with prion disease are subject to retrograde transport and proteasome degradation. Proc Natl Acad Sci U S A *98*, 14955-14960.
Ma, J., and Lindquist, S. (2002). Conversion of PrP to a self-perpetuating PrPSc-like conformation in the cytosol. Science *298*, 1785-1788.
Ma, J., Wollmann, R., and Lindquist, S. (2002). Neurotoxicity and neurodegeneration when PrP accumulates in the cytosol. Science *298*, 1781-1785.
Mabbott, N. A., Bruce, M. E., Botto, M., Walport, M. J., and Pepys, M. B. (2001). Temporary depletion of complement component C3 or genetic deficiency of C1q significantly delays onset of scrapie. Nat Med *7*, 485-487.

Mabbott, N. A., Williams, A., Farquhar, C. F., Pasparakis, M., Kollias, G., and Bruce, M. E. (2000). Tumor necrosis factor alpha-deficient, but not interleukin-6-deficient, mice resist peripheral infection with scrapie. J Virol *74*, 3338-3344.
Maddelein, M. L., Dos Reis, S., Duvezin-Caubet, S., Coulary-Salin, B., and Saupe, S. J. (2002). Amyloid aggregates of the HET-s prion protein are infectious. Proc Natl Acad Sci U S A *99*, 7402-7407.
Magalhaes, A. C., Silva, J. A., Lee, K. S., Martins, V. R., Prado, V. F., Ferguson, S. S., Gomez, M. V., Brentani, R. R., and Prado, M. A. (2002). Endocytic intermediates involved with the intracellular trafficking of a fluorescent cellular prion protein. J Biol Chem *277*, 33311-33318.
Maissen, M., Roeckl, C., Glatzel, M., Goldmann, W., and Aguzzi, A. (2001). Plasminogen binds to disease-associated prion protein of multiple species. Lancet *357*, 2026-2028.
Makrinou, E., Collinge, J., and Antoniou, M. (2002). Genomic characterization of the human prion protein (PrP) gene locus. Mamm Genome *13*, 696-703.
Malthiery, Y., and Lissitzky, S. (1987). Primary structure of human thyroglobulin deduced from the sequence of its 8448-base complementary DNA. Eur J Biochem *165*, 491-498.
Manson, J. C., Clarke, A. R., Hooper, M. L., Aitchison, L., McConnell, I., and Hope, J. (1994). 129/Ola mice carrying a null mutation in PrP that abolishes mRNA production are developmentally normal. Mol Neurobiol *8*, 121-127.
Marella, M., Lehmann, S., Grassi, J., and Chabry, J. (2002). Filipin prevents pathological prion protein accumulation by reducing endocytosis and inducing cellular PrP release. J Biol Chem *277*, 25457-25464.
Markovits, P., Dormont, D., Delpech, B., Court, L., and Latarjet, R. (1981). Trials of in vitro propagation of the scrapie agent in mouse nerve cells. C R Seances Acad Sci III *293*, 413-417.
Marsh, R. F., Bessen, R. A., Lehmann, S., and Hartsough, G. R. (1991). Epidemiological and experimental studies on a new incident of transmissible mink encephalopathy. J Gen Virol *72*, 589-594.
Marsh, R. F., and Hadlow, W. J. (1992). Transmissible mink encephalopathy. Rev Sci Tech *11*, 539-550.
Massimino, M. L., Ballarin, C., Bertoli, A., Casonato, S., Genovesi, S., Negro, A., and Sorgato, M. C. (2004). Human Doppel and prion protein share common membrane microdomains and internalization pathways. Int J Biochem Cell Biol *36*, 2016-2031.
Masters, C. L., Gajdusek, D. C., and Gibbs, C. J. (1981). Creutzfeldt-Jakob disease virus isolations from the Gerstmann-Straussler syndrome with an analysis of the various forms of amyloid plaque deposition in the virus-induced spongiform encephalopathies. Brain *104*, 559-588.
Masters, C. L., and Richardson, E. P. (1978). Subacute spongiform encephalopathy (Creutzfeldt-Jakob disease). The nature and progression of spongiform change. Brain *101*, 333-344.
Mastrangelo, P., Serpell, L., Dafforn, T., Lesk, A., Fraser, P., and Westaway, D. (2002). A cluster of familial Creutzfeldt-Jakob disease mutations recapitulate conserved residues in Doppel: a case of molecular mimicry? FEBS Lett *532*, 21-26.
Matsumoto, M., Mariathasan, S., Nahm, M. H., Baranyay, F., Peschon, J. J., and Chaplin, D. D. (1996). Role of lymphotoxin and the type I TNF receptor in the formation of germinal centers. Science *271*, 1289-1291.
Mayor, S., and Riezman, H. (2004). Sorting GPI-anchored proteins. Nat Rev Mol Cell Biol *5*, 110-120.

McBride, P. A., Eikelenboom, P., Kraal, G., Fraser, H., and Bruce, M. E. (1992). PrP protein is associated with follicular dendritic cells of spleens and lymph nodes in uninfected and scrapie-infected mice. J Pathol *168*, 413-418.
McFarlin, D. E., Raff, M. C., Simpson, E., and Nehlsen, S. H. (1971). Scrapie in immunologically deficient mice. Nature *233*, 336.
McKinley, M. P., Bolton, D. C., and Prusiner, S. B. (1983). A protease-resistant protein is a structural component of the scrapie prion. Cell *35*, 57-62.
Michels, A. A., Kanon, B., Konings, A. W., Ohtsuka, K., Bensaude, O., and Kampinga, H. H. (1997). Hsp70 and Hsp40 chaperone activities in the cytoplasm and the nucleus of mammalian cells. J Biol Chem *272*, 33283-33289.
Miquelis, R., Alquier, C., and Monsigny, M. (1987). The N-acetylglucosamine-specific receptor of the thyroid. Binding characteristics, partial characterization, and potential role. J Biol Chem *262*, 15291-15298.
Mironov, A., Jr., Latawiec, D., Wille, H., Bouzamondo-Bernstein, E., Legname, G., Williamson, R. A., Burton, D., DeArmond, S. J., Prusiner, S. B., and Peters, P. J. (2003). Cytosolic prion protein in neurons. J Neurosci *23*, 7183-7193.
Montrasio, F., Cozzio, A., Flechsig, E., Rossi, D., Klein, M. A., Rulicke, T., Raeber, A. J., Vosshenrich, C. A., Proft, J., Aguzzi, A., and Weissmann, C. (2001). B lymphocyte-restricted expression of prion protein does not enable prion replication in prion protein knockout mice. Proc Natl Acad Sci U S A *98*, 4034-4037.
Montrasio, F., Frigg, R., Glatzel, M., Klein, M. A., Mackay, F., Aguzzi, A., and Weissmann, C. (2000). Impaired prion replication in spleens of mice lacking functional follicular dendritic cells. Science *288*, 1257-1259.
Moore, R. C., Lee, I. Y., Silverman, G. L., Harrison, P. M., Strome, R., Heinrich, C., Karunaratne, A., Pasternak, S. H., Chishti, M. A., Liang, Y., *et al.* (1999). Ataxia in prion protein (PrP)-deficient mice is associated with upregulation of the novel PrP-like protein doppel [In Process Citation]. J Mol Biol *292*, 797-817.
Moore, R. C., Mastrangelo, P., Bouzamondo, E., Heinrich, C., Legname, G., Prusiner, S. B., Hood, L., Westaway, D., DeArmond, S. J., and Tremblay, P. (2001). Doppel-induced cerebellar degeneration in transgenic mice. Proc Natl Acad Sci U S A *98*, 15288-15293.
Mouillet-Richard, S., Ermonval, M., Chebassier, C., Laplanche, J. L., Lehmann, S., Launay, J. M., and Kellermann, O. (2000). Signal transduction through prion protein. Science *289*, 1925-1928.
Mouillet-Richard, S., Pietri, M., Schneider, B., Vidal, C., Mutel, V., Launay, J. M., and Kellermann, O. (2005). Modulation of serotonergic receptor signaling and cross-talk by prion protein. J Biol Chem *280*, 4592-4601.
Naslavsky, N., Stein, R., Yanai, A., Friedlander, G., and Taraboulos, A. (1997). Characterization of detergent-insoluble complexes containing the cellular prion protein and its scrapie isoform. J Biol Chem *272*, 6324-6331.
Neutra, M. R., Frey, A., and Kraehenbuhl, J. P. (1996). Epithelial M cells: gateways for mucosal infection and immunization. Cell *86*, 345-348.
Nicholson, E. M., Mo, H., Prusiner, S. B., Cohen, F. E., and Marqusee, S. (2002). Differences between the prion protein and its homolog Doppel: a partially structured state with implications for scrapie formation. J Mol Biol *316*, 807-815.
Nieznanski, K., Nieznanska, H., Skowronek, K. J., Osiecka, K. M., and Stepkowski, D. (2005). Direct interaction between prion protein and tubulin. Biochem Biophys Res Commun *334*, 403-411.
Nishida, N., Tremblay, P., Sugimoto, T., Shigematsu, K., Shirabe, S., Petromilli, C., Erpel, S. P., Nakaoke, R., Atarashi, R., Houtani, T., *et al.* (1999). A mouse prion protein

transgene rescues mice deficient for the prion protein gene from purkinje cell degeneration and demyelination. Lab Invest *79*, 689-697.
Norstrom, E. M., and Mastrianni, J. A. (2005). The AGAAAAGA palindrome in PrP is required to generate a productive PrPSc-PrPC complex that leads to prion propagation. J Biol Chem *280*, 27236-27243.
Oesch, B., Westaway, D., Walchli, M., McKinley, M. P., Kent, S. B., Aebersold, R., Barry, R. A., Tempst, P., Teplow, D. B., Hood, L. E., and Weissmann, C. (1985). A cellular gene encodes scrapie PrP 27-30 protein. Cell *40*, 735-746.
Ohtsuka, K. (1993). Cloning of a cDNA for heat-shock protein hsp40, a human homologue of bacterial DnaJ. Biochem Biophys Res Commun *197*, 235-240.
Owen, F., Poulter, M., Collinge, J., Leach, M., Lofthouse, R., Crow, T. J., and Harding, A. E. (1992). A dementing illness associated with a novel insertion in the prion protein gene. Brain Res Mol Brain Res *13*, 155-157.
Paitel, E., Alves da Costa, C., Vilette, D., Grassi, J., and Checler, F. (2002). Overexpression of PrPc triggers caspase 3 activation: potentiation by proteasome inhibitors and blockade by anti-PrP antibodies. J Neurochem *83*, 1208-1214.
Paitel, E., Sunyach, C., Alves da Costa, C., Bourdon, J. C., Vincent, B., and Checler, F. (2004). Primary cultured neurons devoid of cellular prion display lower responsiveness to staurosporine through the control of p53 at both transcriptional and post-transcriptional levels. J Biol Chem *279*, 612-618.
Palmer, M. S., Dryden, A. J., Hughes, J. T., and Collinge, J. (1991). Homozygous prion protein genotype predisposes to sporadic Creutzfeldt-Jakob disease. Nature *352*, 340-342.
Pan, K. M., Baldwin, M., Nguyen, J., Gasset, M., Serban, A., Groth, D., Mehlhorn, I., Huang, Z., Fletterick, R. J., Cohen, F. E., and al, e. (1993a). Conversion of alpha-helices into beta-sheets features in the formation of the scrapie prion proteins. ProcNatlAcadSciUSA.
Pan, K. M., Baldwin, M., Nguyen, J., Gasset, M., Serban, A., Groth, D., Mehlhorn, I., Huang, Z., Fletterick, R. J., Cohen, F. E., and et al. (1993b). Conversion of alpha-helices into beta-sheets features in the formation of the scrapie prion proteins. Proc Natl Acad Sci U S A *90*, 10962-10966.
Pan, K. M., Stahl, N., and Prusiner, S. B. (1992). Purification and properties of the cellular prion protein from Syrian hamster brain. Protein Sci *1*, 1343-1352.
Pan, T., Wong, B. S., Liu, T., Li, R., Petersen, R. B., and Sy, M. S. (2002). Cell-surface prion protein interacts with glycosaminoglycans. Biochem J *368*, 81-90.
Parchi, P., Zou, W., Wang, W., Brown, P., Capellari, S., Ghetti, B., Kopp, N., Schulz-Schaeffer, W. J., Kretzschmar, H. A., Head, M. W., *et al.* (2000). Genetic influence on the structural variations of the abnormal prion protein. Proc Natl Acad Sci U S A *97*, 10168-10172.
Pattison, I. (1965a). Experiments with scrapie with special reference to the nature of the agent and the pathology of the disease. *Slow, latent and temperate virus infections*, 249-257.
Pattison, I. H. (1965b). Resistance of the scrapie agent to formalin. J Comp Pathol *75*, 159-164.
Pattison, I. H., Hoare, M. N., Jebbett, J. N., and Watson, W. A. (1972). Spread of scrapie to sheep and goats by oral dosing with foetal membranes from scrapie-affected sheep. Vet Rec *90*, 465-468.
Pattison, I. H., and Millson, G. C. (1961). Scrapie produced experimentally in goats with special reference to the clinical syndrome. J Comp Pathol *71*, 101-109.

Pauly, P. C., and Harris, D. A. (1998). Copper stimulates endocytosis of the prion protein. J Biol Chem *273*, 33107-33110.
Peretz, D., Williamson, R. A., Kaneko, K., Vergara, J., Leclerc, E., Schmitt-Ulms, G., Mehlhorn, I. R., Legname, G., Wormald, M. R., Rudd, P. M., *et al.* (2001). Antibodies inhibit prion propagation and clear cell cultures of prion infectivity. Nature *412*, 739-743.
Peters, P. J., Mironov, A., Jr., Peretz, D., van Donselaar, E., Leclerc, E., Erpel, S., DeArmond, S. J., Burton, D. R., Williamson, R. A., Vey, M., and Prusiner, S. B. (2003). Trafficking of prion proteins through a caveolae-mediated endosomal pathway. J Cell Biol *162*, 703-717.
Pocchiari, M. (1994). Prions and related neurological diseases. Mol Aspects Med *15*, 195-291.
Powell Jackson, J., Weller, R. O., Kennedy, P., Preece, M. A., Whitcombe, E. M., and Newsom Davis, J. (1985). Creutzfeldt-Jakob disease after administration of human growth hormone. Lancet *2*, 244-246.
Priola, S. A. (1999). Prion protein and species barriers in the transmissible spongiform encephalopathies. Biomed Pharmacother *53*, 27-33.
Prusiner, S. B. (1982). Novel proteinaceous infectious particles cause scrapie. Science *216*, 136-144.
Prusiner, S. B. (1989). Scrapie prions. Annu Rev Microbiol *43*, 345-374.
Prusiner, S. B. (1991). Molecular biology of prion diseases. Science *252*, 1515-1522.
Prusiner, S. B. (1997). Prion diseases and the BSE crisis. Science *278*, 245-251.
Prusiner, S. B. (1998). Prions. Proc Natl Acad Sci U S A *95*, 13363-13383.
Prusiner, S. B., Scott, M., Foster, D., Pan, K. M., Groth, D., Mirenda, C., Torchia, M., Yang, S. L., Serban, D., Carlson, G. A., and et al. (1990). Transgenetic studies implicate interactions between homologous PrP isoforms in scrapie prion replication. Cell *63*, 673-686.
Prusiner, S. B., and Scott, M. R. (1997). Genetics of prions. Annu Rev Genet *31*, 139-175.
Qin, K., Coomaraswamy, J., Mastrangelo, P., Yang, Y., Lugowski, S., Petromilli, C., Prusiner, S. B., Fraser, P. E., Goldberg, J. M., Chakrabartty, A., and Westaway, D. (2003). The PrP-like protein Doppel binds copper. J Biol Chem *278*, 8888-8896.
Race, R., Oldstone, M., and Chesebro, B. (2000). Entry versus blockade of brain infection following oral or intraperitoneal scrapie administration: role of prion protein expression in peripheral nerves and spleen. J Virol *74*, 828-833.
Race, R. E., Caughey, B., Graham, K., Ernst, D., and Chesebro, B. (1988). Analyses of frequency of infection, specific infectivity, and prion protein biosynthesis in scrapie-infected neuroblastoma cell clones. J Virol *62*, 2845-2849.
Raeber, A. J., Borchelt, D. R., Scott, M., and Prusiner, S. B. (1992). Attempts to convert the cellular prion protein into the scrapie isoform in cell-free systems. J Virol *66*, 6155-6163.
Rieger, R., Edenhofer, F., Lasmezas, C. I., and Weiss, S. (1997). The human 37-kDa laminin receptor precursor interacts with the prion protein in eukaryotic cells [see comments]. Nat Med *3*, 1383-1388.
Riek, R., Hornemann, S., Wider, G., Billeter, M., Glockshuber, R., and Wuthrich, K. (1996). NMR structure of the mouse prion protein domain PrP(121-321). Nature *382*, 180-182.
Rine, J., and Kim, S. H. (1990). A role for isoprenoid lipids in the localization and function of an oncoprotein. New Biol *2*, 219-226.

Rohwer, R. G. (1991). The scrapie agent: "a virus by any other name". Curr Top Microbiol Immunol *172*, 195-232.
Rossi, D., Cozzio, A., Flechsig, E., Klein, M. A., Rulicke, T., Aguzzi, A., and Weissmann, C. (2001). Onset of ataxia and Purkinje cell loss in PrP null mice inversely correlated with Dpl level in brain. Embo J *20*, 694-702.
Roucou, X., Giannopoulos, P. N., Zhang, Y., Jodoin, J., Goodyer, C. G., and LeBlanc, A. (2005). Cellular prion protein inhibits proapoptotic Bax conformational change in human neurons and in breast carcinoma MCF-7 cells. Cell Death Differ *12*, 783-795.
Roucou, X., Guo, Q., Zhang, Y., Goodyer, C. G., and LeBlanc, A. C. (2003). Cytosolic prion protein is not toxic and protects against Bax-mediated cell death in human primary neurons. J Biol Chem *278*, 40877-40881.
Rubenstein, R., Carp, R. I., and Callahan, S. M. (1984). In vitro replication of scrapie agent in a neuronal model: infection of PC12 cells. J Gen Virol *65*, 2191-2198.
Saborio, G. P., Permanne, B., and Soto, C. (2001). Sensitive detection of pathological prion protein by cyclic amplification of protein misfolding. Nature *411*, 810-813.
Safar, J., Wille, H., Itri, V., Groth, D., Serban, H., Torchia, M., Cohen, F. E., and Prusiner, S. B. (1998). Eight prion strains have PrP(Sc) molecules with different conformations [see comments]. Nat Med *4*, 1157-1165.
Safar, J. G., Kellings, K., Serban, A., Groth, D., Cleaver, J. E., Prusiner, S. B., and Riesner, D. (2005). Search for a prion-specific nucleic Acid. J Virol *79*, 10796-10806.
Sakaguchi, S., Katamine, S., Nishida, N., Moriuchi, R., Shigematzu, K., Sugimoto, T., Nakatni, A., Kataoka, Y., Houtani, H., Shirabe, S., *et al.* (1996). Loss of cerebellar Purkinje Cells in aged mice homozygous for a disrupted PrP gene. Nature *380*, 528-531.
Santuccione, A., Sytnyk, V., Leshchyns'ka, I., and Schachner, M. (2005). Prion protein recruits its neuronal receptor NCAM to lipid rafts to activate p59fyn and to enhance neurite outgrowth. J Cell Biol *169*, 341-354.
Sarnataro, D., Campana, V., Paladino, S., Stornaiuolo, M., Nitsch, L., and Zurzolo, C. (2004). PrP(C) association with lipid rafts in the early secretory pathway stabilizes its cellular conformation. Mol Biol Cell *15*, 4031-4042.
Schmitt-Ulms, G., Legname, G., Baldwin, M. A., Ball, H. L., Bradon, N., Bosque, P. J., Crossin, K. L., Edelman, G. M., DeArmond, S. J., Cohen, F. E., and Prusiner, S. B. (2001). Binding of neural cell adhesion molecules (N-CAMs) to the cellular prion protein. J Mol Biol *314*, 1209-1225.
Schätzl, H. M., Laszlo, L., Holtzman, D. M., Tatzelt, J., DeArmond, S. J., Weiner, R. I., Mobley, W. C., and Prusiner, S. B. (1997). A hypothalamic neuronal cell line persistently infected with scrapie prions exhibits apoptosis. J Virol *71*, 8821-8831.
Shmerling, D., Hegyi, I., Fischer, M., Blattler, T., Brandner, S., Gotz, J., Rulicke, T., Flechsig, E., Cozzio, A., von Mering, C., *et al.* (1998). Expression of amino-terminally truncated PrP in the mouse leading to ataxia and specific cerebellar lesions. Cell *93*, 203-214.
Shogomori, H., and Futerman, A. H. (2001). Cholera toxin is found in detergent-insoluble rafts/domains at the cell surface of hippocampal neurons but is internalized via a raft-independent mechanism. J Biol Chem *276*, 9182-9188.
Shyng, S. L., Heuser, J. E., and Harris, D. A. (1994). A glycolipid-anchored prion protein is endocytosed via clathrin-coated pits. J Cell Biol *125*, 1239-1250.
Shyng, S. L., Huber, M. T., and Harris, D. A. (1993). A prion protein cycles between the cell surface and an endocytic compartment in cultured neuroblastoma cells. J Biol Chem *268*, 15922-15928.

Shyng, S. L., Lehmann, S., Moulder, K. L., and Harris, D. A. (1995a). Sulfated glycans stimulate endocytosis of the cellular isoform of the prion protein, PrPC, in cultured cells. J Biol Chem *270*, 30221-30229.
Shyng, S. L., Moulder, K. L., Lesko, A., and Harris, D. A. (1995b). The N-terminal domain of a glycolipid-anchored prion protein is essential for its endocytosis via clathrin-coated pits. J Biol Chem *270*, 14793-14800.
Silverman, G. L., Qin, K., Moore, R. C., Yang, Y., Mastrangelo, P., Tremblay, P., Prusiner, S. B., Cohen, F. E., and Westaway, D. (2000). Doppel is an N-glycosylated, glycosylphosphatidylinositol-anchored protein. Expression in testis and ectopic production in the brains of Prnp(0/0) mice predisposed to Purkinje cell loss. J Biol Chem *275*, 26834-26841.
Simons, K., and Toomre, D. (2000). Lipid rafts and signal transduction. Nat Rev Mol Cell Biol *1*, 31-39.
Skarnes, W. C., Moss, J. E., Hurtley, S. M., and Beddington, R. S. (1995). Capturing genes encoding membrane and secreted proteins important for mouse development. Proc Natl Acad Sci U S A *92*, 6592-6596.
Solforosi, L., Criado, J. R., McGavern, D. B., Wirz, S., Sanchez-Alavez, M., Sugama, S., DeGiorgio, L. A., Volpe, B. T., Wiseman, E., Abalos, G., *et al.* (2004). Cross-linking cellular prion protein triggers neuronal apoptosis in vivo. Science *303*, 1514-1516.
Somerville, R. A., Birkett, C. R., Farquhar, C. F., Hunter, N., Goldmann, W., Dornan, J., Grover, D., Hennion, R. M., Percy, C., Foster, J., and Jeffrey, M. (1997). Immunodetection of PrPSc in spleens of some scrapie-infected sheep but not BSE-infected cows. J Gen Virol *78*, 2389-2396.
Sparrer, H. E., Santoso, A., Szoka, F. C., Jr., and Weissman, J. S. (2000). Evidence for the prion hypothesis: induction of the yeast [PSI+] factor by in vitro- converted Sup35 protein. Science *289*, 595-599.
Spielhaupter, C., and Schatzl, H. M. (2001). PrPC directly interacts with proteins involved in signaling pathways. J Biol Chem *276*, 44604-44612.
Stahl, N., Borchelt, D. R., Hsiao, K., and Prusiner, S. B. (1987). Scrapie prion protein contains a phosphatidylinositol glycolipid. Cell *51*, 229-240.
Stewart, R. S., and Harris, D. A. (2005). A transmembrane form of the prion protein is localized in the Golgi apparatus of neurons. J Biol Chem *280*, 15855-15864.
Stewart, R. S., Piccardo, P., Ghetti, B., and Harris, D. A. (2005). Neurodegenerative illness in transgenic mice expressing a transmembrane form of the prion protein. J Neurosci *25*, 3469-3477.
Stockel, J., and Hartl, F. U. (2001). Chaperonin-mediated de novo generation of prion protein aggregates. J Mol Biol *313*, 861-872.
Sunyach, C., Jen, A., Deng, J., Fitzgerald, K. T., Frobert, Y., Grassi, J., McCaffrey, M. W., and Morris, R. (2003). The mechanism of internalization of glycosylphosphatidylinositol-anchored prion protein. Embo J *22*, 3591-3601.
Supattapone, S., Bosque, P., Muramoto, T., Wille, H., Aagaard, C., Peretz, D., Nguyen, H. O., Heinrich, C., Torchia, M., Safar, J., *et al.* (1999). Prion protein of 106 residues creates an artifical transmission barrier for prion replication in transgenic mice. Cell *96*, 869-878.
Supattapone, S., Muramoto, T., Legname, G., Mehlhorn, I., Cohen, F. E., DeArmond, S. J., Prusiner, S. B., and Scott, M. R. (2001). Identification of two prion protein regions that modify scrapie incubation time. J Virol *75*, 1408-1413.

Swietnicki, W., Petersen, R., Gambetti, P., and Surewicz, W. K. (1997). pH-dependent stability and conformation of the recombinant human prion protein PrP(90-231). J Biol Chem *272*, 27517-27520.
Tanaka, M., Chien, P., Naber, N., Cooke, R., and Weissman, J. S. (2004). Conformational variations in an infectious protein determine prion strain differences. Nature *428*, 323-328.
Taraboulos, A., Raeber, A. J., Borchelt, D. R., Serban, D., and Prusiner, S. B. (1992). Synthesis and trafficking of prion proteins in cultured cells. Mol Biol Cell *3*, 851-863.
Taraboulos, A., Scott, M., Semenov, A., Avraham, D., Laszlo, L., and Prusiner, S. B. (1995). Cholesterol depletion and modification of COOH-terminal targeting sequence of the prion protein inhibit formation of the scrapie isoform. JCell Biol *129*, 121-132.
Telling, G. C., Scott, M., Hsiao, K. K., Foster, D., Yang, S. L., Torchia, M., Sidle, K. C., Collinge, J., DeArmond, S. J., and Prusiner, S. B. (1994). Transmission of Creutzfeldt-Jakob disease from humans to transgenic mice expressing chimeric human-mouse prion protein. Proc Natl Acad Sci U S A *91*, 9936-9940.
Telling, G. C., Scott, M., Mastrianni, J., Gabizon, R., Torchia, M., Cohen, F. E., DeArmond, S. J., and Prusiner, S. B. (1995). Prion propagation in mice expressing human and chimeric PrP transgenes implicates the interaction of cellular PrP with another protein. Cell *83*, 79-90.
Tobler, I., Gaus, S. E., Deboer, T., Achermann, P., Fischer, M., Rulicke, T., Moser, M., Oesch, B., McBride, P. A., and Manson, J. C. (1996). Altered Circadian Activity Rhythms and Sleep in Mice Devoid of Prion Protein. Nature *380*, 639-642.
Townley, D. J., Avery, B. J., Rosen, B., and Skarnes, W. C. (1997). Rapid sequence analysis of gene trap integrations to generate a resource of insertional mutations in mice. Genome Res *7*, 293-298.
Turk, E., Teplow, D. B., Hood, L. E., and Prusiner, S. B. (1988). Purification and properties of the cellular and scrapie hamster prion proteins. Eur J Biochem *176*, 21-30.
Uetz, P., Giot, L., Cagney, G., Mansfield, T. A., Judson, R. S., Knight, J. R., Lockshon, D., Narayan, V., Srinivasan, M., Pochart, P., *et al.* (2000). A comprehensive analysis of protein-protein interactions in Saccharomyces cerevisiae. Nature *403*, 623-627.
Vankeulen, L. J. M., Schreuder, B. E. C., Meloen, R. H., Mooijharkes, G., Vromans, M. E. W., and Langeveld, J. P. M. (1996). Immunohistochemical Detection of Prion Protein in Lymphoid Tissues of Sheep With Natural Scrapie. Journal of Clinical Microbiology *34*, 1228-1231.
Vey, M., Pilkuhn, S., Wille, H., Nixon, R., Dearmond, S. J., Smart, E. J., Anderson, R. G. W., Taraboulos, A., and Prusiner, S. B. (1996). Subcellular Colocalization of the Cellular and Scrapie Prion Proteins in Caveolae-Like Membranous Domains. Proceedings of the National Academy of Sciences of the United States of America *93*, 14945-14949.
Vilette, D., Andreoletti, O., Archer, F., Madelaine, M. F., Vilotte, J. L., Lehmann, S., and Laude, H. (2001). Ex vivo propagation of infectious sheep scrapie agent in heterologous epithelial cells expressing ovine prion protein. Proc Natl Acad Sci U S A *98*, 4055-4059.
Waggoner, D. J., Drisaldi, B., Bartnikas, T. B., Casareno, R. L., Prohaska, J. R., Gitlin, J. D., and Harris, D. A. (2000). Brain Copper Content and Cuproenzyme Activity Do Not Vary with Prion Protein Expression Level. J Biol Chem *275*, 7455-7458.
Weighardt, F., Biamonti, G., and Riva, S. (1996). The roles of heterogeneous nuclear ribonucleoproteins (hnRNP) in RNA metabolism. Bioessays *18*, 747-756.
Weissmann, C. (1991). A 'unified theory' of prion propagation. Nature *352*, 679-683.
Weissmann, C. (2004). The state of the prion. Nat Rev Microbiol *2*, 861-871.

Wells, G. A., Scott, A. C., Johnson, C. T., Gunning, R. F., Hancock, R. D., Jeffrey, M., Dawson, M., and Bradley, R. (1987). A novel progressive spongiform encephalopathy in cattle. VetRec *121*, 419-420.
Wennerberg, K., Rossman, K. L., and Der, C. J. (2005). The Ras superfamily at a glance. J Cell Sci *118*, 843-846.
White, A. R., Enever, P., Tayebi, M., Mushens, R., Linehan, J., Brandner, S., Anstee, D., Collinge, J., and Hawke, S. (2003). Monoclonal antibodies inhibit prion replication and delay the development of prion disease. Nature *422*, 80-83.
Wilesmith, J. W., Ryan, J. B., and Atkinson, M. J. (1991). Bovine spongiform encephalopathy: epidemiological studies on the origin. Vet Rec *128*, 199-203.
Will, R., Ironside JW, Zeidler M, Cousens SN, Estibeiro K, Alperovitch A, Poser S, Pocchiari M, Hofman A, and Smith (1996). A new variant of Creutzfeldt-Jakob disease in the UK. Lancet *347*, 921-925.
Will, R. G. (2003). Acquired prion disease: iatrogenic CJD, variant CJD, kuru. Br Med Bull *66*, 255-265.
Williams, E. S., and Young, S. (1980). Chronic wasting disease of captive mule deer: a spongiform encephalopathy. J Wildl Dis *16*, 89-98.
Wong, C., Xiong, L. W., Horiuchi, M., Raymond, L., Wehrly, K., Chesebro, B., and Caughey, B. (2001). Sulfated glycans and elevated temperature stimulate PrP(Sc)-dependent cell-free formation of protease-resistant prion protein. Embo J *20*, 377-386.
Zanata, S. M., Lopes, M. H., Mercadante, A. F., Hajj, G. N., Chiarini, L. B., Nomizo, R., Freitas, A. R., Cabral, A. L., Lee, K. S., Juliano, M. A., *et al.* (2002). Stress-inducible protein 1 is a cell surface ligand for cellular prion that triggers neuroprotection. Embo J *21*, 3307-3316.
Zerial, M., and McBride, H. (2001). Rab proteins as membrane organizers. Nat Rev Mol Cell Biol *2*, 107-117.
Zobeley, E., Flechsig, E., Cozzio, A., Enari, M., and Weissmann, C. (1999). Infectivity of scrapie prions bound to a stainless steel surface. Mol Med *5*, 240-243.